FINAL REPORT

V/STOL TILT ROTOR STUDY - VOLUME V

A MATHEMATICAL MODEL FOR REAL TIME FLIGHT SIMULATION OF THE BELL MODEL 301 TILT ROTOR RESEARCH AIRCRAFT

MODEL 301

REPORT 301-099-001

NASA CONTRACT NAS 2-6589

BELL HELICOPTER COMPANY
textron

CR114614

V/STOL TILT ROTOR STUDY-VOLUME V

A MATHEMATICAL MODEL FOR REAL TIME FLIGHT SIMULATION OF THE BELL MODEL 301 TILT ROTOR RESEARCH AIRCRAFT

by

P. B. HARENDRA
M. J. JOGLEKAR
T. M. GAFFEY
R. L. MARR

BELL HELICOPTER COMPANY REPORT NO. 301-099-001

April 13, 1973

Prepared Under Contract No. NAS2-6599 by
Bell Helicopter Company, A Textron Company
Fort Worth, Texas

for

National Aeronautics and Space Administration
Ames Research Center

and

United States Army Airmobility Research and Development
Laboratory, Ames Directorate

This Data is Furnished in Accordance
With the Provisions of Contract NAS2-6599

Foreword

This report is one of a series prepared by the Bell Helicopter Company, Fort Worth, Texas for the National Aeronautics and Space Administration, Ames Research Center, Moffett Field, California under contract NAS2-6599. These Tilt Rotor Research Aircraft studies were jointly funded by NASA and the U. S. Army Air Mobility Research and Development Laboratory, Ames Directorate.

The Administrative Contracting Officer was Mr. Richard J. Abbott. The Technical Monitor was Mr. Martin D. Maisel, Tilt Rotor Research Aircraft Project Office. Mr. Gary B. Churchill, Tilt Rotor Research Aircraft Project provided technical support of the effort reported in Volume V.

Volume I -- V/STOL Tilt Rotor Study, Conceptual Design -- CR11441

Volume II -- V/STOL Tilt Rotor Study, Research Aircraft Design-- CR11442

Volume III -- V/STOL Tilt Rotor Study, Research Aircraft Project Plan--CR11443

Volume IV -- V/STOL Tilt Rotor Study, Wind Tunnel Investigation Plan--CR114444

Volume V -- V/STOL Tilt Rotor Study, A Mathematical Model for Real Time Flight Simulation of the Bell Model 301 Tilt Rotor Research Aircraft--CR114614

Volume VI -- V/STOL Tilt Rotor Study, Hover, Low Speed and Conversion Tests of a Tilt Rotor Aeroelastic Model --CR114615

BELL HELICOPTER COMPANY

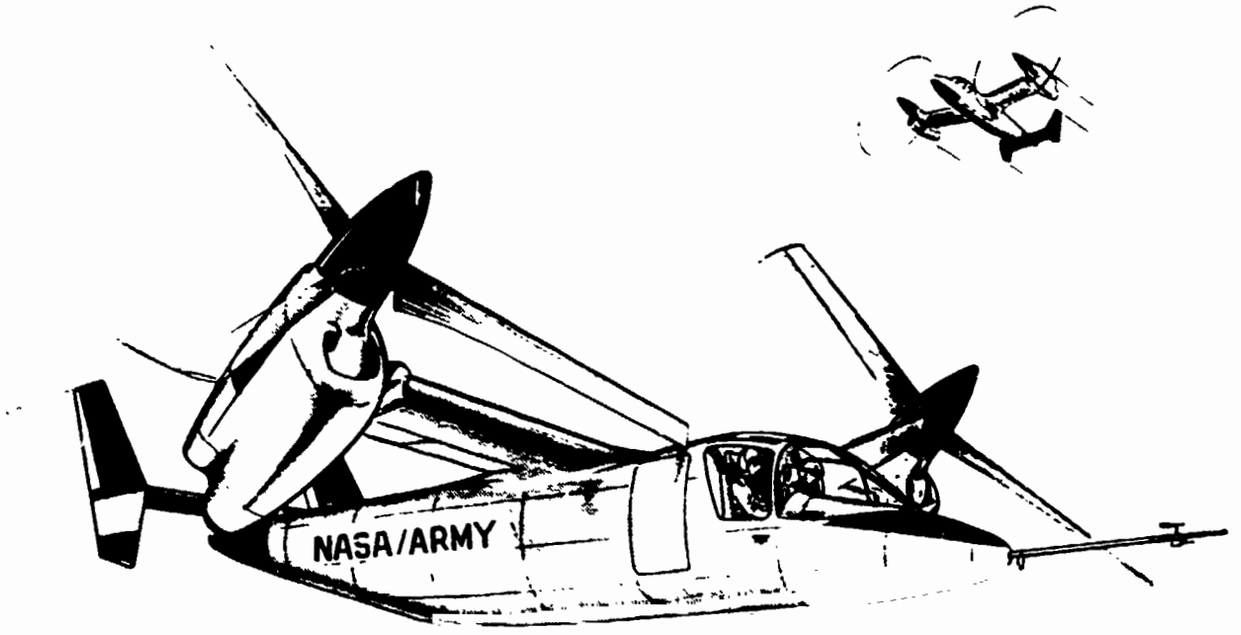

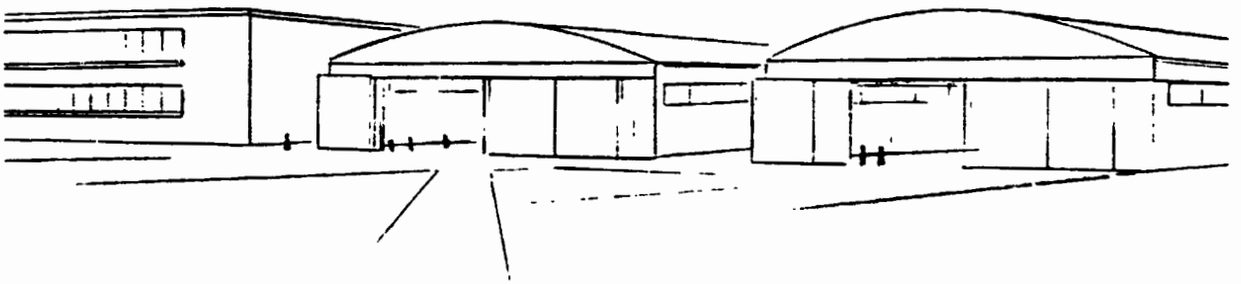

BELL MODEL 301 TILT ROTOR
RESEARCH AIRCRAFT

TABLE OF CONTENTS

Section		Page
	LIST OF ILLUSTRATIONS	iv
	LIST OF TABLES	vi
	LIST OF SYMBOLS	vii
I.	SUMMARY	I-1
II.	DESCRIPTION OF THE MATHEMATICAL MODEL	II-1
	A. Coordinate Systems and Sign Conventions	II-1
	B. Rotor Math Model	II-1
	C. Airframe Aerodynamics	II-3
	D. Rotor Wake-Airframe Aerodynamic Interaction	II-5
	E. Flight Controls	II-7
	F. Drive System and Engines	II-7
	G. Automatic Flight Control System	II-9
	H. Equations of Motion and Coordinate Transformations	II-10
III.	VALIDATION OF THE MATHEMATICAL MODEL	III-1
	A. Rotor Performance	III-1
	B. Airframe Aerodynamics	III-1
	C. Rotor Wake-Airframe Aerodynamic Interaction	III-2
	D. Stability Derivatives	III-2
	E. Static Stability	III-3
	F. Dynamic Stability	III-3
	G. Control Power and Damping	III-3
IV.	CONTRACTOR EVALUATION OF FSAA SIMULATION	IV-1
	A. Mathematical Model and Computer Program Deficiencies	IV-1
	B. Simulator Hardware Deficiencies	IV-2
V.	RECOMMENDATIONS FOR FURTHER DEVELOPMENT OF MODEL 301 SIMULATION	V-1
	A. Mathematical Model and Computer Program	V-1
	B. Simulator Hardware	V-2
VI.	REFERENCES	VI-1
APPENDIX A - MATHEMATICAL MODEL EQUATIONS		A-1
APPENDIX B - MODEL 301 INPUT DATA		B-1

LIST OF ILLUSTRATIONS

Number		Page
I-1	Block Diagram of Mathematical Model	I-3
II-1	Rotor Axes Systems and Sign Convention	II-11
II-2	Side-By-Side Rotor Effect on Induced Velocity	II-12
II-3	Wing-Pylon Lift Coefficient Versus Angle of Attack	II-13
II-4	Wing-Pylon Drag Coefficient Versus Angle of Attack	II-14
II-5	Compressibility Correction to Wing-Pylon Lift Coefficient	II-15
II-6	Compressibility Correction to Wing-Pylon Drag Coefficient	II-16
II-7	Wing-Pylon Lift Coefficient at Large Negative Angles of Attack	II-17
II-8	Wing-Pylon Drag Coefficient at Large Negative Angles of Attack	II-18
II-9	Sign Conventions and Notation for Horizontal Stabilizer and Vertical Fin Aerodynamics	II-19
II-10	Horizontal Stabilizer Lift Coefficient Versus Angle of Attack	II-20
II-11	Horizontal Stabilizer Drag Coefficient Versus Angle of Attack	II-21
II-12	Wing-Pylon Wake Deflection at Horizontal Stabilizer	II-22
II-13	Vertical Stabilizer Side Force Coefficient Versus Sideslip Angle	II-23
II-14	Vertical Stabilizer Drag Coefficient Versus Sideslip Angle	II-24
II-15	Sign Convention and Notation for Mathematical Model of Rotor Wake - Wing Interaction	II-25
II-16	Model of Rotor Wake Induced Velocity at Horizontal Stabilizer	II-26
II-17	Representation of In-Ground Effect Rolling Moment	II-27
II-18	Schematic of Model 301 Flight Control System	II-28
II-19	Computer Representation of Flight Control System Wash-Out Schedule With Conversion Angle	II-29
II-20	Schematic of SCAS Pitch Channel Network	II-30
III-1	Rotor Performance Correlation - Hover	III-7
III-2	Rotor Performance Correlation - $\alpha_m = 75^\circ$	III-8
III-3	Rotor Performance Correlation - $\alpha_m = 60^\circ$	III-9

LIST OF ILLUSTRATIONS (Cont'd)

Number		Page
III-4	Rotor Performance Correlation - $\alpha_m = 30°$	III-10
III-5	Rotor Performance Correlation - $\alpha_m = 0°$	III-11
III-6	Rotor Rate Derivative Correlation	III-12
III-7	Airplane Mode Lift Coefficient Correlation	III-13
III-8	Helicopter Mode Lift Coefficient Correlation	III-14
III-9	Airplane Mode Drag Coefficient Correlation	III-15
III-10	Helicopter Mode Drag Coefficient Correlation	III-16
III-11	Airplane Mode Pitching Moment Correlation	III-17
III-12	Helicopter Mode Pitching Moment Correlation	III-18
III-13	Airplane Mode Sideforce Coefficient Correlation	III-19
III-14	Helicopter Mode Sideforce Coefficient Correlation	III-20
III-15	Airplane Mode Rolling Moment Coefficient Correlation	III-21
III-16	Helicopter Mode Rolling Moment Coefficient Correlation	III-22
III-17	Airplane Mode Yawing Moment Coefficient Correlation	III-23
III-18	Helicopter Mode Yawing Moment Coefficient Correlation	III-24
III-19	Aileron Control Power Correlation	III-25
III-20	Rotor Wake Effect on Wing Lift	III-26
III-21	Level Flight Trim Condition Correlation	III-27
III-22	Comparison of Longitudinal Oscillatory Mode Characteristics With MIL-F-83300 Response Requirements	III-28
III-23	Comparison of Lateral-Directional Oscillatory Mode Characteristics With MIL-F-83300 Response Requirements	III-29
III-24	Helicopter and Conversion Mode Control Power Correlation	III-30
III-25	Airplane Mode Control Power Correlation	III-31
III-26	Aircraft Damping Correlation	III-32

LIST OF TABLES

Number		Page
III-1	Stability Derivative Correlation	III-4
III-2	Flight Mode Characteristics Correlation	III-6

LIST OF SYMBOLS

This section describes the symbols used for the time dependent variables that are passed between the subsystems (see subsystems block diagram, Section I).

Key to Nomenclature:

X, Y, Z	Indicate body axes forces
D, Y', L	Indicate wind axes forces
l, M, N	Indicate body axes moments
l', M', N'	Indicate wind axes moments

Subscripts

F	Fuselage
W	Wing
WP	Wing-pylon
H	Horizontal stabilizer
V	Vertical stabilizer
R	Right rotor
L	Left rotor
SP	Shaft pivot point
P	Pylon
MG	Main gear
NG	Nose gear
a	Aileron
e	Elevator
r	Rudder
PA	Pilot station
CG	Aircraft center of gravity
R/W	Due to rotor at wing
R/H	Due to rotor at horizontal stabilizer
R/V	Due to rotor at vertical stabilizers
W/H	Due to wing at horizontal stabilizer
$\vert^{B}_{R/W}$	Due to rotor at wing in body axes
$\vert^{B}_{R/H}$	Due to rotor at horizontal stabilizer, in body axes
$\vert^{B}_{R/V}$	Due to rotor at vertical stabilizers, in body axes

Symbol	Description	Units
a_0, a_1, a_2	Blade lift coefficients	$\frac{1}{ad}$, $\frac{1}{\mu}$, $\frac{1}{\mu^2}$

Symbol	Description	Units
a_{OL}	Steady flapping component, left rotor	rad
a_{OR}	Steady flapping component, right rotor	rad
a_{1L}	F/A flapping, left rotor + backward	rad
$\dot{a}_{1L}$	F/A flapping rate, left rotor	rad/sec
a_{1R}	F/A flapping, right rotor + backward	rad
a_{1R}	F/A flapping rate, right rotor	rad/sec
B	Blade tip loss factor	ND
BL_{CG}	Butt line of aircraft C.G.	In.
B_{1L}	Forward cyclic input, left rotor	rad
B_{1R}	Forward cyclic input, right rotor	rad
b_{1L}	Lateral flapping, left rotor, + outboard edge down	rad
$\dot{b}_{1L}$	Lateral flapping rate, left rotor	rad/sec
b_{1R}	Lateral flapping, right rotor, + outboard edge down	rad
$\dot{b}_{1R}$	Lateral flapping rate, right rotor	rad/sec
C_{β}	Prandtl-Glauert factor, page A-33	
C_{RF}	Rotor thrust coefficient (see page A-18)	ND
C_{T_L}	Thrust coefficient, left rotor	ND
C_{T_R}	Thrust coefficient, right rotor	ND
D_F	Aero drag on fuselage	Lb.
D_H	Aero drag on horizontal stabilizer	Lb.
D_{iWPL}	Aero drag on portion of left wing-pylon immersed in rotor wake	Lb.
D_{iWPL}	Aero drag on portion of right wing-pylon immersed in rotor wake	Lb.
D_{MG}	Aero drag on main landing gear	Lb.
D_{NG}	Aero drag on nose landing gear	Lb.
D_{VL}	Aero drag on left vertical fin	Lb.
D_{VR}	Aero drag on right vertical fin	Lb.
D_{WP}	Aero drag on portion of wing-pylon in freestream	Lb.
E	Distance from takeoff point in the direction grid-East (+ East)	Nautical Miles
$\dot{E}$	Eastward velocity of aircraft	Knots
ESAS, RSAS, ASAS	SCAS actuator inputs to the elevator, rudder, and aileron, respectively	In.

Symbol	Description	Units
F_{LN}, F_T, F_{PD}	Stick and pedal forces from pilot (+ fwd, + right. + right)	Lb.
F_X	Flap position indicator	-
H_L	Aero H-force on left rotor + backward (upward) in mast axis system	Lb.
HP_{RL}	HP required to drive left rotor	HP
HP_{RR}	HP required to drive right rotor	HP
H_R	Aero H force on right rotor + backward (upward) in mast axis system	Lb.
h	Radar altitude of aircraft	ft
$\dot{h}$	Aircraft climb rate	ft/sec
I_{XX}	Aircraft rolling inertia, body axes	slug ft^2
I_{XZ}	Aircraft product of inertia, body axes	slug ft^2
I_{YY}	Aircraft pitching inertia, body axes	slug ft^2
I_{ZZ}	Aircraft yawing inertia, body axes	slug ft^2
K_e	Elevator effectiveness factor, p. B-26	
L_F	Aero lift on fuselage	Lb.
L_H	Aero lift on horizontal stabilizer	Lb.
L_{iWPL}	Aero lift on portion of left wing pylon immersed in rotor wake	Lb.
L_{iWPR}	Aero lift on portion of right wing-pylon immersed in rotor wake	Lb.
L_{LG}	Landing gear position indicator	ND
L_{WP}	Aero lift on portion of wing-pylon in freestrea	Lb.
l_A, M_A, N_A	Total rolling, pitching and yawing moment on aircraft about body X, Y, Z axes	Lb.
l_F, M_F, N_F	Rolling, pitching and yawing moments on fuselage about body X, Y, Z axes	Lb Ft
l_L, M_L, N_L	Rolling, pitching and yawing moments about body X,Y,Z axes, due to left rotor forces	Lb Ft
l_R, M_R, N_R	Rolling, pitching and yawing moments about X,Y,Z axes, due to right rotor forces	Lb Ft
l_{WP}, M_{WP}, N_{WP}	Rolling, pitching and yawing moments due to wing-pylon, about body X,Y,Z axes	Lb Ft

Symbol	Description	Units
$l'_{WP}, M'_{WP}, N'_{WP}$	Rolling, pitching and yawing moments due to wing-pylon in wind axes system	Lb ft
L_{XH}, L_{YH}, L_{ZH}	Distance from the CG to swashplate, Body X, Y, Z axes	ft
M_H	Aero pitching moment due to horizontal stabilizer in body axes	Lb ft
M'_H	Aero pitching moment due to horizontal stabilizer in wind axes	Lb ft
M_N	Mach number	ND
M_{a1L}	F/A flapping restraint moment exerted by left rotor on airframe, mast axes system (nose up)	Lb ft
M_{a1R}	F/A flapping restraint moment exerted by right rotor on airframe, mast axes system (nose up)	Lb ft
l_{b1L}	Lateral flapping restraint moment exerted by left rotor on airframe, mast axes system (hub outboard)	Lb ft
l_{b1R}	Lateral flapping restraint moment exerted by right rotor on airframe, mast axes system (hub outboard)	Lb ft
N_N	Distance from takeoff point in the direction grid-North (+ North)	Naut. Miles
N_X, N_Y, N_Z	Linear acceleration components of aircraft cg in body axes system	g
P_{AX}, P_{AY}, P_{AZ}	Position of aircraft cg w r t ground	Naut. Miles
P_a	Ambient pressure, absolute	psia
p,q,r	Aircraft roll, pitch and yaw rates in body axes system	rad/sec
$\dot{p},\dot{q},\dot{r}$	Aircraft angular accelerations in body axes system	rad/sec^2
Q_L	Left rotor aero torque, + trying to slow rotor down, mast axes system	Lb ft
Q_{LPT}	Torque supplied by left power turbine	Lb ft
Q_R	Right rotor aero torque, + trying to slow rotor down, mast axes system	Lb ft
Q_{RPT}	Torque supplied by right power turbine	Lb ft
R	Rotor radius	ft
RPM_{NII}	Power Turbine RPM set at 100% (overspeed Governor	RPM
RPM_P	Proprotor RPM selected by the pilot	RPM

Symbol	Description	Units
R_{WL}	Left rotor wake contraction ratio	ND
SL_{CG}	Station location of aircraft CG	In.
T_L	Left rotor aero. thrust, in mast axis + up (forward)	Lb.
T_R	Right rotor aero, thrust, in mast axis + up (forward)	Lb
T_a	Ambient temperature, absolute	^oK
U,V,W	Velocity of aircraft CG, w.r.t. air, in body axes system, in X,Y,Z direction	Ft/sec
U_{EB},V_{EB},W_{EB}	Velocity components of aircraft CG, w.r.t. air, along earth-based axes	Ft/sec
U_G,V_G,W_G	Ground velocity components of aircraft CG	Ft/sec
U_W,V_W	Wind velocity components w.r.t ground	Ft/sec
$U_i\Big\vert^B_{R/H}$	Induced X-velocity at horizontal stabilizer in body axes system, due to rotors	Ft/sec
$U_i\Big\vert^B_{R/V}$	Induced X-velocity at vertical fins, in body axes system, due to rotor	Ft/sec
$U_i\Big\vert^B_{R/WL}$	Induced X-velocity at left wing, in body axes system, due to rotor	Ft/sec
$U_i\Big\vert^B_{R/WR}$	Induced X-velocity at right wing, in body axes system, due to rotor	Ft/sec
V_{CAS}	Calibrated airspeed	MPH
V_T	Total linear velocity of aircraft c.g. w.r.t. air	Ft/sec
WL_{CG}	Waterline of aircraft CG	In.
W_{iL}	Uniform component of induced velocity at left rotor, + downward, mast axes system	Ft/sec
W_{iR}	Uniform component of induced velocity at right rotor, + downward, mast axes system	Ft/sec

Symbol	Description	Units
$W_i\Big\|^{B}_{R/H}$	Induced Z-velocity at horizontal stabilizer, in body axes system, due to rotors	Ft/sec
$W_i\Big\|^{B}_{R/V}$	Induced Z-velocity at vertical fins, in body axes system, due to rotors	Ft/sec
$W_i\Big\|^{B}_{R/WL}$	Induced Z-velocity at left wing in body axes system, due to rotor	Ft/sec
X_A, Y_A, Z_A	Total forces on the aircraft in X,Y,Z directions, body axes system	Lb.
X_{COL}	Collective stick position, inches from full down	In.
X_F, Y_F, Z_F	Aero forces on the fuselage, in body axes system	Lb.
X_{FL}	Position indicator for flap actuator	ND
X_H, Z_H	Aero forces on horizontal stabilizer, in body axes system	Lb
X_{iWPL}, Z_{iWPL}	Aero forces on portion of left wing-pylon in rotor wake, in body axes system	Lb.
X_{iWPL}, Z_{iWPL}	Aero forces on portion of right wing-pylon in rotor wake, in body axes system	Lb
X_L, Y_L, Z_L	Left rotor forces in body axes system	Lb.
X_{LG}	Position indicator for landing gear actuator	ND
X_{LN}	Longitudinal stick position, inches from full aft	In.
X_{LT}	Lateral stick position, inches from full left	In.
X_{MG}, Z_{MG}	Aero forces on main landing gear, in body axes system	Lb.
X_{NG}, Z_{NG}	Aero forces on nose gear in body axes system	Lb.
X_{PD}	Position of pedal, inches from full left	In.
X_R, Y_R, Z_R	Right rotor forces in body axes system	Lb.

Symbol	Description	Units
X_{VL}, Y_{VL}, Z_{VL}	Aero forces on left fin, in body axes system	Lb.
X_{VR}, Y_{VR}, Z_{VR}	Aero forces on right fin, in body axes system	Lb.
X_{THL}, X_{THR}	Angles of the power levers on the fuel controls	Deg.
X_{WP}, Y_{WP}, Z_{WP}	Aero forces on wing-pylon in freestream, in body axes system	Lb.
X_{β_M}	Position of mast tilt-actuator, percent	ND
α_F	Fuselage angle of attack	rad
$\dot{\alpha}_F$	Rate of change of fuselage angle of attack	rad/sec
$\alpha'_{F\ WR}$	Angle of attack at portion of right wing immersed in rotor wake	rad
$\alpha'_{F\ WR}$	Angle of attack at portion of left wing immersed in rotor wake	rad
α_H	Angle of attack at horizontal stabilizer	rad
α_W	Angle of attack on portion of wing outside rotor wake	rad
β_F	Fuselage sideship angle	rad
β_M	Mast conversion angle, + forward, measured from body (-Z) axis, 0° is vertical, 90° is zero incidence	deg
β_V	Angle of attack at vertical fins	deg
δ_3	Pitch flap coupling	deg
δ_a	Aileron mean deflection angle, + right aileron up	deg
δ_e	Elevator deflection angle, + up	deg
δ_r	Rudder deflection angle, + right pedal	deg
$\epsilon_{W/H}$	Wing wake deflection at horizontal stabilizer	deg
θ_{oL}	Left rotor root collective pitch	deg
$\theta_{oL/G}$	Left rotor collective pitch input from proprotor collective governor	deg

Symbol	Description	Units
θ_{oR}	Right rotor root collective pitch	deg
$\theta_{oR/G}$	Right rotor collective pitch input from proprotor collective governor	deg
λ_{oL}	Inflow ratio at left rotor, neglecting rotor-induced velocity	ND
λ_{oR}	Inflow ratio at right rotor, neglecting rotor-induced velocity	ND
μ_L	Tip speed ratio, left rotor	ND
μ_R	Tip speed ratio, right rotor	ND
ρ	Air density	$Slug/ft^3$
Ψ,θ,ϕ	Euler angles	rad
$\dot{\Psi},\dot{\theta},\dot{\phi}$	Rate of change of Euler angles	rad/sec
Ψ_w,θ_w	Grid heading (+ clockwise from N) and Euler pitch angle of wind	rad
Ω_{EL}	Left engine speed	rad/sec
Ω_{ER}	Right engine speed	rad/sec
Ω_{INT}	Interconnect shaft speed	rad/sec
Ω_L	Left rotor speed w.r.t. aircraft	rad/sec
Ω_{LPT}	Left power turbine speed, same as Ω_{EL}	rad/sec
Ω_R	Right rotor speed w.r.t. aircraft	rad/sec
Ω_{RPT}	Right power turbine speed, same as Ω_{ER}	rad/sec
ϕ_m	Lateral mast tilt	deg
V_n	Distance from CG to gear	In
τ_e	Elevator effectiveness, $\partial\alpha_H/\partial\delta_e$	ND
τ_r	Rudder effectiveness, $\partial\alpha_V/\partial\delta_r$	ND

I. SUMMARY

This report describes a mathematical model for real-time flight simulation of the Bell Model 301 Tilt Rotor Research Aircraft[1]. The mathematical model was developed under Contract NAS 2-6599 for mechanization of the NASA Ames Flight Simulator for Advanced Aircraft (FSAA)[2]. The objective of this program was to obtain a validated mathematical model of the tilt rotor research aircraft to support the aircraft design, pilot training, and proof-of-concept flight testing.

The development of the mathematical model involved the following specific tasks:

(1) Derivation of equations representing the kinematic, dynamic, and aerodynamic characteristics of the Model 301's rotor, airframe, flight control system and subsystem. The mathematical model is described in Section II and the equations are presented in Appendix A. Model 301 parameters required as inputs to the equations are given in Appendix B.

(2) Checkout and validation of the mathematical model. A non-realtime digital computer program was developed at Bell for this purpose. Comparison of performance and stability and control characteristics predicted using the subject mathematical model with experimental data and with predictions using other computer programs is presented in Section III.

(3) Support of the Tilt Rotor Research Aircraft Project simulation effort at NASA Ames. This involved providing technical assistance during checkout and validation of the FSAA/Sigma 8 mechanization of the mathematical model, Program BELTR (Program BELTR was developed by Computer Science Corporation under a separate contract and was used for the real time simulation) and evaluation of the simulation by Bell Helicopter Company experimental test pilots. The results of the evaluation are given in Section IV and recommendations for further development of the mathematical model and the simulation are given in Section V.

The structure of the mathematical model is indicated by the block diagram shown in Figure I-1. The mathematical model differs from that for a conventional fixed-wing aircraft principally in the added requirements to represent the dynamics and aerodynamics of the rotors, the interaction of the rotor wake with the airframe, and the rotor control and drive systems (Subsystems 1, 2, 8(a) and 19 in Figure I-1). The portion of the block diagram enclosed by a dashed line is common to all simulation mathematical models; in the BELTR Program the equations given in this report were replaced by CSC program BASIC[3] which contains essentially identical equations and is used for all FSAA simulations. The landing gear oleo forces were also generated using the BASIC program.

The rigorousness of the mathematical model of the tilt-rotor research aircraft was constrained by two factors. One was the requirement to keep the fast loop computational time (this was a two loop simulation) to less than 50 milliseconds in order to maintain real time simulation. To achieve this it was necessary to limit the rotor representation to steady, linearized, aerodynamics with uniform inflow and to approximate the rotor following time. Rotor stall and compressibility effects are only used to define a limit for the maximum rotor thrust coefficient as a function of advance ratio. This rotor math model is satisfactory for most handling qualities studies, but may be inadequate to evaluate flight conditions or maneuvers where stall, compressibility or rotor dynamics are significant.

The second factor constraining the rigorousness of the mathematical model was the lack of sufficient experimental data on the rotor wake-airframe aerodynamic interactions such as the rotors' downwash (or upwash) at the horizontal tail. The model of the rotor wake-airframe interaction is presently based on a limited amount of data from the tests of a powered model of a tilt-rotor aircraft similar to the Model 301[4]. Tests of a powered model of the Model 301 to obtain detailed information on the rotor wake-airframe aerodynamic interaction have been completed and will be used to refine the model of this important characteristic of the tilt rotor VTOL.

FOLDOUT FRAME

BELL HELICOPTER COMPANY

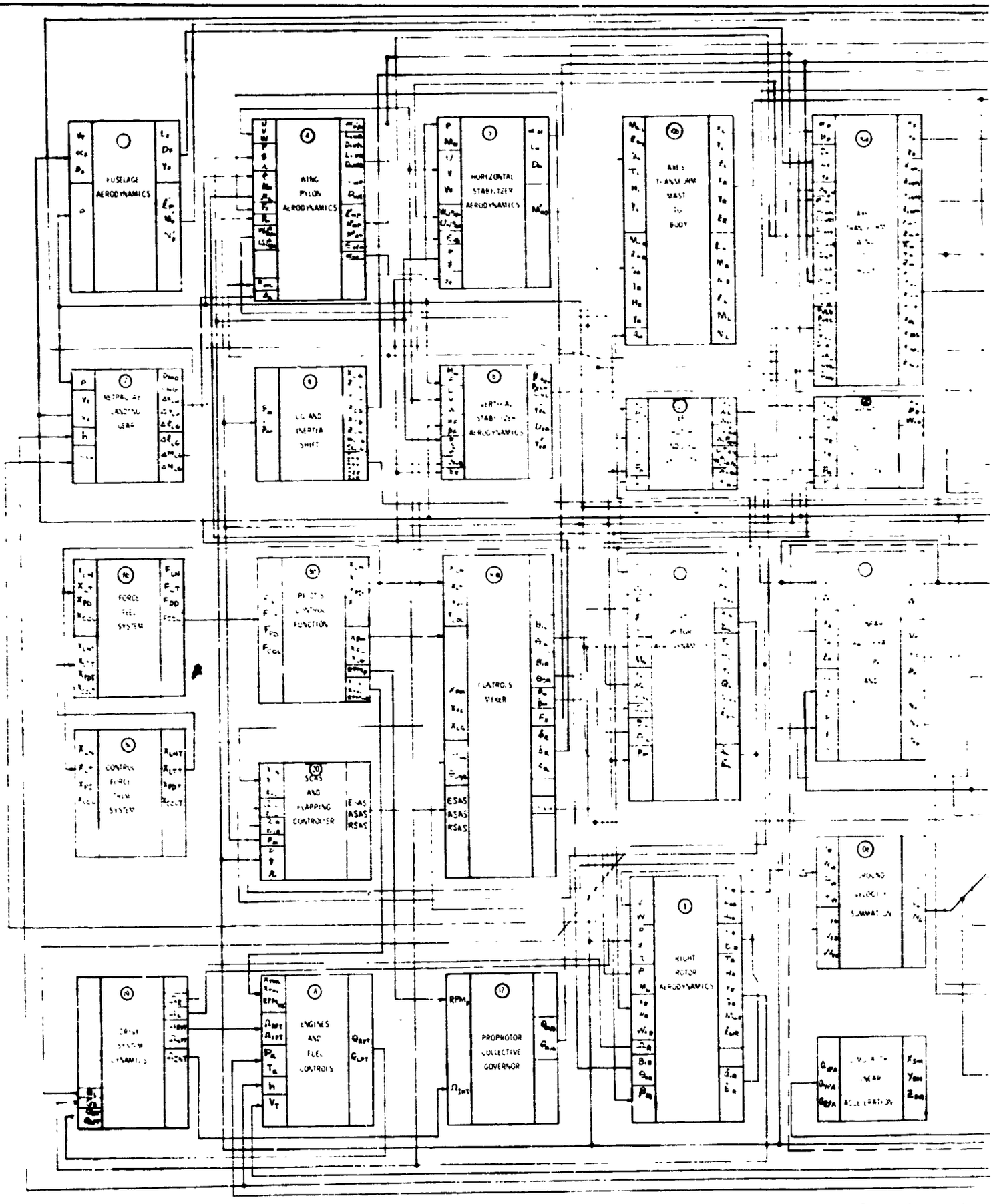

Figure I-1. Block Diagram of Mathematica

FOLDOUT FRAME 2

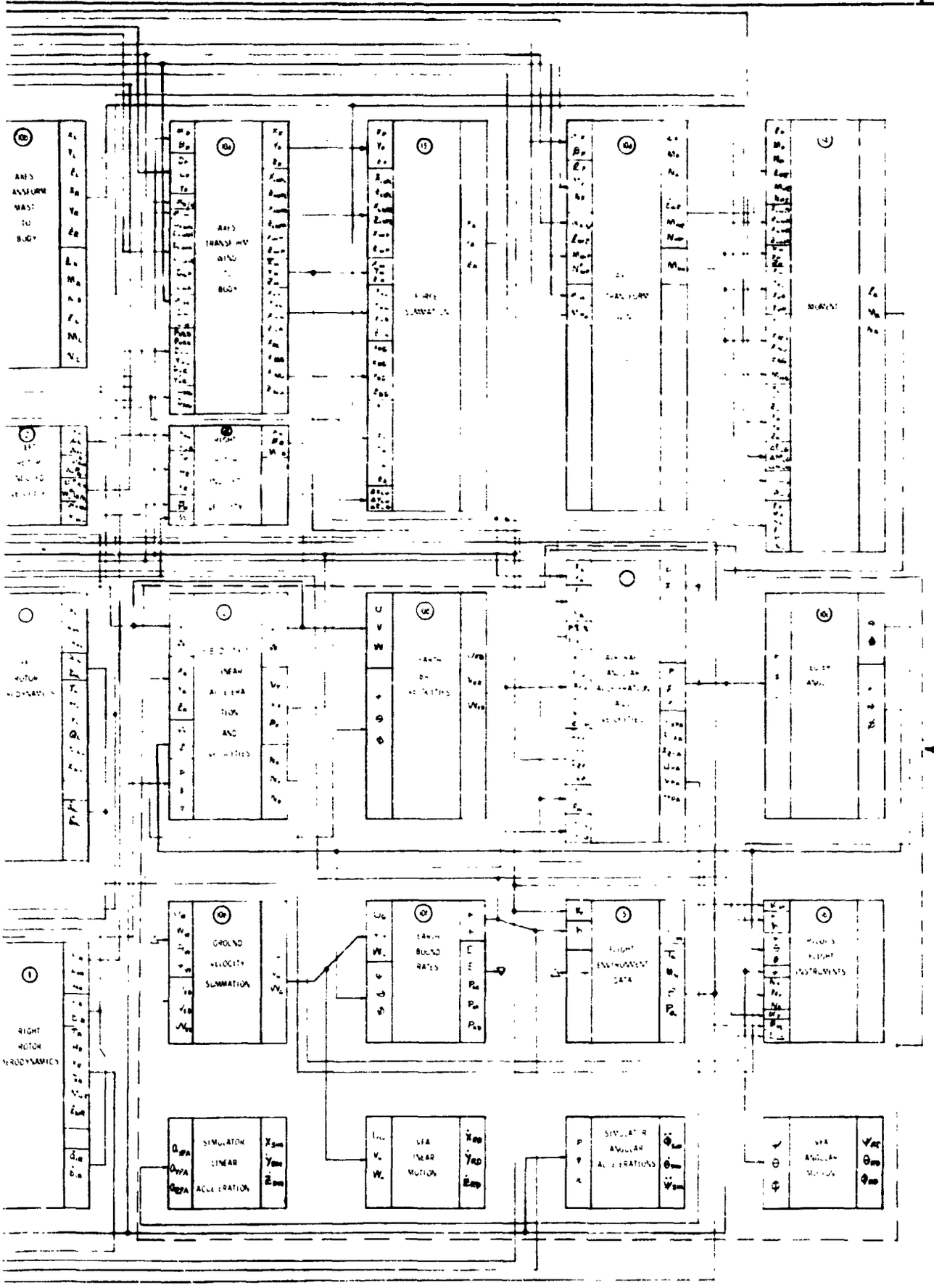

1. Block Diagram of Mathematical Model

II. DESCRIPTION OF THE MATHEMATICAL MODEL

This section describes the mathematical models of the components of the tilt rotor aircraft; the rotors, the airframe, the control system, the engines and drive system, and the automatic flight control systems (Subsystems 1, 2, 3, 4, 5, 6, 7, 8, 9, 17, 18, 19 and 20 in Figure I-1). The math model used for the equations of motion (Subsystems 10 through 16) follows that of Reference 5. The coordinate systems, sign conventions and equations of motion are also described.

A. Coordinate Systems and Sign Conventions

Earth, body, wind and mast axes systems are used in the mathematical model. The rotor flapping, forces and moments are calculated in a "wind-mast" axis system while the airframe aerodynamic forces and moments are calculated in a wind axis system. Forces and moments from the rotor and airframe are resolved into the body axis system for solution of the aircraft equations of motion. The flight path of the aircraft is described with reference to earth fixed axes with the aircraft orientation given by the Euler angles, Ψ, θ, and ϕ, in that order of rotation.

The mast axis system and sign convention used for the rotor are shown in Figure II-1. The rotor flapping, forces and moments are calculated in the "wind-mast" axis system ($\bar{a}_1$, $\bar{b}_1$, $\bar{T}$, $\bar{H}$, and $\bar{Y}$) and are then transformed into the mast axis system (a_1, b_1 T_1 H and Y).

B. Rotor Math Model (Subsystem 1)

1. Rotor Forces and Moments

The mathematical model of the rotor is similar to that given in References 6 and 7 except that it is derived in a mast axis system (the theory in Reference 6 is based on an axis system perpendicular to the axis of no flapping i.e. the tip-path-plane, and that of Reference 7 is based on the axis of no feathering) and contains provisions for proprotor characteristics such as non-linear twist, flapping restraint and pitch-flap coupling.

The major assumptions that are made in the rotor math model are:

(1) Average values for the lift curve slope and profile drag coefficient are used over the span of the blade. These are adjusted to approximate the rotor thrust and power required characteristics.

(2) The blade angle of attack α_r is approximated by $\sin\alpha_r$. Substitution of $\sin\alpha_r$ for α_r in the blade element equations makes it possible to develop equations for rotor forces without restricting blade pitch, θ, and inflow angle, ϕ, to small angles.

(3) Blade stall and compressibility effects are approximated by limiting the maximum rotor thrust coefficient as a function of advance ratio and by arbitrarily modifying coefficients in the rotor power required equation (rotor profile drag is increased as a function of the cubes of the rotor inflow and advance ratios multiplied by empirically adjusted coefficients).

(4) Blade flapping with respect to the mast is assumed small so that the small angle assumption can be made. And harmonics of flapping greater than one-per-rev are ignored.

(5) The blade flapping due to cyclic inputs is assumed to occur instantaneously, i.e. the flapping equations assume the rotor is in an equilibrium condition. This assumption was made because of limits imposed by the computer computation time. Differential equations for blade flapping that would properly account for the rotor following time were determined to require a solution time in excess of that allowable for real time simulation. Furthermore there is a transport lag between the time a control input is made at the cab and the time aircraft response is updated at the cab, of from one to two frame times (0.050 to 0.10 seconds). By neglecting the rotor following time in the equation of motion, it is approximated by the cab-control input to computer time lag (for example, in hover the rotor following time is 0.08 seconds compared to an average computation lag time of 0.075 seconds).

2. Rotor Induced Velocity

The rotor induced velocity is computed by calculating the induced velocity of an isolated, out of ground effect rotor and modifying the induced velocity to account for the side-by-side rotor effect and for operation in ground effect.

The mean value of the isolated, out-of-ground effect rotor induced velocity is approximated using a modified expression from Reference 8.

$$v_i = \frac{(\Omega R)C}{\sqrt{0.866\lambda^2 + \mu^2} + \dfrac{0.6|C_T|^{1.5}\left(|C_T| - 8/3\lambda|\lambda|\right)}{\left(|C| + 8\mu^2\right)\left(|C| + 8\lambda^2\right)}}$$

where $C = C_T/2B^2$

(the 0.866 factor on λ^2 has been added to improve power correlation in hover)

The side-by-side rotor effect on the rotor induced velocity is approximated using an expression derived in Reference 9.

$$\Delta v_i = x_{SS} \frac{(\Omega R) C_T}{2B^2 \mu}$$

The factor x_{SS} is called the mutual induction coefficient and is obtained from Figure 3.7 of Reference 9. The term Δv_i is added to the induced velocity for the isolated rotor.

In the determination of x_{SS}, the increased mass flow of the side-by-side configuration is taken into account and the rotor wakes are assumed to remain separate if the distance between the rotor centers is greater than the rotor diameter. The value of x_{SS} depends on the direction of rotation, the distance between the rotors, the advance ratio and the rotor angle of attack. The value of x_{SS} given in Reference 9 is valid for μ greater than 0.15. In this analysis the value of x_{SS} for μ less than 0.15 has been approximated by providing a smooth transition between a value of x_{SS} equal to zero at $\mu = .06$ and the value at $\mu = 0.15$.

The reduction in induced velocity caused by ground proximity is computed using the expression

$$v_{i_{IGE}} = v_{i_{OGE}} \left[1 + (G-1) \left(\frac{\sqrt{U^2 + V^2}}{30} - 1 \right) \right]$$

where $G = 0.76 + 0.24\ h/D$ for $h \leq D$

and $G = 1.0$ if $h > D$

The constants 0.76 and 0.24 in the expression for G were derived from model test data. The factor $\sqrt{U^2 + V^2}/30$ washes out the effect of ground proximity with forward speed; at 30 feet per second and greater the effect is completely washed out.

The major assumption made with regard to induced velocity is that it is uniform over the rotor disc. The main effect of this assumption is that lateral flapping is underpredicted in the low speed helicopter regime ($\mu = 0.05$ to 0.2). However, lateral flapping has only a second order effect on stability and control characteristics in the helicopter mode so this is not a serious limitation. Presently the tandem rotor effect is neglected when in sideward flight. This effect was not included in the initial development of the mathematical model since other factors significant to sideward flight simulation are only approximated.

C. Airframe Aerodynamics (Subsystem Nos. 3, 4, 5 and 6)

The fuselage, wing-pylon assembly, horizontal tail and vertical fins are modeled separately to facilitate accounting for the influence of the rotor

wake on the airframe aerodynamics. In general the airframe aerodynamics are extracted from wind tunnel test data; where wind tunnel data was not available characteristics were estimated using References 10, 11, and 12.

1. Fuselage (Subsystem No. 3)

Equations for the fuselage lift, drag, side force, pitching moment, yawing moment and rolling moment are referenced to the wind axis system and defined at the fuselage aerodynamics center. The coefficients in the equations for angles of attack and sideslip less than or equal to 20 degrees are based on wind tunnel data. For angles of attack greater than 20 degrees the coefficients have been approximated.

Aircraft angular rates and the rotors wakes are neglected in calculating the fuselage aerodynamic forces and moments.

2. Wing-Pylon Assembly (Subsystem No. 4)

The wing-pylon aerodynamic forces and moments are defined in the local wind axis system. Wing-body interference effects are included in the aerodynamic data.

Calculation of the wing aerodynamic forces and moments is made in two parts; (1) lift and drag generated by the rotors wakes, and (2) the forces and moments generated by the free stream flow. The math model of item (1) is discussed in Section II.3. Item (2) is discussed in the paragraph below.

The wing-pylon lift and drag generated by the freestream flow are functions of angle of attack, conversion angle, flap setting and Mach number. The pitching moment is a function of flap setting. Wing-pylon lift and drag coefficients are provided for mast angles of 0 degrees and 90 degrees, and for four flap settings as shown in Figures II-3 and II-4. Coefficients for intermediate mast angles and flap settings are obtained by interpolation. Mach number corrections are made only for the flaps-up airplane mode condition as shown in Figures II-5 and II-6. The aerodynamic coefficients for angles of attack up to stall are based on wind tunnel data; at angles of attack above stall the coefficients shown in Figures II-7 and II-8 are approximated based on the test data shown in Reference 11.

The angle of attack of the wing is modified to reflect the induction effect of the thrusting rotors. The expression for the wing angle of attack is,

$$\alpha_W = \alpha_F - 0.26\, x_{R/W} * \frac{2C_{RF}}{MAX^2(\mu,\ 0.15)} * 57.3$$

Where $x_{R/W}$, the induction coefficient is a function of the distance between the rotor and the wing, and C_{RF} is the non dimensionalized rotor force coefficient.

The lateral-directional aerodynamic forces and moments are calculated using equations for stability derivatives from Reference 10. Compressibility effects and the wing loading are included in the lateral-directional characteristics. The dihedral effect of the wing-pylon is based on wind tunnel test data and is a function of angle of attack and flap setting. The aileron effectiveness is also based on wind tunnel data and is a function of angle of attack, mast angle and flaperon deflection.

3. Horizontal Tail (Subsystem No. 5)

The dynamic pressure and angle of attack at the horizontal stabilizer as shown in Figure II-9(a) takes into account wing-body blockage, mast angle, the wing-pylon wake, the rotor wake and the aircraft attitude and angular velocity. The lift and drag coefficients shown in Figures II-10 and II-11 of the stabilizer are determined from wind-tunnel test data for angles of attack up to stall. Above stall the coefficients are approximated using data from Reference 11.

The downwash at the horizontal stabilizer due to the wing-pylon shown in Figure II-12 is determined from wind tunnel data for angles of attack up to stall. Above wing stall the downwash is approximated using data for a high wing-low tail configuration given in Reference 12.

The downwash at the horizontal stabilizer due to the rotor wake is discussed in Section II.3.

4. Vertical Fins (Subsystem No. 6)

The forces and moments on the left and right fins are computed separately to account for the variation in rotor wake effects with sideslip. The dynamic pressure and angle of attack at the fins as shown in Figure II-9(b) take into account the wing-body blockage, mast angle, wing-pylon wake, rotor wake and fuselage attitude and angular rates. The lift and drag coefficients of the fins shown in Figures II-13 and II-14 are determined from wind tunnel data for angles of attack up to stall. Above stall the coefficients are approximated using data from Reference 11.

The sidewash at the fins is a function of flap setting, mast angle, fuselage angle of attack and sideslip angle.

D. Rotor Wake - Airframe Aerodynamic Interaction (Subsystem No. 2 and parts of 4, 5 and 6)

The rotor wake-airframe aerodynamic interference representation consists of three parts:

(1) The effect of the rotor wakes on the wing lift and drag.

(2) The effect of the rotor wakes on the horizontal stabilizer and vertical fins lift and drag.

(3) The net rolling moment induced by the rotor wake-airframe-ground interaction when hovering near the ground.

1. Rotor Wake Effect on the Wing

As noted in Section II.C.2.2 the calculation of the wing aerodynamic forces and moments due to rotor wake effects is made separately from the forces and moments generated by the freestream flow. The calculation of the rotor wake effect involves calculating the area and angle of attack and dynamic pressure of the portion of the wing immersed in the wake; Figure II-15 illustrates the representation of this effect.

The area of the wing immersed in the rotor wake, S_{iW} (shown in Figure II-15) is computed as a function of wake radius, conversion angle, wake angle of attack and sideslip angle of the fuselage. The expression used to compute wake radius of a hovering rotor as a function of vertical distance from the rotor disc is derived in Reference 13. Experimental data also shows that the contracted wake remains stable as it reaches the wing and horizontal stabilizer surfaces. The equation for the wake radius (Equation 3 of Reference 13) has been simplified since the wing and stabilizer surfaces are located at approximately .4R below the rotor disc.

$$R_W = \{0.78 + 0.22 \text{ Exp } [-(0.3 + 2 Z\sqrt{C_{RF}} + 60 C_{RF})]\} * R$$

The rotor induced velocity at the wing varies with speed and mast tilt and is given by the following expression:

$$W_i\Big|_{R/W} = (K_0 + K_1 \mu + K_2 \mu^2 + K_3\lambda + K_4\lambda^2) W_{iL}$$

where the constants K_i are determined from powered rotor test data. Wing loads at high negative incidences caused by the rotor wake at low speeds are determined using lift and drag coefficient data tables that are defined up to angles of attack of ±90 degrees.

Asymmetric flight at low speeds, which causes unequal portion of the left and right wing to be affected by the left and right rotor wakes and generates roll and yaw moments, is taken into account.

2. Rotor Wake Effect at Horizontal Stabilizer and Vertical Fins

The rotor induced velocity at the horizontal stabilizer and vertical fins is based on data from wind tunnel tests of a powered model. The velocity induced at the tail by the rotors was derived by analysis of aircraft pitching moment data with the tail on and off, and with and without the rotors. Figure II-16 shows the induced velocity at the tail (normal to the horizontal stabilizer chordline) as a function of airspeed and mast angle.

The following expression is used to approximate the velocity variation shown in Figure II-16.

$$W_i\Big|_{R/H} = \left[h_0 + h_1\beta_M + (h_2 + h_3\beta_M)\left(\frac{(U-168.89 + h_4\beta_M)^2}{168.89}\right)\right]^* W_{iL}$$

The coefficients h_0 through h_4 were determined by curve fit of the test data. W_{iL} is the induced velocity at the left rotor.

The induced velocity at the empennage is presently based on the value for trimmed level flight, and is invarient with angle of attack and sideslip. Data from tests of a powered aeroelastic model indicates a significant variation in induced velocity with angle of attack and/or sideslip. This new data will be used to refine the present representation of the rotor wake effect on the empennage.

3. Rolling Moment Induced by Rotor Wake-Airframe Ground Interaction

When hovering in ground effect ($h/D < 1.5$) an unstable roll moment is generated by aerodynamic interaction between the rotor wake, the wing and the ground. Figure II-17 shows the rolling moment as a function of h/D measured with 1/5th scale powered model of the Model 301. This effect is represented in the math model by a polynomial equation for the rolling moment, curve fitted to the test data, and applied at the aircraft center of gravity.

E. Flight Controls (Subsystem No. 8)

The flight controls representation consists of a controls mixing model, and a force gradient model.

The Model 301 flight control system is illustrated schematically in Figure II-18. The math model of the system represents the mixing of the pilot and automatic flight control inputs, wash out of the rotor controls as a function of mast angle and airspeed and conversion, landing gear, and flap controls. Wash out schedules are illustrated in Figure II-19 and are given in tabular form in the math model. The math model does not include friction or free play. The time constants of the control actuators are assumed zero, since in practice they are less than the computer frame time.

The pedal and cyclic stick longitudinal and lateral gradients are specified as a function of airspeed. The location of the gradient detent (zero force position) may be moved by the pilot to trim out steady stick forces.

F. Drive System and Engines (Subsystems 18 and 19)

The drive system is represented by the zero frequency symmetric mode, e.g. the rotors speed up or slow down in response to the unbalance between

aerodynamic torque and engine torque. The frequencies of the flexible modes of the drive system (3.67 cps and 11.8 cps for the first antisymmetric and second symmetric modes respectively) are too high to significantly influence the simulation.

The engine and power turbine (N_{II}) governor models are composed of equations to calculate engine horsepower during transient and steady state operation. The equations are based on the operating characteristics of the combined engine-fuel control system. This approach was taken rather than one involving time constants, inertias and derivation of engine components to minimize the computational requirements.

The engine equations are derived in terms of the optimum power turbine speed and the horsepower developed at that speed. For a given throttle setting (or fuel flow rate) the engine will develop the maximum horsepower if the turbine is operating at the optimum speed. The commanded optimum power, referred to sea level, standard, static conditions is given by

$$HP_{ROC} = \begin{cases} K_3 X_{TH}^2 + K_9 X_{TH} + K_{10} & (\text{for } T_a \le K_7) \\ \left[1-K_{11}(T_a-K_7)\right]\left[K_{12} + K_{13}(X_{TH}-K_{14})\right]\left[K_8 X_{TH}^2 + K_9 X_{TH} + K_{10}\right] & (\text{for } T_a > K_7) \end{cases}$$

where K_8 through K_{14} are constants derived to fit the engine power versus throttle (X_{TH}) setting characteristics given in the engine installation manual[14].

The referenced optimum power HP_{RO} at any time t, after a power lever change is given by the equation

$$HP_{RO} = (HP_{RO})_0 + \int_{t_o}^{t} \frac{dHP_{ROP}}{dt}\, dt$$

where HP_{RO_0} is the power before the change in the power lever position and $\frac{dHP_{ROP}}{dt}$ is the engine power acceleration schedule and is given as

$$\frac{dHP_{ROP}}{dt} = \text{sign}\,(HP_{ROC} - HP_{RO}) * \text{MIN}\left\{1, \frac{[100]\left[1 - \frac{HP_{RO}}{HP_{ROC}}\right]}{pctmxp}\right\} f\left(HP_{RO}, h\right)$$

where f (HP_{RO}, h) is the engine power acceleration schedule, derived to correlate with measured engine acceleration characteristics.

The actual horsepower HP is then computed by correcting the referred optimum horsepower, HP_{RO}, for nonstandard conditions using the following equation

$$HP = \left[HP_{RO}\, \delta \sqrt{\theta}\right] \left[K_1 \left(\frac{\Omega_R}{\Omega_{RO}}\right)^2 + K_2 \left(\frac{\Omega_R}{\Omega_{RO}}\right) + K_3\right]$$

where K_1, K_2, and K_3 are constants used to curve fit the power to the engine characteristics given in the installation manual, Ω_R is the actual power turbine speed and Ω_{RO} is the referred optimum power turbine speed, and δ and θ are terms used to correct for nonstandard pressure and temperature, respectively.

The equations used for the power turbine governon (N_{II}) are similar to those for the engine except that the optimum power is referred to the N_{II} speed commanded by the pilot rather than the throttle setting. It should be noted that in the Model 301 the N_{II} governing speed is set at that corresponding to the rotor limit speed so that the N_{II} governor is only used to help prevent overspeeding.

G. Automatic Flight Control System (Subsystem No. 17 and 20)

The Model 301's rotor rpm governor and Stability and Control Augmentation System (SCAS) are represented in the math model.

1. Rotor RPM Governor (Subsystem No. 17)

The rotor RPM governor representation consists of a single channel model of the feedback network. In the Model 301 the rotor blade collective pitch is changed so as to maintain constant rpm; the blade pitch is proportional to the integral of the error in rpm (e.g. the difference between the actual and the pilot selected rpm) so that any steady error is completely washed out. The gain of the integral feedback is very low so the governor will not destabilize structural modes.

A position gain is used in parallel with the integral gain to provide damping to the rotor rotational mode under conditions of low inflow, such as in low power descents in helicopter mode. The position gain is phased out as the pylons are converted to airplane mode to prevent destabilizing structural modes.

Control of the RPM governor consists of a thumb operated, three position switch spring loaded-to-center, located on the power lever head. Pushing the switch forward, increases the reference rpm by 20 rpm for each second the switch is depressed; pulling aft decreases the reference rpm by 20 rpm per second. A pointer on the rotor tachometer indicates the selected rpm. This system was modeled in the FSAA cab. At present, this modeling does not include capability to evaluate failure modes.

2. SCAS (Subsystem No. 20)

The SCAS math model consists of a single channel representation of the electronic network; SCAS actuator characteristics are not modeled, however, total system authorities are used. A typical channel is shown in Figure II-20. Each channel has three functional circuits; rate feedback to augment the aircraft damping, attitude feedback for attitude retention, and pilot input feed forward to improve the apparent response to pilot control inputs. The pitch channel has, in addition, an airspeed feedback loop (this loop was implemented but not used).

The main feature of the SCAS math model is representation of the systems gains. All gains are functions of both airspeed and pylon angle. This feature was incorporated to facilitate optimizing the SCAS during the design phase.

The attitudes and airspeed hold circuits are switched off or on by the position of the pedals and cyclic stick. When the longitudinal cyclic stick is trimmed (e.g., in the force detent) the pitch channel holds are switched on; when untrimmed the pitch channel holds are switched off. When the lateral cyclic stick and the pedals are trimmed the roll and yaw attitudes holds are switched on; when either the pedal or the lateral cyclic is out of trim the roll and yaw holds are switched off.

H. Equations of Motion and Coordinate Transformations (Subsystem 9, 10, 11, 12)

The equations of motion used to solve for the six degrees of freedom flight path are identical to the ones given in Reference 5. Change in aircraft c.g. location and inertia due to pylon tilt are computed. Equations derived to compute pilot station acceleration take into account the c.g. acceleration due to pylon tilt rate and the c.g. offset location. However, the effects of mast tilt acceleration and rate on the body pitch acceleration and rate are assumed to be small and therefore neglected. The pylon degrees of freedom are neglected as the Model 301 wing-pylon natural frequencies are well above the frequency capability of the simulation software and hardware.

Transformation of forces and moments from wind to body axes and from mast to body axes is required for a number of subsystems. These transformations are given in Subsystem 10. The transformation for the rotor equations are given in Subsystem No. 1. Rotor forces and moments are computed in the wind axis and referenced to the mast. This is noted throughout this report as the "wind-mast" axis system as described in Figure II-1. The forces and moments computed in this axis system are then transformed to the mast axis system. Transformation of rotor forces and moments to the body axis system are given in Section 10b.

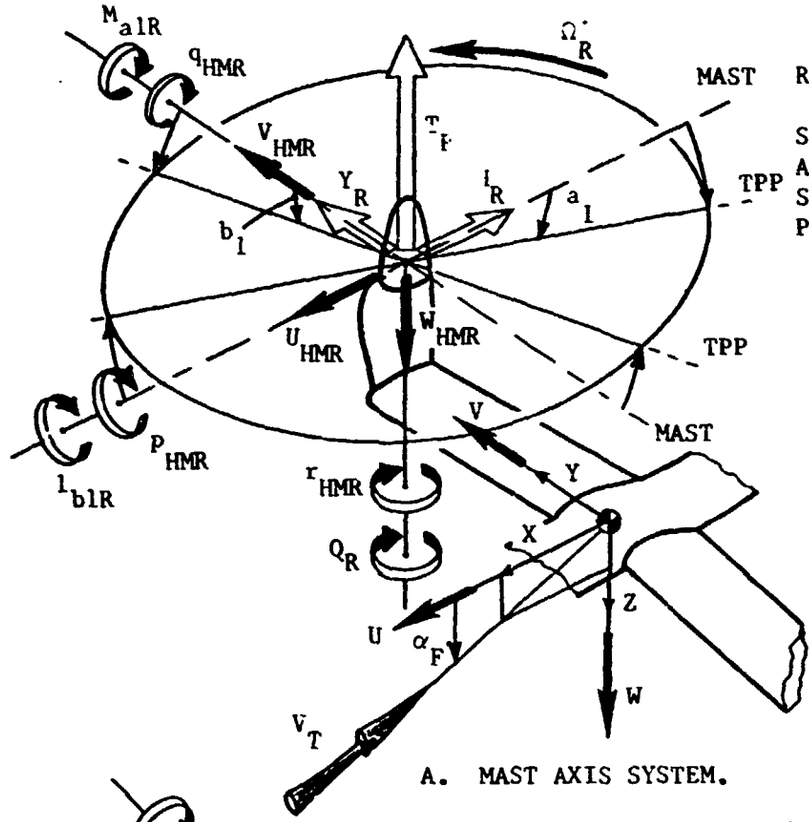

A. MAST AXIS SYSTEM.

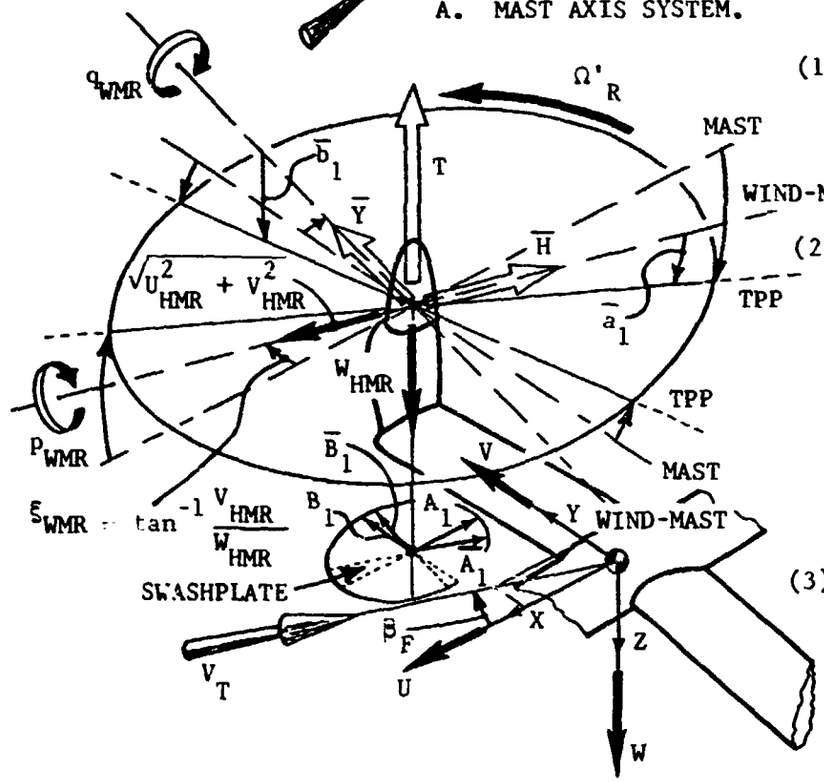

B. "WIND-MAST" AXIS SYSTEM.

RIGHT ROTOR SHOWN

SIGN CONVENTIONS ON RIGHT AND LEFT SIDE ARE COMPLETELY SYMMETRICAL ABOUT AIRCRAFT PLANE-OF-SYMMETRY

(1) U, V, W_{HMR} ARE TRANSFORMED FROM BODY (FUSELAGE) AXIS SYSTEM -

(2) FLAPPING AND PERFORMANCE CALCULATIONS ARE MADE IN WIND-MAST SYSTEM OBTAINED BY RESOLVING U_{HMR} AND V_{HMR} INTO A SINGLE WIND VECTOR AS SHOWN IN (B) BELOW

(3) T, $\bar{H}$, $\bar{Y}$, $\bar{a}_1$ AND $\bar{b}_1$ ARE CALCULATED IN WIND-MAST AXIS SYSTEM - THEN TRANSFORMED TO MAST AXIS SYSTEM TO OBTAIN T, H, Y, a_1 AND b_1.

Figure II-1. Rotor Axes Systems and Sign Conventions

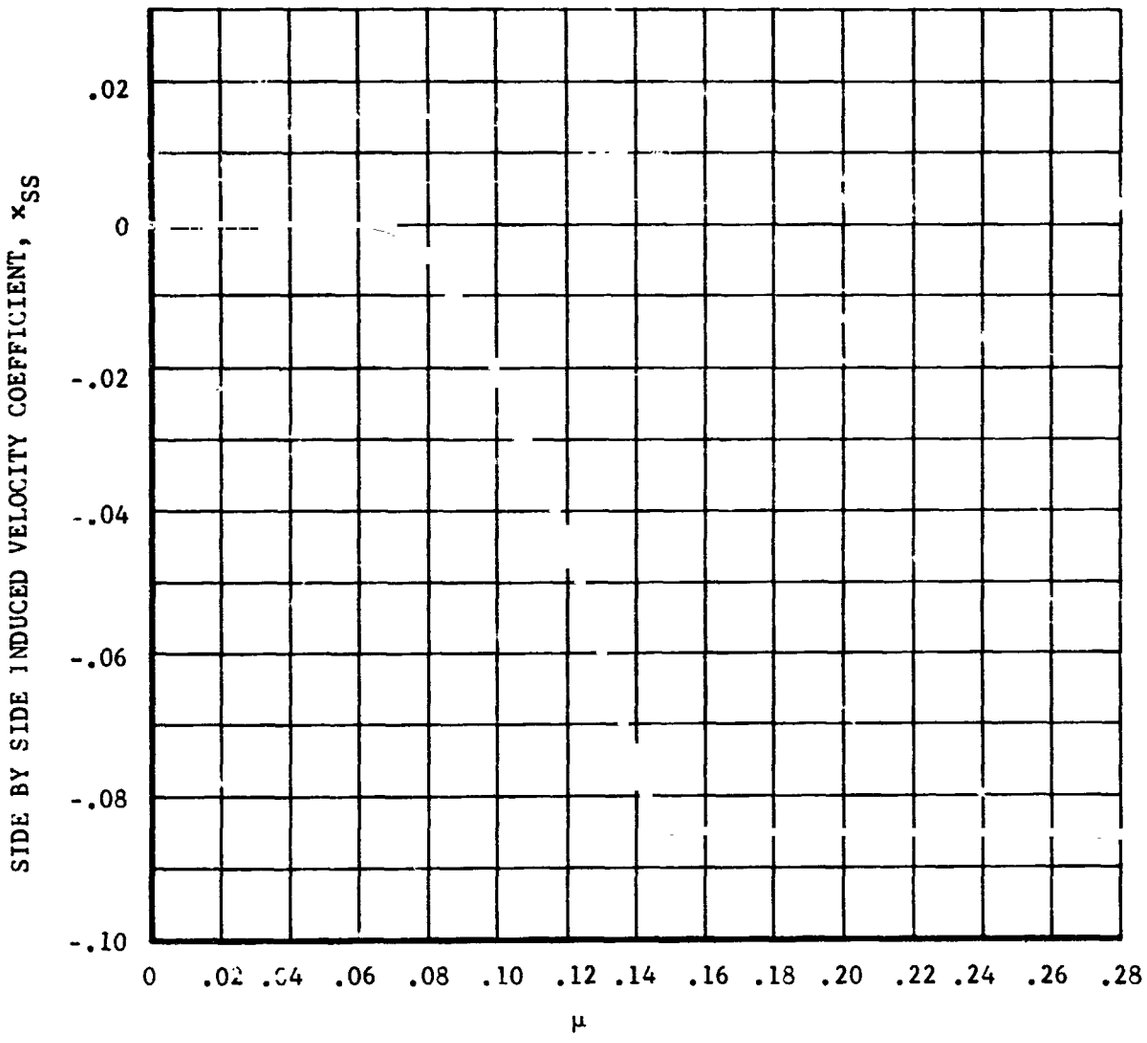

Figure II-2. Side-By-Side Rotor Effect on Induced Velocity

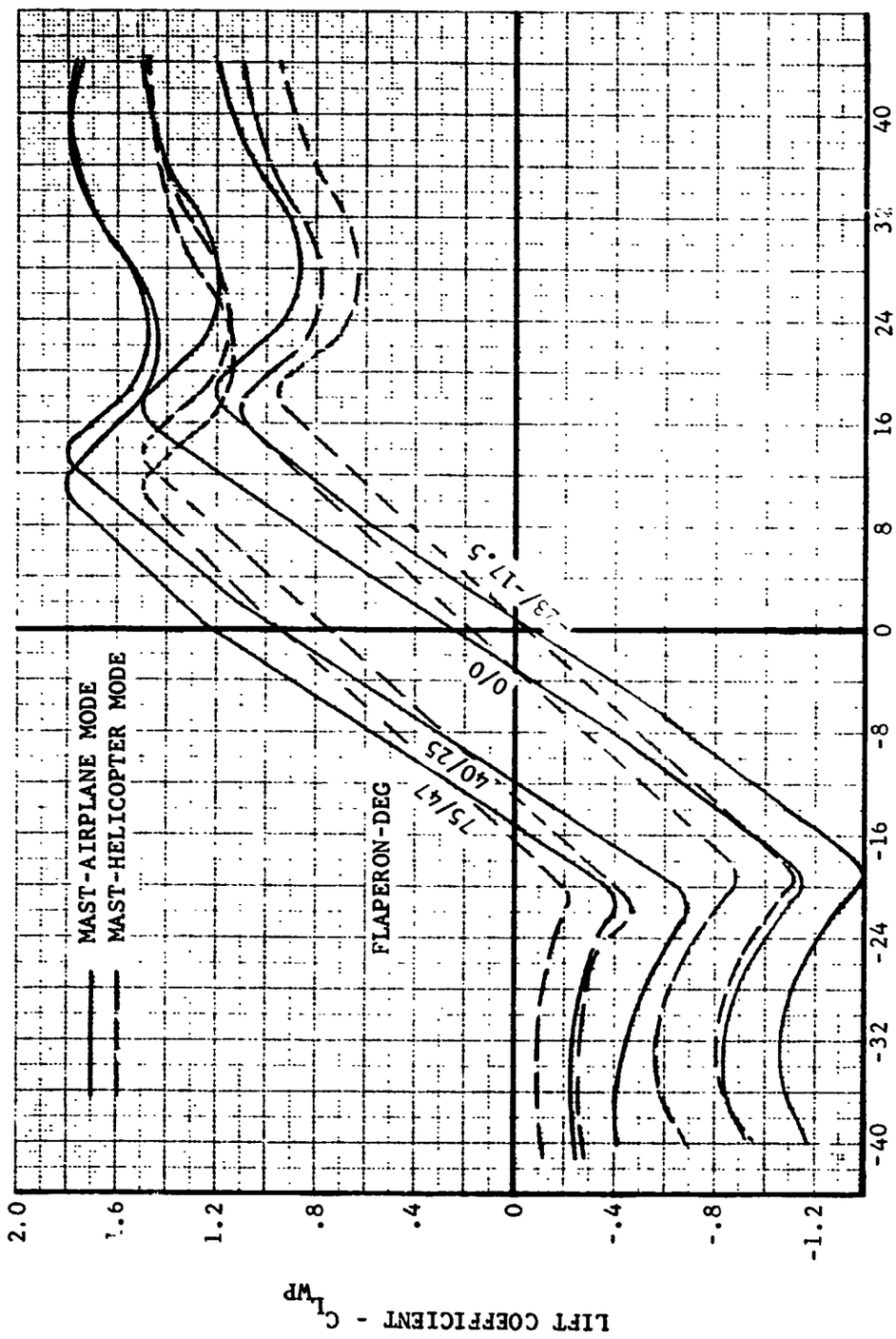

Figure II-3. Wing-Pylon Lift Coefficient Versus Angle of Attack

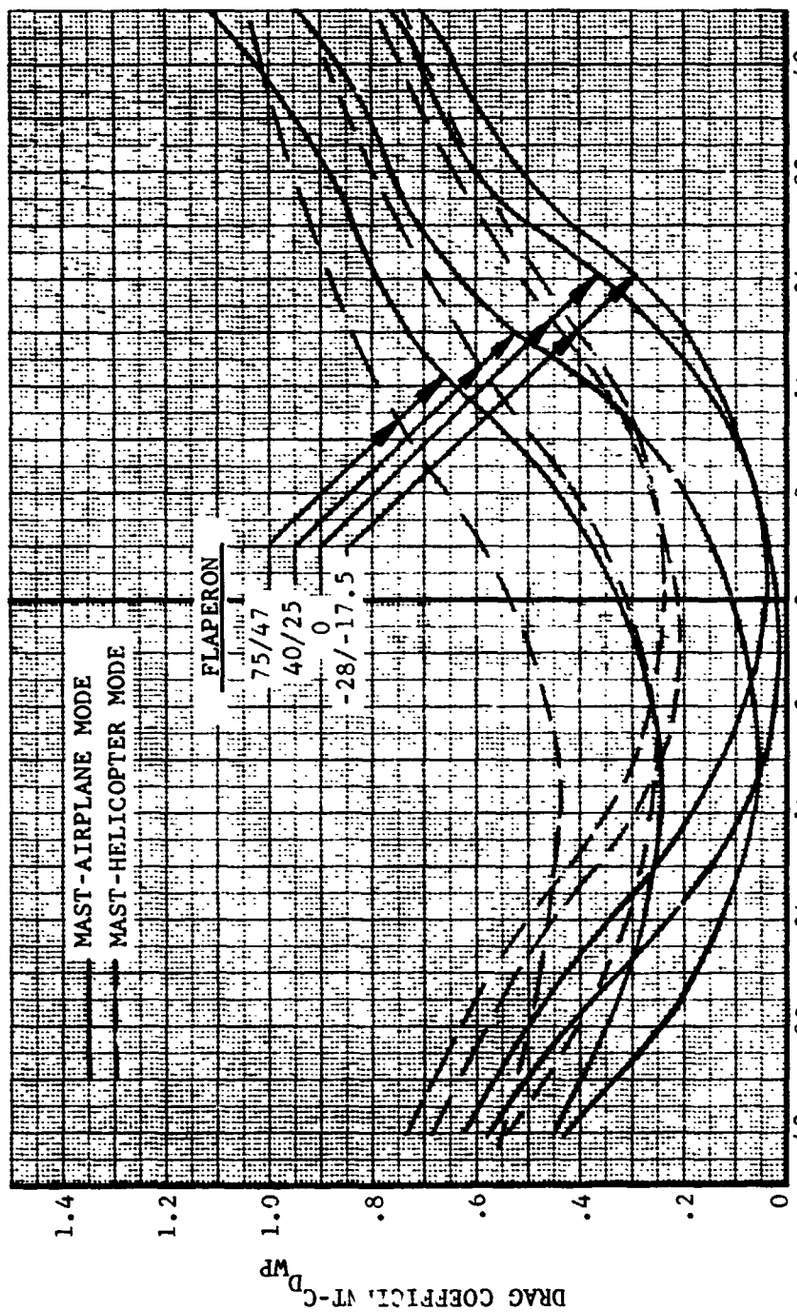

Figure II-4. Wing-Pylon Drag Coefficient Versus Angle of Attack

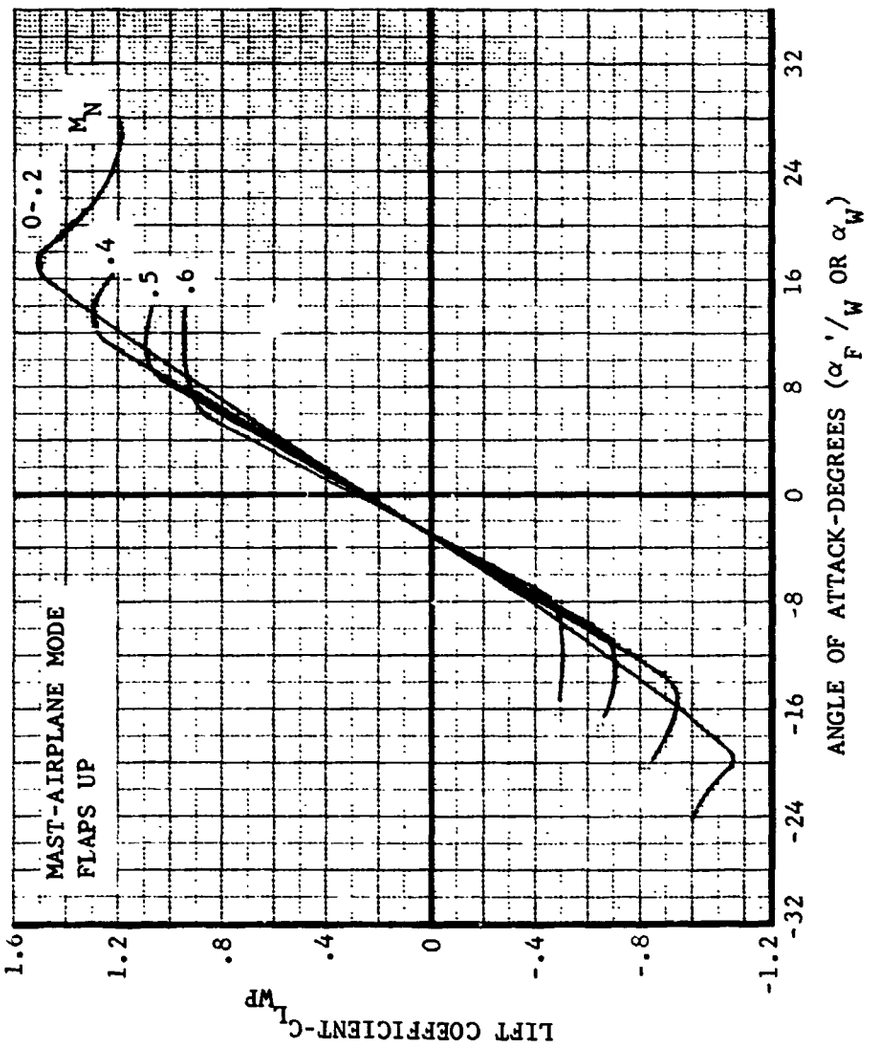

Figure II-5. Compressibility Correction to Wing-Pylon Lift Coefficient

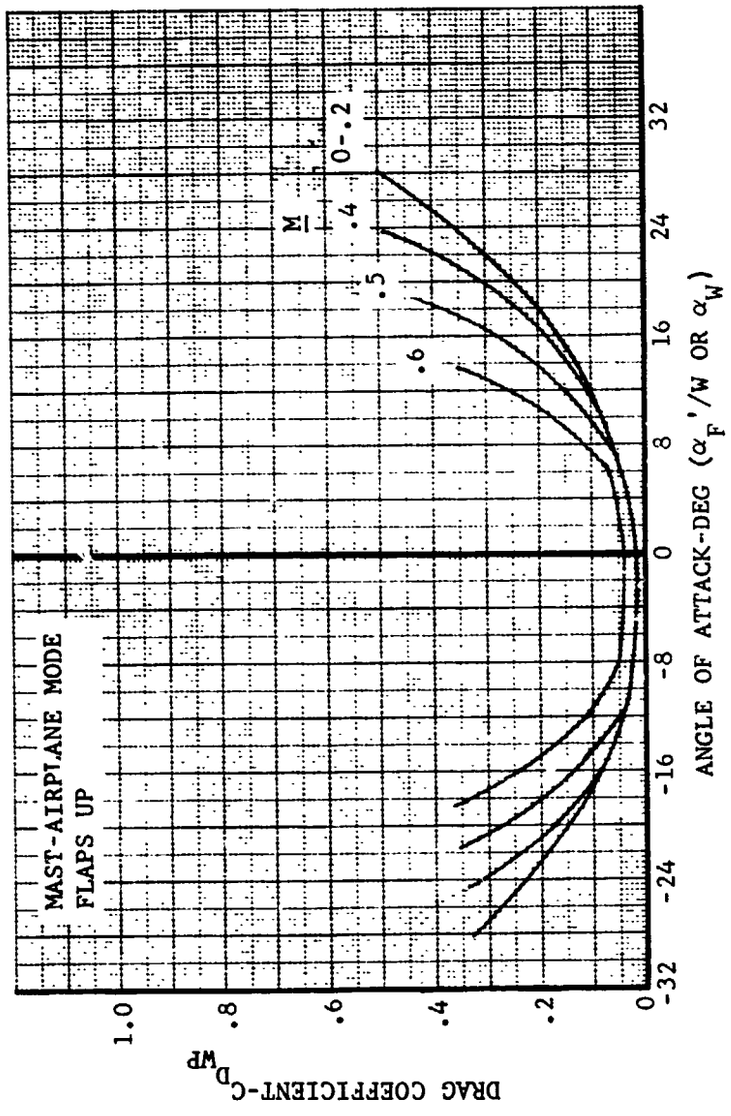

Figure II-6. Compressibility Correction to Wing-Pylon Drag Coefficient

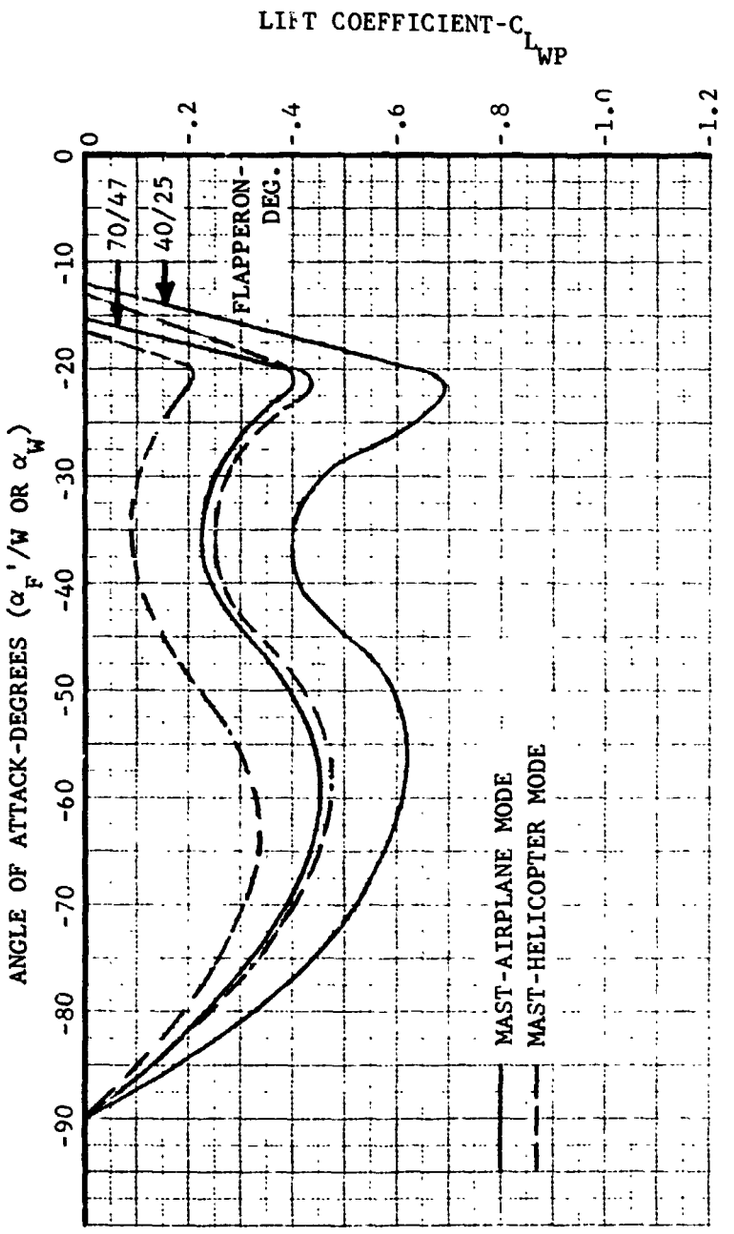

Figure II-7. Wing-Pylon Lift Coefficient at Large Negative Angles of Attack

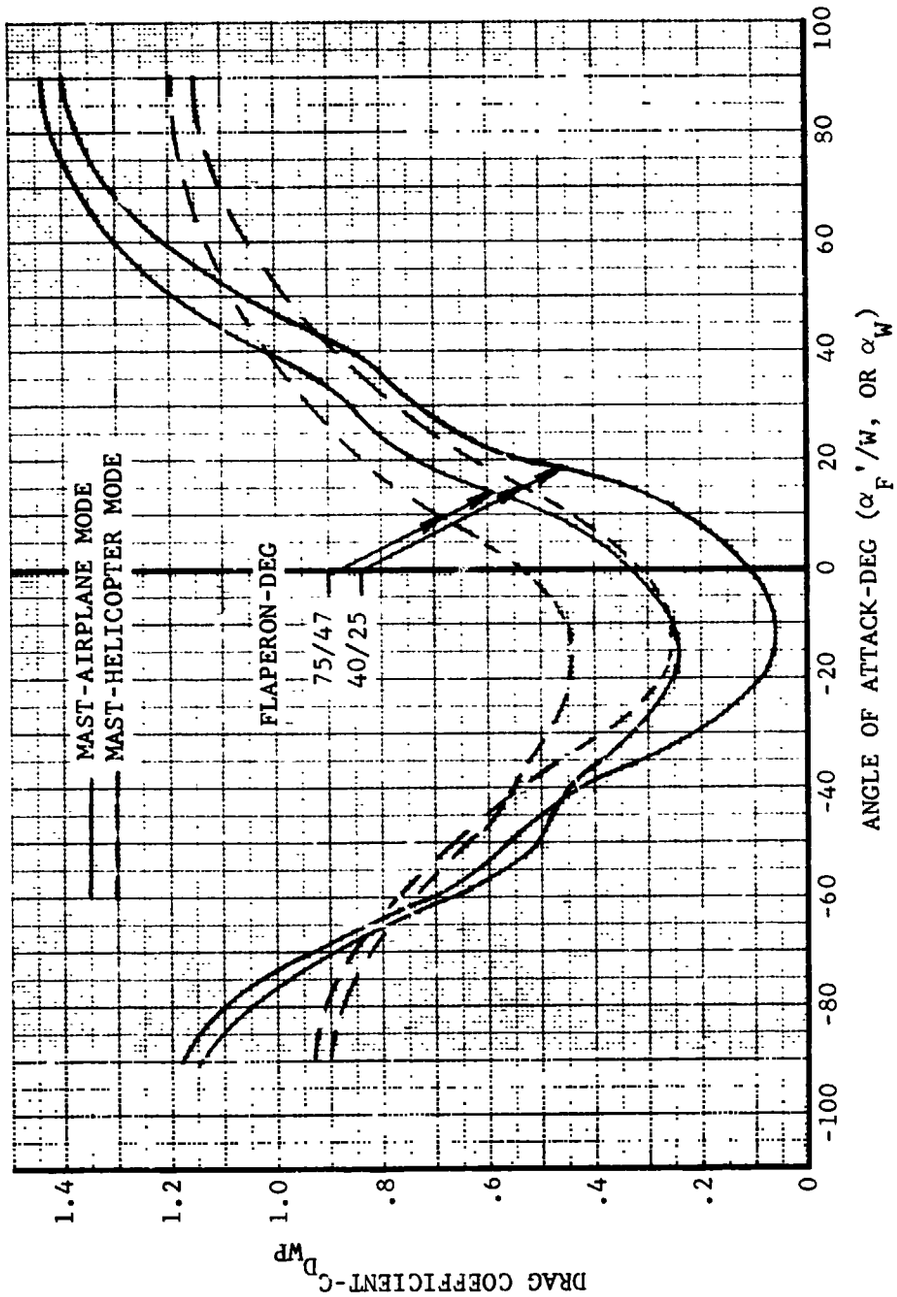

Figure II-8. Wing-Pylon Drag Coefficient at Large Negative Angles of Attack

NOTE: Angles shown are positive values in mathematical model sign convention.

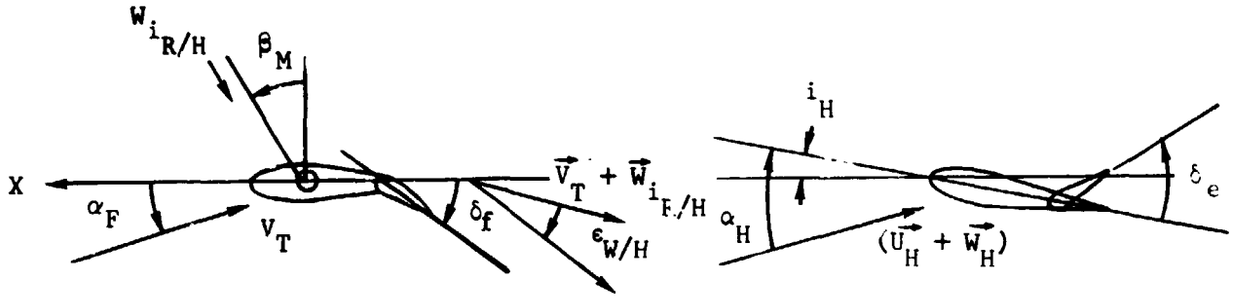

Wing Fuselage Vector Diagram

Horizontal Stabilizer Vector Diagram

a.

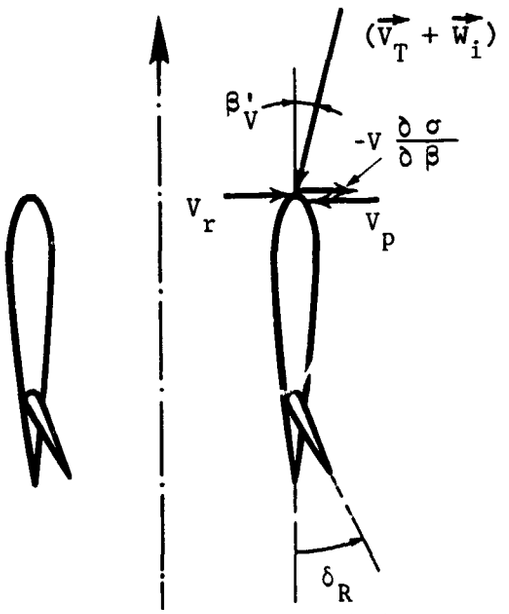

b. Vertical Stabilizer Vector Diagram

Figure II-9. Sign Conventions and Notation for Horizontal Stabilizer and Vertical Fin Aerodynamics

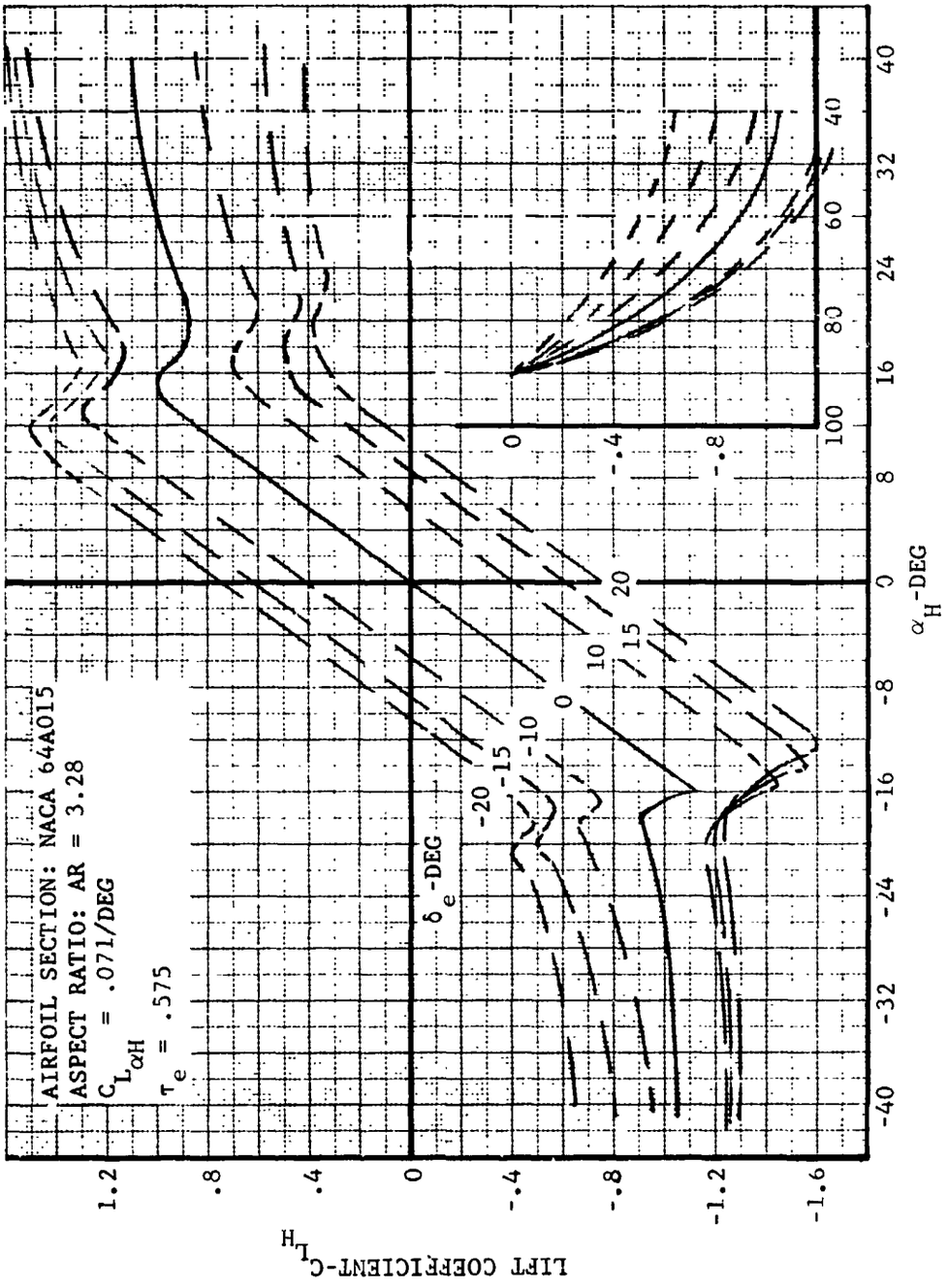

Figure II-10. Horizontal Stabilizer Lift Coefficient Versus Angle of Attack

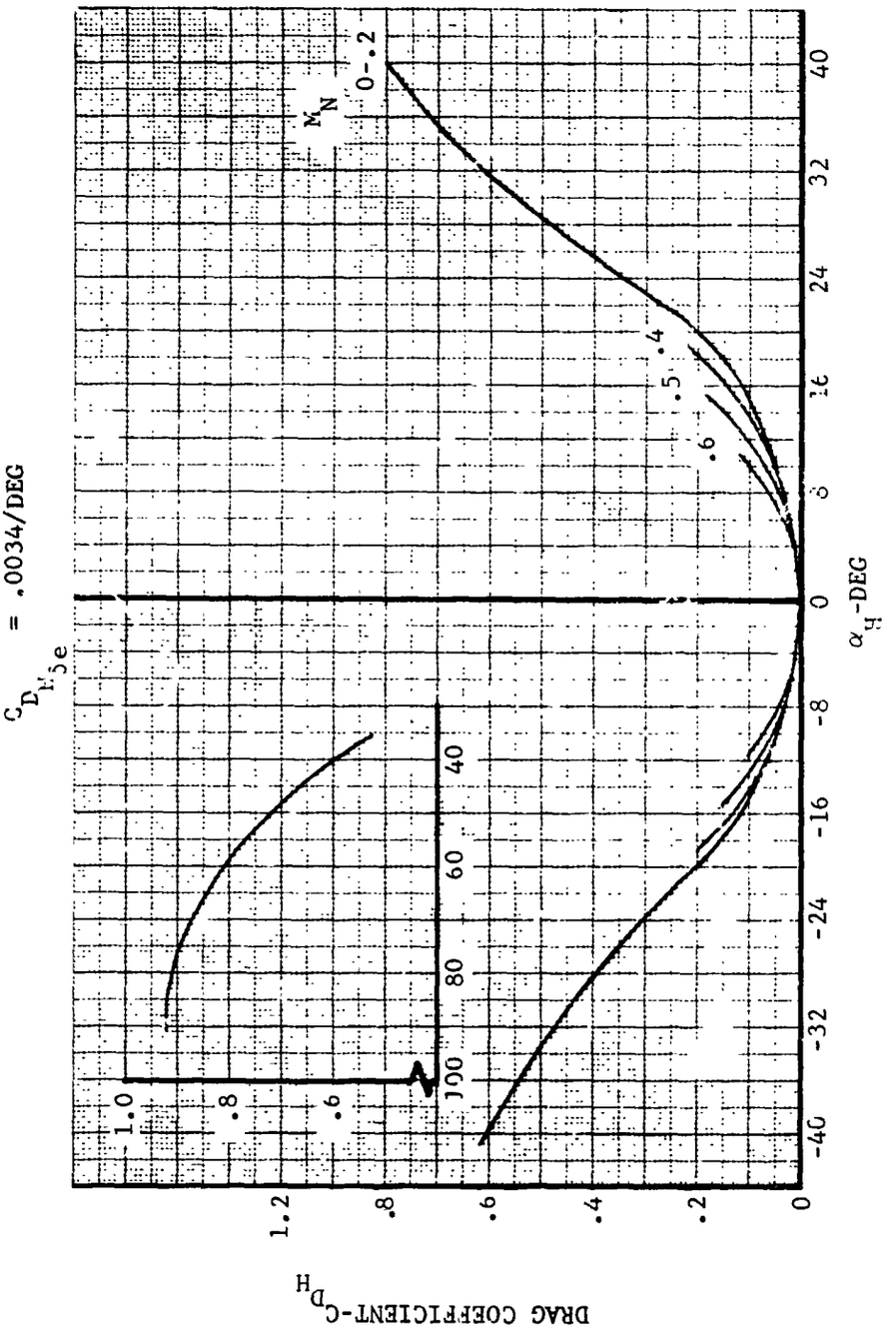

Figure II-11. Horizontal Stabilizer Drag Coefficient Versus Angle of Attack

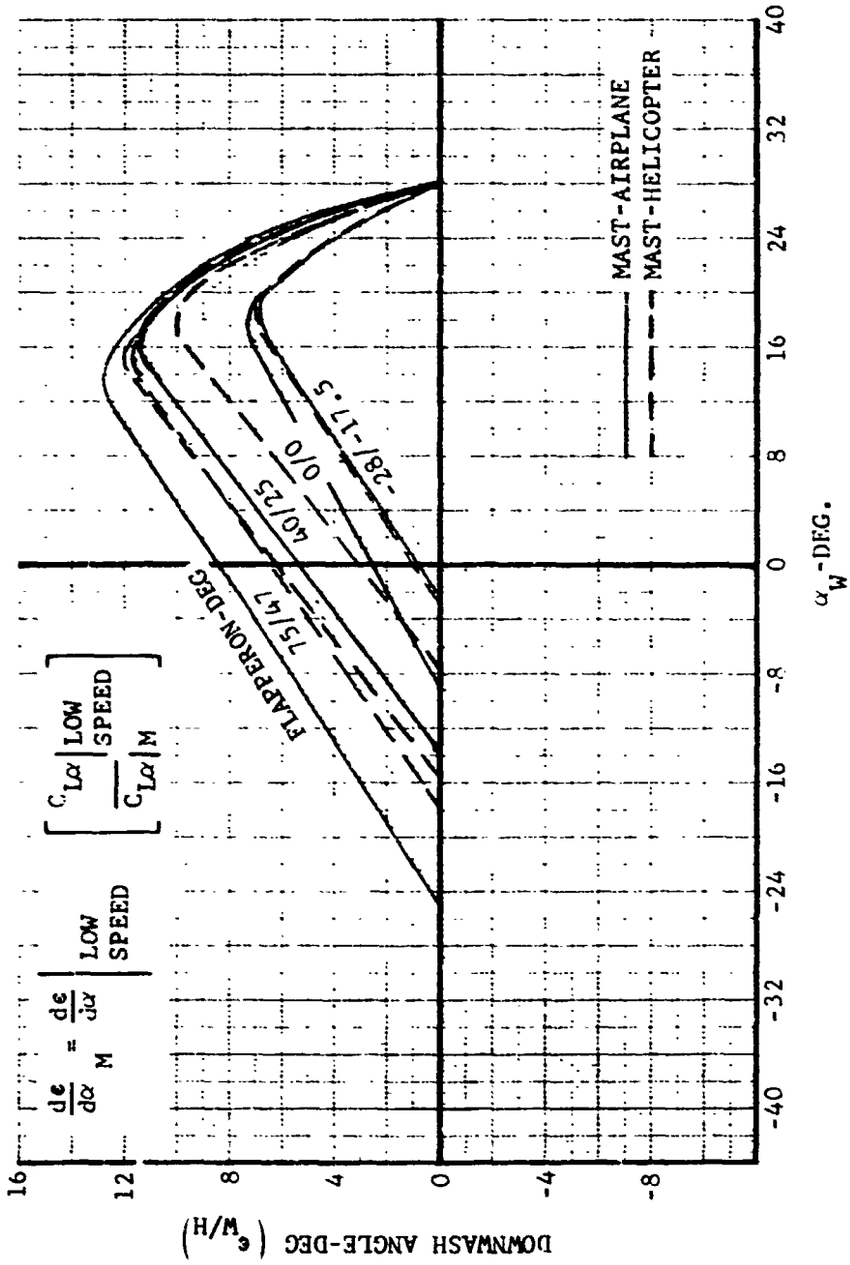

Figure II-12. Wing-Pylon Wake Deflection at Horizontal Stabilizer

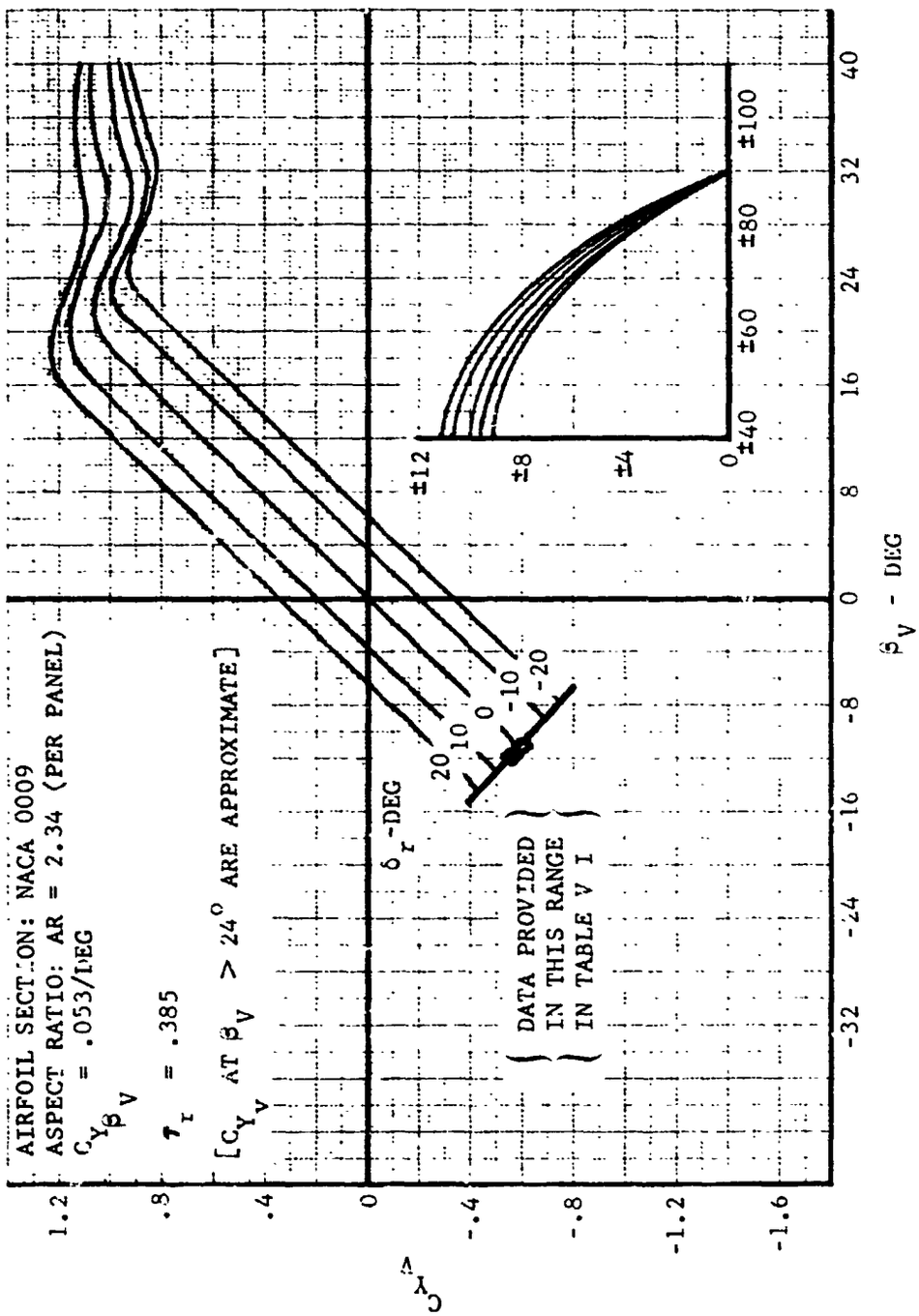

Figure II-13. Vertical Stabilizer Side Force Coefficient Versus Sideslip Angle

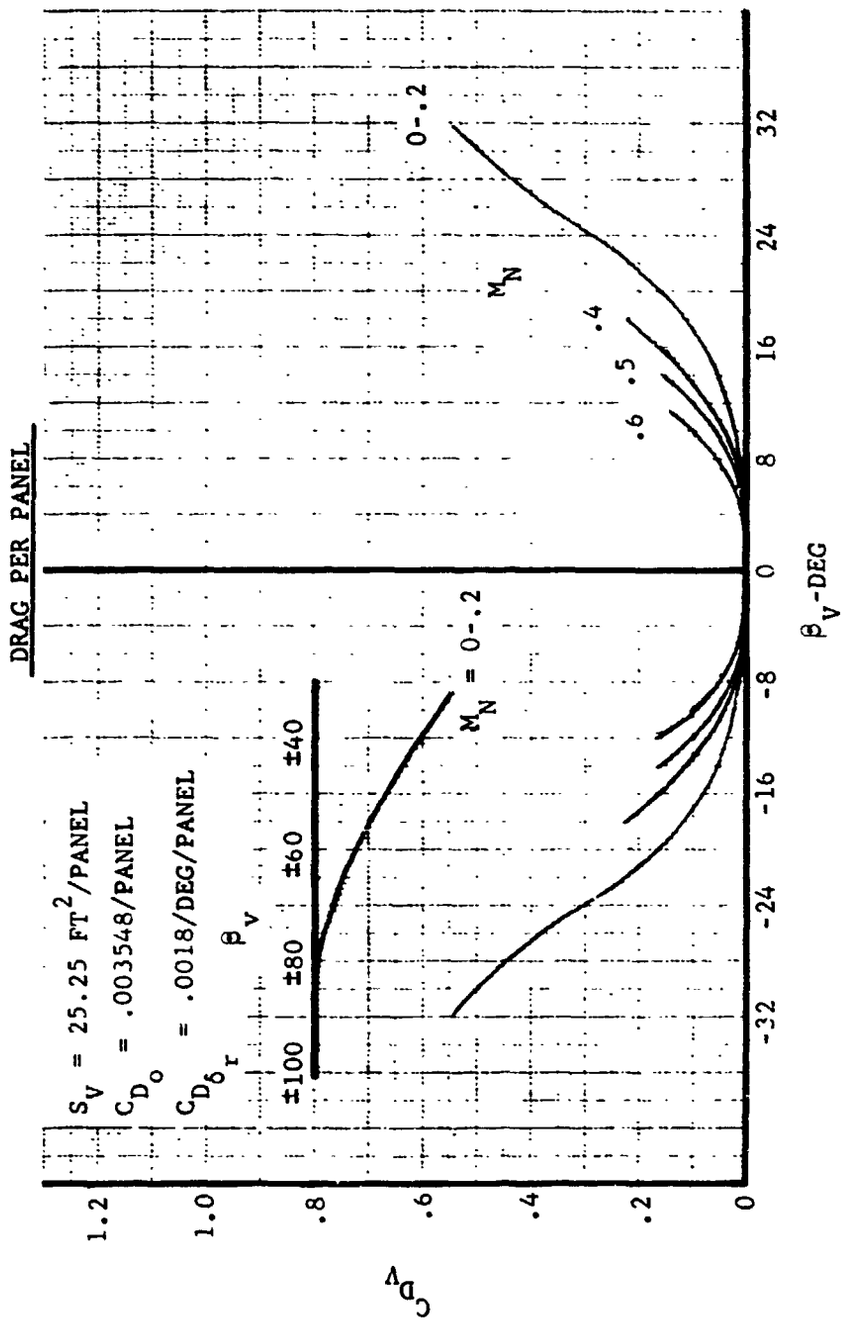

Figure II-14. Vertical Stabilizer Drag Coefficient Versus Sideslip Angles

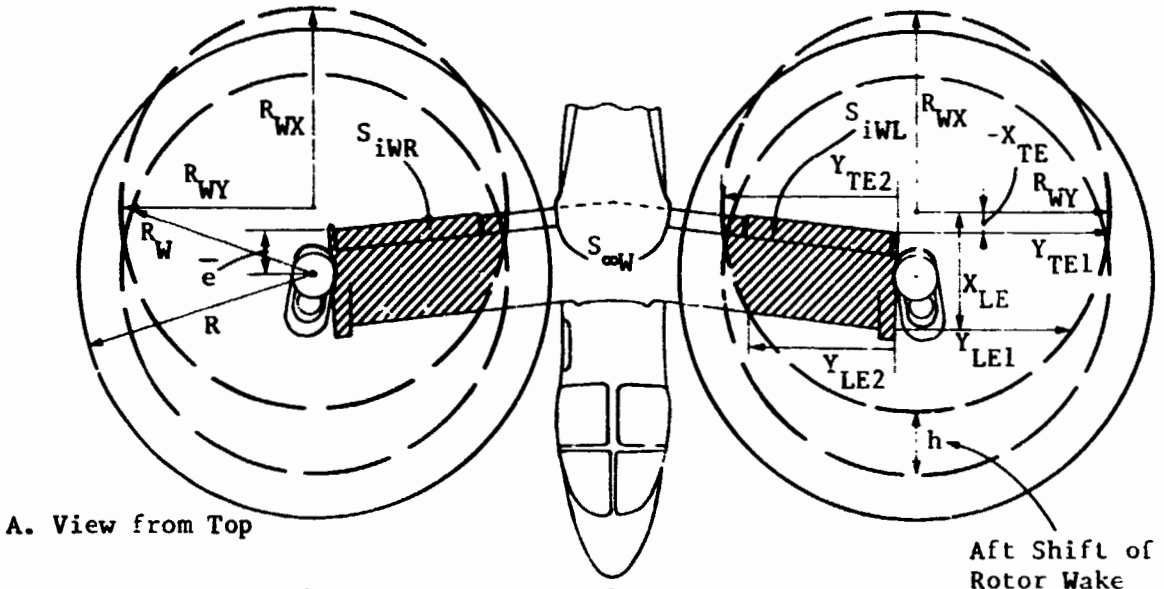

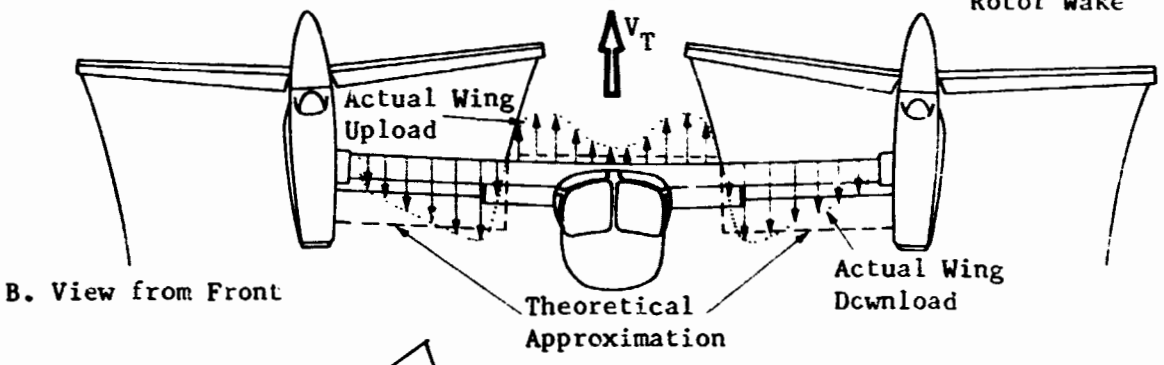

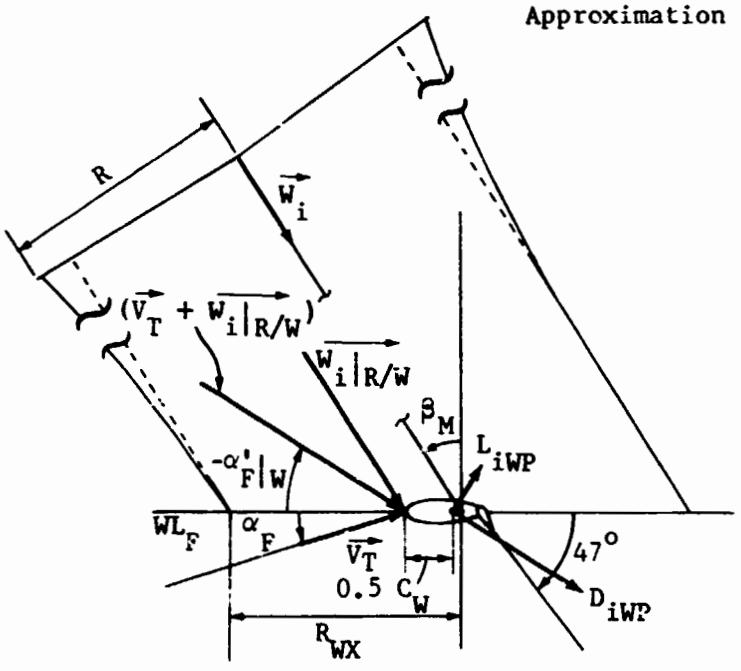

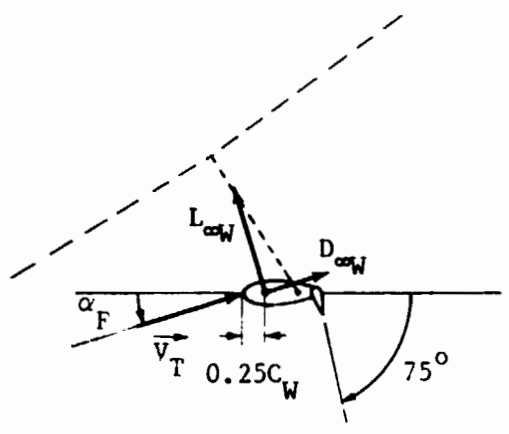

Figure II-15. Sign Convention and Notation for Mathematical Model of Rotor Wake - Wing Interaction

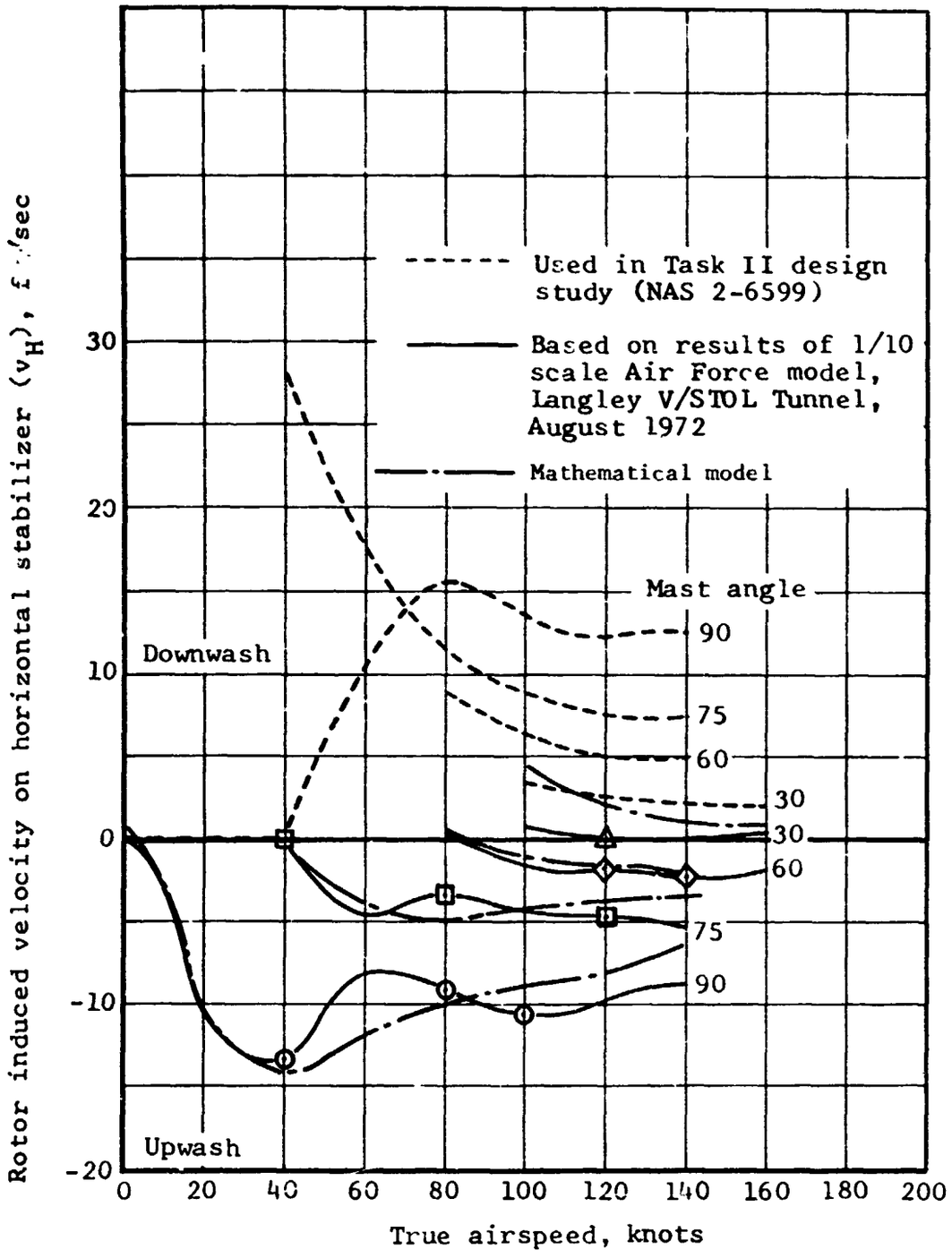

Figure II-16. Model of Rotor Wake Induced Velocity at Horizontal Stabilizer

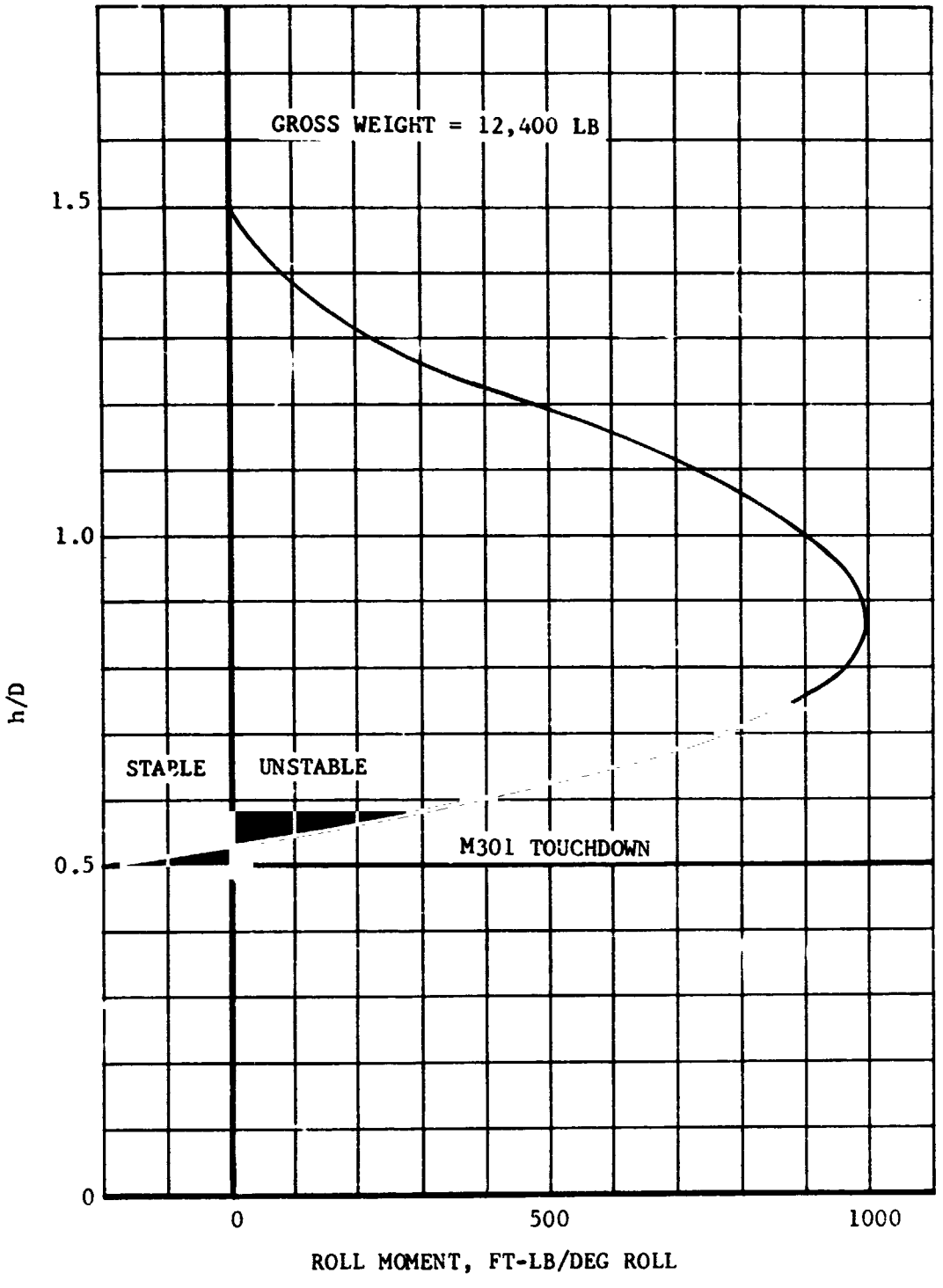

Figure II-17. Representation of In-Ground Effect Rolling Moment

FOLDOUT FRAME

BELL HELICOPTER COMPANY

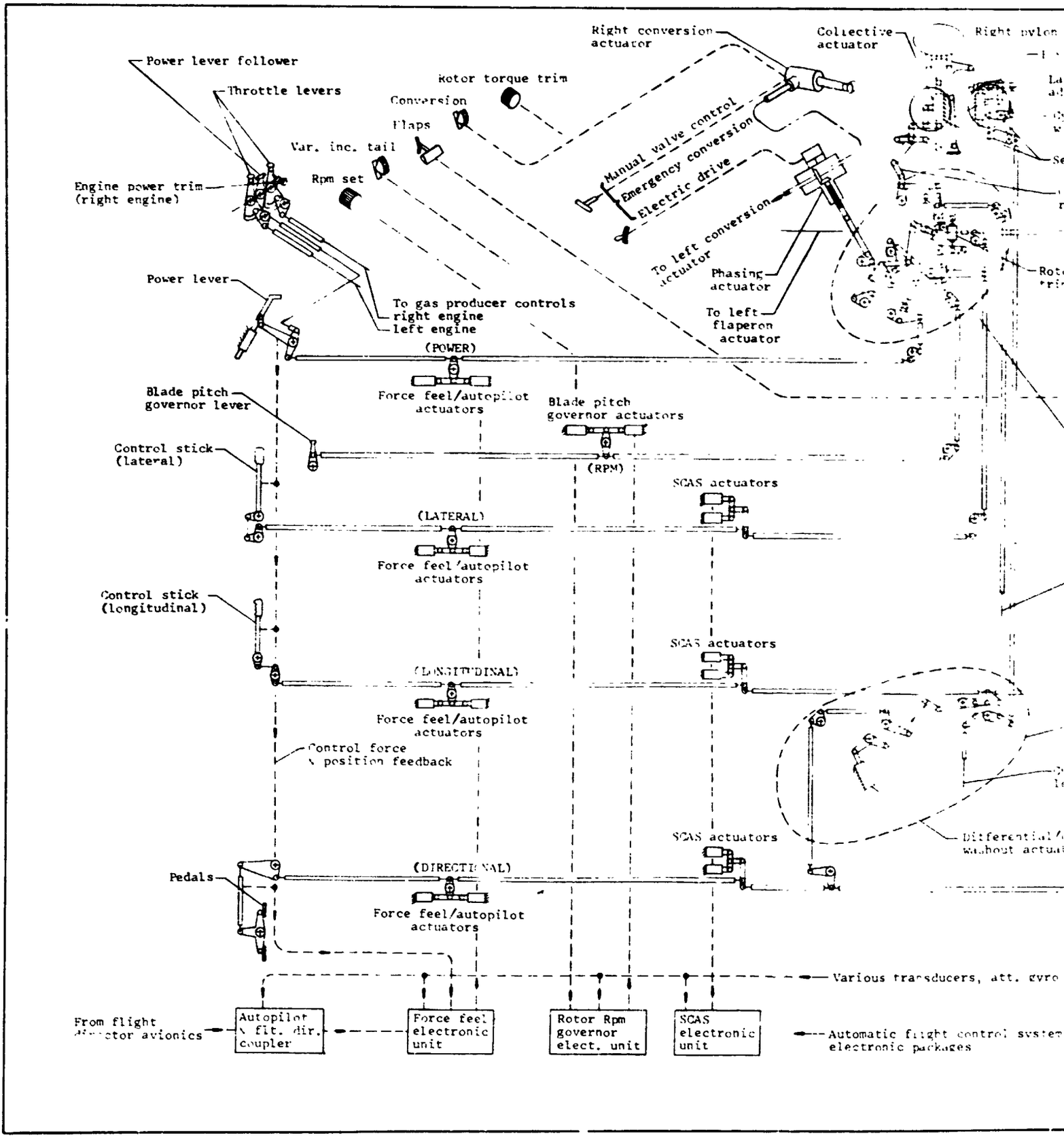

Figure II-18. Schematic of Model 301 Flight

FOLDOUT FRAME 2

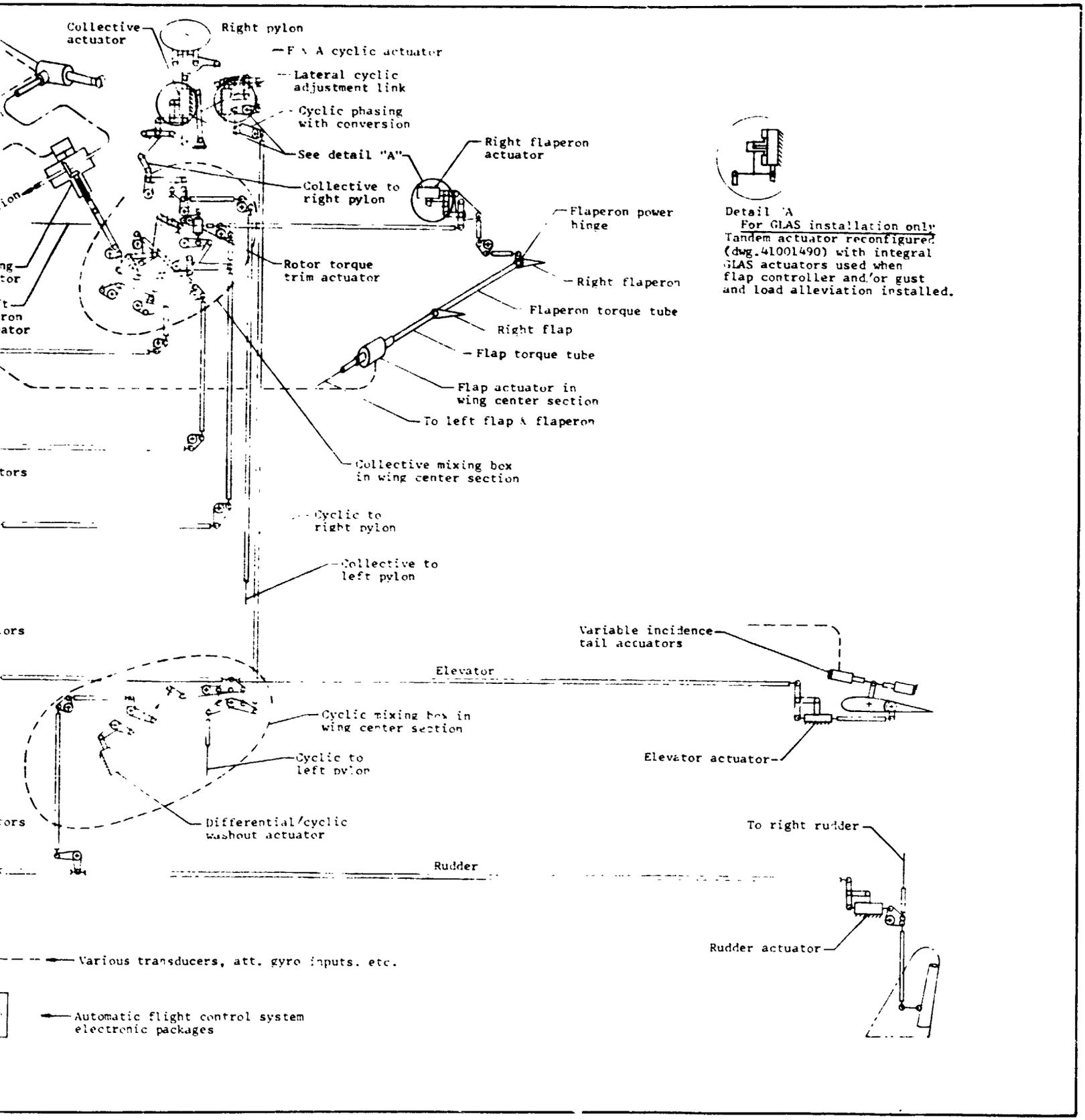

Schematic of Model 301 Flight Control System

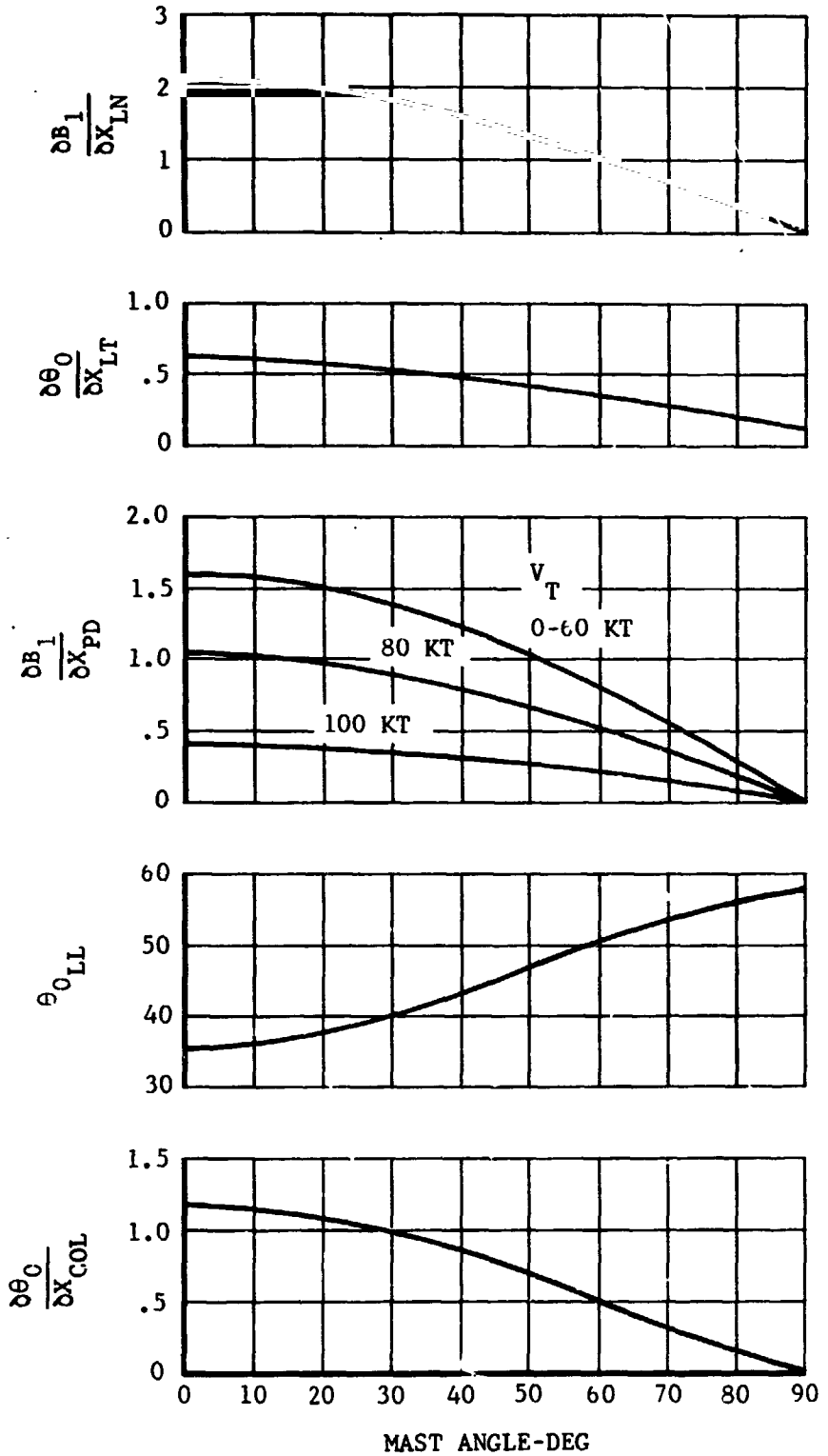

Figure II-19. Computer Representation of Flight Control System Wash-Out Schedule With Conversion Angle

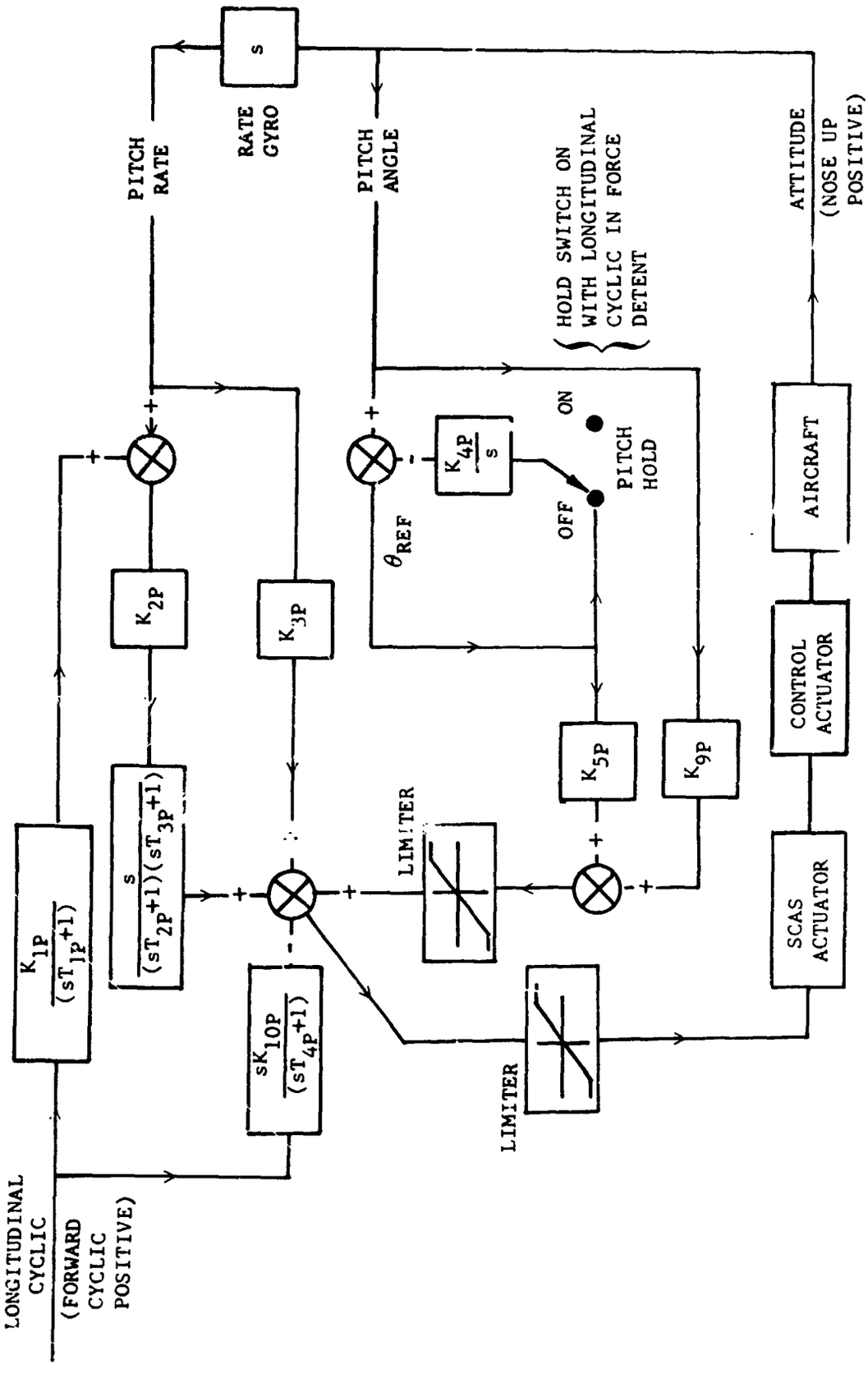

Figure II-20. Schematic of SCAS Pitch Channel Network

III. VALIDATION OF THE MATHEMATICAL MODEL

The accuracy of the mathematical model has been investigated with regard to rotor performance and force characteristics, airframe aerodynamics, rotor wake - airframe aerodynamic interaction, static and dynamic stability characteristics and control power and damping. Test data were used for comparison where avilable; when test data were not available the mathematical model was compared with BHC computer program C81, the program used to predict the Model 301's stability, control, and handling qualities presented in Reference 1.

A. Rotor Performance and Force Characteristics

Rotor forces and power required are compared with data from wind tunnel and whirl tests of the Model 301's 25-foot diameter rotor (References 15 and 16) in Figures III-1 through III-5. In general the correlation reflects the neglect of stall and compressibility in the mathematical model. For a given lift, power required is calculated slightly low and propulsive force slightly high. Collective pitch and longitudinal cyclic are calculated accurately.

Figure III-6 compares the rotor damping characteristics with those calculated with program C81. Agreement between the two analyses is good.

B. Airframe Force and Moment Characteristics

As noted in Section II.3 the mathematical model of the airframe force and moment characteristics in the angle of attack and sideslip range below stall are based on wind tunnel data. In the mathematical model, the wind tunnel data has been broken down into the contributions of major components; the fuselage, the wing-pylon assembly, the horizontal stabilizers and the fins. Above stall the force and moment characteristics have been approximated.

In order to verify that the force and moment data add up to equal that of the complete airframe a computer "wind tunnel" test of the airframe math model (with the rotors removed) was conducted. The mathematical model force and moment characteristics are compared to the wind tunnel data in Figures III-7 through III-11. Data from two tests are shown: LTV Low Speed Wind Tunnel Test No. 408 performed at a Reynolds number of 1.2 by 10^6 and NASA Langley Transonic Dynamics Test No. 195 performed at a Reynolds number of 3.8 by 10^6. Vortex generators were installed on the wing during the LTV test to simulate wing stall characteristics at the full-scale Reynolds numbers.

The reasons for significant difference between the mathematical model and the test data are as follows:

- Lift Coefficient (Figures III-7 and III-8). Correlation is good for angles of attack up to stall but above stall the mathematical

model lift coefficient is high. This error is caused by the assumed lift characteristic above stall (Reference 11) and will be corrected for the Phase II simulations.

- Pitching Moment Coefficient (Figures III-11 and III-12). The pitching moment characteristic of the full-scale aircraft is estimated to be close to the TDT test data, hence the mathematical model has been adjusted to obtain the slope of the TDT data. The discontinuity in the mathematical model pitching moment coefficient at positive and negative stall angles is caused by the assumed characteristics of the wing downwash and the fuselage pitching moment above stall. The difference in pitching moment at zero angle of attack as shown in Figure III-11 results from an assumption made in the mathematical model - that the wing-pylon zero pitching moment is independent of pylon tilt angle. This will be modified for Phase II simulations.

- Rolling Moment Coefficient (Figures III-15 and III-16). The mathematical model defines wing-pylon dihedral effects accurately up to ±10 degrees sideslip angle. Beyond this range, the dihedral stability of wing-pylon is maintained constant. (The test data do not show zero rolling moment at zero yaw because of model asymmetry.)

Figure III-19 compares the mathematical model aileron control power variation with angle of attack with test data. The decrease in roll control power at high angles of attack is accurately represented.

C. Rotor Wake - Airframe Aerodynamic Interaction

The rotor wake induced velocity at the horizontal tail and the unstable rolling moment in-ground effect are represented using a polynomial fit of test data. The curve fit and test data are compared in Figure II-16.

The effect of the rotor downwash on wing lift is calculated using the analytical model discussed in Section II.D. This effect is compared to test data (from a model of a similar aircraft) in Figure III-20. One to one agreement is not expected because of differences in the configuration of the Model 301 and that of the model. What is significant is the trend in down load with airspeed which is quite good.

D. Stability Derivatives

Stability derivatives calculated with the mathematical model are compared with those calculated with program C81 in Table III-1. Significant differences between the mathematical model and C81 derivatives are evident but are not fully understood. One of the reasons for the difference in the longitudinal derivatives may be explained by the fact that C81 airframe inputs are linear below the stall angle of attack, whereas the mathematical model accounts for the variation in the coefficients with angle of attack. The lateral-directional derivatives are in better agreement since both the programs use stability derivatives for airframe

inputs; the difference in derivatives is primarily caused by differences in the rotor mathematical models.

However, the differences in computed derivatives of the two programs are small enough that the resulting dynamic stability characteristics are similar, as discussed later in Section IV.F.

E. Static Stability

Figure III-21 compares the level flight trim longitudinal stick position, blade root collective pitch, and fuselage pitch attitude calculated with the mathematical model with those calculated with program C81. These are in good agreement with the exception of the longitudinal stick position at airspeeds below 50 knots. This difference is caused by the difference in the wing download representation in the two programs. In C81 the center of pressure of the download does not vary with airspeed; in the simulator mathematical model the download center of pressure moves aft with increasing airspeed.

F. Dynamic Stability

Flight mode characteristics calculated with the mathematical model are compared with those calculated by program C81 in Table III-2. Note that characteristics for the mathematical model were determined both from response time histories and by solving the characteristic equations using the derivatives given in Table III-1. The differences in the flight mode characteristics (particularly for the phugoid mode) may be caused by the rotor rpm degree of freedom being active when the response time histories were obtained. A higher short period damping predicted by program C81 is due to a higher estimate of the wing downwash lag derivative $C_{m_{\dot{\alpha}}}$. Differences in short period frequencies are primarily due to inaccuracies in the rotor mathematical model computation of inplane forces resulting from a neglect of stall effects.

The flight mode characteristics computed by the two programs are compared with the MIL-F-83300 level 1 requirements in Figures III-22 and III-23. Characteristics computed from these two programs are such that they meet the level 1 requirements and would be expected to produce similar pilot evaluation.

G. Control Sensitivity and Damping

Figures III-24 and III-25 compare the control sensitivity calculated with the mathematical model with that calculated with program C81. Agreement is good except for the control power at $\alpha_{mast} = 30^{\circ}$. Investigation of this difference revealed that the C81 data is in error at this mast angle; the mathematical model reflects the correct sensitivity.

Comparison of aircraft damping characteristics as shown in Figure III-26 is good throughout the speed and pylon tilt range.

TABLE III-1 COMPARISON OF STABILITY DERIVATIVES WITH THOSE COMPUTED BY PROGRAM C81

G. W. = 13,000 LB., AFT CG, SEA LEVEL STANDARD

DERIVATIVE \ FLIGHT CONDITION	HELICOPTER MODE α_M=90° FLAPS 40/25		CONVERSION MODE α_M=60° FLAPS 40/25		CONVERSION MODE α_M=30° FLAPS 40/25		AIRPLANE MODE α_M=0° FLAPS 0°/0°	
	565 RPM	120 KNOTS	565 RPM	120 KNOTS	565 RPM	140 KNOTS	458 RPM	260 KNOTS
	(1)	(2)	(1)	(2)	(1)	(2)	(1)	(2)
$-C_{X_U}$	.865	.95	1.64	1.59	3.19	3.05	1.22	.125
$-C_{Z_U}$	1.34	.83	.54	.36	.82	.61	1.46	.61
$-C_{M_U}$	.29	-.49	-.64	-.67	-1.26	-.99	-.887	-.058
$-C_{X_\alpha}$	.605	.675	-2.72	-1.87	-2.06	-1.80	-.201	-.246
$-C_{Z_\alpha}$	9.105	8.45	8.30	8.01	6.59	6.35	6.47	6.47
$-C_{M_\alpha}$	3.5	1.74	2.67	2.61	1.85	2.36	1.32	1.17
$-C_{X_q}$	-.013	-1.21	5.33	1.17	5.16	1.42	-.551	-.41
$-C_{M_q}$	39.9	37.4	33.7	39.2	29.2	35.8	29.8	33.8
$-C_{Y_\beta}$	1.77	1.95	1.8	1.61	1.87	1.62	1.83	1.87
$-C_{l_\beta}$	.365	305	.285	.106	.289	.202	.318	.312
$-C_{N_\beta}$	-.371	-.474	-.38	-.46	-.303	-.34	-.242	-.305
$-C_{Y_P}$	.45	.344	-.03	-.72	-.517	-.366	.188	.0064
$-C_{l_P}$	3.13	3.2	2.7	3.0	2.06	1.96	1.34	1.28

Cont'd on Next Page

TABLE III-1 COMPARISON OF STABILITY DERIVATIVES WITH THOSE COMPUTED BY PROGRAM C81 (CONTINUED)

G. W. = 13,000 LB., AFT CG, SEA LEVEL STANDARD

FLIGHT CONDITION / DERIVATIVE	HELICOPTER MODE α_M=90° F 40/25		CONVERSION MODE α_M=60° FLAPS 40/25		CONVERSION MODE α_M=30° FLAPS 40/25		AIRPLANE MODE α_M=0°, FLAPS 0°/0°	
	565 RPM	120 KNOTS	565 RPM	120 KNOTS	565 RPM	140 KNOTS	458 RPM	260 KNOTS
	(1)	(2)	(1)	(2)	(1)	(2)	(1)	(2)
$-C_{N_p}$	-.635	-.276	.43	.74	.734	.94	.19	.26
$-C_{l_r}$	-.936	-.44	.002	.384	.234	.664	.414	.388
$-C_{N_r}$	1.13	1.03	1.015	1.206	1.54	1.86	1.22	1.24
C_{L_o}	1.48	1.48	1.48	1.48	1.085	1.085	.314	.314

(1) Mathematical Model - Constant RPM and Collective Pitch

(2) C81 Program - Constant RPM, for $\alpha_M < 20°$ Collective Pitch Adjusted to Maintain Constant Torque

TABLE III-2 COMPARISON OF FLIGHT MODE CHARACTERISTICS WITH THOSE PREDICTED BY PROGRAM C81

G. W. = 13,000 LB., AFT CG, SEA LEVEL STANDARD

FLIGHT MODE \ FLIGHT CONDITION		HELICOPTER MODE α_M=90°, F_x-40°/25° 565 RPM 120 KNOTS	CONVERSION MODE α_M=60°, F_x-40°/25° 565 RPM 120 KNOTS	CONVERSION MODE α_M=30° F_x-40°/25° 565 RPM 140 KNOTS	AIRPLANE MODE α_M=0° F_x-0°/0° 458 RPM 260 KNOTS
SHORT PERIOD	(1)	P=2.0 $t_{1/2}$=1.0	P=3.2 $t_{1/2}$ < 1/2	P=2.9 $t_{1/2}$=0.6	P=1.6 $t_{1/2}$=0.35
	(2)	P=1.9 $t_{1/2}$= .48	P=2.2 $t_{1/2}$ 0.53	P=2.4 $t_{1/2}$=0.55	P=1.5 $t_{1/2}$=0.31
	(3)	P=4.6 $t_{1/2}$=0.35	P=2.2 $t_{1/2}$=0.37	P-2.0 $t_{1/2}$=0.35	P=1.3 $t_{1/2}$=0.26
PHUGOID	(1)	P > 30 $t_{1/2}$=7.5	P=29.5 $t_{1/2}$=25.0	P=28.5 $t_{1/2}$=28.0	P=27.7 $t_{1/2}$=30.6
	(2)	P=51.6 $t_{1/2}$=20.4	P=23.2 $t_{1/2}$= 9.5	P=20.0 $t_{1/2}$= 5.1	P=45.0 $t_{1/2}$=56.0
	(3)	P=32.0 $t_{1/2}$=14.0	P=41.0 $t_{1/2}$= 8.0	P=46.0 $t_{1/2}$= 4.0	P=56.0 $t_{1/2}$=48.0
DUTCH ROLL	(1)	P= 4.8 $t_{1/2}$= 3.0	P= 4.0 $t_{1/2}$= 3.6	P= 4.0 $t_{1/2}$= 3.5	P= 2.4 $t_{1/2}$= 1.6
	(2)	P= 4.6 $t_{1/2}$= 2.24	P= 4.1 $t_{1/2}$= 3.4	P= 1.95 $t_{1/2}$= .25	P= 2.6 $t_{1/2}$= 1.41
	(3)	P= 4.0 $t_{1/2}$= 2.9	P= 3.9 $t_{1/2}$= 2.2	P- 4.0 $t_{1/2}$= 1.8	P= 2.2 $t_{1/2}$= 1.0
SPIRAL	(1)	$t_{1/2}$=16	$t_{1/2}$=16.5	$t_{1/2}$= 7.4	$t_{1/2}$= 9.8
	(3)	$t_{1/2}$=17.5	$t_{1/2}$=16.4	$t_{1/2}$= 6.3	$t_{1/2}$= 8.3
ROLL CONVERGENCE	(1)	τ_R= 0.6	τ_R= 1.5	τ_R= 0.8	τ_R= 0.52
	(2)	τ_R= 0.63	τ_R= 0.61	τ_R= 0.63	τ_R= 0.57
	(3)	τ_R= 0.44	τ_R= 0.46	τ_R= 0.52	τ_R= 0.58

NOTE: Period, P, time to one half amplitude, $t_{1/2}$, are in seconds and time constant τ is per second.

(1) Mathematical Model - Characteristics extracted from time histories of airplane response to control inputs.

(2) - Characteristics obtained by solving characteristic equation using stability derivatives determined from the Mathematical Model (Table III-1)

(3) C81 Program - Characteristics obtained by solving characteristic equation using stability derivatives (data from Section 6, BHC Report 301-199-002).

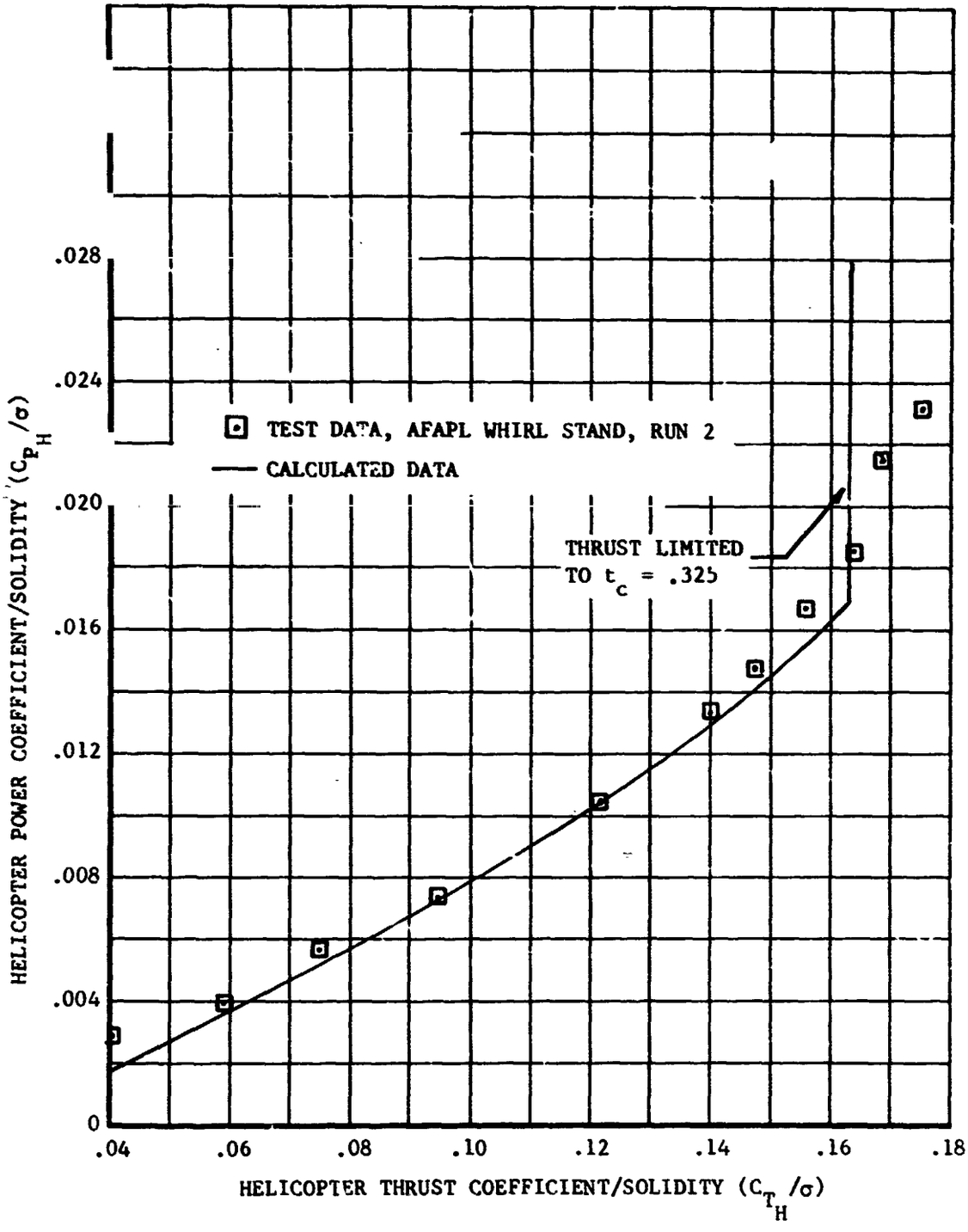

Figure III-1. Rotor Performance Correlation - Hover

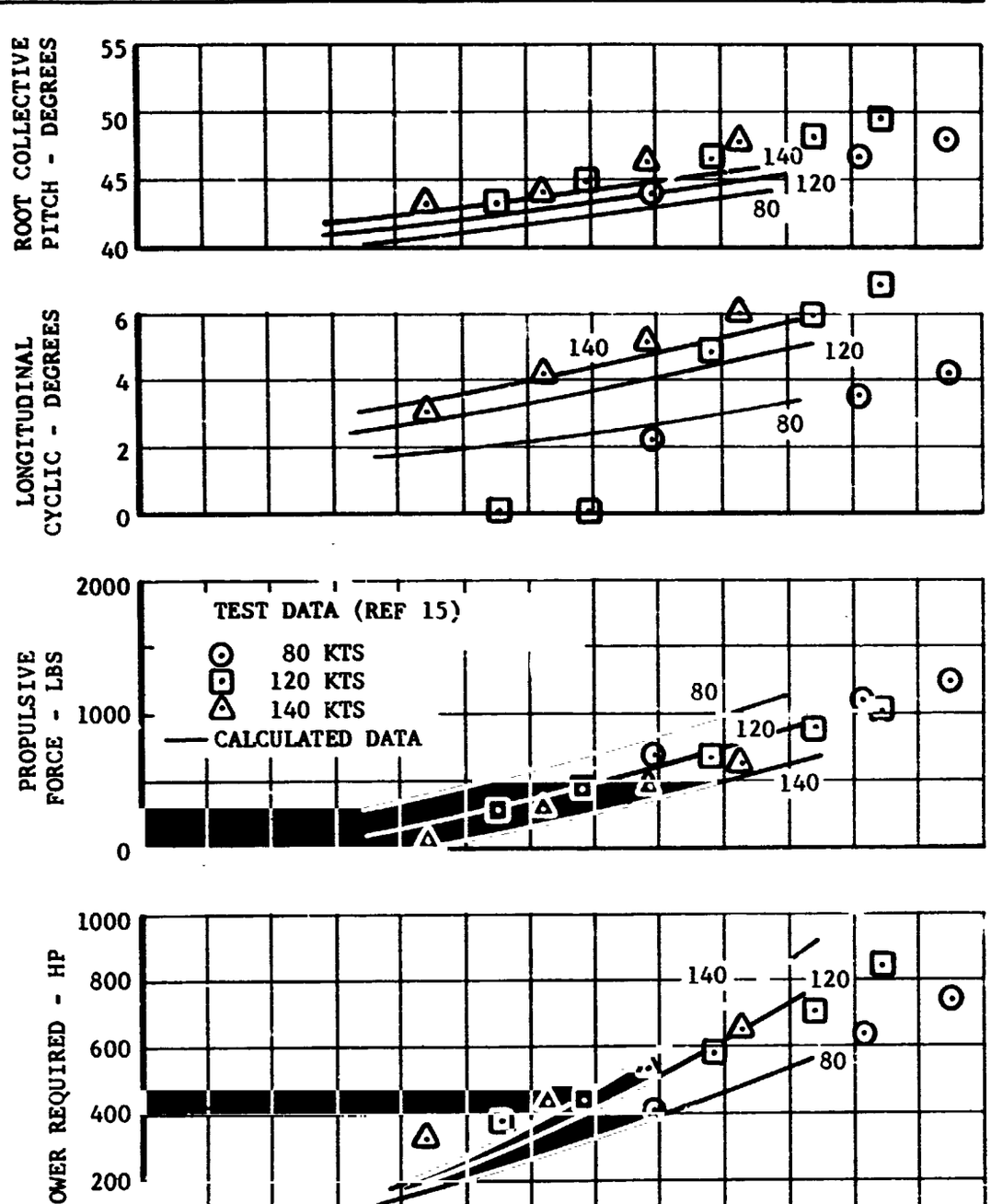

Figure III-2. Rotor Performance Correlation - $\alpha_m = 75°$

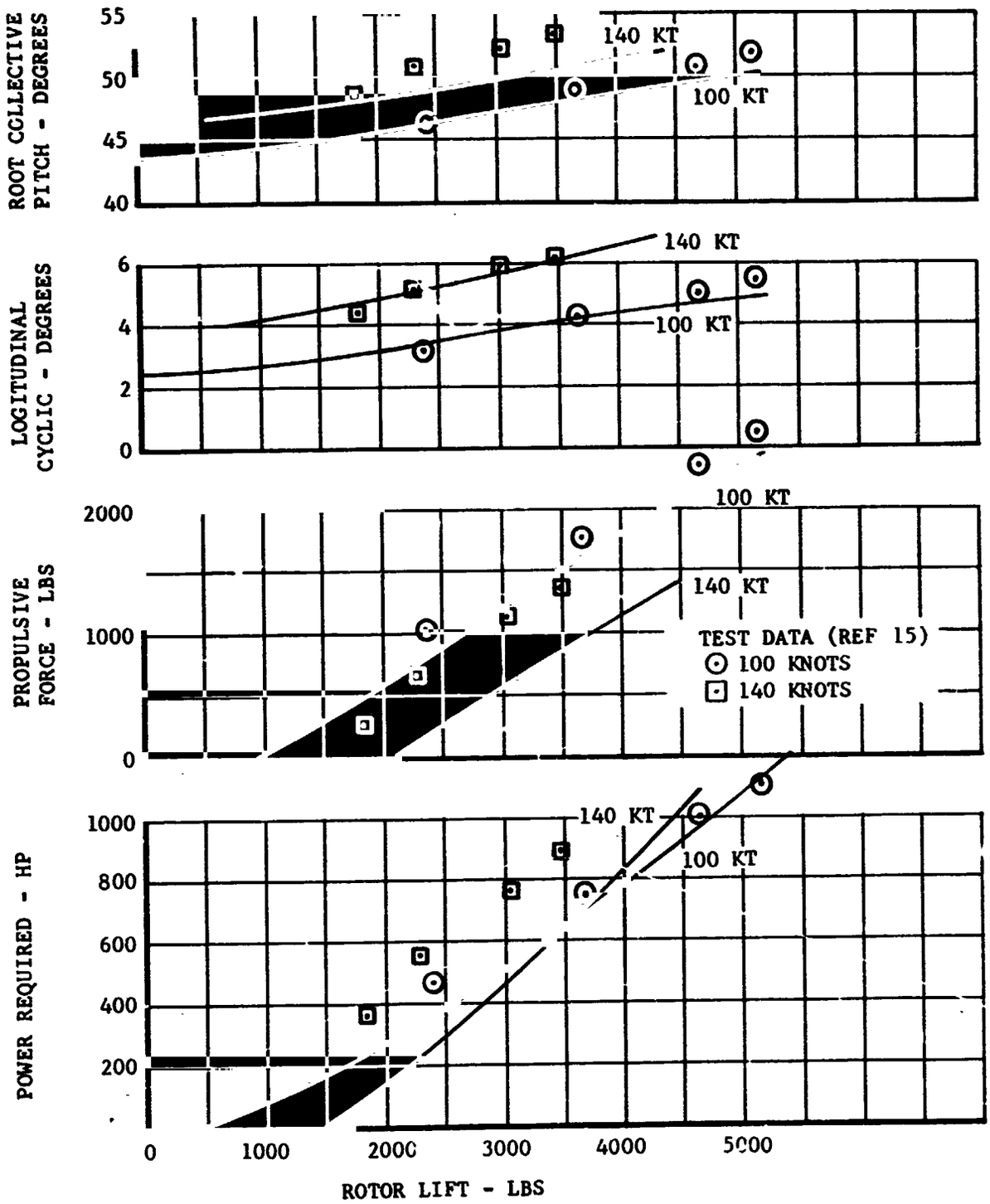

Figure III-3. Rotor Performance Correlation - $\alpha_m = 60°$

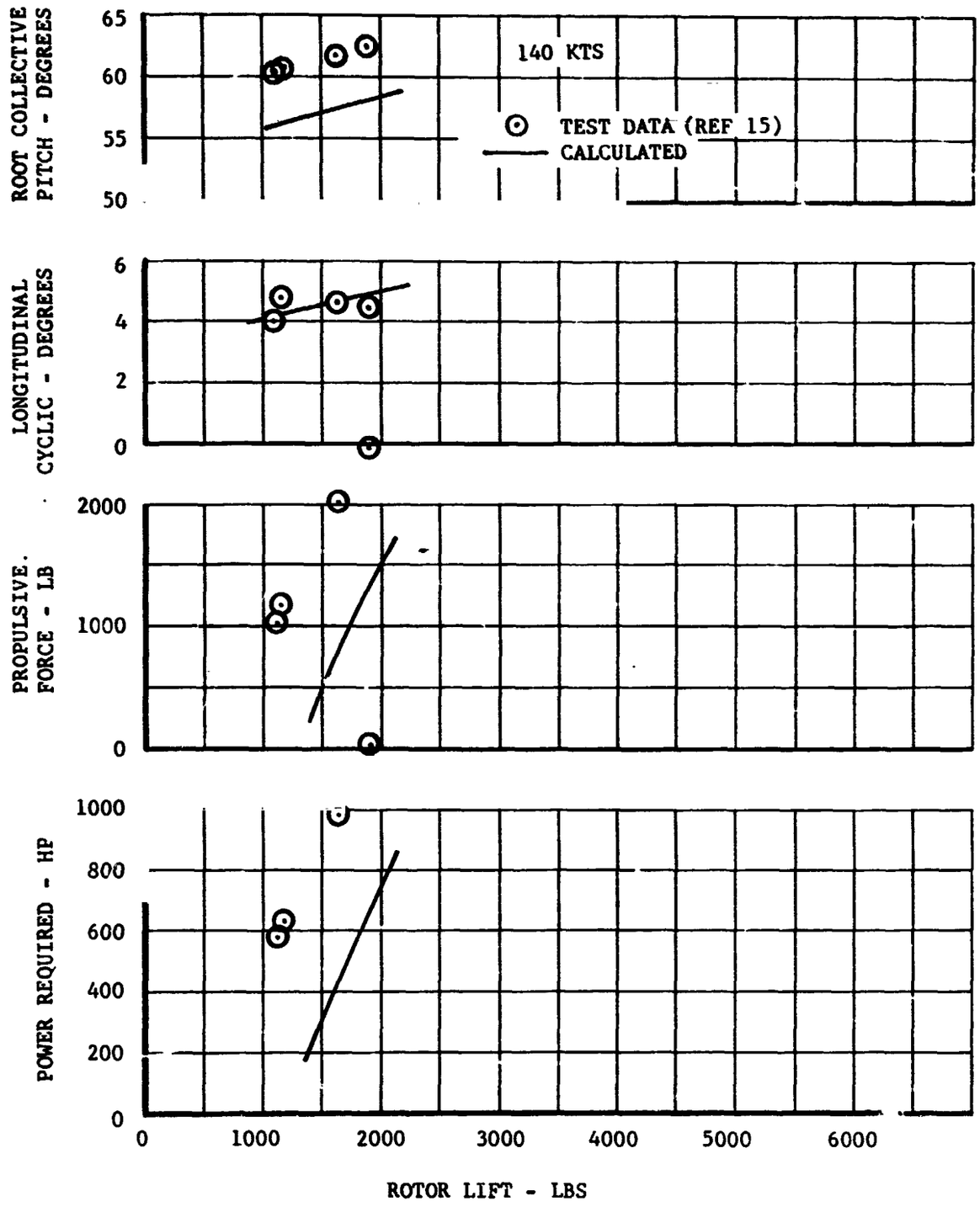

Figure III-4. Rotor Performance Correlation - $\alpha_m = 30°$

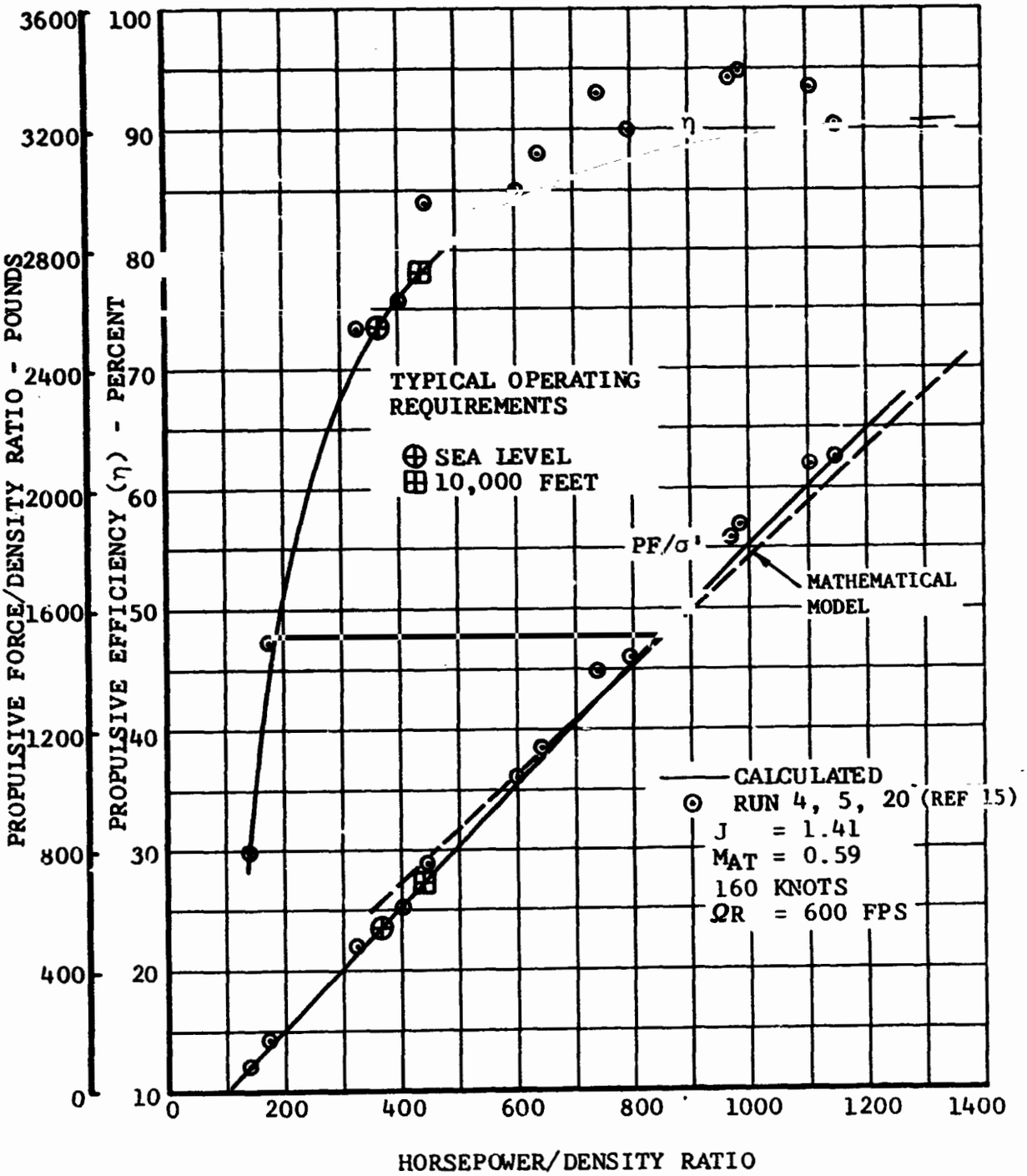

Figure III-5. Rotor Performance Correlation - $\alpha_m = 0°$

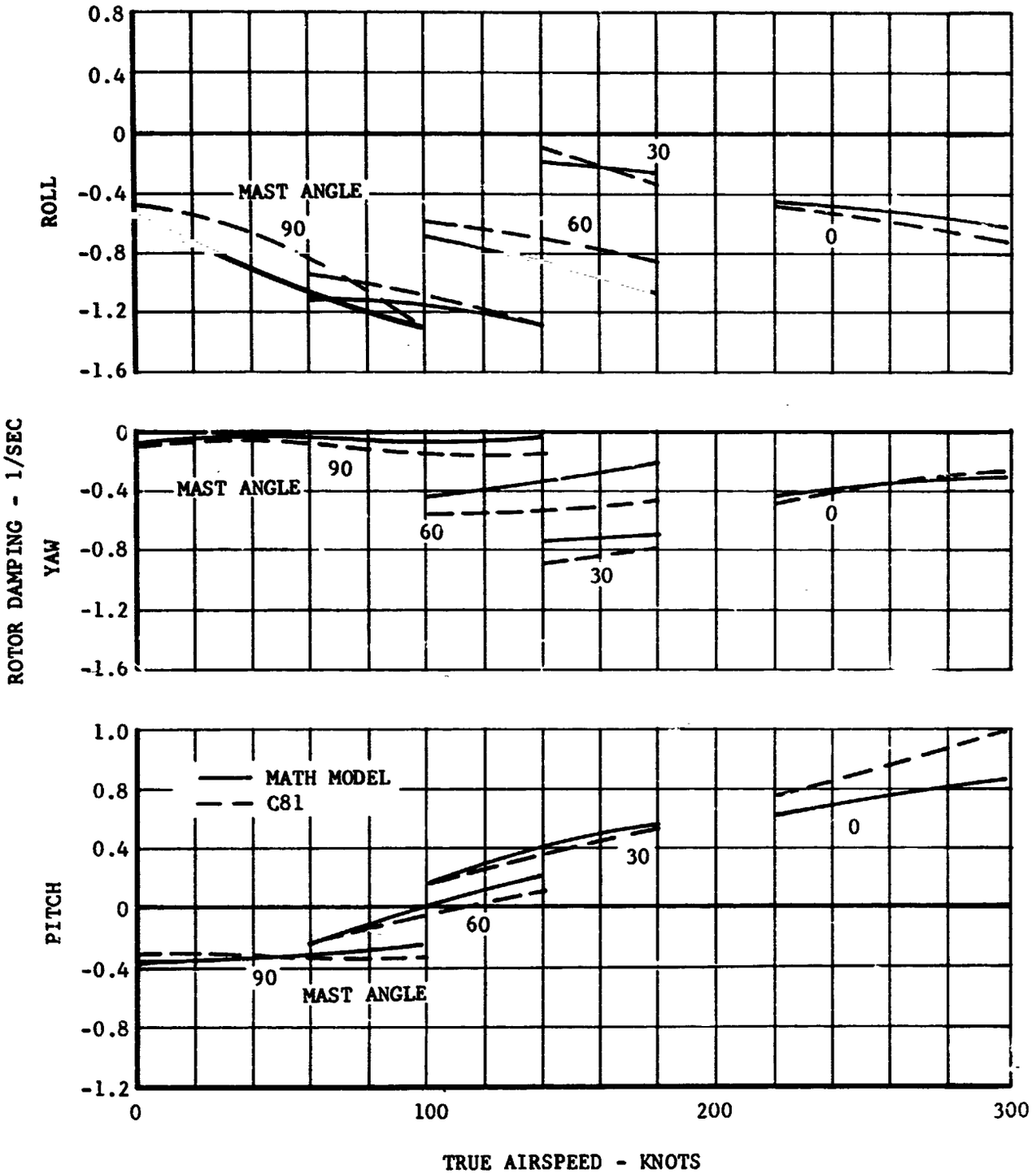

Figure III-6. Rotor Rate Derivative Correlation

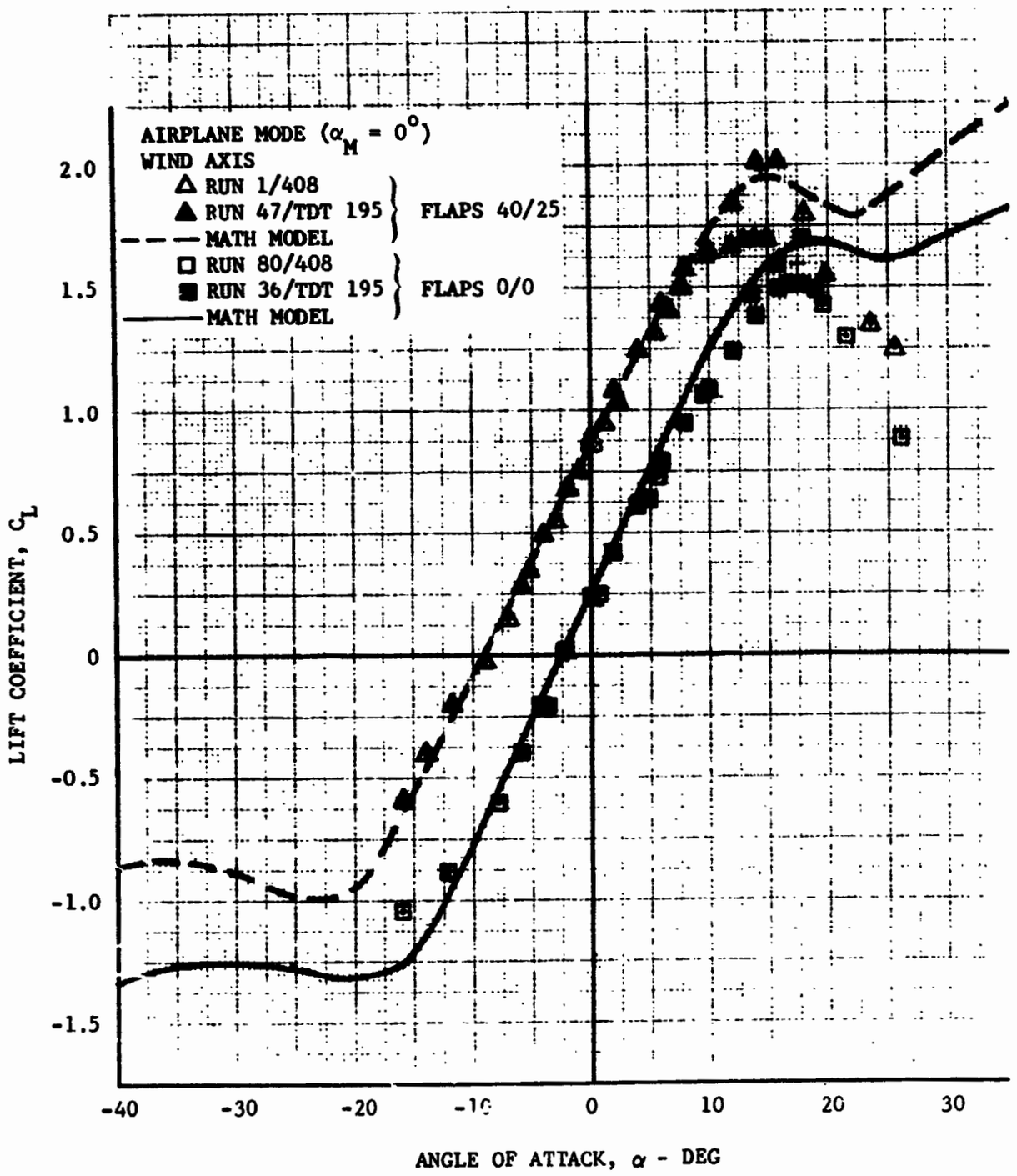

Figure III-7. Airplane Mode Lift Coefficient Correlation

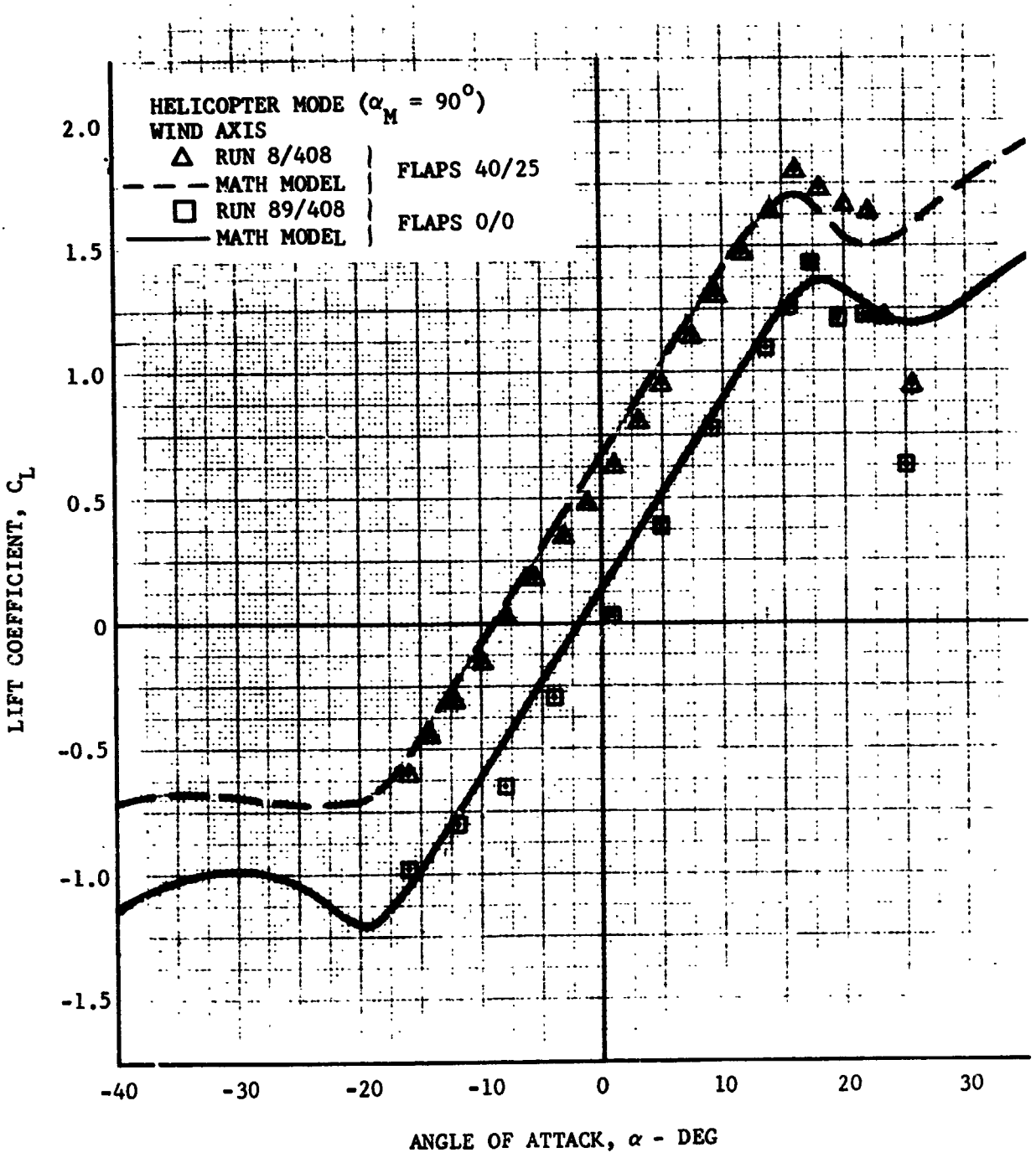

Figure III-8. Helicopter Mode Lift Coefficient Correlation

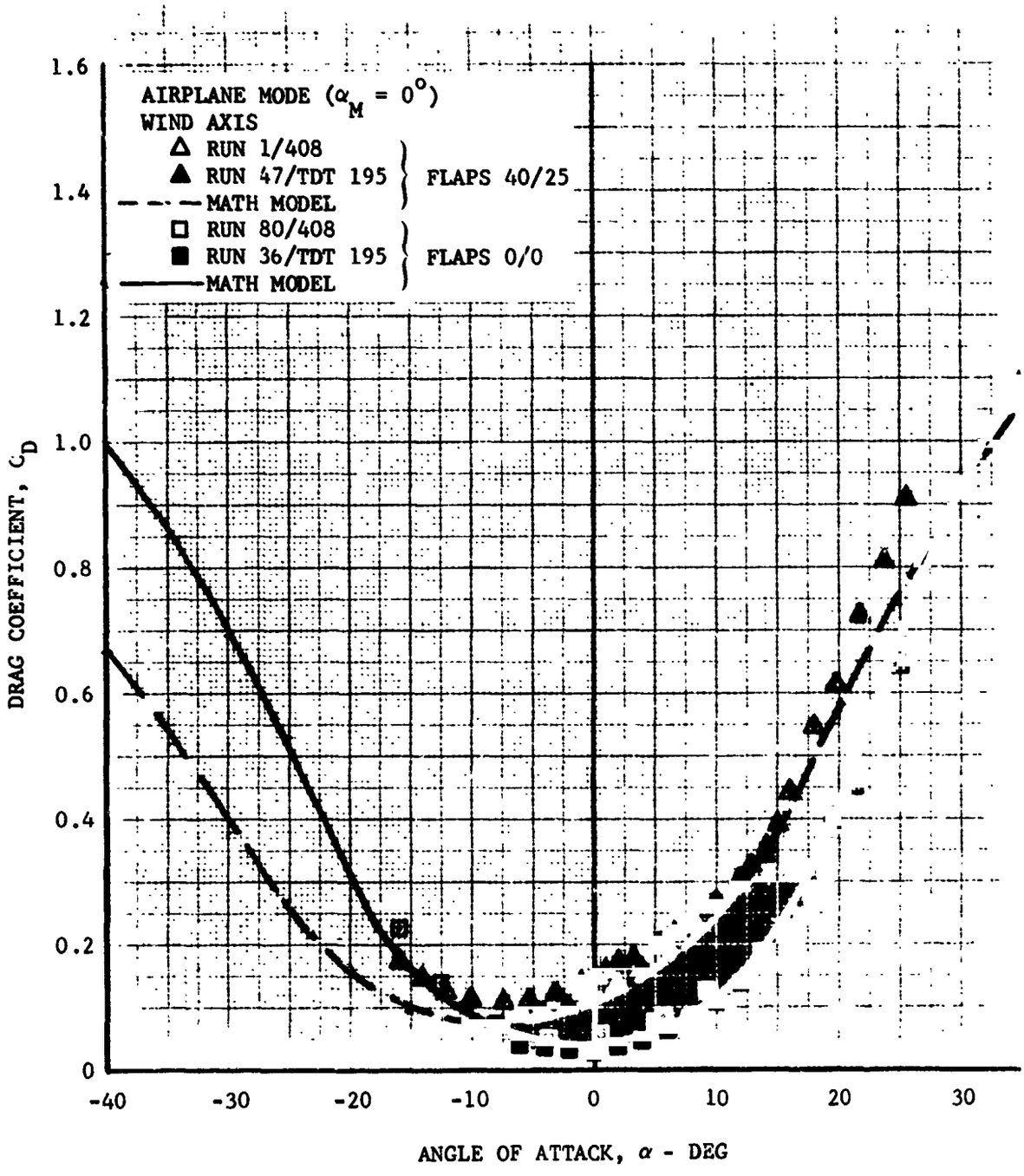

Figure III-9. Airplane Mode Drag Coefficient Correlation

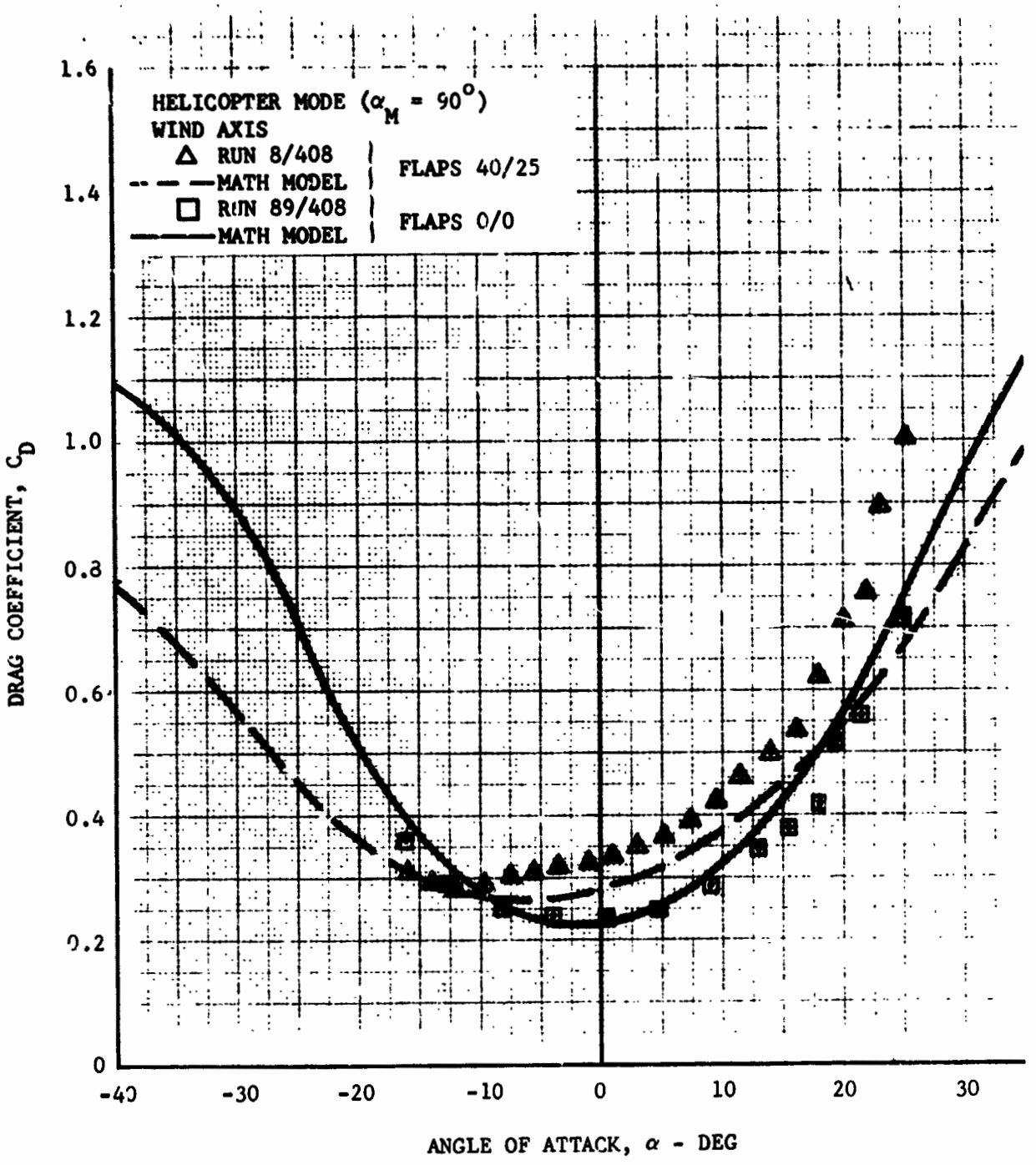

Figure III-10. Helicopter Mode Drag Coefficient Correlation

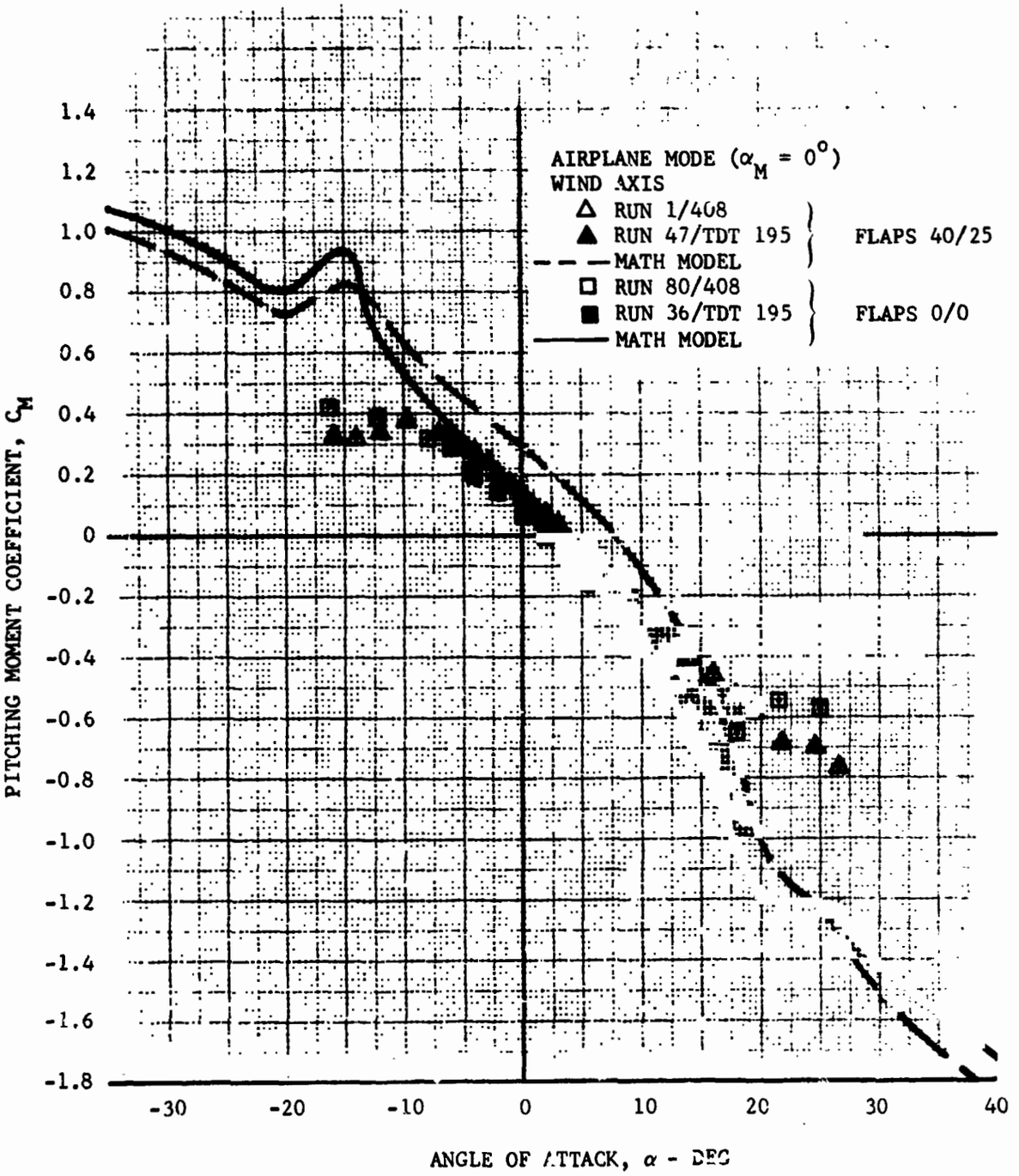

Figure III-11. Airplane Mode Pitching Moment Correlation

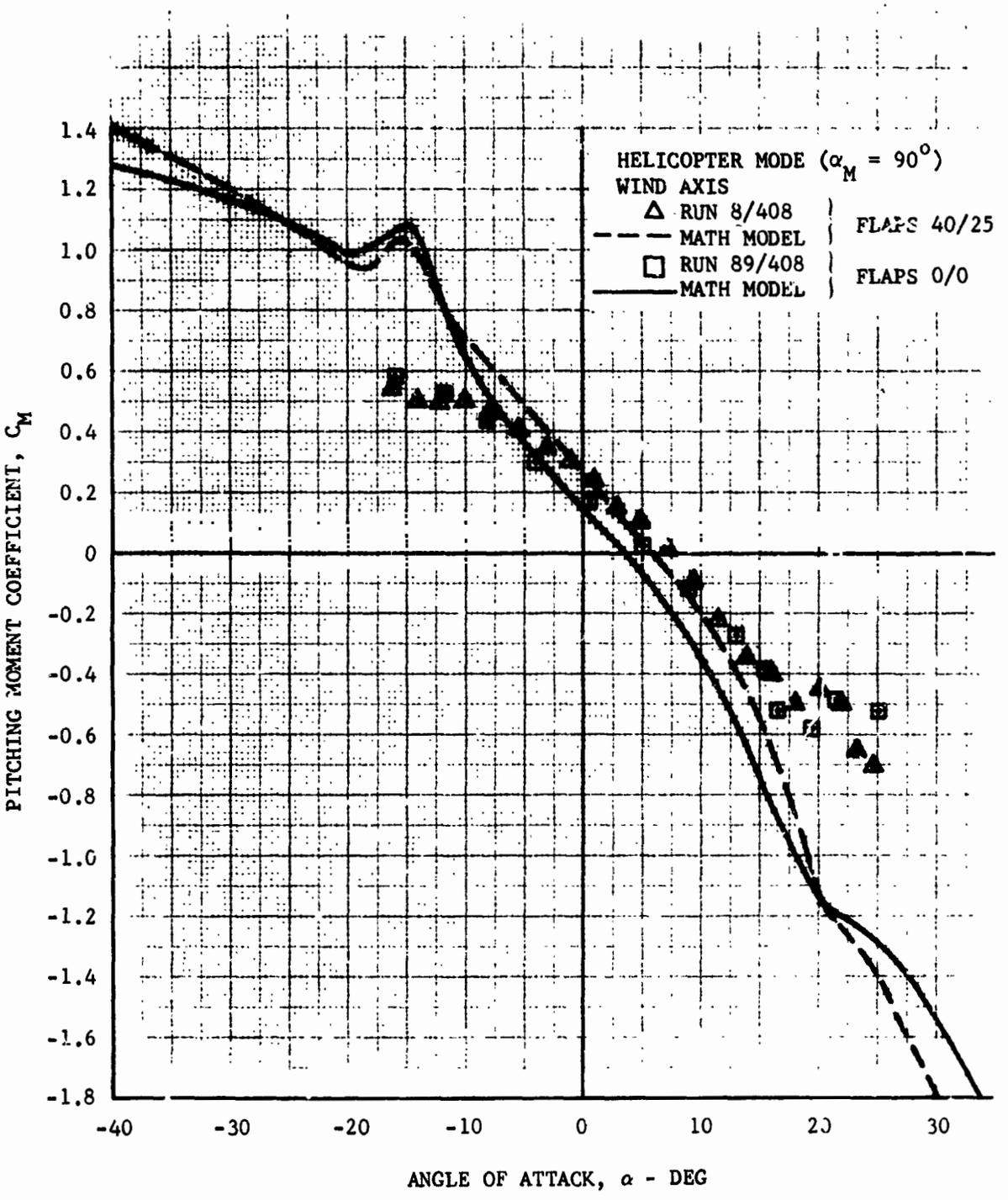

Figure III-12. Helicopter Mode Pitching Moment Correlation

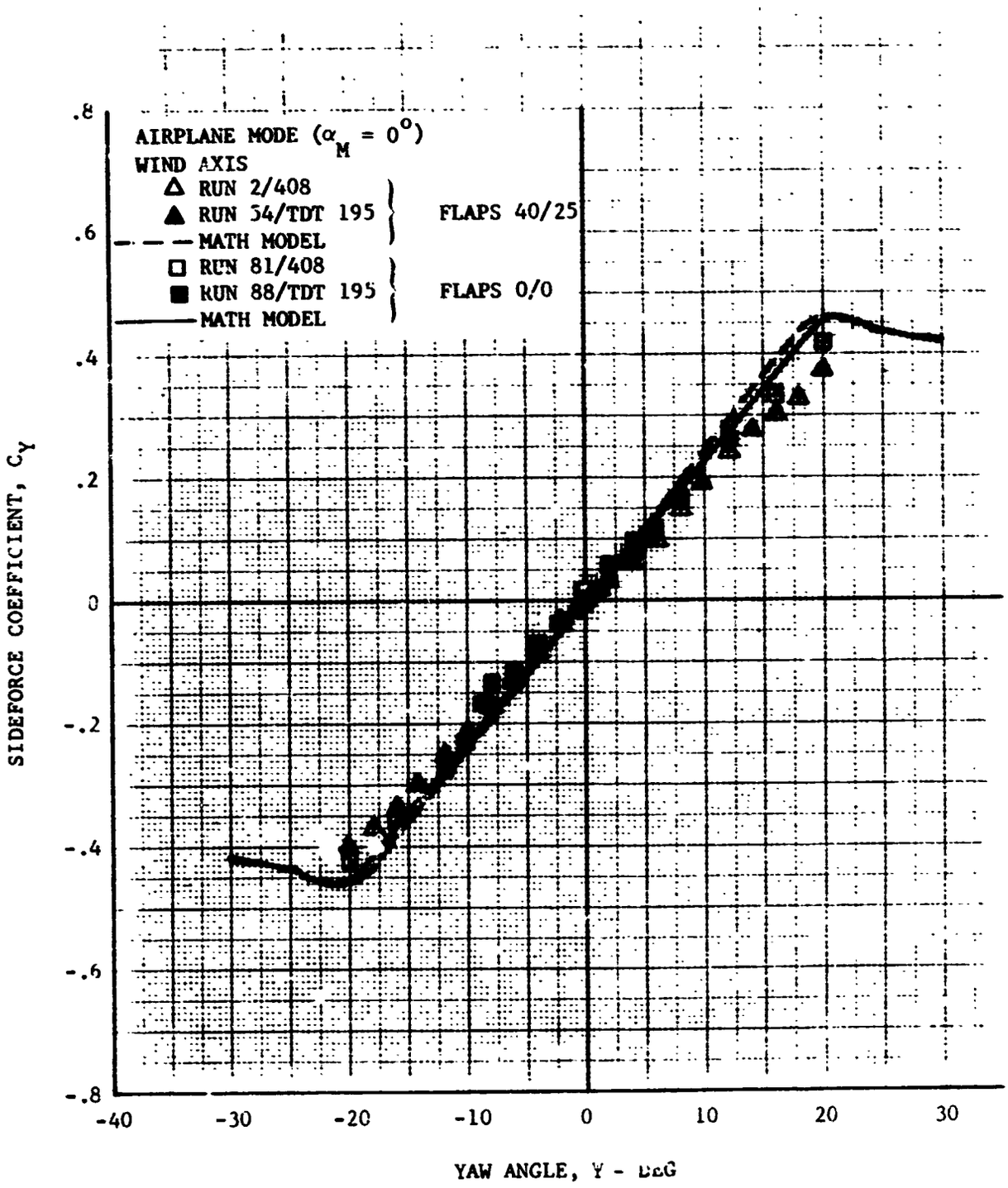

Figure III-13. Airplane Mode Sideforce Coefficient Correlation

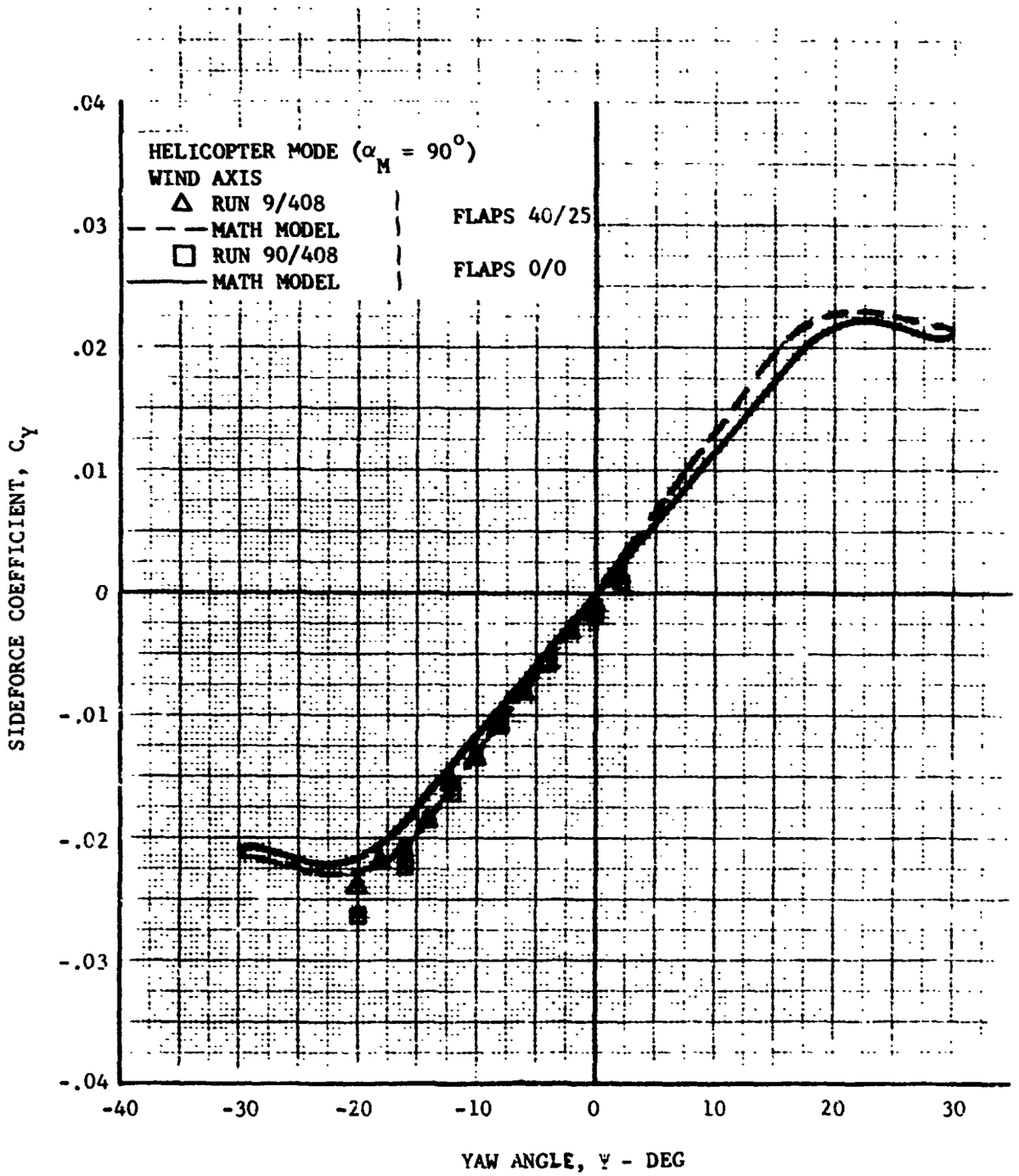

Figure III-14. Helicopter Mode Sideforce Coefficient Correlation

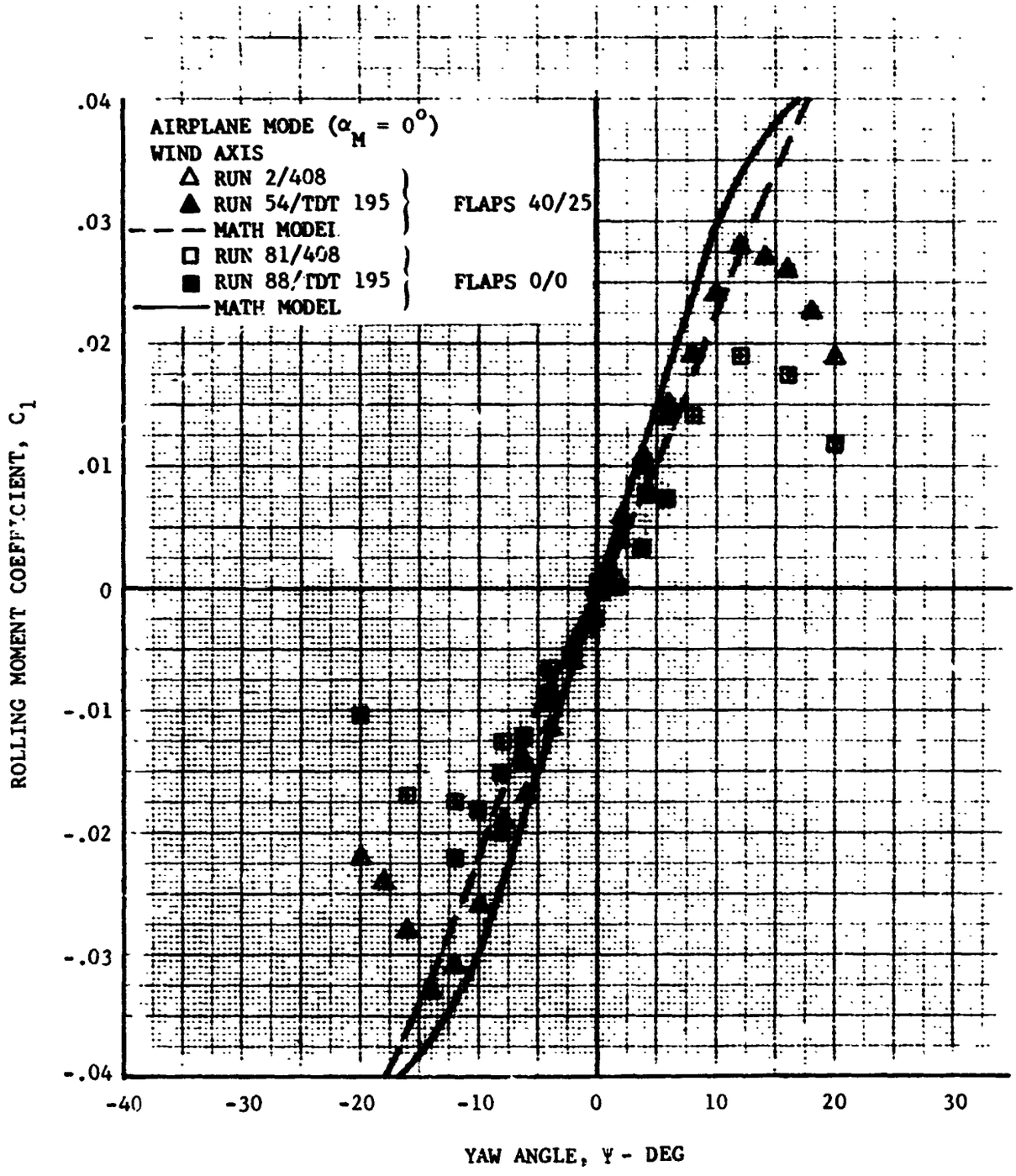

Figure III-15. Airplane Mode Rolling Moment Coefficient Correlation

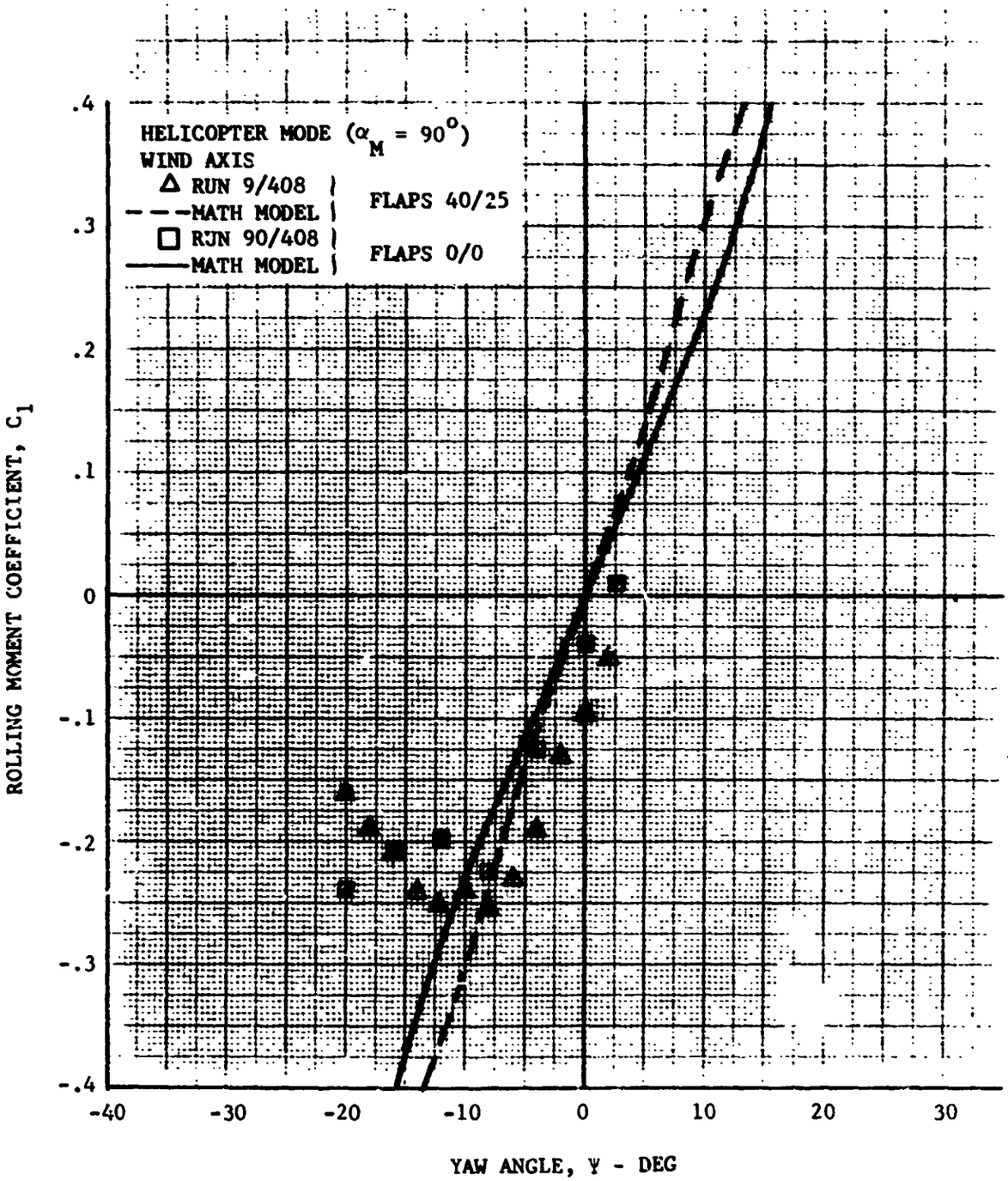

Figure III-16. Helicopter Mode Rolling Moment Coefficient Correlation

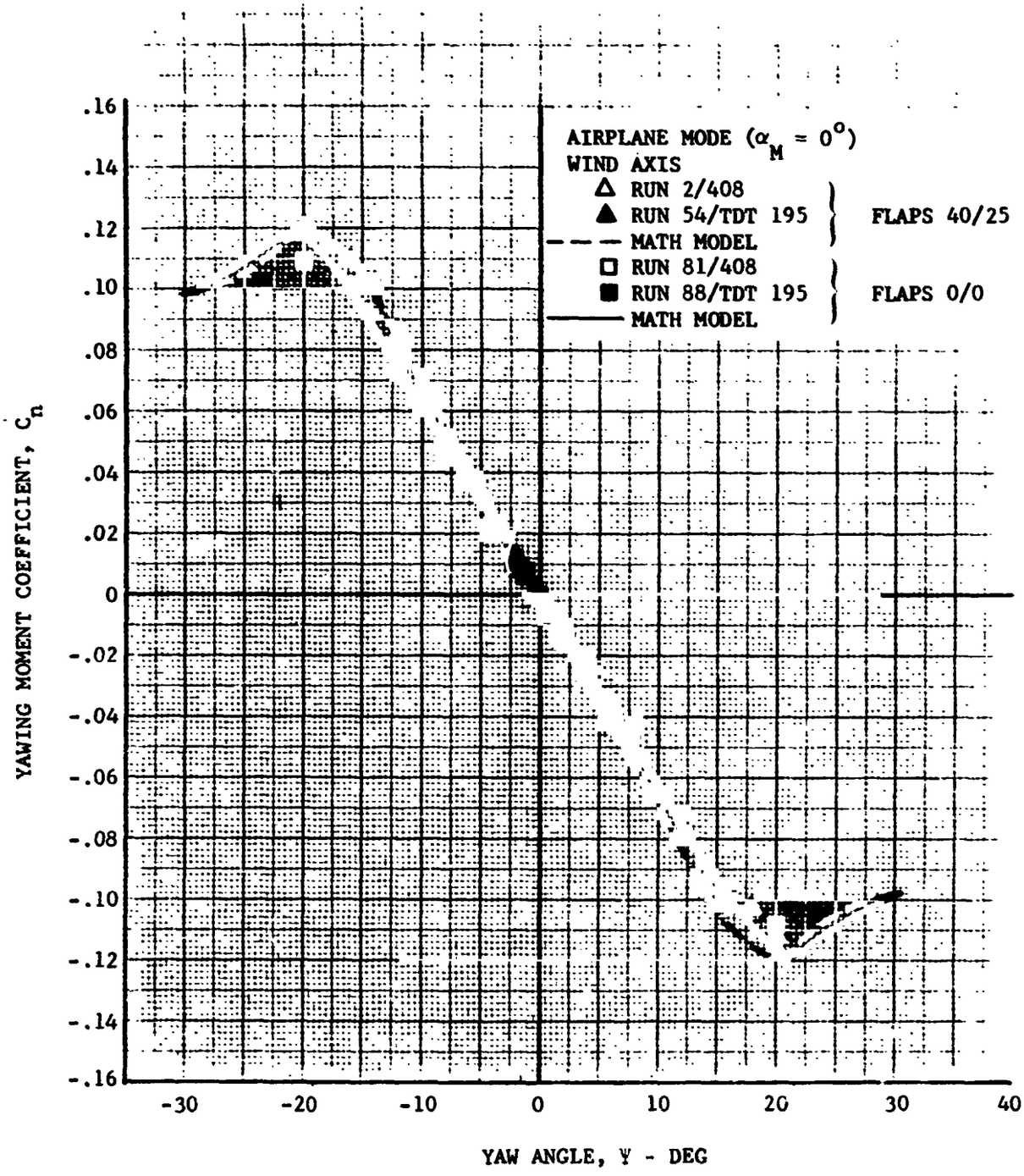

Figure III-17. Airplane Mode Yawing Moment Coefficient Correlation

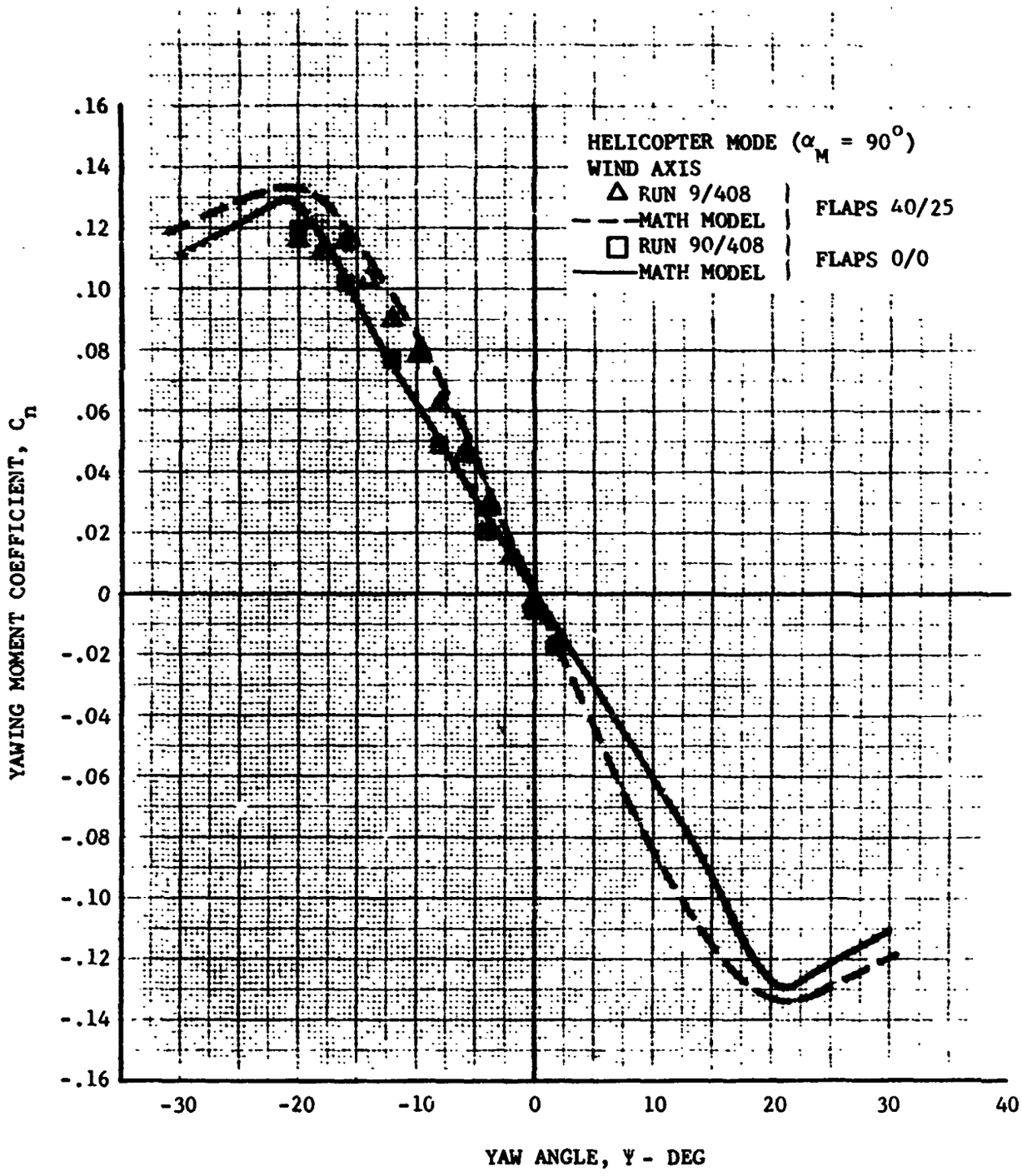

Figure III-18. Helicopter Mode Yawing Moment Coefficient Correlation

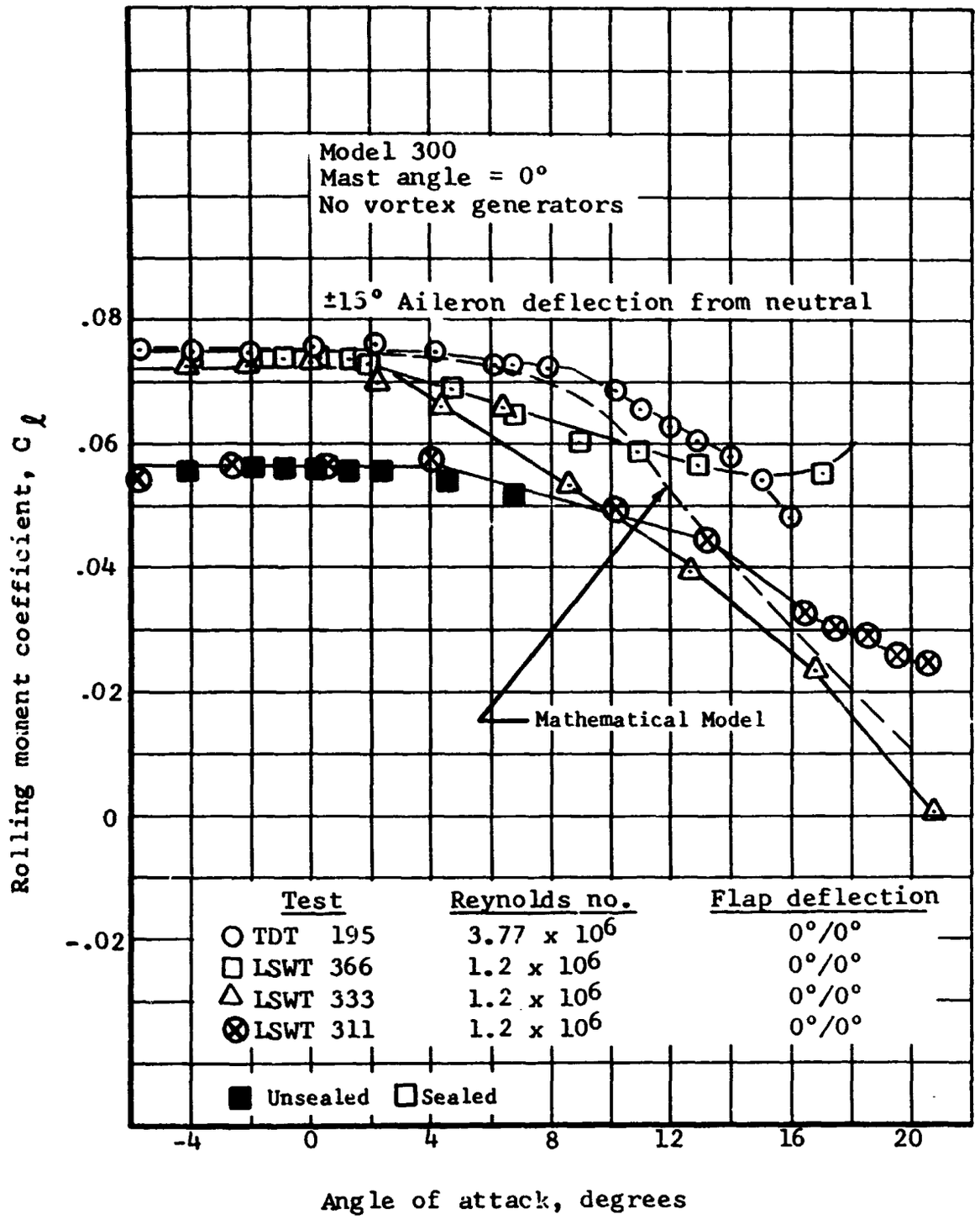

Figure III-19. Aileron Control Power Correlation

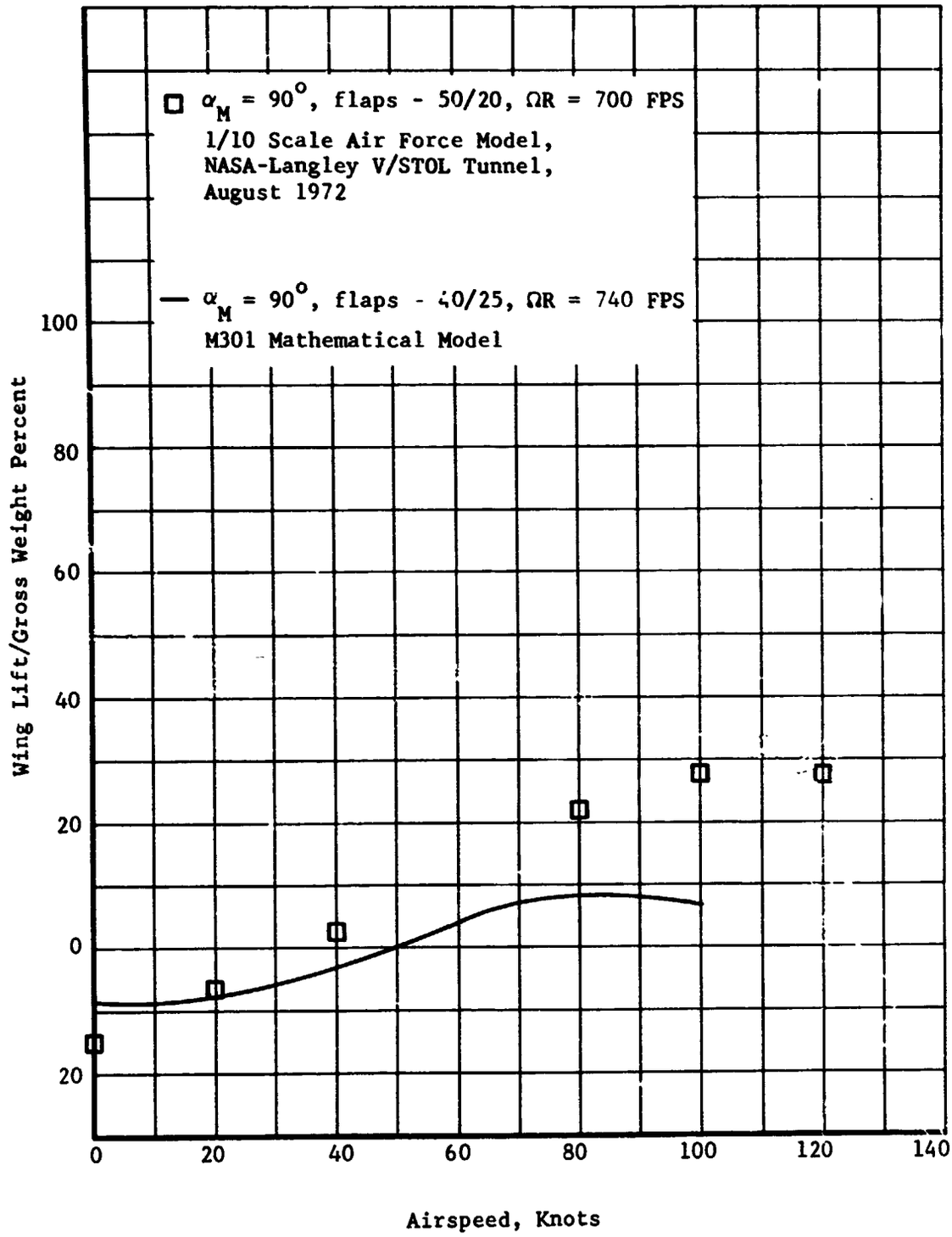

Figure III-20. Rotor Wake Effect on Wing Lift

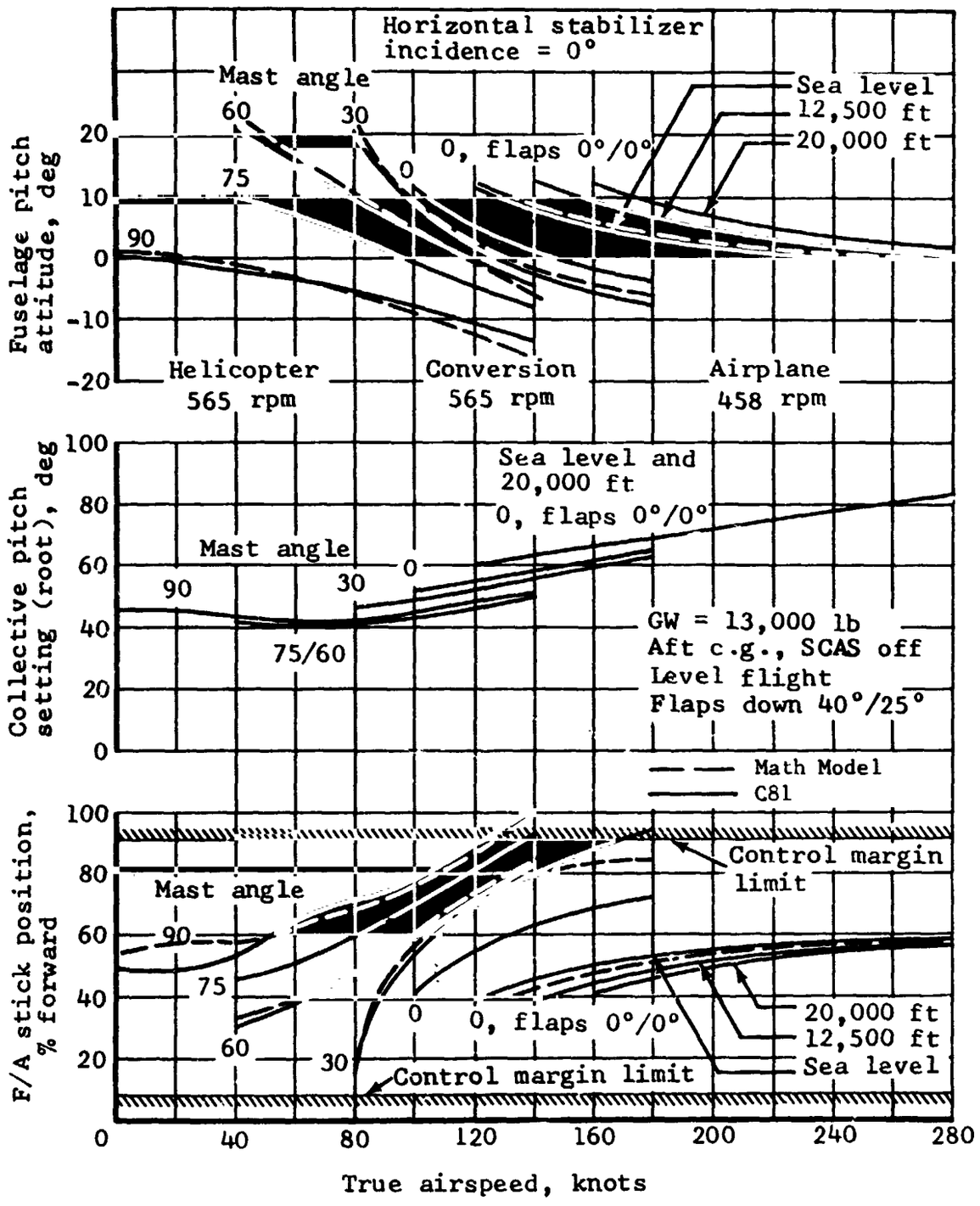

Figure III-21. Level Flight Trim Condition Correlation

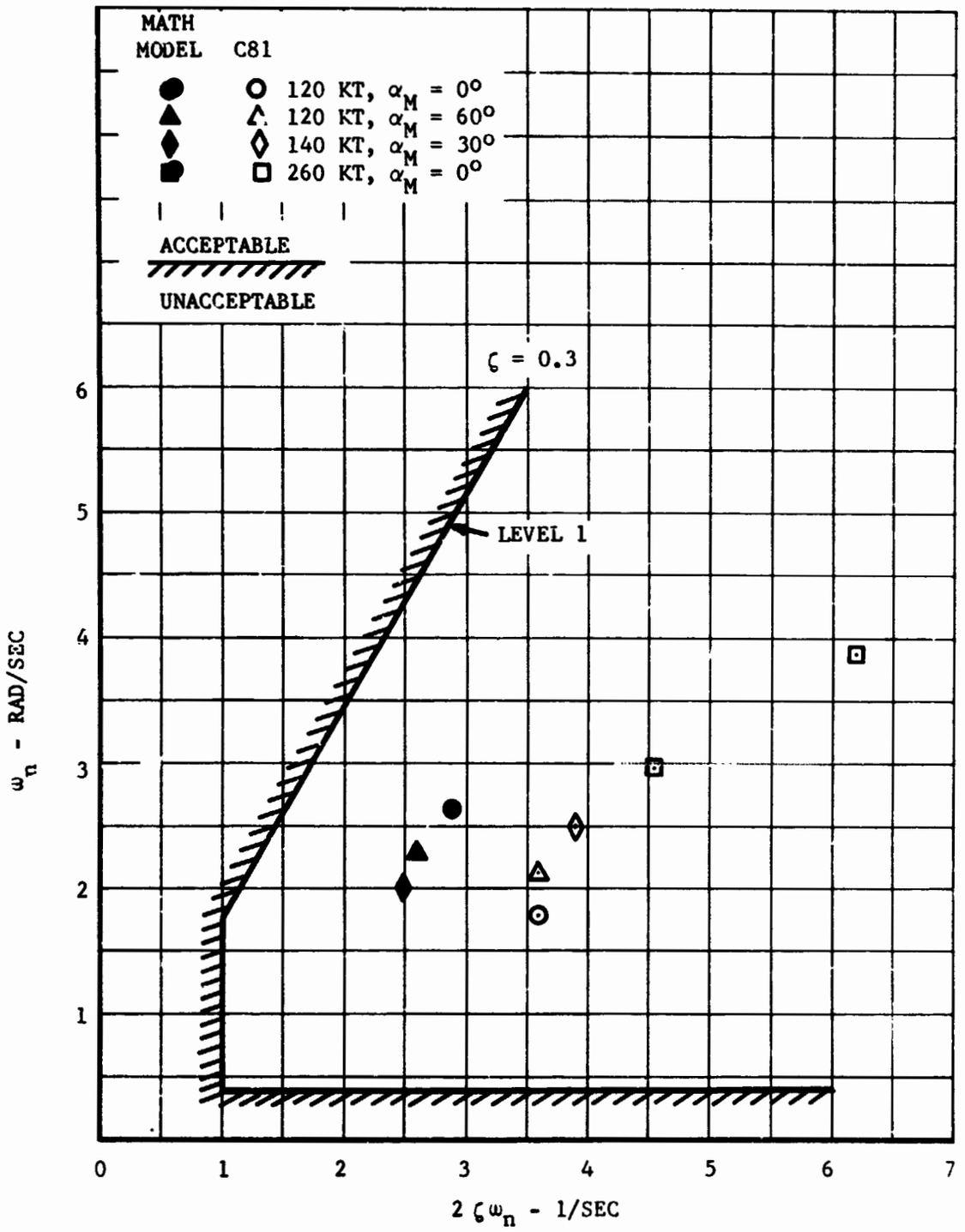

Figure III-22. Comparison of Longitudinal Oscillatory Mode Characteristics With MIL-F-83300 Response Requirements

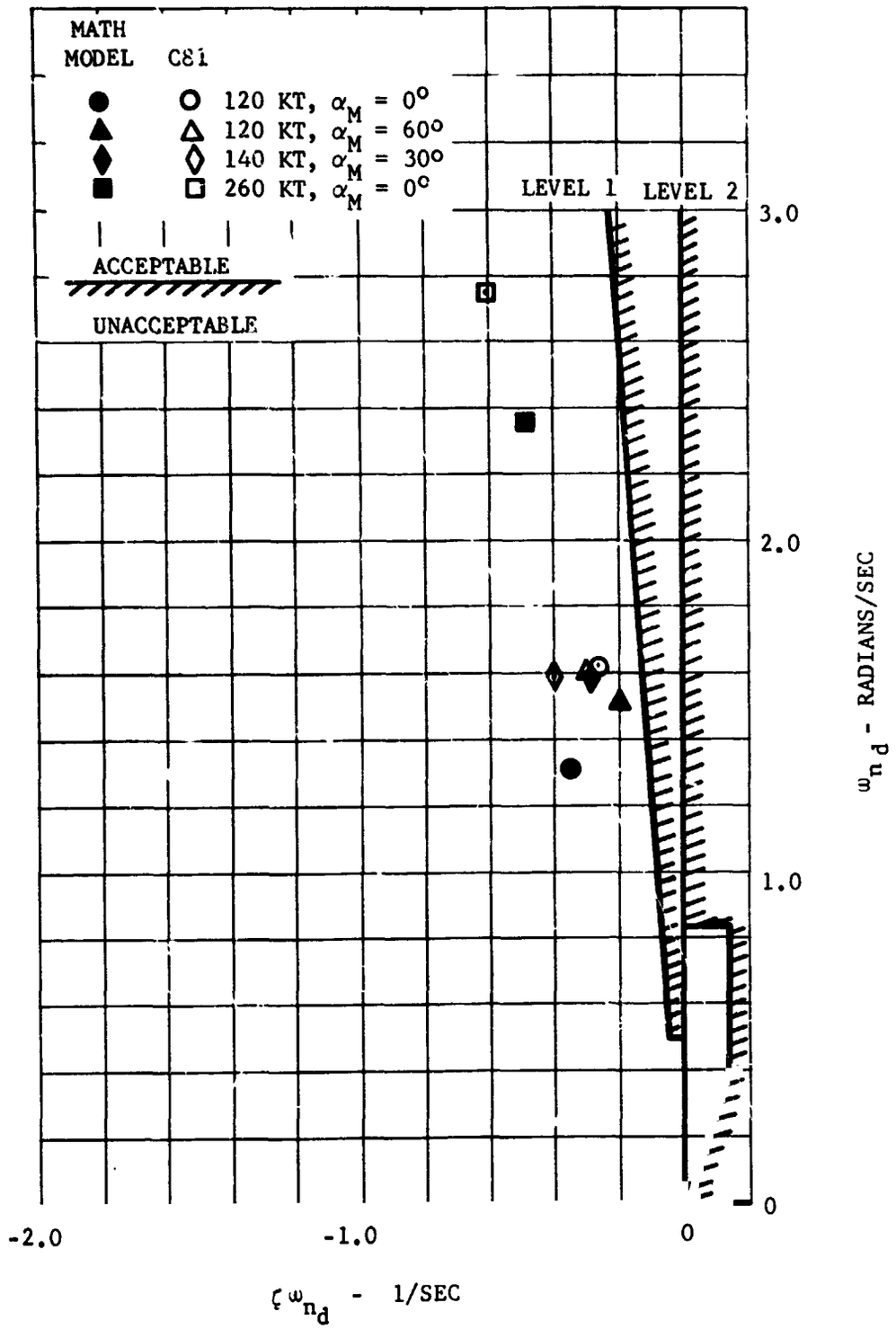

Figure III-23. Comparison of Lateral-Directional Oscillatory Mode Characteristics With MIL-F-83300 Response Requirements

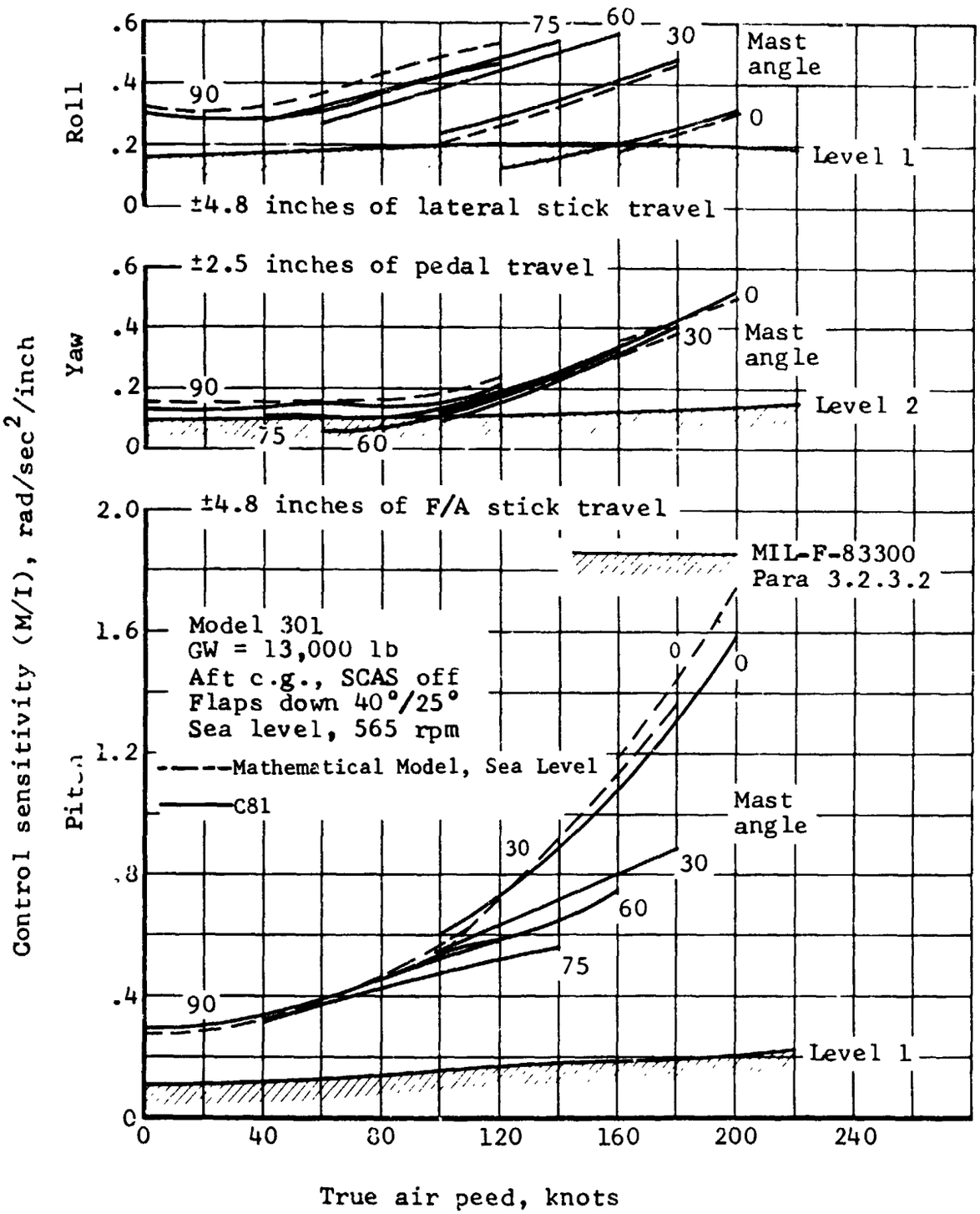

Figure III-24. Helicopter Conversion Mode Control Sensitivity Correlation

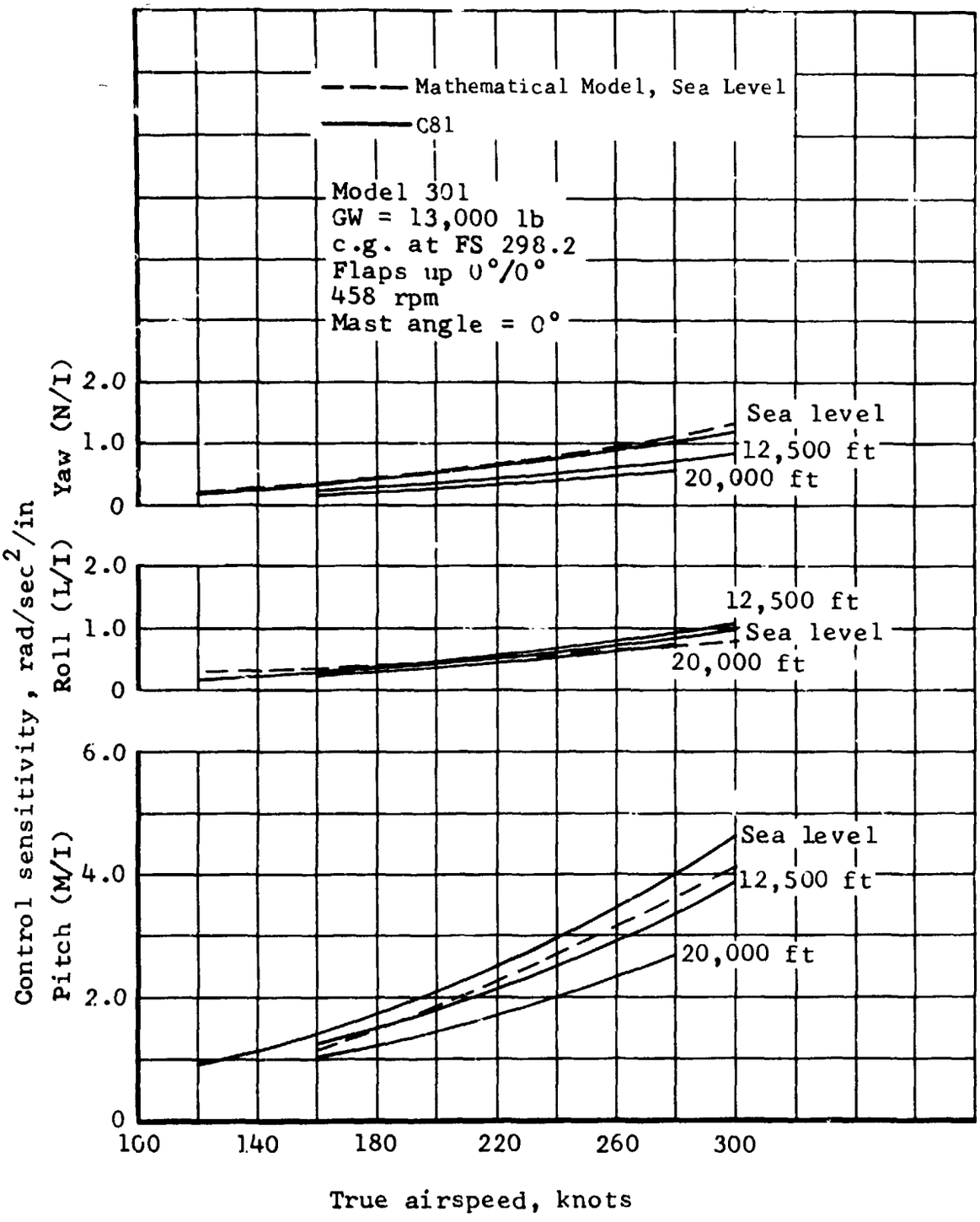

Figure III-25. Airplane Mode Control Sensitivity Correlation

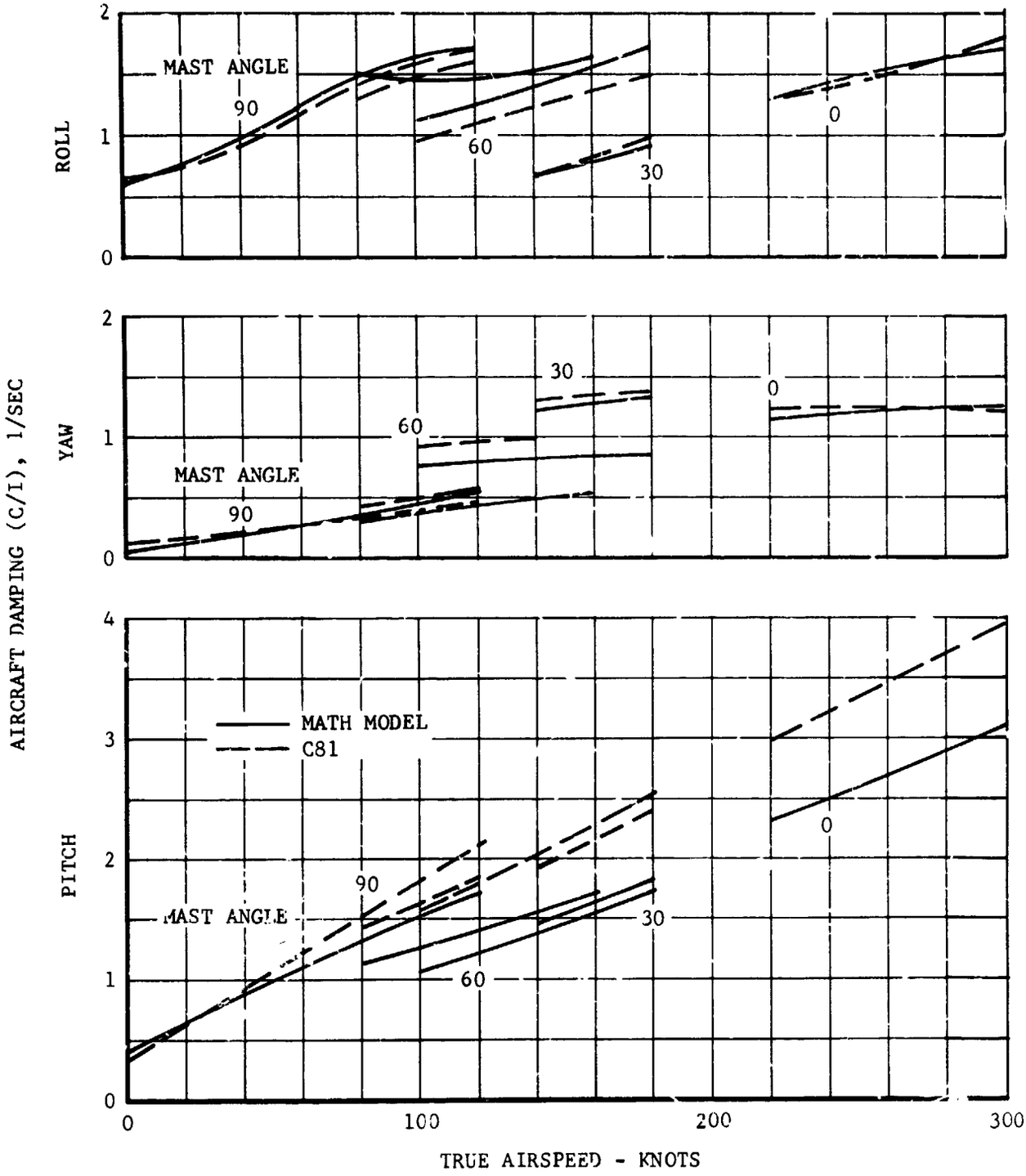

Figure III-26. Aircraft Damping Correlation

IV. CONTRACTOR EVALUATION OF FSAA SIMULATION

Contractor evaluation of the Model 301 research aircraft simulation on the NASA Ames FSAA to define deficiencies of the math model, computer program, and the simulator hardware was conducted prior to formal evaluation by the Army/NASA Tilt Rotor Project Office.

A. Math Model and Computer Program Deficiencies

(1) The rotor math model does not include stall or compressibility. The requirement to include these effects in the math model was deleted in order to meet the schedule for the Army/NASA evaluation. However, the first order effects of stall and compressibility have been included by limiting thrust to a value determined using an analysis which includes stall and compressibility and by arbitrarily modifying the rotor power required equation to obtain the correct power at maximum speed in the helicopter and airplane modes.

The rotor flapping time constant is approximated by the transport delay lagging the response to cyclic stick inputs by the computer frame time (0.048 seconds). This gives a minimum delay of 0.048 seconds and a maximum of 0.096 seconds compared to the rotor time constant in hover of 0.08 seconds.

A uniform inflow is assumed which means that lateral flapping in helicopter mode is inaccurate, and the tandem rotor effect on rotor induced velocity in sideward flight is not represented.

(2) Airframe aerodynamics are not adequate in rearward and sideward flight as accurate aerodynamics are limited to $\alpha,\beta = \pm 20$ degrees. While wing and tail stall are represented, the wing downwash at the tail is believed subject to error at angles of attack above wing stall.

A change in wing flap setting produces an abrupt change in lift, drag, and pitching moment. The flap setting changes instantaneously and is therefore not representative.

Wing dihedral effects are accurate only for sideslip angles less than ±12 degrees.

(3) Rotor downwash at the horizontal tail is accurate only for level flight as it is not varied as a function of angle of attack or sideslip.

Wake recirculation effects at the horizontal tail in ground effect are not accounted for.

(4) The SCAS and RPM governor systems have not been optimized. Further work on these systems is planned for the Phase II simulations.

However, their performance is satisfactory for preliminary evaluation of aircraft characteristics.

(5) With the aircraft on the ground and at full down collective pitch, a high frequency oscillation (approximately 5 cps) occurs. This apparently results from an unstable interaction between the landing gear math model and the rotor induced velocity math model. Raising the collective approximately one inch eliminates the oscillation.

(6) Several unexplainable computer "crashes" occurred when flying at α_{mast} = 60 degrees. These were not repetitive, in that flying back to the same condition did not result in a "crash". The cause of this problem has not yet been determined.

B. Simulator Hardware Deficiencies

(1) The cab controls are not representative of the Model 301. The cyclic stick has too much inertia which affects the pilots ability to hover (particularly SCAS off). In hover, numerous rapid and small amplitude motions are required. The high inertia causes a lag and an overshoot, resulting in over controlling. The cyclic also has an excess amount of free play in the force detent. The cyclic, with force feel on, is too "viscous" feeling. Smooth inputs and exact return to trim are difficult. Additionally, there is a ratcheting feel when moving the cyclic fore and aft.

With the force gradient off (magnetic brake button depressed) unacceptable high inertia and viscous damping forces are present. When the brake is released there is a large stick jump.

The pedals also have a high inertia causing lag and overshoot.

(2) The visual system has no peripheral capability making hovering flight very difficult. The resolution of the display is low causing difficulty in perception of small velocity and attitude changes further increasing the difficulty in hover.

(3) The instrument panel is a compromise between the two contractors, consequently the panel layout is not that of the Model 301.

(4) The absence of noise and vibration cues characteristic of rotary wing VTOL's reduces the flight condition information provided the pilot.

V. RECOMMENDATIONS FOR FURTHER DEVELOPMENT OF MODEL 301 SIMULATION

The following modifications and additions to the mathematical model, computer program, and FSAA hardware are recommended for implementation prior to the Phase II simulations:

A. Mathematical Model and Computer Program

1. Rotor

The rotor tip-path-plane flapping degrees of freedom should be included in the mathematical model to improve prediction of transient flapping and rotor inplane shear forces. Differential equations for rotor flapping have already been derived but were not implemented because they required a large increase in computer frame time. The problem with implementing the differential equations lies with the forward precession flapping mode which has a natural frequency of approximately two-per-rev. In order to include the flapping degrees of freedom in the mathematical model it will be necessary to find a means of eliminating the foward precession mode from the solution of the differential equations.

The rotor induced velocity must be modified to include non-uniform inflow and the tandem rotor effect in sideward flight.

2. Airframe

The mathematical model of the airframe aerodynamics should be extended to include ±180 degrees of angle of attack and sideslip so that the aerodynamics are completely valid in vertical, rearward, and sideward flight. Data from the tests of the Model 301 powered aeroelastic model can be used to guide this effort.

The wing downwash representation at angles of attack above wing stall should be improved.

The computer program should be modified to interpolate between flap settings and the flap extend/retract time should be added to the mathematical model.

A representation of the airframe buffet which accompanies lifting surface stall should be added to the model to provide the pilot with a stall cue

3. Rotor Wake-Airframe-Ground Interaction

The mathematical model of the rotor wake effects on the horizontal stabilizer and fins should be modified to reflect data from the test of the Model 301 powered aeroelastic model.

Ground effects on the wing and horizontal tail should be added to improve representation of STOL mode take off and landing.

4. Flight Controls and Subsystems

The mathematical model should be modified to include failures in the subsystems. This will require modeling all channels of the SCAS and RPM governor, the potential failure modes, and failure indicators.

5. Engine and Drive System

A mathematical model of the second engine and the refinements required to improve simulation of engine failure should be incorportated.

B. Simulator Hardware

1. Cab Cockpit

The FSAA cockpit should be mock-up to represent the Model 301 instrument panel layout, pedal and cyclic stick inertia and free play characteristics (new hardware will probably be necessary), and the power management system. In order to use the simulation to optimize the cockpit layout it will be necessary to represent exactly the location, size and shape of the various levers manipulated by the pilot. It will also be necessary to represent the instrument location and face characteristics. Location of all switches, knobs and indicator lights should be represented.

2. Noise Cues

A noise cue generator having noise characteristics appropriate to the Model 301 should be developed. The generator should include rotor, engine and drive system noise which varies as a function of rpm, power setting, conversion angle and airspeed.

VI. LIST OF REFERENCES

1. Anon: V/STOL Tilt Rotor Research Aircraft, Bell Helicopter Company Report Nos. 301-199-001 through 301-199-012, January 1973.

2. Rathert, G. A. Jr.: NASA Ames Simulation Sciences Division Simulator Facilities Description Sheets, April 1970.

3. McFarland, R. E.: Basic Flight Design, Computer Sciences Corporation PRO 103-71, 14 May 1971.

4. Anon: Wind Tunnel Tests of a Tilt-Proprotor Model (NASA Contract NAS1-11582), Bell Helicopter Company, February 1973.

5. Etkin, B.: Dynamics of Flight, John Wiley and Sons, 1959.

6. Gessow, A. and Crim, A.: An Extension of Lifting Rotor Theory to Cover Operation at Large Angles of Attack and High Inflow Conditions, NACA TN 2665, April 1952.

7. Castles, W. Jr. and New, N.: A Blade Element Analysis for Lifting Rotors That is Applicable for Large Inflow and Blade Angles and Any Reasonable Blade Geometry, NACA TN 2656, 1952.

8. Drees, J. M.: A Theory of Airflow Through Rotors and Its Application to Some Helicopter Problems, The Journal of The Helicopter Association of Great Britain, Vol. 3, No. 2, September 1949.

9. Mil, M. L., et al: Helicopter Calculation and Design - Volume 1, Aerodynamics, NASA TTF-494, September 1967.

10. Anon: USAF Stability and Control Datcom, Air Force Flight Dynamics Laboratory. Wright-Patterson Air Force Base, October 1960 (Revised September 1970).

11. Knight, Maud Wenzinger, C. J.: Wind Tunnel Tests on a Series of Wing Models Through a Large Angle of Attack Range, Part I - Force Tests, NACA Report No. 317.

12. Byrnes, A. L. et al: Effect of Horizontal Stabilizer Vertical Location on the Design of Large Transport Aircraft, Journal of Aircraft, April 1966.

13. Landgrebe, A.: An Analytical and Experimental Investigation of Helicopter Rotor Hover Performance and Wake Geometric Characteristics, USAAMRDL TR71-024.

14. Anon: T-53-L-11 Gas Turbine Engine Installation Instructions, Lycoming Report No. 13611.1, August 1966.

15. Anon: Advancement of Proprotor Technology, Task II - Wind Tunnel Test Results, NASA Contractor Report CR114363, September 1971.

16. Foster, R. and Sambell, K.: Full-Scale Hover Test of a 25-Foot Tilt Rotor, - Interim Report, Bell Helicopter Company Report No. 300-099-009, March 1973.

APPENDIX A

EQUATIONS FOR TILT-ROTOR FLIGHT SIMULATION PROGRAM

SUBSYSTEM NO. 1: ROTOR AERODYNAMICS

INPUTS

A. Variables

Subsystem Block No.	Symbol	Units
12		
	U	Ft/Sec
	V	Ft/Sec
11	W	Ft/Sec
	p	Rad/Sec
15	q	Rad/Sec
	r	Rad/Sec
8a	ρ	$Slug/Ft^3$
	M_N	1
2	β_N	Rad
19	W_{iR}	Ft/Sec
8a	Ω_R	Rad/Sec
	B_{1R}	Rad
	θ_{OR}	Rad
	A_{1R}	
2	W_{iL}	Ft/Sec
19	Ω_L	Rad/Sec
8a	B_{1L}	Rad
	θ_{OL}	Rad
	A_{1L}	
9	h_H	Ft

B. Coefficients

	Units
a_o, a_1, a_2	$1/rad, 1/\mu, 1/\mu^2$
$\delta_o, \delta_1, \delta_2$	$ND, 1/Deg, 1/Deg^2$
B	ND
C_T	ND
X_{SS}	ND

EQUATIONS

A. Blade Twist Constants (One Time Per Rotor)

$$K_{SO,m} = \frac{1}{\theta_1^m}\left[\cos\left(\theta_1^m X_m\right) - \cos\left(\theta_1^m X_{m-1}\right)\right]$$

$$K_{CO,m} = \frac{1}{\theta_1^m}\left[\sin\left(\theta_1^m X_{m-1}\right) - \sin\left(\theta_1^m X_m\right)\right]$$

$$K_{S1,m} = \frac{1}{\theta_1^m}\left[K_{CO,m} - \left(\left(X_{m-1}\cos\left(\theta_1^m X_{m-1}\right) - X_m \cos\left(\theta_1^m X_m\right)\right)\right)\right]$$

$$K_{C1,m} = \frac{-1}{\theta_1^m}\left[K_{SO,m} - \left(\left(X_{m-1}\sin\left(\theta_1^m X_{m-1}\right) - X_m \sin\left(\theta_1^m X_m\right)\right)\right)\right]$$

$$K_{S2,m} = \frac{2}{\theta_1^m} K_{C1,m} - \frac{1}{\theta_1^m}\left[(X_m - 1)^2 \cos\left(\theta_1^m X_{m-1}\right) - (X_m)^2 \cos\left(\theta_1^m X_m\right)\right]$$

$$K_{C2,m} = \frac{-2}{\theta_1^m} K_{S1,m} + \frac{1}{\theta_1^m}\left[(X_m - 1)^2 \sin\left(\theta_1^m X_{m-1}\right) - (X_m)^2 \sin\left(\theta_1^m X_m\right)\right]$$

$$K_{S3,m} = \frac{3}{\theta_1^m} K_{C2,m} - \frac{1}{\theta_1^m}\left[(X_{m-1})^3 \cos\left(\theta_1^m X_{m-1}\right) - (X_m)^3 \cos\left(\theta_1^m X_m\right)\right]$$

$$K_{C3,m} = \frac{-3}{\theta_1^m} K_{S2,m} + \frac{1}{\theta_1^m}\left[(X_{m-1})^3 \sin\left(\theta_1^m X_{m-1}\right) - (X_m)^3 \sin\left(\theta_1^m X_m\right)\right]$$

Where θ_1^m = twist rate of m^{th} segment $= \left(\frac{\theta_m - (\theta_{m-1})}{X_m - (X_{m-1})}\right)$

X_m = Radial station of m^{th} segment

θ_m = Blade pitch angle at m^{th} segment

$K_{Cn,m}$ = Blade twist constants

(n = 0, 1, 2, 3)

m = No. of segments of starting from tip (R = B) to root (R = 0)

Define,

$$TW1_n = \sum_1^m K_{Cn,m} \cos \Delta \theta_{Om}$$

$$TW2_n = \sum_1^m K_{Cn,m} \sin \Delta \theta_{Om}$$

$$TW3_n = \sum_1^m K_{Sn,m} \sin \Delta \theta_{Om}$$

$$TW4_n = \sum_1^m K_{Sn,m} \cos \Delta \theta_{Om}$$

Where, $\Delta \theta_{Om} = (\theta_m - \theta_R) - X_m \theta_1^m$, θ_R Blade pitch at the rotor center.

B. Initial Transformation Equations (One Time Per Rotor)

$$A = \pi R^2$$

$$DN' = AR^2$$

$$TD3 = TAN (\delta_3)$$

$$\sigma = \frac{n_b c_b}{\pi R}$$

$$\gamma' = \frac{cR^4}{I_b}$$

$$\gamma_m = p\gamma'$$

C. Long Term Transformations

1. Rotor Angular Velocity in Space.

$$\Omega'_R = \Omega_R + p \sin \beta_M \cos \phi_M + q \cos \beta_M \sin \phi_M - r \cos \beta_M \cos \phi_M$$

$$\Omega'_L = \Omega_L + p \sin \beta_M \cos \phi_M + q \cos \beta_M \sin \phi_M + r \cos \beta_M \cos \phi_M$$

2. 'Wind-Mast' Axis Angular Rates

Right Rotor

$$p_{WMR} = p_{HMR} \cos \xi_{WMR} + q_{HMR} \sin \xi_{WMR}$$

$$q_{WMR} = -p_{HMR} \sin \xi_{WMR} + q_{HMR} \cos \xi_{WMR}$$

where

$$p_{HMR} = p \cos \beta_M - q \sin \beta_M \sin \phi_M + r \sin \beta_M \cos \phi_M$$

$$q_{HMR} = q \cos \phi_M + r \sin \phi_M$$

$$\underset{p}{\Lambda}_{WMR} = \frac{p_{WMR}}{\Omega'_R} \qquad \underset{q}{\Lambda} = \frac{q_{WMR}}{\Omega'_R}$$

ξ_{WMR} - Wind azimuth angle defined to be equal to $\tan^{-1} \frac{V_{HMR}}{U_{HMR}}$

Left Rotor

$$p_{WML} = p_{HML} \cos \xi_{WML} + q_{HML} \sin \xi_{WML}$$

$$q_{WML} = -p_{HML} \sin \xi_{WML} + q_{HML} \cos \xi_{WML}$$

where

$$p_{HML} = -p \cos \beta_M - q \sin \beta_M \sin \phi_M - r \sin \beta_M \cos \phi_M$$

$$q_{HML} = q \cos \phi_M - r \sin \phi_M$$

$$\overset{\Lambda}{p}_{WML} = \frac{p_{WML}}{\Omega' L} \qquad \overset{\Lambda}{q}_{WML} = \frac{q_{WML}}{\Omega' L}$$

ξ_{WML} - Wind azimuth angle defined to be equal to $\tan^{-1} \frac{V_{HML}}{U_{HML}}$

3. Rotor Hub Velocity - Mast Axes

Right Rotor

$$U_{HMR} = U_{HBR} \cos \beta_M - V_{HBR} \sin \beta_M \sin \phi_M + W_{HBR} \sin \beta_M \cos \phi_M$$

$$V_{HMR} = V_{HBR} \cos \phi_M + W_{HBR} \sin \phi_M$$

$$W_{HMR} = -U_{HBR} \sin \beta_M - V_{HBR} \cos \beta_M \sin \phi_M + W_{HBR} \cos \beta_M \cos \phi_M$$

where,

$$U_{HBR} = U - q * L_{ZH} - r * L_{YH} \quad | \quad L_{XH} = \frac{(SL_{CG} - SL_{SP})}{12} + l_M \sin \beta_M \cos \phi_M$$

$$V_{HBR} = V + p * L_{ZH} + r * L_{XH} \quad | \quad L_{YH} = \frac{(BL_{SP} - BL_{CG})}{12} + l_M \sin \phi_M$$

$$W_{HBR} = W + p * L_{YH} - q * L_{XH} \quad | \quad L_{ZH} = \frac{(WL_{SP} - WL_{CG})}{12} + l_M \cos \beta_M \cos \phi_M$$

Left Rotor

$$U_{HML} = U_{HBL} \cos \beta_M + V_{HBL} \sin \beta_M \sin \phi_M + W_{HBL} \sin \beta_M \cos \phi_M$$

$$V_{HML} = -V_{HBL} \cos \phi_M + W_{HBL} \sin \phi_M$$

$$W_{HBL} = -U_{HBL} \sin \beta_M + V_{HBL} \cos \beta_M \sin \phi_M + W_{HBL} \cos \beta_M \cos \phi_M$$

where,

$$U_{HBL} = U - q * L_{ZH} + r * L_{YH}$$

$$V_{HBL} = V + p * L_{ZH} + r * L_{XH}$$

$$W_{HBL} = W - p * L_{YH} - q * L_{XH}$$

4. Aerodynamic Coefficients

Right Rotor

$$DN_R = \rho \Omega'^2_R \, DN'$$

$$DNQ_R = DN_R \, (\Omega'_R R/550)$$

$$\mu_R = \frac{\left[U^2_{HMR} + V^2_{HMR}\right]^{\frac{1}{2}}}{\Omega'_R R}$$

$$\lambda_{OR} = - \frac{W_{HMR}}{\Omega'_R R}$$

$$\xi_{WMR} = \text{TAN}^{-1} \frac{V_{HMR}}{U_{HMR}}$$

$$a_R = a_0 + \mu_R (a_1 - a_2 \mu_R) \qquad (a_0, a_1, a_2 \text{ - blade lift coefficients})$$

$$C_{KFAR} = \frac{2/3 \, K_{FA}}{I_b \Omega'^2_R} \quad ; \quad C_{KLTR} = \frac{2/3 \, K_{LT}}{I_b \Omega'^2_R}$$

$$\gamma_R = \frac{\rho a_R \, c R^4}{I_b} \left[1 + \frac{\mu_R}{2}\right] = \gamma_{MR} \left[1 + \frac{\mu_R}{2}\right]$$

$$\gamma_{MR} = \gamma_M \, a_R$$

Define,

$$Q_R = 0.5\,\sigma\, a_R\, (DN_R)$$

(For Left rotor replace subscript R with L)

D. Short Term Transformations
(Every update Cycle)

1. 'Wind-Market' Axis Cyclic Inputs
Right Rotor

$$\bar{A}_{1R} = A_{1R} \cos \xi_{WMR} - B_{1R} \sin \xi_{WMR}$$

$$\bar{B}_{1R} = A_{1R} \sin \xi_{WMR} + B_{1R} \cos \xi_{WMR}$$

(For left rotor replace subscript R with L)

2. Blade Pitch Constants
Right Rotor

$$C_{SnR} = (TW1_n - TW3_n) \sin \theta_{OR} + (TW2_n + TW4_n) \cos \theta_{OR}$$

$$C_{CnR} = -(TW2_n + TW4_n) \sin \theta_{OR} + (TW1_n - TW3_n) \cos \theta_{OR}$$

(For left rotor replace subscript R with L)

3. Performance Parameters
Right Rotor

$$\alpha_{rR} = \frac{7C_{TR}}{\sigma\, a_R}$$

$$C_{d_{fR}} = [\delta_0 + \alpha_{rR}\,(\delta_1 + \alpha_{rR}\,\delta_2)] \,/\, 2a_R$$

(For left rotor replace subscript R with L)

4. Thrust and Induced Velocity
Right Rotor

$$G = (0.76 + .24 * \frac{h_H}{2R})$$

$$\text{If } \sqrt{U^2 + V^2} > 30 \text{ OR } G > 1 \text{ SET } G = 1$$

(D1) $$Q_{3R} = \frac{T_R}{2B^2\, DN_R}$$

$$Q_{5R} = 0.6(|Q_{3R}|^{1.5})/(|Q_{3R}| + 8\mu_R^2)$$

$$\lambda_R = \lambda_{OR} + \lambda_{iR}$$

(D2) $$Q_{1R} = \lambda_{OR} + \frac{Q_{3R}\left[1 + (G-1)\left(\frac{\sqrt{U^2+V^2}}{30} - 1\right)^2\right]}{(\mu_R^2 + .866\,\lambda_R^2)^{.5} + \frac{Q_{5R}\,(|Q_{3R}| - {}^8/_3\,\lambda_R\,|\lambda_R|)}{(|Q_{3R}| + 8\,\lambda_R^2)}}$$

$$+ \frac{x_{ss}\, f(\mu_R)\, Q_{3R}}{\mu_R}$$

$$\lambda_{iR} = Q_{1R} - \lambda_{OR}$$

If $(|Q_{1R} - \lambda_R| > .001\,|\lambda_{iR}|)$ set $\lambda_R = Q_{1R}$ Go to (D2) (In IC only)

$$\lambda_R = 0.7\,Q_{1R} + 0.3\,\lambda_R$$

$$T_{2R} = Q_{6R}\left\{C_{S2R} + C_{SOR}\,\frac{\mu_R^2}{2} - \lambda_R\,(C_{C1R} + C_{d_{fR}}) - \frac{\bar{B}_1}{2}\left[\mu_R\,(C_{SOR}\,\lambda_R + 2\,C_{C1R})\right]\right\}$$

If $(|T_{2R} - T_R| > .001\,|T_R|)$ set $T_R = T_{2R}$ Go to (D1)

$$T_R = T_{2R}$$

$$C_{T_R} = \frac{T_R}{DN_R}$$

$$W_{iR} = \lambda_{iR}\,(\Omega'_R\,R)$$

(For λ_{iR} Initilization use $\lambda_{iR} = \text{Sign}\,Q_{3R} * (Q_{3R})^{.5}$)

Thrust Limit

If $T_R > \bar{T}_{(\mu)}$, Set $T_R = \bar{T}_R$

$$\bar{T}_R = C_{\bar{T}}\,f(\mu) * DN_R$$

(For Left Rotor replace subscript R with L)

5. Rotor Flapping (Wind-Mast Axis System)
Right Rotor

$$\begin{bmatrix} AR(1,1) & AR(1,2) & AR(1,3) \\ AR(2,1) & AR(2,2) & AR(2,3) \\ AR(3,1) & AR(3,2) & AR(3,3) \end{bmatrix} \begin{bmatrix} a_{0R} \\ a_{1R} \\ b_{1R} \end{bmatrix} = \begin{bmatrix} BR(1) \\ BR(2) \\ BR(3) \end{bmatrix}$$

$$AR(1,1) = \frac{2}{\gamma_{MR}} + \frac{\mu_R}{2} \bar{A}_{1R} C_{S2R}$$

$$AR(1,2) = \frac{1}{2} \bar{B}_{1R} \left(C_{S3R} - \frac{\mu_R^2}{4} C_{S1R}\right)$$

$$AR(1,3) = -\frac{1}{2} A_{1R} \left(C_{S3R} + \frac{\mu_R^2}{4} C_{S1R}\right) - \mu_R \tan\delta_3 \left(C_{C2R} + \frac{\lambda R}{2} C_{S1R}\right)$$

$$AR(2,1) = \frac{\mu_R^2}{4} \bar{A}_{1R} C_{S1R}$$

$$AR(2,2) = C_{C3R} - \frac{1}{4} \mu_R^2 \left(C_{C1R} + C_{d_{fR}}\right) + \frac{1}{2} \left[C_{d_{fR}} + \mu_R \bar{B}_{1R} C_{S2R}\right]$$

$$AR(2,3) = -\frac{\mu_R}{2} \bar{A}_{1R} C_{S2R} - C_{KLTR}$$

$$- \tan\delta_3 \left(C_{C3R} + \frac{3}{4} \mu_R^2 C_{C1R} + \lambda_R C_{S2R}\right)$$

$$AR(3,1) = -\mu_R \left[C_{C2R} + \frac{2}{3} C_{d_{fR}} + \frac{\mu_R}{4} \bar{B}_{1R} C_{S1R}\right]$$

$$AR(3,2) = \frac{\mu_R}{2} \bar{A}_{1R} C_{S2R} + C_{KFAR}$$

$$+ \tan\delta_3 \left(\frac{3}{4} \mu_R^2 C_{C1R} + \lambda_R C_{S2R} + C_{C3R}\right)$$

$$AR(3,3) = C_{C3R} + \frac{1}{2}\left\{C_{d_{fR}} + \mu_R\left[\bar{B}_{1R}\, C_{S2R} + \frac{\dot{\lambda}}{2}\,\mu_R\,(C_{C1R} + C_{d_{fR}})\right]\right\}$$

$$BR(1) = C_{S3R} + \frac{\mu_R^2}{2}\, C_{S1R} - \lambda_R\, C_{C2R} - \mu_R\, \bar{E}_{1R}\,(C_{C2R} + \frac{\lambda_R}{2}\, C_{S1R})$$

$$BR(2) = \mu_R\left[2\, C_{S2R} - \lambda_R\,(C_{C1R} + C_{d_{fR}})\right]$$
$$- \bar{B}_{1R}\,(C_{C3R} + \frac{3}{4}\mu_R^2\, C_{C1R} + \lambda_R\, C_{S2R}) - 4\,\frac{\hat{q}_{WMR}}{\gamma_{MR}}$$

$$BR(3) = \bar{A}_{1R}\,(\frac{\mu_R^2}{4}\, C_{C1R} + \lambda_R\, C_{S2R} + C_{C3R}) - \frac{4\hat{p}_{WMR}}{\gamma_{MR}}$$

6. Rotor flapping in mast axis system

$$a_{1R} = \bar{a}_{1R} \cos \xi_{WMR} + \bar{b}_{1R} \sin \xi_{WMR}$$

$$b_{1R} = -\bar{a}_{1R} \sin \xi_{WMR} + \bar{b}_{1R} \cos \xi_{WMR}$$

(For left rotor replace R with L)

7. Rotor Inplane Forces in Wind-Mast Axis System (Right Rotor)

$$\bar{H}_R = Q_{6R}\left\{\frac{1}{2}\, C_{SOR}\,\mu_R\,\lambda_R + C_{S2R}\left(\bar{a}_{1R} - \frac{\hat{p}}{2}\right) - \frac{1}{3}\, C_{C1R}\,\lambda_R\,\bar{b}_{1R}\right.$$

$$\left. + C_{C1R}\left[\frac{\mu_R}{2}\,(a_{OR}^2 + \bar{a}_{1R}^2) - \frac{3}{2}\,\lambda_R\,\bar{a}_{1R} + \hat{p}\,\lambda\right]\right.$$

(Equation Continued on Next Page)

$$- \frac{\bar{B}_{1R}}{2}\left[C_{SOR}\,\lambda_R^2 + C_{S2R}\,\bar{a}_{1R}^{\,2} + C_{C1R}\,(\lambda_R + \mu_R\,\bar{a}_{1R})\right]$$

$$+ \frac{A_{1R}}{2}\left[\frac{1}{4}\,C_{SOR}\,\lambda_R\mu_R\,\bar{b}_{1R} + C_{S1R}\,\lambda_R\,a_{OR} + C_{C2R}\,a_{OR}\right] + C_{d_{fR}}\,\mu_R\Bigg\}$$

$$\bar{Y}_R = Q_{6R}\Bigg\{C_{S2R}\left(\bar{b}_{1R} - \frac{\Lambda_q}{2}\right) - \frac{3}{2}\,C_{S1R}\,\mu_R\,a_{OR} - \frac{3}{2}\,C_{C1R}\,\lambda_R\,\bar{b}_{1R}$$

$$+ \frac{1}{3}\,C_{C1R}\,\lambda_R\,\bar{a}_{1R} - C_{C1R}\,\lambda_R\,\Lambda_q$$

$$+ \bar{B}_{1R}\Big[-\frac{1}{8}\,C_{SOR}\,\lambda_R\,\mu_R\,\bar{b}_{1R} + \frac{1}{2}\,C_{S1R}\,\lambda_R\,a_{OR}$$

$$+ \frac{1}{2}\,C_{C2R}\,a_{OR} - C_{C1R}\,\mu_R\,\bar{b}_{1R}\Big]$$

$$+ \frac{\bar{A}_{1R}}{2}\Big[C_{SOR}\,\lambda_R\,(\lambda_R - \mu_R\,\bar{a}_{1R}) + C_{S2R}\,\bar{b}_{1R}^{\,2}$$

$$+ C_{C1R}\,(\lambda_R - \mu_R\,\bar{a}_{1R})\Big]\Bigg\}$$

8. Rotor Inplane Forces in Mast Axis System

$$H_R = \bar{H}_R \cos \xi_{WMR} + \bar{Y}_R \sin \xi_{WMR}$$

$$Y_R = -\bar{H}_R \sin \xi_{WMR} + \bar{Y}_R \cos \xi_{WMR}$$

(For Left rotor replace subscript R with L)

9. Rotor Power and Torque Required

$$HP_{REQ\ R} = (DNQ_R)\frac{\sigma a_R}{2}\Bigg\{C_{C1R}\left(\lambda_R \mu_R \bar{a}_{1R} - \lambda_R^2\right) + C_{S2R}\lambda_R - \frac{1}{2}C_{C3R}\left(a^2_{1R} + b^2_{1R}\right) + \frac{1}{2}C_{d_{fR}}\left(1 + 280\,\mu^3_R + 60\,\lambda^3_R\right) - \bar{B}_{1R}\left[\frac{1}{2}C_{C3R}\bar{a}_{1R} + \frac{1}{2}C_{C1R}\lambda_R\mu_R + C_{S2P}\lambda_R\bar{a}_{1R}\right] + \bar{A}_{1R}\left[\frac{1}{2}C_{C3R}\bar{b}_{1R} - \frac{1}{2}C_{C2R}\mu_R a_{OR} + C_{S2R}\lambda_R\bar{b}_{1R}\right]\Bigg\}$$

$$Q_R = \frac{(550)\,HP_{REQ\ R}}{\Omega'_R}$$

(For Left rotor replace subscript R with L)

10. Rotor Moments in Mast Axis System

$$M_{a_{1R}} = K_{FA}\,a_{1R}$$

$$l_{b_{1R}} = K_{LT}\,b_{1R}$$

(For left rotor replace subscript R with L)

OUTPUTS

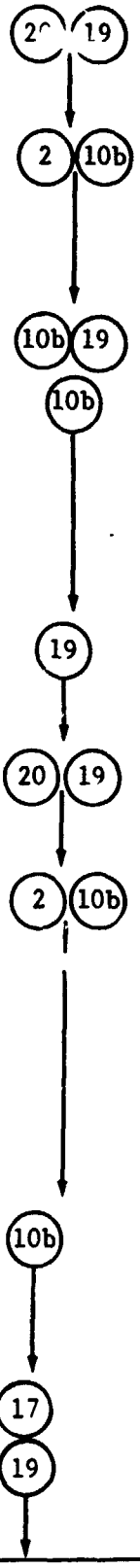

Symbol	Units
a_{1R}	Rad
b_{1R}	Rad
T_R	Lbs
H_R	Lbs
Y_R	Lbs
Q_R	Lb/Ft
$M_{a_{1R}}$	Lb/Ft
$l_{b_{1R}}$	Lb/Ft
$HP_{REQ\ R}$	HP
$\dot{a}_{1R}$	Rad/Sec
$\dot{b}_{1R}$	Rad/Sec
a_{1L}	Rad
b_{1L}	Rad
T_L	Lbs
H_L	Lbs
Y_L	Lbs
W_{iL}	Ft/Sec
Q_L	Lb/Ft
$M_{a_{1L}}$	Lb/Ft
$l_{b_{1L}}$	Lb/Ft
$HP_{REQ\ L}$	HP
$\dot{a}_{1L}$	Rad/Sec
$\dot{b}_{1L}$	Rad/Sec

SUBSYSTEM NO. 2: ROTOR INDUCED VELOCITIES

INPUTS:

A. Variables

Subsystem Block No.	Symbol	Units
1	T_R	Lbs
	H_R	Lbs
	Y_R	
	T_L	Lbs
	H_L	Lbs
	Y_L	Lbs
	W_{iL}	Ft/Sec
8a	β_M	Rad

B. Coefficients

	Units
K_0, K_1, K_2, K_3, K_4	ND
h_0, h_1, h_2, h_3, h_4	ND

EQUATIONS:

Rotor Wake

$$R_{WL} = R\left\{0.78 + 0.22\ EXP\left[-(0.3 + 2Z\sqrt{C_{RFL}} + 60\ C_{RFL})\right]\right\}$$

where

$$Z = \frac{(WL_{HUB} - WL_W)\beta_M = 0}{12R}$$

$$C_{RFL} = \frac{\left(T_L^{\ 2} + H_L^{\ 2} + Y_L^{\ 2}\right)^{\frac{1}{2}}}{\rho\ \pi\ \Omega_L'^{\ 2}\ R^4}$$

Rotor Wake at Wing, Horizontal Stabilizer and Vertical Stabilizer in Mast Axes

(For rotor wake effects on the left and right wing, on the horizontal stabilizer and on the vertical stabilizer, the values of the left rotor induced velocity will be used.)

Wing

$$W_i\Big|_{R/WL} = (K_0 + K_1\ \mu_L + K_2\ \mu_L^2 + K_3\ \lambda_L + K_4\ \lambda_L^2)\ W_{iL}$$

Horizontal Stabilizer

$$W_i\Big|_{R/H} = \left[h_0 + h_1\ \beta_M + (h_2 + h_3\ \beta_M)\left(\frac{(U - 168.89 + h_4\ \beta_M)}{168.89}\right)^2\right]\ W_{iL}$$

Vertical Stabilizer

$$W_i\Big|_{R/V} = W_i\Big|_{R/H}$$

Components of Rotor Wake in Body Axes:

Wing:

$$U_i\Big|^B_{R/WL} = W_i\Big|_{R/WL} \sin \beta_M$$

$$W_i\Big|^B_{R/WL} = -W_i\Big|_{R/WL} \cos \beta_M$$

Horizontal Stabilizer:

$$U_i\Big|^B_{R/H} = W_i\Big|_{R/H} \sin \beta_M$$

$$W_i\Big|^B_{R/H} = -W_i\Big|_{R/H} \cos \beta_M$$

Vertical Stabilizer:

$$U_i\Big|^B_{R/V} = U_i\Big|^B_{R/H}$$

$$W_i\Big|^B_{R/V} = W_i\Big|^B_{R/H}$$

OUTPUTS

Subsystem Block No.	Symbol	Units
4	$U_i\|^{B}_{R/WL}$	Ft/Sec
	$W_i\|^{B}_{R/WL}$	Ft/Sec
	R_{WL}	Ft/Sec
5	$U_i\|^{B}_{R/H}$	Ft/Sec
	$W_i\|^{B}_{R/H}$	Ft/Sec
6	$U_i\|^{B}_{R/V}$	Ft/Sec
	$W_i\|^{B}_{R/V}$	Ft/Sec

SUBSYSTEM NO. 3-FUSELAGE AERODYNAMICS

INPUTS

A. Variables

Subsystem Block No.	Symbol	Units
(12)	V_T	Ft/Sec
	α_F	Deg
	β_F	Deg

B. Aerodynamic Coefficients

	Units
L_0, L_1	$Ft^2, \frac{Ft^2}{Deg}$
D_0, D_1, D_2, D_3, D_4	$Ft^2, \frac{Ft^2}{Deg}, \frac{Ft^2}{Deg^2}, \frac{Ft^2}{Deg}, Ft^2$
M_0, M_1, M_2	$Ft^3, \frac{Ft^3}{Deg}, \frac{Ft^3}{Deg}$
Y_0, Y_1, Y_2	$Ft^2, \frac{Ft^2}{Deg}, \frac{Ft^2}{Deg^2}$
l_0, l_1	$Ft^3, \frac{Ft^3}{Deg}$
N_0, N_1	$Ft^3, \frac{Ft^3}{Deg}$

EQUATIONS:

$$q_F = \frac{1}{2} \rho V_T^2$$

For α_F and $\beta_F \leq 20^\circ$

$$L_F = q_F (L_0 + L_1 \alpha_F)$$

$$D_F = q_F (D_0 + D_1 \alpha_F + D_2 \alpha_F^2 + D_3 |\beta_F|)$$

$$M'_F = q_F (M_0 + M_1 \alpha_F + M_2 |\beta_F|) = q_F (M_\alpha f(\alpha_F) + M_2 |\beta_F|)$$

$$Y'_F = q_F (Y_0 + Y_1 \beta_F + Y_2 \beta_F |\beta_F|)$$

$$l'_F = q_F (l_0 + l_1 \beta_F)$$

$$N'_F = q_F (N_0 + N_1 \beta_F)$$

For α_F and $\beta_F > 20^\circ$

For $\alpha_F > 20^\circ$, $\beta_F < 70^\circ$

$$\left.\begin{aligned} L_F &= L_F \\ D_F &= D_F \end{aligned}\right\} \quad \text{at } \alpha_F = \pm 20^\circ$$

$M_F = M_F$ at $\alpha_F = \pm 40^\circ$, $\beta_F = \pm 20^\circ$

$20^\circ < \beta_F < 70^\circ$

$$\left.\begin{aligned} Y'_F &= Y'_F \\ l'_F &= l'_F \\ N'_F &= N'_F \end{aligned}\right\} \quad \text{At } \beta_F = \pm 20^\circ$$

For $\beta_F > 70^\circ$,

$$L_F = M_F = Y'_F = l'_F = N'_F = 0 \qquad D_F = q_F D_4$$

} Wind axis system

OUTPUTS:

Subsystem Block No.	Symbol	Units
10a	L_F	Lbs.
	D_F	Lbs.
	Y'_F	Lbs.
	M'_F	Ft-Lbs
	l'_F	Ft-Lbs
	N'_F	Ft-Lbs

SUBSYSTEM NO. 4-WING-PYLON AERODYNAMICS

INPUTS:

A. Variables

Subsystem Block No.	Symbol	Units
2	$U_i\|^B_{R/WL}$	Ft/sec
	$W_i\|^B_{R/WL}$	Ft/sec
	R_{WL}	Ft
8a	β_M	Deg
	F_X	F_1, F_2, F_3, F_4
	δ_a	Deg
12	V_T	Ft/sec
	α_F	Deg
	β_F	Deg
	U	Ft/sec
	V	Ft/sec
	W	Ft/sec
15	ρ	$Slug/ft^3$
	M_N	ND
11	p	Rad/sec
	q	Rad/sec
	r	Rad/sec

B. Aerodynamic Coefficients

	Units
$C_{L_{WP}}$, $C_{L_{\delta a}}$	ND, 1/Deg
C_{DWP}	ND
$C_{MO_{WP}}$	ND
$\epsilon_{W/H}$	Deg
$X_{R/W}$, $X_{W/R}$	ND, ND
$C_{y\beta}\Big\vert_{M_N = 0}$	1/Rad
$C_{yp}/C_L\Big\vert_{M_N = 0}$	1/Rad
$C_{yr}\Big\vert_{M_N = 0}$	1/Rad
$C\ell_\beta\Big\vert_{\substack{C_L = 0 \\ M_N = 0}}$, $C\ell_\beta/C_{LWP}\Big\vert_{M_N = 0}$	1/Rad, 1/Rad
$C\ell_p\Big\vert_{\substack{C_L = 0 \\ M_N = 0}}$	1/Rad
$C\ell_r/C_{LWP}\Big\vert_{M_N = 0}$, $\Delta C\ell r/(\frac{\partial\alpha}{\partial\delta_f})\,\delta_f$	1/Rad, 1/Deg
$C_{n\beta}\Big\vert_{\substack{M_N = 0, \\ C_L = 0}}$, $C_{n\beta}/C_{L^2_{WP}}\Big\vert_{M_N = 0}$	1/Rad, 1/Rad
$C_{np}/C_{LWP}\Big\vert_{M_N = 0}$	1/Rad
$C_{nr}/C_{L^2_{WP}}$, $C_{nr}/C_{D_{o_{WP}}}$	1/Rad, 1/Rad
$C\ell_{\delta a}$, $\ell_{\delta a}$	1/Deg, ND
$n_{o\delta a}$, $K_{n\delta a}$	1/Deg, ND
K_{np}	ND

7872 8-76

EQUATIONS

A. Wing Aerodynamics Affected by Rotor Wake

Computation of wing areas S_{iWR} and S_{iWL} under the rotor wakes.

In this subsection, K is a dummy subscript. It is replaced by R and L while computing S_{iWR} and S_{iWL} respectively.

The logical flow chart shows the sequence of computations necessary for determining S_{iWK}.

$F_1(C_{1K}, C_{2K})$ and $F_2(C_{1K}, C_{2K})$ are procedures representing computation of a contribution to the wing-area in a rotor wake.

$F_1(C_{1K}, C_{2K})$

$$S_{iWK} = S_{iWK} + A_{1K}$$

$$XA_K = XA_K + XA_{1K}$$

$$YA_K = YA_K + XA_{1K} \sin \delta_K$$

$F_2(C_{1K}, C_{2K})$

$$S_{iWK} = S_{iWK} + \frac{1}{2} A_{1K} + \frac{R_{WYK}}{2R_{WXK}} (\sin \delta_k)(C_{2K}^2 - C_{1K}^2)$$

$$- Y_{TIPK}(C_{2K} - C_{1K})$$

$$XA_K = XA_K + \frac{1}{2} XA_{1K} + \frac{R_{WYK}}{3R_{WXK}} (\sin \delta_K)(C_{2K}^3 - C_{1K}^3)$$

$$- Y_{T1PK} (C_{2K}^3 - C_{1K}^3)$$

$$YA_K = YA_K + \left[\frac{1}{2}XA_{1K} \sin \delta_K + \frac{R_{WYK}}{6R_{WXK}} (\sin^2 \delta_K - \cos^2 \delta_K)\right.$$

$$\left.(C_{2K}^3 - C_{1K}^3) + \frac{1}{2} (R_{WXK} R_{WYK} \cos^2 \delta_K - Y_{T1PK}^2) * (C_{2K} - C_{1K})\right] \frac{R_{WYX}}{R_{WXK}}$$

where:

$$\theta_{C_{1K}} = \sin^{-1} \frac{C_{1K}}{R_{WXK}}$$

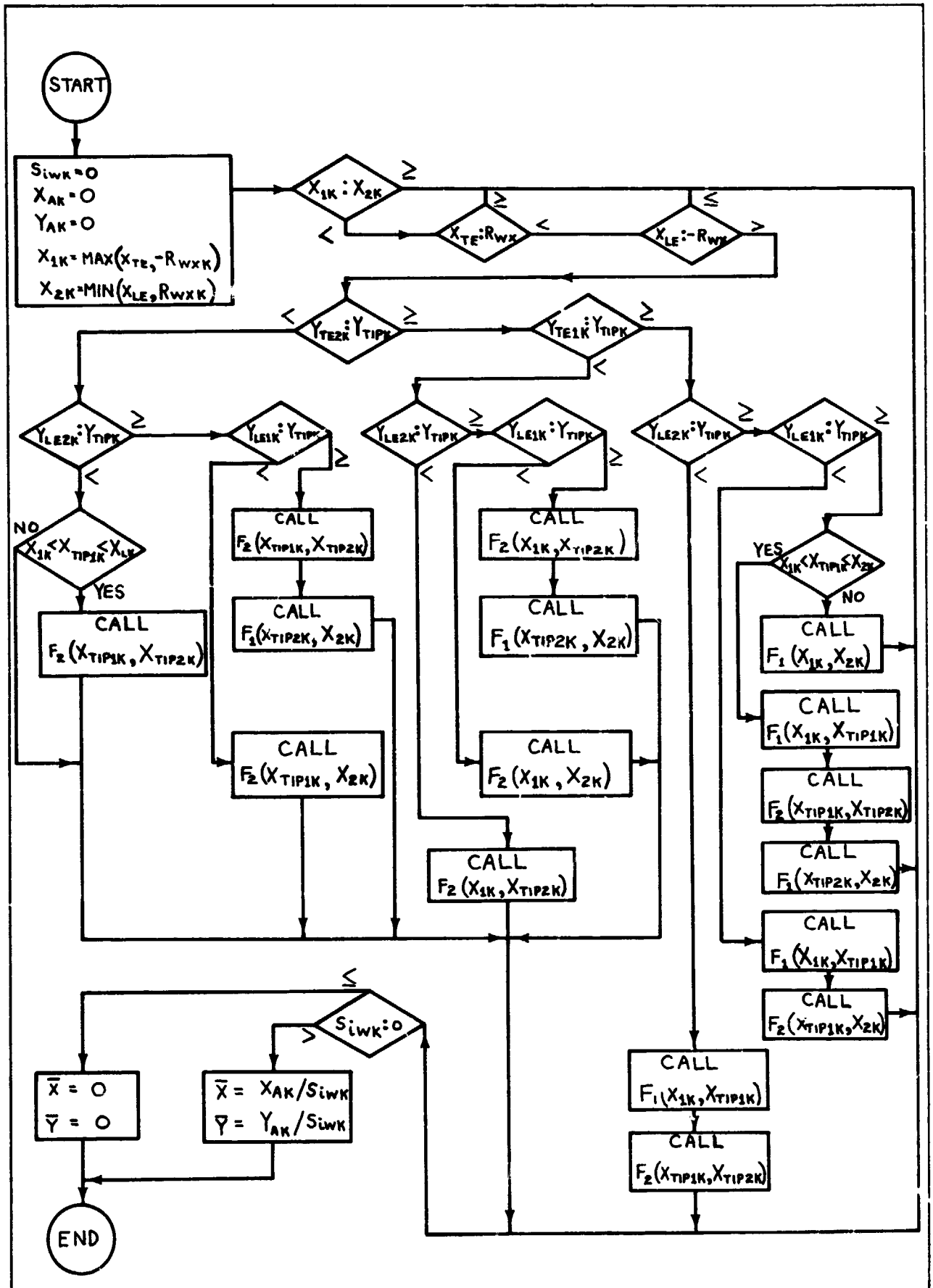

$$\theta_{C_{2K}} = \sin^{-1} \frac{C_{2K}}{R_{WXK}}$$

$$A_{1K} = R_{WXK} R_{WYK} |\cos\delta_K| \left[\sin \theta_{C_{2K}} \cos \theta_{C_{2K}} - \sin \theta_{C_{1K}} \cos \theta_{C_{1K}} + \theta_{C_{2K}} - \theta_{C_{1K}} \right]$$

$$XA_{1K} = - \frac{2}{3} \frac{R_{WYK}}{R_{WXK}} |\cos \delta_K| \left[(R_{WXK}^2 - C_{2K}^2)^{3/2} - (R_{WXK}^2 - C_{1K}^2)^{3/2} \right]$$

and:

$$l' = l_M \cos \beta_M$$

$$U_{WK} = - U - W_i|_{R/WL} \sin \beta_M$$

$$V_{WR} = V, \; V_{WL} = -V$$

$$W_{WK} = - W + W_i|_{R/WL} \cos \beta_M$$

If MAX ($|U_{WK}|$, $|V_{WK}|$) > 100 $|W_{WK}|$

Use:

$$\frac{U_{WK}}{W_{WK}} = \frac{100 \; U_{WK}}{\text{MAX} (U_{WK}, V_{WK})}$$

$$\frac{V_{WK}}{W_{WK}} = \frac{100 \; V_{WK}}{\text{MAX} (U_{WK}, V_{WK})}$$

$\bar{\epsilon}$ is the distance forward from wing trailing edge to shaft pivot.

$$\bar{\epsilon} = \frac{(SL_{WTE} - SL_{SP})}{12}$$

$$X_{TEK} = - \bar{\epsilon} - l_M \sin \beta_M - l' \frac{U_{WK}}{W_{WK}}$$

$$X_{LEK} = c_W + X_{TEK}$$

$$Y_{T1PK} = - \frac{V_{WK}}{W_{WK}} l'$$

$$\delta_K = \tan^{-1} \left(\frac{V_{WK}}{W_{WK}} \sin \beta_M \right)$$

$$R_{WXK} = \left| R_{WK} \left(- \cos \beta_M + \frac{U_{WK}}{W_{WK}} \sin \beta_M \right) \right|$$

$$R_{WYK} = R_{WK} \sqrt{1 + \left(\frac{V_{WK}}{W_{WK}} \sin \beta_M \right)^2}$$

$$\text{If } \left(R^2 - X^2 \text{ or } R^2 - Y^2 \right) \leq 0 \text{ then } \left(\sqrt{R^2 - X^2} \text{ or } \sqrt{R^2 - Y^2} \right) = 0$$

$$\text{If } X_{TE}^2 > R_{WK}^2 \text{ and } X_{TE} > 0, \text{ then } S_{iWK} = 0$$

$$Y_{TE1K} = \frac{R_{WYK}}{R_{WXK}} \left(X_{TEK} \sin \delta_K - |\cos \delta_K| \sqrt{R_{WXK}^2 - X_{TEK}^2} \right)$$

$$Y_{TE2K} = \frac{R_{WYK}}{R_{WXK}} \left(X_{TEK} \sin \delta_K + |\cos \delta_K| \sqrt{R_{WXK}^2 - X_{TEK}^2} \right)$$

$$\text{If } X_{LE}^2 > R_{WX}^2 \text{ and } X_{LE} < 0 \text{ then } S_{iWK} = 0$$

$$Y_{LE1K} = \frac{R_{WYK}}{R_{WXK}} \left(X_{LEK} \sin \delta_K - |\cos \delta_K| \sqrt{R_{WXK}^2 - X_{LEK}^2} \right)$$

$$Y_{LE2K} = \frac{R_{WYK}}{R_{WXK}}\left(X_{LEK}\sin\delta_K + |\cos\delta_K|\sqrt{R^2_{WXK} - X^2_{LEK}}\right)$$

If $Y^2_{TIP} > R^2_{WY}$ and $Y_{TIP} > 0$ then $S_{iWK} = 0$

$$X_{T1P1K} = \frac{R_{WXK}}{R_{WYK}}\left(Y_{T1PK}\sin\delta_K - |\cos\delta_K|\sqrt{R^2_{WYK} - Y^2_{T1KK}}\right)$$

$$X_{T1P2K} = \frac{R_{WXK}}{R_{WYK}}\left(Y_{T1PK}\sin\delta_K + |\cos\delta_K|\sqrt{R^2_{WYK} - Y^2_{T1PK}}\right)$$

$$r_{XWK} = SL_{CG} - SL_{WTE} - X_{TEK} + \bar{X}_K$$

$$r_{YWK} = BL_{SP} - BL_{CG} + Y_{T1PK} - \bar{Y}_R \text{(for right wing)}$$

$$= -BL_{SP} + BL_{CG} - Y_{T1PK} + \bar{Y}_L \text{(for left wing)}$$

where: $\bar{X}_K = \frac{XA_K}{S_{iWK}}$

$$\bar{Y}_K = \frac{YA_K}{S_{iWK}}$$

If $\beta_M > 30^\circ$, set $S_{iWL}, S_{iWR} = 0$

Total Velocity:

$$V_{T_{iWL}} = \left[\left(U + U_i\Big|^B_{R/WL}\right)^2 + V^2 + \left(W + W_i\Big|^B_{R/WL}\right)^2\right]^{1/2}$$

Resultant angle of sideslip,

$$\beta'_F|_W = \text{Tan}^{-1}\frac{V}{\left[\left(U + U_i\Big|^B_{R/WL}\right)^2 + \left(W + W_i\Big|^B_{R/WL}\right)^2\right]^{1/2}}$$

Resultant angle of attack

$$\alpha'_F\Big|_{WL} = \tan^{-1}\left[\frac{W + W_i\Big|^{B}_{R/WL}}{U + U_i\Big|^{B}_{R/WL}}\right]$$

Dynamic pressure:

$$q_{iWPL} = \frac{1}{2}\rho V^2_{T_{iWL}}$$

Lift in (local) wind axis system:

(left): $L_{iWPL} = q_{iWPL} S_{iWL} C_{L_{WP}}$

(right): $L_{iWPR} = q_{iWPL} S_{iWR} C_{L_{WP}}$

Drag in (local) wind axis system:

(left): $D_{iWPL} = q_{iWPL} S_{iWL} C_{D_{WP}}$

(right): $D_{iWPR} = q_{iWPL} S_{iWR} C_{D_{WP}}$

B. Wing Aerodynamics in freestream flow

(Wing area subjected to freestream - $S_{\infty W}$)

$$S_{\infty W} = S_W - (S_{iWL} + S_{iWR})$$

Dynamic Pressure:

$$q_F = \frac{1}{2}\rho V^2_T$$

Rotor flow field effects at wing:

$$\Delta\alpha_{F_r/W} = 0.26\, x_{R/W}\, \frac{2C_{RF}}{MAX^2\,(\mu_L,\ .15)} \quad (57.3)$$

Angle of Attack at the wing:

$$\alpha_W = \alpha_F - \Delta\alpha_{R/W}$$

Lift in (local) wind axis system:

$$L_{WP} = q_F\, S_{\infty W} \left[C_{L_{WP}} + C_{L_{\delta a}} * \delta a \right]$$

Drag:

$$D_{WP} = q_F\, S_{\infty W}\, C_{D_{WP}}\, f(\alpha_W,\ \beta_M,\ F_x,\ M_N)$$

Note: $C_{L_{WP}}$ here is a function of α_W

Pitching moment:

$$M'_{O_{WP}} = q_F\, S_{\infty W}\, c_W\, C_{M_{OWP}}$$

C. Lateral-Directional Equations

Prandtl - Glauert compressibility factor C_β:

$$C_\beta = \frac{AR_W + 4\cos\left(\Lambda_{c/4}\right)_W}{AR_W\, B_C + 4\cos\left(\Lambda_{c/4}\right)_W}$$

where:

$$B_C = \sqrt{1 - M_N^2 \cos^2\left(\Lambda_{c/4}\right)_W}$$

for $U > 15$ ft/sec,

Y - Force in the (local) wind axis system:

$$Y_{WP} = q_F S_{\infty W} \left[C_{Y_\beta} \beta_F + \frac{b_W}{2U} (C_{Y_p} p' + C_{Y_r} r') \right]$$

Roll and yaw moments in (local) wind axis:

$$l'_{WP} = q_F S_{\infty W} b_W \left[C_{l_\beta} \beta_F + \frac{b_W}{2U} (C_{l_p} p' + C_{l_r} r') + C_{l_{\delta_a}} \delta_a \right]$$

$$N'_{WP} = q_F S_{\infty W} b_W \left[C_{n_\beta} \beta_F + \frac{b_W}{2U} (C_{n_p} p' + C_{n_r} r') + C_{n_{\delta_a}} \delta_a \right]$$

where the aircraft angular velocities in wind axis system are,

$$p' = p \cos \alpha_W \cos \beta_F + q \sin \beta_F + r \sin \alpha_W \cos \beta_F$$

$$r' = -p \sin \alpha_W + r \cos \alpha_W$$

and the lateral-directional stability derivatives are,

1. $C_{Y_\beta} = \left(C_{Y_\beta} \Big|_{M_N =} \right)_0 (C_\beta)$

2. $C_{Y_p} = \left(\frac{C_{Y_p}}{C_L} \Big| M_N = 0 \right) \left(C_{L_{WP}} \right) (C_\beta) \left(\frac{AR_W B_C + \cos (\Lambda_{c/4\ W})}{AR_W + \cos (\Lambda_{c/4\ W})} \right)$

3. $C_{Y_r} = \left(C_{Y_r} \Big|_{M_N = 0} \right) (C_\beta)$

4. $C_{l_\beta} = \left(C_{l_\beta} \Big| \begin{matrix} C_L = 0 \\ M_N = 0 \end{matrix} \right) (C_\beta) + \left(\frac{C_{l_\beta}}{C_{L_{WP}}} \Big| M_N = 0 \right) C_{L_{WP}}$

$\left(C_{l_\beta} \Big| \begin{matrix} C_L = 0 \\ M_N = 0 \end{matrix} \right) = 0$ for $|\beta_F| > 15$ Deg

5. $$C_{l_p} = \left[C_{l_p} \middle| \begin{matrix} C_L = 0 \\ M_N = 0 \end{matrix} \right] (C_\beta) * \left[\frac{\left. \frac{\partial C_{L_{WP}}}{\partial \alpha_W} \right| \alpha_W}{\left. \frac{\partial C_{L_{WP}}}{\partial \alpha_W} \right| C_{L_{WP}} = 0} \right] - \frac{1}{8} \left[C_{D_{WP}} - \frac{C_{L_{WP}}^2}{\pi AR_W} \right]$$

6. $$C_{l_r} = \left\{ \left(1 + \frac{AR_W (1 - B_c)^2}{2B_c (AR_W B_c + 2)} \right) \left. \frac{C_{l_r}}{C_{L_{WP}}} \right| M_N = 0 \right\} C_{L_{WP}} + \left[\left. \frac{\Delta C_{l_r}}{\frac{d\alpha}{d\delta_f}} \right| \delta_f \right] \left(\frac{d\alpha}{d\delta_F} \right) \delta_F$$

If F_1 then $\delta_F = 0^\circ$

If F_2 then $\delta_F = 30^\circ$

If F_3 then $\delta_F = 60^\circ$

If F_4 then $\delta_F = -15^\circ$

7. $$C_{l_{\delta_a}} = K_{l_{\delta_a}} * C_{l_{\delta_a}} \left| \begin{matrix} F_1 \\ \alpha_W < 8^\circ \end{matrix} \right.$$

Where,

$$K_{l_{\delta_a}} - f(F_x, \beta_M, \alpha_W)$$

8. $$C_{n_\beta} = \left(C_{n_\beta} \middle| \begin{matrix} C_L = 0 \\ M_N = 0 \end{matrix} \right) * (C_\beta) + \left(\frac{C_{n_\beta}}{C_{L_{WP}}^2} \right) \Bigg|_{M_N = 0} * \left(C_{L_{WP}} \right)^2$$

9. $$C_{n_p} = -C_{l_p}\alpha_W - K_{n_p}\left[-C_{l_p}\alpha_W - \left((C_\beta)\frac{AR_W\ B_c}{AP_W}\ \frac{C_{np}}{C_{L_{WP}}}\ \Big|_{M_N = 0}\right)^* C_{l_{WP}}\right]$$

10. $$C_{n_r} = \left(\frac{C_{n_r}}{C_{L_{WP}}}\right)\left(C_{L_{WP}}\right)^2 + \left(\frac{C_{n_r}}{C_{D_{0_{WP}}}}\right) C_{D_{0_{WP}}}\Big|_{\alpha_W = 0}$$

11. $$C_{n_{\delta_a}} = K_{n_{o\delta a}} + K_{n_{\delta_a}}\ C_{l_{\delta_a}}\ C_{L_{WP}}$$

D. Wing Wake Deflection at Horizontal Tail is a function of angle of attack at the inboard section of the wing, mast tilt, flap deflection derived from test data.

$$\varepsilon_{W/H} = f(\alpha_W, \beta_M, F_x)$$

OUTPUTS:

Subsystem Block No.	Symbol	Units
5	$\epsilon_{W/H}$	Deg
10a	$\alpha'_{F\|W}$, $\beta'_{F\|W}$	Deg
	L_{iWPL}	Lbs
	L_{iWPR}	Lbs
	D_{iWPL}	Lbs
	D_{iWPR}	Lbs
	α_W	Deg
	L_{WP}	Lbs
	D_{WP}	Lbs
	$M'_{O_{WP}}$	Ft-Lbs
	Y'_{WP}	Lbs
	l'_{WP}	Ft-Lbs
	N'_{WP}	Ft-Lbs

SUBSYSTEM NO. 5-HORIZONTAL STABILIZER AERODYNAMICS

INPUTS:

A. Variables

Subsystem Block No.	Symbol	Units
9	SL_{CG}	In
11	q	Rad/Sec
2	$U_i\|^B_{R/H}$	Ft/Sec
	$W_i\|^B_{R/H}$	Ft/Sec
8a	β_M	Deg
	δ_e	Deg
	i_H	Deg
12	U	Ft/Sec
	V	Ft/Sec
	W	Ft/Sec
	$\dot{\alpha}_F$	Rad/Sec
	β_F	Rad
15	M_N	ND
	ρ	$Slug/ft^3$

B. Aerodynamic Coefficients

τ_H	ND
K_e	ND
C_{L_H}, $C_{L_{H\beta}}$	ND, 1/Deg
C_{D_H}	ND
C_{M_H}	ND
τ_e	ND

EQUATIONS

Body-axes velocity components due to vector $\left(\vec{V_T} + \overrightarrow{W_i|_{R/H}}\right)$

$$U_{R/H} = U + U_i\Big|^{B}_{R/H}$$

$$W_{R/H} = W + W_i\Big|^{B}_{R/H}$$

$U_{R/H}$ and $W_{R/H}$ affected by wing wake ($\epsilon_{W/H}$) and body pitch rate (q),

$$U_H = U_{R/H} \cos(\epsilon_{W/H}) + W_{R/H} \sin(\epsilon_{W/H})$$

$$W_H = -U_{R/H} \sin(\epsilon_{W/H}) + W_{R/H} \cos(\epsilon_{W/H}) + l_{XH}\, q$$

where,

$$\epsilon_{W/H} = f(\alpha_W, \beta_M, F_x, M_N)$$

$$l_{XH} = (SL_H - SL_{CG})\frac{1}{12}$$

Total velocity:

$$V_{HT} = \sqrt{U_H^2 + V^2 + W_H^2}$$

Angle of attack for lift equation:

$$\alpha_{HL} = i_H + \tan^{-1}\left(\frac{W_H}{U_H}\right) \quad (\text{for } M_N < 1.0)$$

$$= i_H + \tan^{-1}\left(\frac{W_H}{U_H}\right) - (K_e\tau_e)\delta_e \quad (\text{for } M_N > 1.0)$$

Angle of attack for drag equation:

$$\alpha_{HD} = i_H + \tan^{-1}\left(\frac{W_H}{U_H}\right) - (K_e\tau_e)\,\delta_e$$

Dynamic pressure:

$$q_H = \frac{1}{2} \rho V_{HT}^2 (\eta_H)$$

Lift in (local) wind axes:

For $U < 67.5$ ft/sec, set $\dot{\alpha}_F = 0$; if $U \leq 35$, set $U = 35$ ft/sec

$$L_H = q_H S_H \left\{ C_{L_H}(\alpha_{HL}, \delta_e, M_N) + \frac{l_{XH}}{U} \left(\frac{\partial C_{LH}}{\partial \alpha_{HL}}\right) \left(\frac{\partial \epsilon_{W/H}}{\partial \alpha_W}\right) \dot{\alpha}_F + C_{Y_{H\beta}} |\beta_F| \right\}$$

For $|\beta_F| > 15^\circ$, $L_{H_\beta} = L_{H_\beta}$ AT $|\beta_F| = 15^\circ$

Drag in (local) wind axes:

$$D_H = q_H S_H C_{D_H} (\alpha_{HD}, M_N)$$

Local angle of attack (for resolving forces)

$$\alpha_H = \tan^{-1} \left(\frac{W_H}{U_H}\right)$$

Pitching moment:

$$M'_H = q_H S_H C_H C_{M_H} f(\alpha_H, M_N)$$

OUTPUTS:

Subsystem Block No.	Symbol	Units
10a	α_H	Deg
	L_H	Lbs
	D_H	Lbs
	M'_H	Ft-lbs

SUBSYSTEM NO. 6-VERTICAL STABILIZER AERODYNAMICS

INPUTS:

A. Variables

Subsystem Block No.	Symbol	Units
(12)	U	Ft/sec
	V	Ft/sec
	W	Ft/sec
(11)	p	Rad/sec
	q	Rad/sec
	r	Rad/sec
(2)	$U_i\|^{B}_{R/V}$	Ft/sec
	$W_i\|^{B}_{R/V}$	Ft/sec
(15)	M_N	ND
	ρ	$Slug/ft^3$
	δ_R	Deg
(8a)	β_M	Deg
	F_x	F_1, F_2, F_3, F_4
(12)	β_F	Deg
	α_H	Deg
(9)	SL_{CG}	In.
	WL_{CG}	In.

B. Aerodynamic Coefficients

$(1 - \partial\sigma/\partial_{\beta F})$	ND
$C_{Y_V}\|^{F_1}_{\beta_M = 90}$	ND
C_{D_V}	ND
$\partial\sigma/\partial\hat{p}$, $\partial\sigma/\partial\hat{r}$	ND
r	ND

EQUATIONS

The H-Tail is represented as a left and right fin. Velocity at the left fin,

$$V_{V_L}^2 = \left\{ (U + U_i\Big|_{R/V}^{B} - q*l_{ZV} + r*l_{YV})^2 + (V - r*l_{XV} + p*l_{ZV})^2 + (W - W_i\Big|_{R/V}^{B} + q*l_{XV} - p*l_{YV})^2 \right\}$$

$$\left.\begin{aligned} U_i\Big|_{R/V}^{B} &= 0 \\ W_i\Big|_{R/V}^{B} &= 0 \end{aligned}\right\} \text{ for } \left\{\begin{aligned} &5^\circ < \beta_F < 28^\circ \\ &|\beta_F| > 60^\circ \end{aligned}\right.$$

where,

$$l_{XV} = (SL_V - SL_{CG})\frac{1}{12}$$

$$l_{YV} = (BL_V - BL_{CG})\frac{1}{12}$$

$$l_{ZV} = (WL_V - WL_{CG})\frac{1}{12}$$

Velocity at right fin,

$$V_{VR}^2 = \left\{ (U + U_i\Big|_{R/V}^{B} - q*l_{ZV} - r*l_{YV})^2 + (V - r*l_{XV} + p*l_{ZV})^2 + (W - W_i\Big|_{R/V}^{B} + q*l_{XV} + p*l_{YV})^2 \right\}$$

$$\left.\begin{aligned} U_i\Big|_{R/V}^{B} &= 0 \\ W_i\Big|_{R/V}^{B} &= 0 \end{aligned}\right\} \text{ for } \left\{\begin{aligned} &-5^\circ > \beta_F > -28^\circ \\ &|\beta_F| > 60^\circ \end{aligned}\right.$$

Define sideslip angle due to vector $(\vec{V_T} + \overrightarrow{W_{i\ R/V}})$

$$\beta'_{VL,R} = \tan^{-1}\left\{ \frac{V}{\sqrt{(U + U_i\Big|_{R/V}^{B})^2 + (W + W_i\Big|_{R/V}^{B})^2}} \right\}$$

De ine Zero Rudder Sideslip Angle, if $(U + U_i|^B_{R/V}) \leq 10$, set = 10.0 ft/sec

$$\beta_{VL,R_o} = \left\{ \beta'_{VL,R}\left(1 - \frac{\partial\sigma}{\partial\beta}\right) + \frac{b_W}{2\left(U + U_i\big|^B_{R/V}\right)} \left[\left(\frac{2\, l_{ZV}}{b_W} - \frac{\partial\sigma}{\partial \overset{\Lambda}{p}} \right) p \right. \right.$$

$$\left. \left. - \left(\frac{2\, l_{XV}}{b_W} + \frac{\partial\sigma}{\partial \overset{\Lambda}{r}} \right) r \right] \right\} \quad (57.3)$$

Sideslip Angle for Y Force Equation,

$$\beta_{VYL,R} = \beta_{VL,R_o} \quad (\text{For } M_N < 1.0)$$

$$= \beta_{VL,R_o} + (K_R \tau_R) * \delta_R \quad (\text{for } M_N > 1.0)$$

Sideslip Angle for Drag Equation,

$$\beta_{VDL,R} = \beta_{VL,R_o} + (K_R \tau_R) * \delta_R$$

Dynamic Pressure,

$$q_{VL} = (1/2\ \rho\ V_{VL}^2)\ \eta_V \text{ and } q_{VR} = (1/2\ \rho\ V_{VR}^2)\ \eta_V$$

Forces in the local wind axes are,

$$Y'_{VL} = \frac{1}{2} S_V\ q_{VL}\ C_{Y_V}$$

$$Y'_{VR} = \frac{1}{2} S_V\ q_{VR}\ C_{Y_V}$$

$$D_{VL} = \frac{1}{2} S_V\ q_{VL}\ C_{D_V}$$

$$D_{VR} = \frac{1}{2} S_V\ q_{VL}\ C_{D_V}$$

OUTPUTS:

Subsystem Block No.	Symbol	Units
10a	$\beta_{VL'R_o}$	Deg
	Y'_{VL}	Lbs
	Y'_{VR}	Lbs
	D_{VL}	Lbs
	D_{VR}	Lbs

SUBSYSTEM NO. 7: RETRACTABLE LANDING GEAR

INPUTS:

A. Variables

Subsystem Block No.	Symbol	Units
(8a)	L_{LG}	ND
(10f)	h	Ft
(12)	α_F	Deg
↓	V_T, W_G	Ft/Sec
(15)	ρ	Slug/Ft^3
(10c)	θ, ϕ	Deg

B. Aerodynamic Coefficients

$D_{OMGU}(t)$	$D_{OMGD}(t)$
$D_{ONGU}(t)$	$D_{ONGD}(t)$

C. Strut Force Coefficients

K_{ST1}	K_{ST2}	K_{ST3}
D_{ST1}	D_{ST2}	D_{ST3}
B_{G1}	B_{G2}	B_{G3}
μ_o	μ_1	μ_S

Landing Gear Locations

$$X_n = SL_{CG} - SL_{Gn}$$

$$Y_n = BL_{CG} - BL_{Gn}$$

$$Z_n = WL_{CG} - WL_{Gn}$$

Butt lines positive to right. Water lines defined with zero loads in landing gears.

Where,

n = 1, 2, 3

1 = Left Main Gear
2 = Right Main Gear
3 = Nose Gear

Aerodynamic Force Equations

$$q_F = \frac{1}{2} \rho V_T^2$$

A. Gears Down

$$D_{MG} = q_F D_{MOGD}(t)$$

$$D_{NG} = q_F D_{ONGD}(t)$$

B. Gears Up

$$D_{MG} = q_F D_{OMGU}(t)$$

$$D_{NG} = q_F D_{ONGU}(t)$$

Strut Force Equations

Strut Deflection

$$h_{G\theta n} = X_n \sin \theta - Z_n \cos \theta - \gamma_n$$

$$h_{G\phi n} = [Y_n \sin \phi + (Z_n + \gamma_n)(\cos \phi - 1)] \cos \theta$$

$$h_{Tn} = (h + h_{G\theta n} - h_{G\phi n})/(\cos \theta \cos \phi)$$

Strut Deflection Rate

$$\dot{h}_{Tn} = + W_G \left(\frac{1}{\cos \theta \cos \phi} \right) + X_n q - Y_n p$$

Strut Vertical Force

IF $h_{Tn} > 0$, $F_{GZn} = 0$

IF $h_{Tn} < 0$,

$$F_{GZn} = K_{STn} h_{Tn} + D_{STn} \dot{h}_{Tn}$$

Strut Longitudinal Force

$$F_{\mu n} = - (\mu_o + \mu_1 B_{Gn}) F_{GZn} \frac{U}{|U|}$$

IF $U = 0$, $F_{\mu n} = 0$.

Strut Side Force

IF $V = 0$, $F_{Sn} = 0$

IF $V \neq 0$, $F_{Sn} = -\mu_s F_{GZn} \frac{V}{|V|}$

Force and Moment Contributions of Gear Struts

$$\Delta X_n = F_{\mu n} - F_{GZn}\theta$$

$$\Delta Y_n = F_{Sn} + F_{GZn}\phi$$

$$\Delta Z_n = F_{\mu n}\,\theta - F_{Sn}\,\phi + F_{GZn}$$

$$\Delta M_n = -\Delta Z_n X_n + \Delta X_n\,(Z_n + \gamma_n + h_{Tn})$$

$$\Delta l_n = -\Delta Z_n Y_n - \Delta Y_n\,(Z_n + \gamma_n + h_{Tn})$$

$$\Delta N_n = -\Delta X_n Y_n + X_n\,\Delta Y_n$$

$$\Delta X_{LG} = \sum_{1}^{3} \Delta X_n$$

$$\Delta Y_{LG} = \sum_{1}^{3} \Delta Y_n$$

$$\Delta Z_{LG} = \sum_{1}^{3} \Delta Z_n$$

$$\Delta l_{LG} = \sum_{1}^{3} \Delta l_n$$

$$\Delta M_{LG} = \sum_{1}^{3} \Delta M_n$$

$$\Delta N_{LG} = \sum_{1}^{3} \Delta N_n$$

OUTPUTS

Subsystem Block No.	Symbol	Units
10a	D_{LG}	Lbs
	D_{NG}	Lbs
13	ΔX_{LG}	Lbs
	ΔY_{LG}	Lbs
	ΔZ_{LG}	Lbs
14	Δl_{LG}	Lb. ft
	ΔM_{LG}	Lb. ft
	ΔN_{LG}	Lb. ft

SUBSYSTEM NO. 8a CONTROLS MIXER

INPUTS:

A. Variables

Subsystem Block No.	Symbol	Units
17	$\theta_{OL/G}$, $\theta_{OR/G}$	Deg
8d	X_{LN}	Inch
	X_{LT}	Inch
	X_{PD}	Inch
	X_{COL}	Deg
20	ESAS	Deg
	RSAS	Deg
	ASAS	Deg
8d	X_{P_M}	Fwd, 0, Aft
	X_{FL}	F_1, F_2, F_3, F_4
	X_{LG}	UP, DN
11	V_T	Ft/Sec

B. Control System Gearing

$\partial B_1/\partial X_{LN}$, $\partial B_1/\partial X_{PD}$	Deg/In, Deg/In
$\partial\theta_o/\partial X_{LT}$, $\partial\theta_o/\partial X_{COL}$, $\theta_{o_{LL}}$	Deg/In, Deg/In, Deg
$\partial\delta_R/\partial X_{LN}$, $\partial\delta_R/\partial X_{PD}$	Deg/In, Deg/In
$\partial\delta a/\partial X_{LT}$	Deg, In

This page left blank

FOLDOUT FRAME

BELL HELICOPTER COMPANY

CONTROL SYSTEM BLOCK DIAGRAM

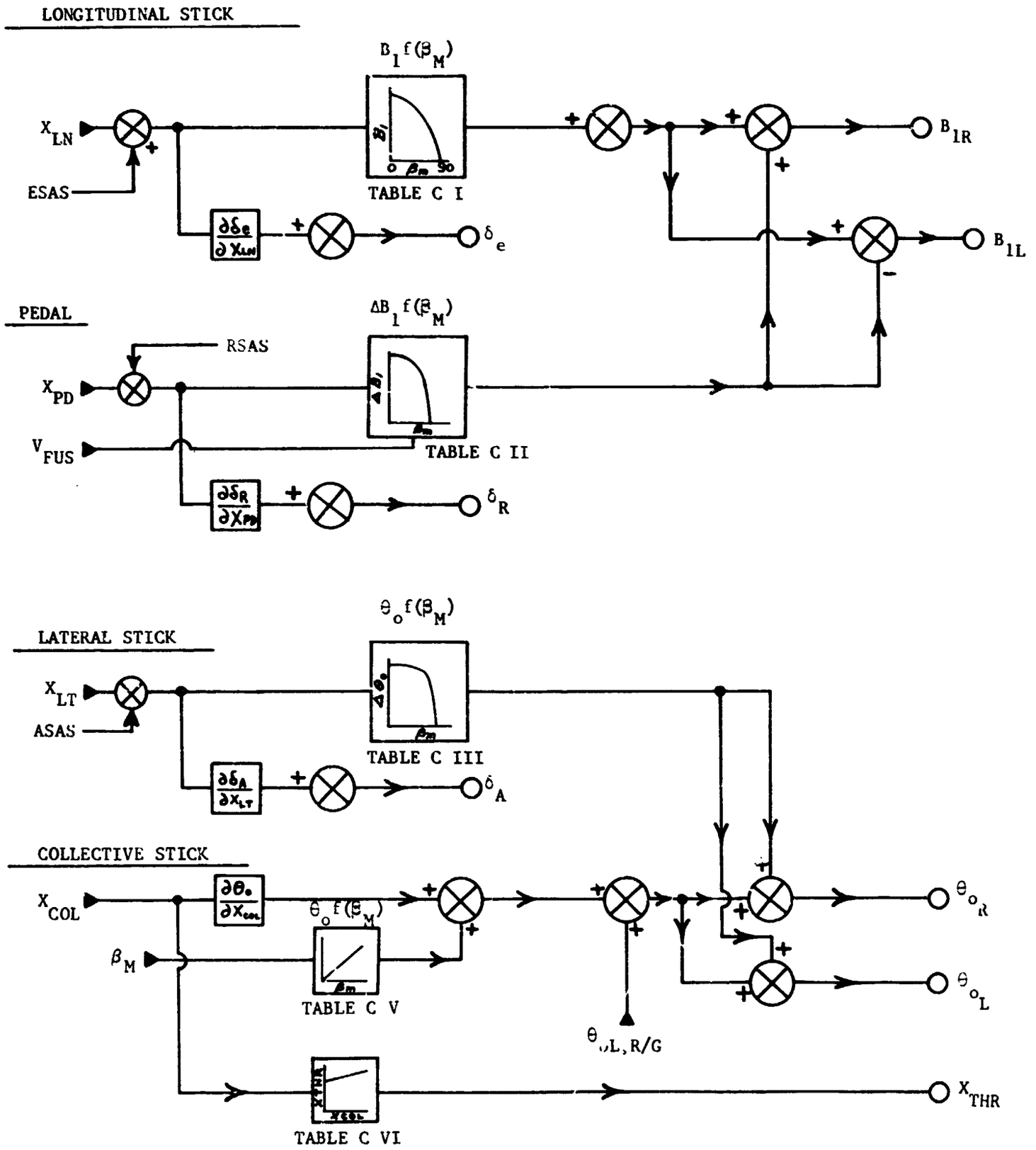

FOLDOUT FRAME 2

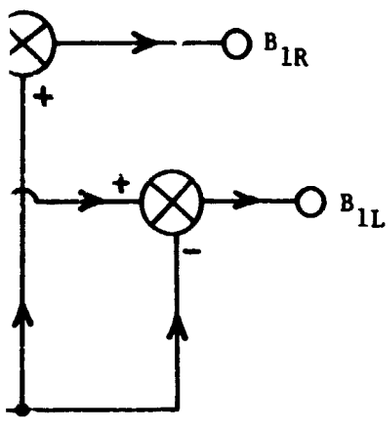

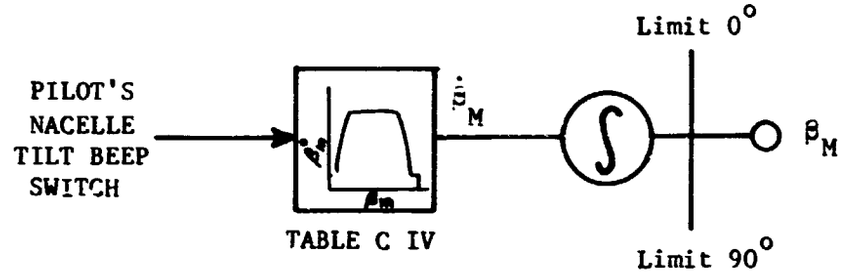

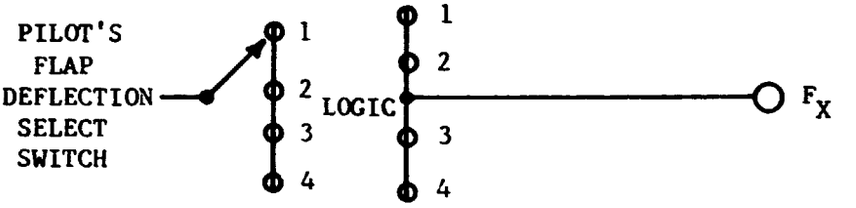

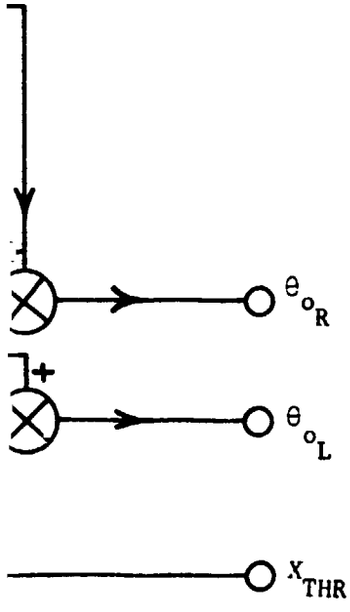

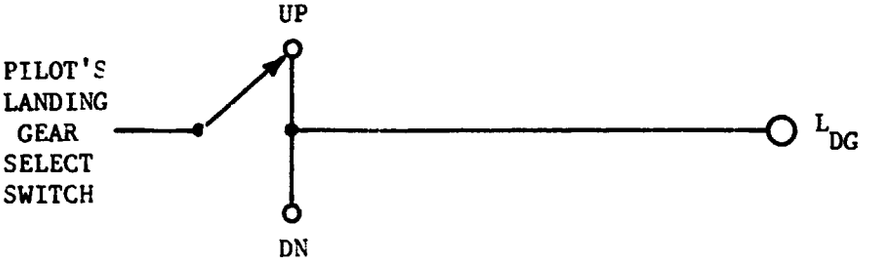

EQUATIONS

A. Collective Pitch

$$\theta_{OR} = \left(\partial\theta_0 / \partial X_{COL}\right) * X_{COL} + \theta_{OLL} + \theta_{OR/G}$$

$$-\left(\frac{\partial\theta_0}{\partial X_{LT}}\right) * (X_{LT} - X_{LTN} + ASAS)$$

$$\theta_{OL} = \left(\partial\theta_0 / \partial X_{COL}\right) * X_{COL} + \theta_{OLL} + \theta_{OL/G}$$

$$+\left(\frac{\partial\theta_0}{\partial X_{LT}}\right) * (X_{LTN} + ASAS)$$

B. Longitudinal Cyclic

$$B_{1R} = \left(\frac{\partial B_1}{\partial X_{LN}}\right) * (X_{LN} - X_{LNN} + ESAS)$$

$$-\left(\frac{\partial B_1}{\partial X_{PD}}\right) * (X_{PD} - X_{PDN} + RSAS)$$

$$B_{1L} = \left(\frac{\partial B_1}{\partial X_{LN}}\right) * (X_{LN} - X_{LNN} + ESAS)$$

$$+\left(\frac{\partial B_1}{\partial X_{PD}}\right) * (X_{PD} - X_{PDN} + RSAS)$$

C. Elevator, Rudder, Aileron

$$\delta_e = \frac{\partial \delta_e}{\partial X_{LN}} * (X_{LN} - X_{LNN} + ESAS)$$

$$\delta_r = \frac{\partial \delta_r}{\partial X_{PD}} * (X_{PD} - X_{PDN} + RSAS)$$

$$\delta_a = \frac{\partial \delta_a}{\partial X_{LT}} * (X_{LT} - X_{LTN} + ASAS)$$

D. Nacelle Tilt

$$\dot{\beta}_M - f(\beta_M) * (1, 0, -1) \text{ (Fwd, Neutral, Aft)}$$

$$\beta_M = \int_0^t \beta_M \, dt \qquad \text{Limits } 90^\circ \leq \beta_M \leq -5^\circ$$

E. Flap Selector

Flap/Flaperon Setting is:

F_1	(0,0)	
F_2	(40,25)	Use to select table
F_3	(75,47)	
F_4	(-28, -17.5)	

F. Landing Gear Selector

$$L_{DG} = [0,1] \text{ (Up, Down)}$$

G. Variable Incidence Stabilizer

$$i_H = i_{HO}\Big|_{X_{LN} = X_{LNN}} + i_{H1}\,(X_{LN} - X_{LNN}) + i_{H2}\,(X_{LN} - X_{LNN})^2$$

$$+ i_{H3}\Big|_{X_{COL} = 0} + i_{H4}\,X_{COL}$$

OUTPUTS:

Subsystem Block No.	Symbol	Units
1	θ_{OR}	Deg
	θ_{OL}	Deg
	B_{1L}	Deg
	B_{1R}	Deg
5	δ_e	Deg
	i_H	Deg
6	δ_R	Deg
4	δ_a	Deg
4	F_X	(F_1, F_2, F_3, F_4)
7	L_{DG}	ND
9	$\dot{\beta}_M$	Deg/Sec
	β_M	Deg

SUBSYSTEM NO. 8b: FORCE FEEL SYSTEM

INPUTS:

A. Variables

Subsystem Block No.	Symbol	Units
8d	X_{LN}	Inch
	X_{LT}	Inch
	X_{PD}	Inch
8c	X_{LNT}	Inch
	X_{LTT}	Inch
	X_{PDT}	Inch
	V_T	Knots

B. Stick Force Gradients

F_{LN0}, F_{LT0}, F_{PD0}	Lb/In
F_{LN1}, F_{LN2}; F_{LT1}, F_{LT2}; F_{PD1}, F_{PD2}	Lb/In/Ft/Sec
F_4	Lb/In
V_1, V_2	Kts

EQUATIONS:

$$F_{LN} = \left[F_{LN_0} + F_{LN_1}\ (V_T - V_1) + F_{LN_2}\ (V_T - V_2)\right] * \left|(X_{LN} - X_{LNT})\right|$$

$$F_{LT} = \left[F_{LT_0} + F_{LT_1}\ (V_T - V_1) + F_{LT_2}\ (V_T - V_2)\right] * \left|(X_{LT} - X_{LTT})\right|$$

$$F_{PD} = \left[F_{PD_0} + F_{PD_1}\ (V_T - V_1) + F_{PD_2}(V_T - V_2)\right] * \left|(X_{PD} - X_{PDT})\right|$$

$$F_{COL} = F_4 * \left|X_{COL}\right|$$

OUTPUTS:

Subsystem Block No.	Symbol	Units
8d	F_{LN}	Pounds
	F_{LT}	Pounds
	F_{PD}	Pounds
	F_{COL}	Pounds

SUBSYSTEM NO. 8c: CONTROL FORCE TRIM SYSTEM

INPUTS:

A. Variables

Subsystem Block No.	Symbol	Units
8d	X_{LN}	Inch
	X_{LT}	Inch
	X_{PD}	Inch
	B_{FT}	On or Off

EQUATIONS:

If trim button is depressed (B_{FT} ON)

$$X_{LNT} = X_{LN}$$

$$X_{LTT} = X_{LT}$$

$$X_{PDT} = X_{PD}$$

If trim button is not depressed (B_{FT} OFF)

$$X_{LNT} = X_{LNT}$$

$$X_{LTT} = X_{LTT}$$

$$X_{PDT} = X_{PDT}$$

OUTPUTS:

Subsystem Block No.	Symbol	Units
8b ↓	X_{LNT}	Inch
	X_{LTT}	Inch
	X_{PDT}	Inch

SUBSYSTEM NO. 8d: PILOT'S CONTROL FUNCTION

INPUTS:

A. Variables

Subsystem Block No.	Symbol	Units
8b	F_{LN}	Pounds
	F_{LT}	Pounds
	F_{PD}	Pounds
	F_{COL}	Pounds

EQUATIONS:

Pilot in the Loop

OUTPUTS:

Subsystem Block No.	Symbol	Control Mechanism	Units
8a	X_{LN}	Long. Stick	Inch
	X_{LT}	Lat. Stick	Inch
	X_{PD}	Pedal	Inch
	X_{COL}	Coll. Stick	Inch
	X_{β_M}	Beep Switch	Fwd, Neut., Aft
	X_{FL}	Grip (Floor Mounted) Switch	F_X Up, Down
	X_{LG}		
17	RPM_p	Beep	RPM
8c	B_{FT}	Switch	ON/OFF

Subsystem Block No.	Symbol	Control Mechanism	Units
8a	X_{PSAS}	Switch	ON/OFF
	X_{RSAS}	Switch	ON/OFF
	X_{YSAS}	Switch	ON/OFF

SUBSYSTEM NO. 9-CG AND INERTIA SHIFT WITH PYLON TILT

INPUTS

A. Variables

Subsystem Block No.	Symbol	Units
(8a) ↓	β_M	Deg.
	$\dot{\beta}_M$	Rad/Sec.
(10f)	h	Ft.

B. Inertia Coefficients

K_{I1}, K_{I2}, K_{I3}, K_{I4}, $\frac{\text{Slugs - Ft}^2}{\text{Deg.}}$

EQUATIONS

CG Displacement as a Function of Pylon Tilt Angle

$$X_{CG} = Z \sin \beta_M + X (1 - \cos \beta_M)$$

$$Z_{CG} = Z (1 - \cos \beta_M) - X \sin \beta_m$$

Where,

$$X = \frac{W_P}{GW} (SL_{SP} - SL_P)$$

$$Z = \frac{W_P}{GW} (WL_{SP} - WL_P)$$

CG Location,

$$SL_{CG} = SL_{CG}\Big|_{\beta_m = 0} + X_{CG}$$

$$WL_{CG} = WL_{CG}\Big|_{\beta_m = 0} + Z_{CG}$$

Rotor Hub Height From Ground,

$$h_H = h + \left\{ l_m \cos \beta_m + \frac{(WL_{SP} - WL_{CG})}{12} \right\}$$

CG Velocity Due to Pylon Tilt Rate,

$$\dot{X}_{CG} = Z [\dot{\beta}_M * \cos \beta_M] + X[\dot{\beta}_M * \sin \beta_M]$$

$$\dot{Z}_{CG} = Z[\dot{\beta}_M * \sin \beta_M] - X[\dot{\beta}_M * \cos \beta_M]$$

CG Acceleration (Neglecting $\ddot{\beta}_M$)

$$\ddot{X}_{CG} = -Z\,[\dot{\beta}_M * \sin \beta_M] + X[\dot{\beta}_M^2 * \cos \beta_M]$$

$$\ddot{Z}_{CG} = Z\,[\dot{\beta}_M^2 * \cos \beta_M] + X[\dot{\beta}_M^2 * \sin \beta_M]$$

Aircraft Inertia Change Due to Pylon Tilt

$$I_{XX} = I_{XX}\Big|_{\beta_M = 0} - K_{I1}\,\beta_M$$

$$I_{YY} = I_{YY}\Big|_{\beta_M = 0} - K_{I2}\,\beta_M$$

$$I_{ZZ} = I_{ZZ}\Big|_{\beta_M = 0} + K_{I3}\,\beta_M$$

$$I_{XZ} = I_{XZ}\Big|_{\beta_M = 0} - K_{I4}\,\beta_M$$

OUTPUTS

Subsystem Block No.	Symbol	Units
11, 14	SL_{CG}	Inch
	WL_{CG}	Inch
11	X_{CG}	Inch
	Z_{CG}	Inch
	$\dot{X}_{CG}$	Inch/sec
	$\dot{Z}_{CG}$	Inch/sec
	$\ddot{X}$	Inch/sec^2
	$\ddot{Z}_{CG}$	Inch/sec^2
	I_{XX}	Slug - Ft^2
	I_{YY}	Slug - Ft^2
	I_{ZZ}	Slug - Ft^2
	I_{XZ}	Slug - Ft^2
1, 14	h_H	Ft

SUBSYSTEM NO. 10: AXES TRANSFORMATIONS

10a. Transformation of Airframe Aerodynamic Forces and Moments from Wind to Body Axes

INPUTS:

Subsystem Block No.	Symbol	Units
3	α_F	Rad
	β_F	Rad
	L_F	Lbs.
	D_F	Lbs
	Y'_F	Lbs
	M'_F	Ft-Lbs
	l'_F	Ft-Lbs
	N'_F	Ft-Lbs
4	$\alpha'_{F/W}$	Rad
	$\beta'_{F/W}$	Rad
	L_{iWPL}	Lbs
	L_{iWPR}	Lbs
	D_{iWPL}	Lbs
	D_{iWPR}	Lbs
	α_W	Rad
	L_{WP}	Lbs
	D_{WP}	Lbs
	$M'_{O_{NP}}$	Ft-Lbs
	Y'_{WP}	Lbs
	l'_{WP}	Ft-Lbs
	N'_{WP}	Ft-Lbs

7872 55426

Subsystem Block No.	Symbol	Units
5	α_H	Rad
	L_H	Lbs
	D_H	Lbs
	M'_H	Ft-Lbs
6	$\beta_{VL'Ro}$	Rad
	Y'_{VL}	Lbs
	Y'_{VR}	Lbs
	D_{VL}	Lbs
	D_{VR}	Lbs
7	D_{MG}	Lbs
	D_{NG}	Lbs

7872 85426

EQUATIONS:

A. General Form of Transformation

$$\begin{bmatrix} X_i \\ Y_i \\ Z_i \end{bmatrix}_{Body} = \begin{bmatrix} \cos\alpha_i \cos\beta_i & -\cos\alpha_i \sin\beta_i & -\sin\alpha_i \\ \sin\beta_i & \cos\beta_i & 0 \\ \sin\alpha_i \cos\beta_i & -\sin\alpha_i \sin\beta_i & \cos\alpha_i \end{bmatrix} \begin{bmatrix} X_i \\ -Y_i \\ Z_i \end{bmatrix}_{Wind}$$

This transformation matrix is also used for the moment transformation. α_i and β_i are the component angle of attack and sideslip angle, respectively.

B. Transformation of Fuselage Forces and Moments

$$X_F = -D \cos\alpha_F \cos\beta_F - Y'_F \cos\alpha_F \sin\beta_F + L_F \sin\alpha_F$$

$$Y_F = -D_F \sin\beta_F + Y'_F \cos\beta_F$$

$$Z_F = -D_F \sin\alpha_F \cos\beta_F - Y'_F \sin\alpha_F \sin\beta_F - L_F \cos\alpha_F$$

$$L_F = l'_F \cos\alpha_F \cos\beta_F - M'_F \cos\alpha_F \sin\beta_F - N'_F \sin\alpha_F$$

$$M_F = l'_F \sin\beta_F + M'_F \cos\beta_F$$

$$N_F = l'_F \sin\alpha_F \cos\beta_F - M'_F \sin\alpha_F \sin\beta_F + N'_F \cos\alpha_F$$

7872 55426

C. Transformation of Wing Forces and Moments

1. Forces Generated by Rotor Wake

$$X_{iWPR} = -D_{iWPR} \cos \alpha'_{F/W} \cos \beta'_{F/W} + L_{iWPR} \sin \alpha'_{F/W}$$

$$Y_{iWPR} = -D_{iWPR} \sin \beta'_{F/W}$$

$$Z_{iWPR} = -D_{iWPR} \sin \alpha'_{F/W} \cos \beta'_{F/W} - L_{iWPR} \cos \alpha'_{F/W}$$

2. Forces and Moments Generated by Freestream Flow

$$X_{WP} = -D_{WP} \cos \alpha_W \cos \beta_F - Y'_{WP} \cos \alpha_W \sin \beta_F + L_{WP} \sin \alpha_W$$

$$Y_{WP} = -D_{WP} \sin \beta_F + Y'_{WP} \cos \beta_F$$

$$Z_{WP} = -D_{WP} \sin \alpha_W \cos \beta_F - Y'_{WP} \sin \alpha_W \sin \beta_F - L_{WP} \cos \alpha_W$$

$$L_{WP} = l'_{WP} \cos \alpha_W \cos \beta_F - M'_{O_{WP}} \cos \alpha_W \sin \beta_F - N'_{WP} \sin \alpha_W$$

$$M_{WP} = l'_{WP} \sin \beta_F + M'_{O_{WP}} \cos \beta_F$$

$$N_{WP} = l'_{WP} \sin \alpha_W \cos \beta_F - M'_{O_{WP}} \sin \alpha_W \sin \beta_F + N'_{WP} \cos \alpha_W$$

D. Transformation of Horizontal Stabilizer Forces and Moments

$$X_H = -D_H \cos \alpha_H \cos \beta_F + L_H \sin \alpha_H$$

$$Y_H = -D_H \sin \beta_F$$

$$Z_H = -D_H \sin \alpha_H \cos \beta_F - L_H \cos \alpha_H$$

7872 55426

$$l_H = -M'_H \cos \alpha_H \sin \beta_F$$

$$M_H = M'_H \cos \beta_F$$

$$N_H = -M'_H \sin \alpha_H \sin \beta_F$$

E. Transformation of Vertical Stabilizer Forces.

$$X_{VR} = -D_{VR} \cos \alpha_H \cos \beta_{VR_o} + Y'_{VR} \cos \alpha_H \sin \beta_{VR_o}$$

$$Y_{VR} = -D_{VR} \sin \beta_{VR_o} - Y'_{VR} \cos \beta_{VR_o}$$

$$Z_{VR} = -D_{VR} \sin \alpha_H \cos \beta_{VR_o} + Y'_{VR} \sin \alpha_H \sin \beta_{VR_o}$$

F. Transformation of Landing Gear Aerodynamic Forces

$$X_{MG} = -D_{MG} \cos \alpha_F \cos \beta_F$$

$$Y_{MG} = -D_{MG} \sin \beta_F$$

$$Z_{MG} = -D_{MG} \sin \alpha_F \cos \beta_F$$

7872 55426

OUTPUTS:

Subsystem Block No.	Symbol	Units
13, 14	$(X, Y, Z)_F$	Lbs
	$(X, Z)_{iWPL}$	Lbs
	$(Z, Z)_{iWPR}$	Lbs
	$(Z, Y, Z)_{WP}$	Lbs
	$(X, Y, Z)_H$	Lbs
	$(X, Z)_{MG}$	Lbs
	$(X, Z)_{NG}$	Lbs
	$(X, Y)_{VL}$	Lbs
	$(X, Y)_{VR}$	Lbs
14	l_F	Ft-Lbs
	M_F	Ft-Lbs
	N_F	Ft-Lbs
	l_{WP}	Ft-Lbs
	M_{WP}	Ft-Lbs
	N_{WP}	Ft-Lbs
	l_H	Ft-Lbs
	M_H	Ft-Lbs
	N_H	Ft-Lbs

7872 55426

10b. Transformation of Rotor Forces and Moments from Mast to Body Axes

INPUTS:

Subsystem Block No.	Symbol	Units
1	T_R	Lbs
	H_R	Lbs
	Y_R	Lbs
	Q_R	Ft-Lbs
	$M_{a_{1R}}$	Ft-Lbs
	$l_{b_{1R}}$	Ft-Lbs
	T_L	Lbs
	H_L	Lbs
	Y_L	Lbs
	Q_L	Ft-Lbs
	$M_{a_{1L}}$	Ft-Lbs
	$l_{b_{1L}}$	Ft-Lbs
8a	θ_M	Rad

7872 5542

EQUATIONS:

$$X_R = -H_R \cos \beta_M \cos \phi_M - Y_R \sin \beta_M \sin \phi_M + T_R \sin \beta_M \cos \phi_M$$

$$Y_R = H_R \sin \beta_M \sin \phi_M + Y_R \cos \phi_M + T_R \cos \beta_M \sin \phi_M$$

$$Z_R = -H_R \sin \beta_M \cos \phi_M + Y_R \cos \beta_M \sin \phi_M - T_R \cos \beta_M \cos \phi_M$$

$$X_L = -H_L \cos \beta_M \cos \phi_M - Y_L \sin \beta_M \sin \phi_M + T_L \sin \beta_M \cos \phi_M$$

$$Y_L = -H_L \sin \beta_M \sin \phi_M - Y_L \cos \phi_M - T_L \cos \beta_M \sin \phi_M$$

$$Z_L = -H_L \sin \beta_M \cos \phi_M + Y_L \cos \beta_M \sin \phi_M - T_L \cos \beta_M \cos \phi_M$$

$$l_R = l_{b1R} \cos \beta_M \cos \phi_M - M_{A1R} \sin \beta_M \sin \phi_M - Q_R \sin \beta_M \cos \phi_M$$

$$M_R = -l_{b1R} \sin \beta_M \sin \phi_M + M_{A1R} \cos \phi_M - Q_R \cos \beta_M \sin \phi_M$$

$$N_R = l_{b1R} \sin \beta_M \cos \phi_M + M_{A1R} \cos \beta_M \sin \phi_M + Q_R \cos \beta_M \cos \phi_M$$

$$l_L = -l_{b1R} \cos \beta_M \cos \phi_M - M_{A1L} \sin \beta_M \sin \phi_M + Q_L \sin \beta_M \cos \phi_M$$

$$M_L = l_{b1L} \sin \beta_M \sin \phi_M + M_{A1L} \cos \phi_M + Q_L \cos \beta_M \sin \phi_M$$

$$N_L = -l_{b1L} \sin \beta_M \cos \phi_M + M_{A1L} \cos \beta_M \sin \phi_M - Q_L \cos \beta_M \cos \phi_M$$

7872 55426

OUTPUTS:

Subsystem Block No.	Symbol	Units
13	$(X, Y, Z)_R$	Lbs
	$(X, Y, Z)_L$	Lbs
14	$(l, M, N)_R$	Ft-Lbs
	$(l, M, N)_L$	Ft-Lbs

10c. Subsystem for Euler Angles

INPUTS:

Subsystem Block No.	Symbol	Units
11	p	Rad/Sec
	q	Rad/Sec
	r	Rad/Sec
10c	Ψ	Rad
	θ	Rad
	ϕ	Rad

EQUATIONS:

$$\dot{\theta} = q \cos \phi - r \sin \phi$$

$$\dot{\phi} = p + r \tan \theta \cos \phi + q \tan \theta \sin \phi$$

$$\dot{\Psi} = \frac{r \cos \phi + q \sin \phi}{\cos \theta}$$

$$\theta = \int \dot{\theta}\, dt$$

$$\phi = \int \dot{\phi}\, dt$$

$$\Psi = \int \dot{\Psi}\, dt$$

OUTPUTS:

Subsystem Block No.	Symbol	Units
16	$\dot{\Psi}$	Rad/Sec
	$\dot{\theta}$	Rad/Sec
	$\dot{\phi}$	Rad/Sec
10c, 10d, 10f, 12, 16	Ψ	Rad
20, VFA	θ	Rad
	ϕ	Rad

10d. Subsystem for Earth Based Velocities

INPUTS:

Subsystem Block No.	Symbol	Units
10c	Ψ	Rad
	θ	Rad
	ϕ	Rad
11	U	Ft/Sec
	V	Ft/Sec
	W	Ft/Sec

EQUATIONS:

$$U_{EB} = U \cos \Psi \cos \theta + V \cos \Psi \sin \theta \sin \phi - V \sin \Psi \cos \phi + W \cos \Psi \sin \theta \cos \phi + W \sin \Psi \sin \phi - U \text{ wind E}$$

$$V_{EB} = U \sin \Psi \cos \theta + V \cos \Psi \cos \phi + V \sin \Psi \sin \theta \sin \phi + W \sin \Psi \sin \theta \cos \phi - W \cos \Psi \sin \phi - V \text{ wind E}$$

$$W_{EB} = -U \sin \theta + V \cos \theta \sin \phi + W \cos \theta \cos \phi + W \text{ wind E}$$

OUTPUTS:

Subsystem Block Nc.	Symbol	Units
10c	U_{EB}	Ft/Sec
	V_{EB}	Ft/Sec
	W_{EB}	Ft/Sec

10e. Subsystem for Ground Velocity Summation

INPUTS:

Subsystem Block No.	Symbol	Units
Wind	U_W	Ft/Sec
	θ_W	Rad
	Ψ_W	Rad
10d	U_{EB}	Ft/Sec
	V_{EB}	Ft/Sec
	W_{EB}	Ft/Sec

EQUATIONS:

$$U_{WE} = U_W (\cos \Psi_W \cos \theta_W)$$

$$V_{WE} = V_W (-\sin \Psi_W)$$

$$W_{WE} = U_W (\cos \Psi_W \sin \theta_W)$$

$$U_G = U_{EB} - U_{WE}$$

$$V_G = V_{EB} - V_{WE}$$

$$W_G = W_{EB} - W_{WE}$$

OUTPUT:

Subsystem Block No.	Symbol	Units
VFA, 10f	U_G	Ft/Sec
	V_G	Ft/Sec
	W_G	Ft/Sec

10f. Subsystem for Ground Reference Distances

INPUTS:

Subsystem Block No.	Symbol	Units
10e	U_G	Ft/Sec
	V_G	Ft/Sec
	W_G	Ft/Sec
9	WL_{CG}	Inch

EQUATIONS:

$$N_N = \frac{1}{1.6878} \int U_G \, dt, \qquad P_{AX} = N_N + X_0$$

$$E = \frac{1}{1.6878} \int V_G \, dt, \qquad P_{AY} = E + Y_0$$

$$h_0 = \frac{(WL_{CG} - 11.0)}{12} + h_I \quad (h_I \text{ - Initial CG altitude})$$

$$h = -\int W_G \, dt + h_0 \quad , \qquad P_{AZ} = h + h_0$$

$$\dot{h} = -W_G$$

OUTPUTS:

Subsystem Block No.	Symbol	Units
	N_N	NM
	E	NM
9, 15, 16, 18	h	Ft
	P_{AX}	NM
	P_{AY}	NM
	P_{AZ}	Ft
16	$\dot{h}$	Ft/Sec

SUBSYSTEM NO. 11: AIRCRAFT ANGULAR ACCELERATIONS AND VELOCITIES

INPUTS:

A. Variables

Subsystem Block No.	Symbol	Units
13	X_A	Lbs.
	Z_A	Lbs
14	l_A	Lb Ft
	M_A	Lb. Ft.
	N_A	Lb. Ft.
11	$\dot{p}$	Rad/Sec^2
	$\dot{q}$	Rad/Sec^2
	$\dot{r}$	Rad/Sec^2
	p	Rad/Sec
	q	Rad/Sec
	r	Rad/Sec
8a	β_M	Rad
	$\dot{\beta}_M$	Rad/Sec
9	I_{XX}	Slug Ft^2
	I_{YY}	Slug Ft^2
	I_{ZZ}	Slug Ft^2
	I_{XZ}	Slug Ft^2
	X_{CG}, Z_{CG}	Ft
	$\dot{X}_{CG}$, $\dot{Z}_{CG}$	Ft/Sec
	$\ddot{X}_{CG}$, $\ddot{Z}_{CG}$	Ft/Sec^2

Subsystem Block No.	Symbol	Units
9	SL_{CG}	Inch
	WL_{CG}	Inch

EQUATIONS:

A. Aircraft CG Angular Accelerations (Body Axes)

Roll Equation:

$$I_{XX}\,\dot{p} = (I_{YY} - I_{ZZ})\,q\,r + I_{XZ}(\dot{r} + pq) + l_A$$

Pitch Equation:

$$I_{YY}\,\dot{q} = (I_{ZZ} - I_{XX})pr + I_{XZ}(r^2 - p^2) + M_A$$

Yaw Equation:

$$I_{ZZ}\,\dot{r} = (I_{XX} - I_{YY})pq + I_{XZ}(\dot{p} - rq) + N_A$$

Angular Rate Equations:

$$p = \int \dot{p}\,dt$$

$$q = \int \dot{q}\,dt$$

$$r = \int \dot{r}\,dt$$

B. Pilot Station Accelerations (Body Axes)

$$a_{XPA} = \frac{X_A}{m} + (\dot{q} + pr)(Z_{PA} - Z_{CG}) + (q^2 + r^2)(X_{CG} - l_{PA})$$
$$+ Y_{PA}(pq - \dot{r}) - 2q\,\dot{Z}_{CG} - \ddot{X}_{CG}$$

$$a_{YPA} = \frac{Y_A}{m} + (\dot{p} - qr)(Z_{CG} - Z_{PA}) + (\dot{r} + pq)(l_{PA} - X_{CG})$$

$$- Y_{PA}(r^2 + p^2) + 2(p\dot{Z}_{CG} - r\dot{X}_{CG})$$

$$a_{ZPA} = \frac{Z_A}{m} + (\dot{q} - pr)(X_{CG} - l_{PA}) + (p^2 + q^2)(Z_{CG} - Z_{PA})$$

$$+ Y_{PA}(\dot{p} + qr) + 2q\dot{X}_{CG} - \ddot{Z}_{CG}$$

C. Pilot Station Velocities (Body Axes)

$$U_{PA} = U - q * Z'_{PA} - r * Y'_{PA} - \dot{X}_{CG}$$

$$V_{PA} = V + r * l'_{PA} - p * Z'_{PA}$$

$$W_{PA} = W - q * l'_{PA} + p * Y'_{PA} - \dot{Z}_{CG}$$

where, $l'_{PA} = (SL_{CG} - SL_{PA})/12$, $l_{PA} = (SL_{SP} - SL_{PA})/12$

$$Y'_{PA} = (BL_{PA} - BL_{CG})/12, \quad Y_{PA} = \frac{BL_{PA}}{12}$$

$$Z'_{PA} = (WL_{PA} - WL_{CG})/12, \quad Z_{PA} = (WL_{PA} - WL_{SP})/12$$

OUTPUTS

Subsystem Block No.	Symbol	Units
11	$\dot{p}$	Rad/Sec^2
	$\dot{q}$	Rad/Sec^2
	$\dot{r}$	Rad/Sec^2
1, 4, 5, 6, 10c, 11, 12	p	Rad/Sec
FSAA CAB	q	Rad/Sec
	r	Rad/Sec
FSAA CAB	a_{XPA}	Ft/Sec^2
	a_{YPA}	Ft/Sec^2
	a_{ZPA}	Ft/Sec^2
	U_{PA}	Ft/Sec
	V_{PA}	Ft/Sec
	W_{PA}	Ft/Sec

SUBSYSTEM NO. 12: BODY AXIS LINEAR ACCELERATIONS AND VELOCITIES

INPUTS:

A. Variables

Subsystem Block No.	Symbol	Units
13	X_A	Pounds
	X_A	Pounds
	Z_A	Pounds
12	U	Ft/Sec
	V	Ft/Sec
	W	Ft/Sec
11	p	Rad/Sec
	q	Rad/Sec
	r	Rad/Sec
10c	θ	Rad
	ϕ	Rad

EQUATIONS:

$$\dot{U} = -g \sin\theta + Vr - Wq + \frac{X_A}{m}$$

$$\dot{V} = g \cos\theta \sin\phi - rU + Wp + \frac{Y_A}{m}$$

$$\dot{W} = g \cos\theta \cos\phi + qU - pV + \frac{Z_A}{m}$$

$$N_X = \frac{X_A}{GW}$$

$$N_Y = \frac{Y_A}{GW}$$

$$N_Z = \frac{Z_A}{GW}$$

$$U = \int \dot{U}\, dt$$

$$V = \int \dot{V}\, dt$$

$$W = \int \dot{W}\, dt$$

$$V_T = \sqrt{U^2 + V^2 + W^2}$$

Angle of Attack,

$$\alpha_F = \tan^{-1} \frac{W}{U}$$

Angle of sideslip

$$\beta_F = \tan^{-1} \frac{V}{\sqrt{U^2 + W^2}}$$

OUTPUTS:

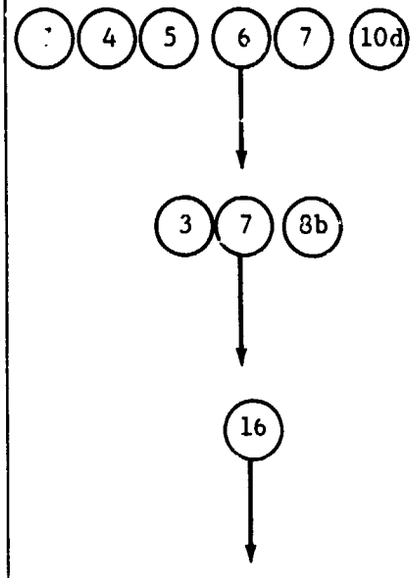

Subsystem Block No.	Symbol	Units
1, 4, 5, 6, 7, 10d	U	Ft/Sec
	V	Ft/Sec
	W	Ft/Sec
3, 7, 8b	V_T	Ft/Sec
	α_F	Rad
	β_F	Rad
16	N_X	g's
	N_Y	g's
	N_Z	g's

SUBSYSTEM NO. 13-FORCE SUMMATION

INPUTS:

Subsystem Block No.	Symbol	Units
10a	$(X, Y, Z)_F$	Lbs.
	$(X, Z)_{iWPL}$	Lbs.
	$(X, Z)_{iWPR}$	Lbs.
	$(X, Y, Z)_{WP}$	Lbs.
	$(X, Y, Z)_H$	Lbs.
	$(X, Z)_{MG}$	Lbs.
	$(X, Z)_{NG}$	Lbs.
	$(X, Y, Z)_L$	Lbs.
	$(X, Y, Z)_R$	Lbs.
	$(X, Y)_{VL}$	Lbs.
	$(X, Y)_{VR}$	Lbs.
	$(\Delta X, \Delta Y, \Delta Z)_{LG}$	Lbs.

EQUATIONS:

$$X_A = X_F + X_{iWPR} + X_{WP} + X_H + X_{MG} + \Delta X_{LG} + X_{NG}$$

$$+ X_L + X_R + X_{VL} + X_{VR} + X_{iWPL}$$

$$Y_A = Y_F + Y_{WP} + \Delta Y_{LG} + Y_L + Y_R + Y_{VL} + Y_{VR} + Y_H$$

$$Z_A = Z_F + Z_{iWPL} + Z_{WP} + Z_H + Z_{MG} + \Delta Z_{LG}$$

$$+ Z_{NG} + Z_L + Z_R + Z_{iWPR}$$

OUTPUTS:

Subsystem Block No.	Symbol	Units
(12)	X_A	Lbs.
	Y_A	Lbs.
	Z_A	Lbs.

SUBSYSTEM NO. 14-MOMENT SUMMATION

INPUTS:

Subsystem Block No.	Symbol	Units
9	SL_{CG}	Inch
	WL_{CG}	Inch
	BL_{CG}	Inch
10a	$(X, Y, Z)_{F}$	Lb.
	$(X, Z)_{iWPL}$	Lb.
	$(X, Z)_{iWPR}$	Lb.
	$(X, Y, Z)_{WP}$	Lb.
	$(X, Y, Z)_{H}$	Lb.
	$(X, Y)_{VL}$	Lb.
	$(X, Y)_{VR}$	Lb.
	$(X, Z)_{MG}$	Lb.
	$(X, Z)_{NG}$	Lb.
10b	$(X, Y, Z)_{L}$	Lb.
	$(X, Y, Z)_{R}$	Lb.
10a	$(l, M, N)_{F}$	Ft.lb
	$(l, M, N)_{WP}$	Ft.lb
	M_{H}	Ft.lb
10b	$(l, M, N)_{L}$	Ft.lb
	$(l, M, N)_{R}$	Ft.lb
	$(\Delta l, \Delta M, \Delta N)_{LG}$	Inch
4	$(r_{XW}, r_{YW})_{R}$	Inch
	$(r_{XW}, r_{YW})_{L}$	Inch
10c	ϕ	Deg.
9	h_{H}	Ft.

EQUATIONS:

$$M_A = X_F\,(WL_{CG} - WL_F)/12 + Z_F(SL_F - SL_{CG})/12 + (X_{iWPL} + X_{iWPR} + X_{WP}) *$$

$$(WL_{CG} - WL_W)/12 - Z_{iWPR} * r_{XWR}/12 - Z_{iWL} * r_{XWL}/12 + Z_{WP}\,(SL_W - SL_{CG})/12$$

$$+ X_H\,(WL_{CG} - WL_H)/12 + Z_H\,(SL_H - SL_{CG})/12 + X_{MG}\,(WL_{CG} - WL_{MG})/12$$

$$+ Z_{MG}\,(SL_{MG} - SL_{CG})/12 + X_{NG}\,(WL_{CG} - WL_{NG})/12 + Z_{NG}\,(SL_{NG} - SL_{CG})/12$$

$$+ (X_{VL} + X_{VR})\,(WL_{CG} - WL_V)/12 + (X_L + X_R)[WL_{CG} - (WL_{SP} + 12\,l_M \cos\beta_M)]/12$$

$$+ (Z_L + Z_R)\,[(SL_{SP} - 12\,l_M \sin\beta_M) - SL_{CG}]/12 + M_F + M_{WP}$$

$$+ M_H + M_L + M_R + \Delta M_{LG}$$

$$l_A = Y_F\,(WL_F - WL_{CG})/12 + Z_{iWPL} * r_{YWL}/12 + Z_{iWPR} * r_{WYR}/12$$

$$+ (Y_{iWPR} + Y_{iWPL} + Y_{WP})\,(WL_W - WL_{CG})/12 + (Y_{VL} + Y_{VR})(WL_V - WL_{CG})/12$$

$$+ (Y_L + Y_R)\,[(WL_{SP} + 12\,l_M \cos\beta_M) - WL_{CG}]/12 + Z_L(BL_{SPL} - BL_{CG})/12$$

$$+ Z_R\,(BL_{SPR} - BL_{CG})/12 + l_F + l_{WP} + l_L + l_R + l_G * \phi + \Delta l_{LG}$$

Where,

$$l_G = \{l_{GO} + l_{G1} * \frac{h_H}{2R} + l_{G2} * (\frac{h_H}{2R})^2 + l_{G3} * (\frac{h_H}{2R})^3\} * e^{(-.1V_T)}$$

For $0.5 \leq \frac{h_H}{2R} \leq 1.4$

$$N_A = Y_F\ (SL_{CG} - SL_F)/12 - X_{iWPL} * r_{YWL}\ /12 - X_{iWPR} * r_{YWR}/12$$

$$+ Y_{iWPR} * r_{XWR}/12 + Y_{iWPL} * r_{XWL}/12 + Y_{WP}\ (SL_{CG} - SL_W)/12$$

$$+ X_L\ (BL_{CG} - BL_{SPL})/12 + X_R\ (BL_{CG} - BL_{SPR})/12 + Y_H\ (SL_{CG} - SL_H)/12$$

$$+ (Y_{VL} + Y_{VR})\ (SL_{CG} - SL_V)/12 + (X_{VL} - X_{VR})\ (BL_{VR} - BL_{CG})/12$$

$$+ (Y_L + Y_R)[SL_{CG} - (SL_{SP} - 12\ l_M \sin \beta_M)]/12 + N_F + N_{WP} + N_L$$

$$+ N_R + \Delta N_{LG}$$

OUTPUTS:

Subsystem Block No.	Symbol	Units
(11)	M_A	Ft.Lb.
	l_A	Ft.Lb.
	N_A	Ft.Lb.

SUBSYSTEM NO. 15: FLIGHT ENVIRONMENT DATA

INPUTS:

A. Variables

Subsystem Block No.	Symbol	Units
(10f)	h	Ft.
(12)	V_T	Ft/Sec

B. Constants

	T_o	^oC

EQUATIONS:

$$T_a = 288.15 - .0019812\ h + T_o$$

$$\theta_T = \frac{T_a}{288.15}$$

$$\delta_T = \left[\frac{T_a}{288.15}\right]^{5.255876}$$

$$\sigma' = \left\{\frac{(1 - .00000687\ h)^{5.255876}}{1 - .000687\ h + \theta_T}\right\}$$

$$\rho = (.002378)(\sigma')$$

$$V_S = 661.48\ (\theta_T)^{1/2}$$

$$M_N = V_T/V_S$$

$$V_{CAS} = 661.48\left[5\left\{\left(1 + \delta_T\left(1 + \frac{.2}{\theta_T}\left(\frac{V_T}{661.48}\right)^2\right)^{7/2} - 1\right)^{2/7} - 1\right\}\right]^{1/2}$$

OUTPUTS:

Subsystem Block No.	Symbol	Units
(1) (3) (4) (5) (6) (7)	ρ	Slugs-Ft^2
(16)	V_{CAS}	MPH
(18)	T_a	^oK
(4) (5) (6)	V_S	Ft/Sec

SUBSYSTEM NO. 16: PILOT'S FLIGHT INSTRUMENTS

COCKPIT INSTRUMENT DISPLAY

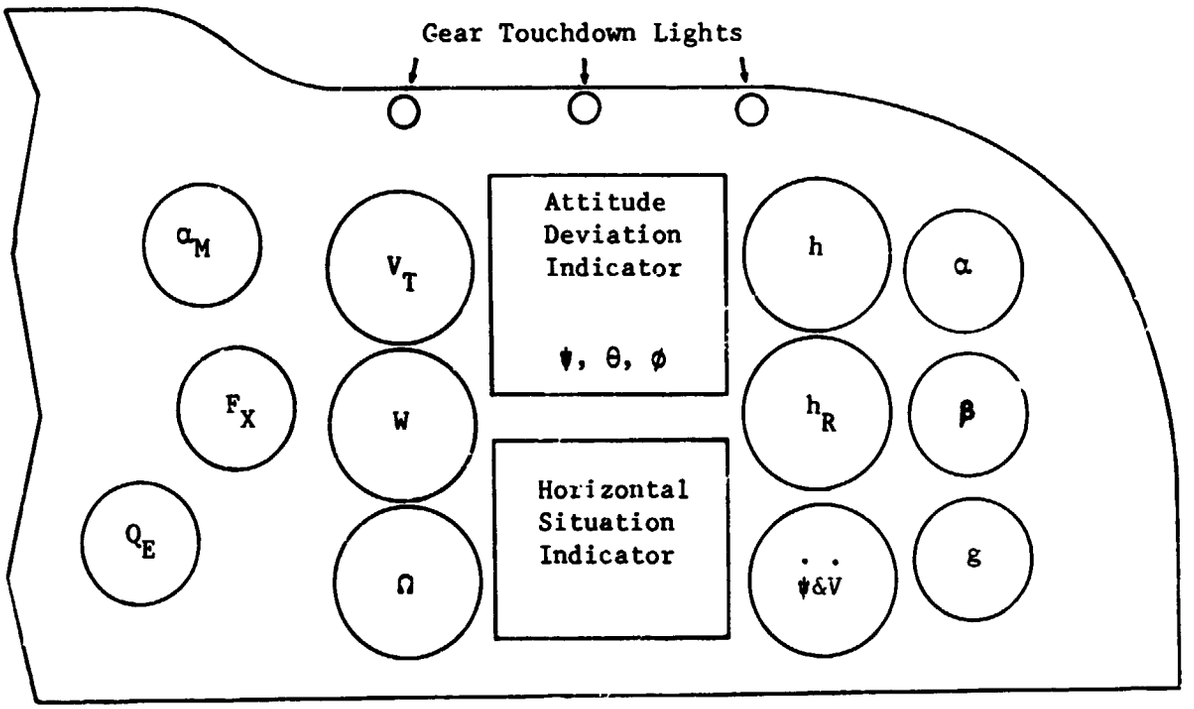

α_M Nacelle Tilt Angle
F_X Flap Position
Q_E Engine Torque
V_T Airspeed
W Vertical Velocity Indicator
Ω Rotor RPM

h Baro Altimeter
h_R Radar Altimeter
$\dot{\psi}\&V$ Turn and Slip
α Angle of Attack
β Side Slip Angle
g Normal Acceleration

FSAA - MODEL 301 PILOTS PANEL

SUBSYSTEM NO. 17: ROTOR COLLECTIVE GOVERNOR

INPUTS:

A. Variables

Subsystem Block No.	Symbol	Units
(8d)	RPM_P	RPM
(19)	Ω_{INT}	Rad/Sec

B. Coefficients

K_{RPG}	ND
K_{IG}	ND
$\frac{\partial \Omega_{0\ INT}}{\partial \Omega_{RO}}$	ND

EQUATIONS:

$$\bar{\theta}_{0G} = K_{RPG}\,(\beta_M) * \left[\frac{1}{s} + K_{IG}\right]\left[\frac{\Omega_{INT} * 9.55}{\left(\frac{\partial \Omega_{INT}}{\partial \Omega_{RO}}\right)} - RPM_P\right] \qquad \left(s \text{ is Laplace operator}\right)$$

If $\bar{\theta}_{0G} > 0$ then $\theta_{0L/G},\ \theta_{0R/G} = MIN\left[\bar{\theta}_{0G},\ \theta_{0G_{max}}\right]$

If $\bar{\theta}_{0G} < 0$ then $\theta_{0L/G},\ \theta_{0R/G} = MIN\left[\bar{\theta}_{0G},\ \theta_{0G_{min}}\right]$

OUTPUTS:

Subsystem Block No.	Symbol	Units
(8a)	$\theta_{0L/G},\ \theta_{0R/G}$	Deg

SUBSYSTEM NO. 18: ENGINES AND FUEL CONTROLS

INPUTS:

A. Variables

Subsystem Block No.	Symbol	Units
8d	X_{THR}	Deg
	X_{THL}	Deg
10f	h	Ft.
12	V_T	Ft/Sec
15	P_a	Psia
	T_a	^oK
19	Ω_{RPT}	Rad/Sec
	Ω_{LPT}	Rad/Sec

B. Engine Coefficients

K_1, K_2, K_3	ND
K_4, K_5, K_6	RPM, RPM/$\sqrt{HP}$, HP
K_7	^oK
K_8, K_9, K_{10}, K_{11}, K_{13}, K_{14}	HP/Deg^2, HP/Deg, HP, $1/^oK$, 1/Deg, $1/Deg^2$, Deg
t_D	Sec
pctmxs, pctmxp	%, %
P_o	Lb/In^2
T_o	^oK

EQUATIONS:

A. Power-Turbine (N_2) Governor

$$HP_{ROPTG} = (HP_{RO})_0 + \int_{t_D}^{t_{PTG}} \frac{dHP_{ROS}}{dt_{PTG}} dt_{PTG}$$

$$\epsilon_S = \left(\frac{9.55 * \Omega_{RPT}}{RPM_{N_{II}}} - 1 \right)$$

$$RPM_{N_{II}} = 22200$$

Integration begins when $|\epsilon_S|$ has exceeded 0.002 for t_D seconds, and continues until $\epsilon_S \leq 0.002$ at which time $(HP_{RO})_0$ is reset to the current HP_{RO}, and t_{PTG} is reset to zero.

$$\frac{dHP_{ROS}}{dt_{PTG}} = \text{sign}(-\epsilon_S) * \text{MIN}\left\{1, \frac{100 * |\epsilon_S|}{\text{pctmxs}}\right\} * f_1(HP_{RO}, h)$$

$$HP_{ROPTG} = \text{MIN}\left\{HP_{ROPTG}, HP_{ROTH}\right\}$$

B. Throttle Control

HP_{ROC} is the commanded referred optimum HP on one engine.

If $X_{THR} \leq 46.0$ $HP_{ROC} = 150.$

If $T_a \leq K_7$,

$$HP_{ROC} = K_8 X_{THR}^2 + K_9 X_{THR} + K_{10}$$

If $T_a > K_7$,

$$HP_{ROC} = [1 - K_{11}\ (T_a - K_7)][K_{12} + K_{13}\ (X_{THR} - K_{14})][K_8\ X_{THR}^2 + K_9\ X_{THR} + K_{10}]$$

$$HP_{ROC} = (HP_{RO})_0 + \int_{t_D}^{t_{HP}} \frac{dHP_{ROT}}{dt_{TH}}\, dt_{TH}$$

$$\epsilon_p = \frac{HP_{ROTH}}{HP_{ROC}} - 1$$

Integration begins when ϵ_p has exceeded 0.002 for t_D seconds, and continues till $\epsilon_p \leq 0.002$, at which time $(HP_{RO})_0$ is reset to the current HP_{RO}, and t_{TH} is reset to zero.

$$\frac{dHP_{ROT}}{dt_{TH}} = \text{SIGN}\ (-\epsilon_p) * \min\left\{1, \frac{100 * \epsilon_p}{\text{pctmxp}}\right\} * f_1\ (HP_{RO}, h)$$

C. Actual Power Developed

Referred optimum horsepower of one engine

$$= HP_{RO} = \min\left\{HP_{ROPTG}, HP_{ROTH}\right\}$$

$$HP = (HP_{RO}\ \delta\ \sqrt{\theta}\ )\left[K_1\left(\frac{9.55 * \Omega\ RPT}{\sqrt{\theta}\ RPM_{RO}}\right)^2 + K_2\left(\frac{9.55 * \Omega\ RPT}{\sqrt{\theta}\ RPM_{RO}}\right) + K_3\right]$$

where $$RPM_{RO} = K_4 + K_5\left\{MAX\ \left[(HP_{RO} - K_6),\ 0.1\right]\right\}^{1/2}$$

$$\delta = \left(\frac{P_a}{P_o}\right)\left[1 + \frac{.0000461\ V_T^2}{T_a}\right]^{7/2}$$

$$\theta = \left(\frac{T_a}{T_o}\right)\left[1 + \frac{.0000461\ V_T^2}{T_a}\right]$$

The actual power developed by the two engines is given by:

$$HP_R = HP * \eta_{ER}$$

$$HP_L = HP * \eta_{EL}$$

η_{ER}	η_{EL}	Comments
1	1	Both engines operating
1	0	Left engine cut
0	1	Right engine out

$$Q_{RPT} = \frac{HP_R * 550}{\Omega_{RPT}}$$

$$Q_{LPT} = \frac{HP_L * 550}{\Omega_{LPT}}$$

Initial values: (at the beginning of simulation)

$$(HP_{RO})_0 = HP_{ROC}$$

OUTPUTS:

Subsystem Block No.	Symbol	Units
19 ↓	Q_{RPT}	Lb. Ft.
	Q_{LPT}	Lb. Ft.

SUBSYSTEM NO. 19: DRIVE SYSTEM DYNAMICS

INPUTS:

A. Variables

Subsystem Block No.	Symbol	Units
1	Q_R	Lb-Ft
	Q_L	Lb-Ft
18	Q_{RPT}	Lb-Ft
	Q_{LPT}	Lb-Ft

B. Constants

Symbol	Units
I_1	$Slug\text{-}Ft^2$
θ_{RPT1}	ND
θ_{INT1}	ND

EQUATIONS:

Drive shaft angular acceleration,

$$\ddot{\xi} = \frac{F_1(t)}{I_1}$$

$$F_1(t) = -(Q_R + Q_L) + \theta_{RPT1}\ (Q_{RPT} + Q_{LPT})$$

$$\Omega_R = \Omega_{R_0} + \dot{\xi}$$

$$\Omega_L = \Omega_R$$

$$\Omega_{RPT} = \Omega_R * \theta_{RPT1}$$

$$\Omega_{LPT} = \Omega_{RPT}$$

$$\Omega_{INT} = \Omega_R * \theta_{INT1}$$

OUTPUTS:

Subsystem Block No.	Symbol	Units
1	Ω_R	Rad/Sec
	Ω_L	Rad/Sec
18	Ω_{RPT}	Rad/Sec
	Ω_{LPT}	Rad/Sec
17	Ω_{INT}	Rad/Sec

SUBSYSTEM NO. 20: STABILITY AND CONTROL AUGMENTATION SYSTEM

INPUTS:

A. Variables

Subsystem Block No.	Symbol	Units
12	V_T	Ft/Sec
	U	Ft/Sec
8a	β_M	Deg
8d	X_{LN}	In.
	X_{LT}	In.
	X_{PD}	In.
10c	P	Rad/Sec
	q	Rad/Sec
	r	Rad/Sec
	Ψ	Rad
	θ	Rad
	φ	Rad

B. SCAS Gains and Time Constants

$K_{1P}[U, \beta_M], \ldots K_{10P}[U, \beta_M]$ (Pitch Gains)

$T_{1P}, T_{2P}, T_{3P}, T_{4P}$ (Pitch Time Constants)

$K_{1Y}[U, \beta_M], \ldots K_{5Y}[U, \beta_M]$ (Yaw Gains)

$T_{1Y}, T_{2Y}, T_{3Y}, T_{4Y}$ (Yaw Time Constants)

$K_{1R}[U, \beta_M], \ldots . K_{10R}[U, \beta_M]$ (Roll Gains)

T_{1R}, T_{2R}, T_{3R} (Roll Time Constants)

EQUATIONS:

A. Pitch SCAS Electronics

$$PSCAS = q * \left[K_{3P} + \frac{s}{(sT_{2P})(sT_{3P} + 1)} \; K_{2P} \right]$$

$$+ (X_{LN} - X_{LNN}) * \left[\frac{s \; K_{1P} \quad * \quad K_{2P}}{(sT_{1P} + 1)(sT_{2P} + 1)(sT_{3P} + 1)} \right]$$

$$+ \; PHOLD$$

(s is Laplace operator)

where,

$$PHOLD = SIGN(\overline{PHOLD}) * MIN \left[\left| \overline{PHOLD} \right| \; , PHOLD_{max} \right]$$

$$\overline{PHOLD} = K_{5P} \quad * \{57.3 * \theta(t) - \theta_{REFD}(t)\}$$

$$+ K_{8P} * \{-U(t) + U_{REFD}(t)\} + K_{9P} * 57.3 * \theta(t)$$

$$\theta_{REFD}(t) = \int_0^t K_{4P} \{K_{6P} * IFPH * [U(t) - U_{REF}(t)]$$

$$+ [1-IFPH(t)] * [57.3 * \theta(t) - \theta_{REFD}(t)]\} \; dt$$

$$\theta_{REFD}(0) = 57.3 * \theta(0)$$

$$U_{REF}(t) = \int_0^t K_{7P} * [1 - IFUH(t)] * [U(t) - U_{REF}(t)] \; dt$$

$$U_{REF}(0) = U(0)$$

PHOLD is the output from the pitch-attitude-hold and airspeed-hold circuits. IFUH and IFPH defined on page A-115.

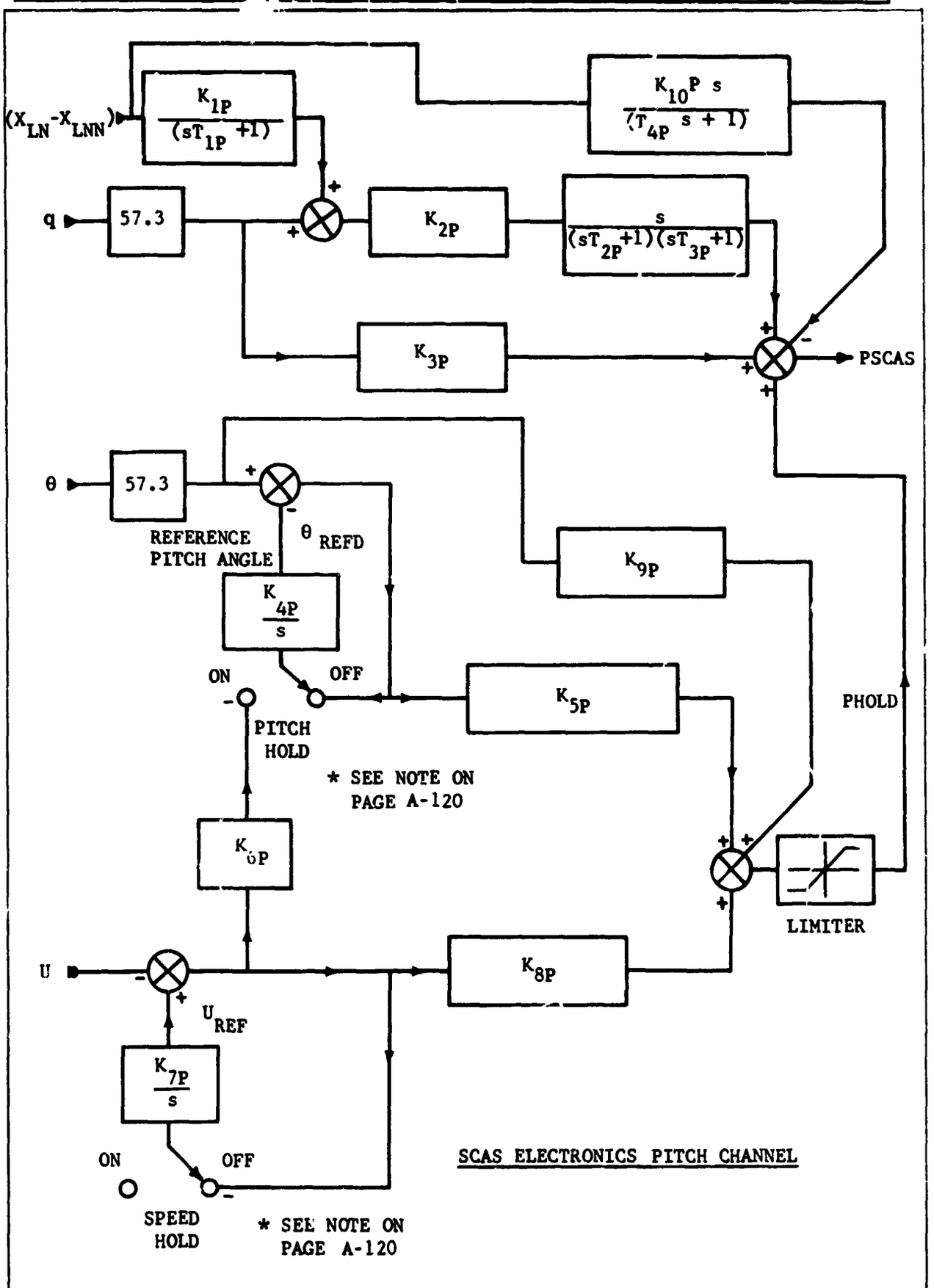

SCAS ELECTRONICS PITCH CHANNEL

IFPH = 0, If pitch-attitude-hold is Off.

= 1, If pitch-attitude-hold is Operative

IFUH = 0, If airspeed-hold is Off.

= 1, If airspeed-hold is Operative and if U $\geq$ 102 Ft/Sec

When the airspeed-hold is tripped off due to U dropping below 102 FPS, it can be re-engaged only manually after the aircraft has reached a new trim-point.

Pitch SCAS Parameters

$$K_{1P} = K_{1PU} * K_{1P\beta_M}$$

$$K_{2P} = K_{2PU} * K_{2P\beta_M}$$

$$K_{3P} = K_{3PU} * K_{3P\beta_M}$$

If IFUH = 0, $K_{5P} = K_{5PU0} * K_{5P\beta_M 0}$

If IFUH = 1, $K_{5P} = K_{5PU1} * K_{5P\beta_M 1}$

$$K_{8P} = K_{8PU} * K_{8P\beta_M}$$

$$K_{9P} = K_{9PU} * K_{9P\beta_M}$$

$$K_{10P} = K_{10P\beta_M}$$

B. Yaw SCAS Electronics

$$YSCAS = -r * \left[K_{3Y} + \frac{s\,K_{2Y}}{(sT_{2Y} + 1)(sT_{3Y} + 1)} \right] + \left(X_{PD} - X_{PDN} \right) * \left[\frac{s\,(sT_{4Y} + 1)\,K_{1Y}}{(sT_{1Y} + 1)(sT_{2Y} + 1)(sT_{3Y} + 1)} \right] + YHOLD$$

where,

$$YHOLD = SIGN\,(\overline{YHOLD}) * MIN\left[\left| \overline{YHOLD} \right| , YHOLD_{max} \right]$$

$$\overline{YHOLD} = K_{5Y} * \{\Psi_{REFD}(t) - 57.3 * \Psi(t)\}$$

$$\Psi_{REFD}(t) = \int_0^t K_{4Y} * [1 - IFYH(t)] * [57.3 * \Psi(t) - \Psi_{REFD}(t)]\,dt$$

$$\Psi_{REFD}(0) = 57.3 * \Psi(0)$$

YHOLD is the output from the yaw-attitude-hold circuit.

IFYH = 0, If yaw-attitude-hold is Off.

= 1, If yaw-attitude-hold is Operative.

Yaw SCAS Parameters

$$K_{1Y} = K_{1YU} * K_{1Y\beta_M}$$

$$K_{2Y} = K_{2YU} * K_{2Y\beta_M}$$

$$K_{3Y} = K_{3YU} * K_{3Y\beta_M}$$

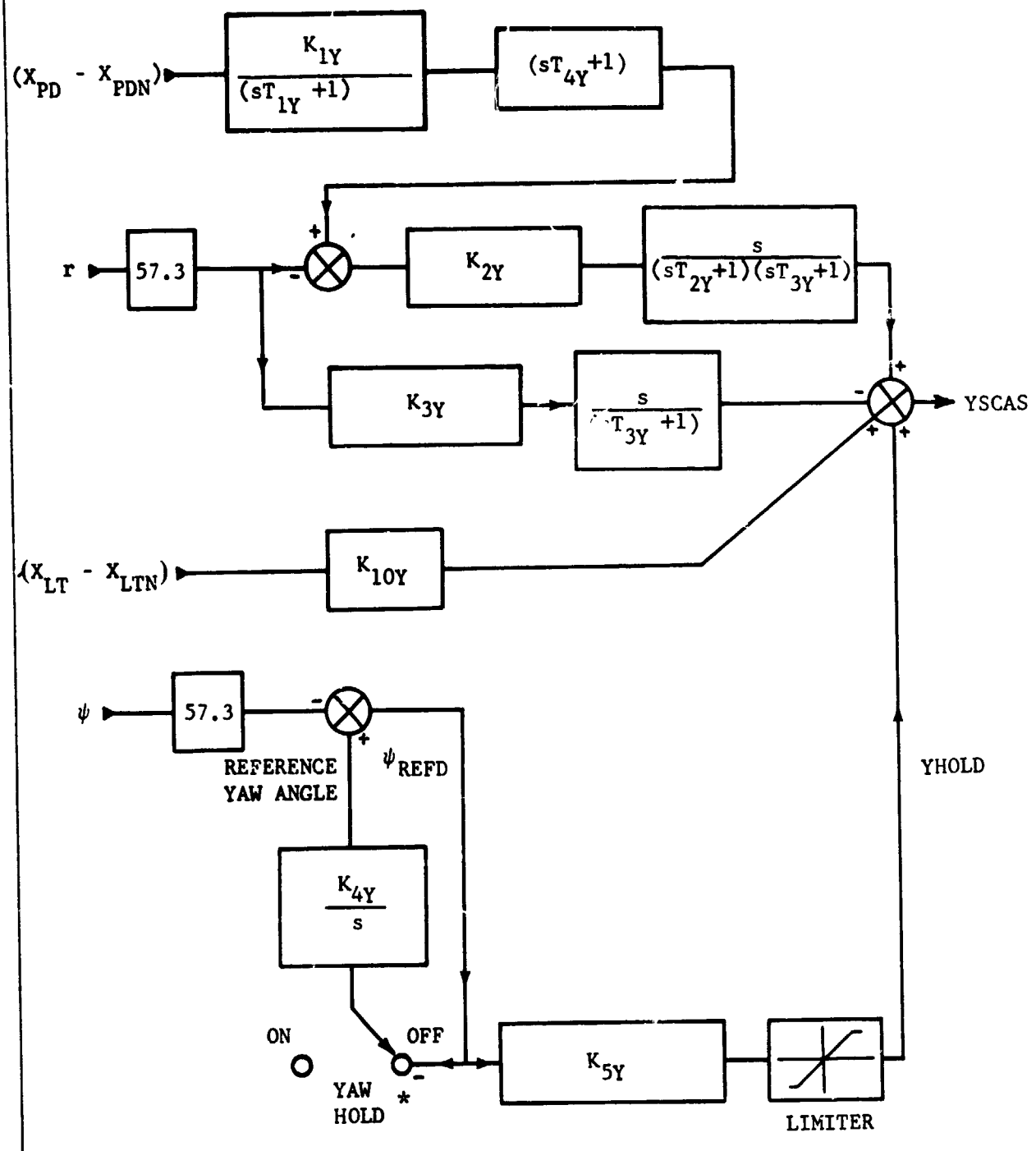

SCAS ELECTRONICS

YAW CHANNEL

*See Note on page A-120

If IFUH = 0, $K_{5Y} = K_{5YU0} * K_{5Y\beta_M}0$

If IFUH = 1, $K_{5Y} = K_{5YU1} * K_{5Y\beta_M}1$

$$K_{10Y} = K_{10Y\beta_M}$$

Roll SCAS Electronics

$$RSCAS = -p * \left[K_{3R} + \frac{s\,K_{2R}}{(sT_{2R} + 1)(sT_{3R} + 1)} \right] + \left(X_{} - X_{LTN} \right) * \left[\frac{s\,K_{1R} * K_{2R}}{(sT_{1R} + 1)(sT_{2R} + 1)(sT_{3R} + 1)} \right] + RHOLD$$

where,

$$RHOLD = SIGN\ \overline{(RHOLD)} * MIN \left[\left| \overline{RHOLD} \right| , RHOLD_{max} \right]$$

$$\overline{RHOLD} = K_{5R} * \left| \phi_{REFD}(t) - 57.3 * \phi(t) \right| - K_{9R} * 57.3 * \phi(t)$$

$$\phi_{REFD}(t) = \int_0^t K_{/R} * [1 - IFRH(t)] * [57.3 * \phi(t) - \phi_{REFD}(t)\ ]\, dt$$

$$\phi_{REFD}(0) = 57.3 * \phi(0)$$

RHOLD is the output from the roll-attitude-hold circuit.

IFRH = 0, If roll-attitude-hold is Off.

= 1, If roll-attitude-hold is Operative.

SCAS ELECTRONICS

ROLL CHANNEL

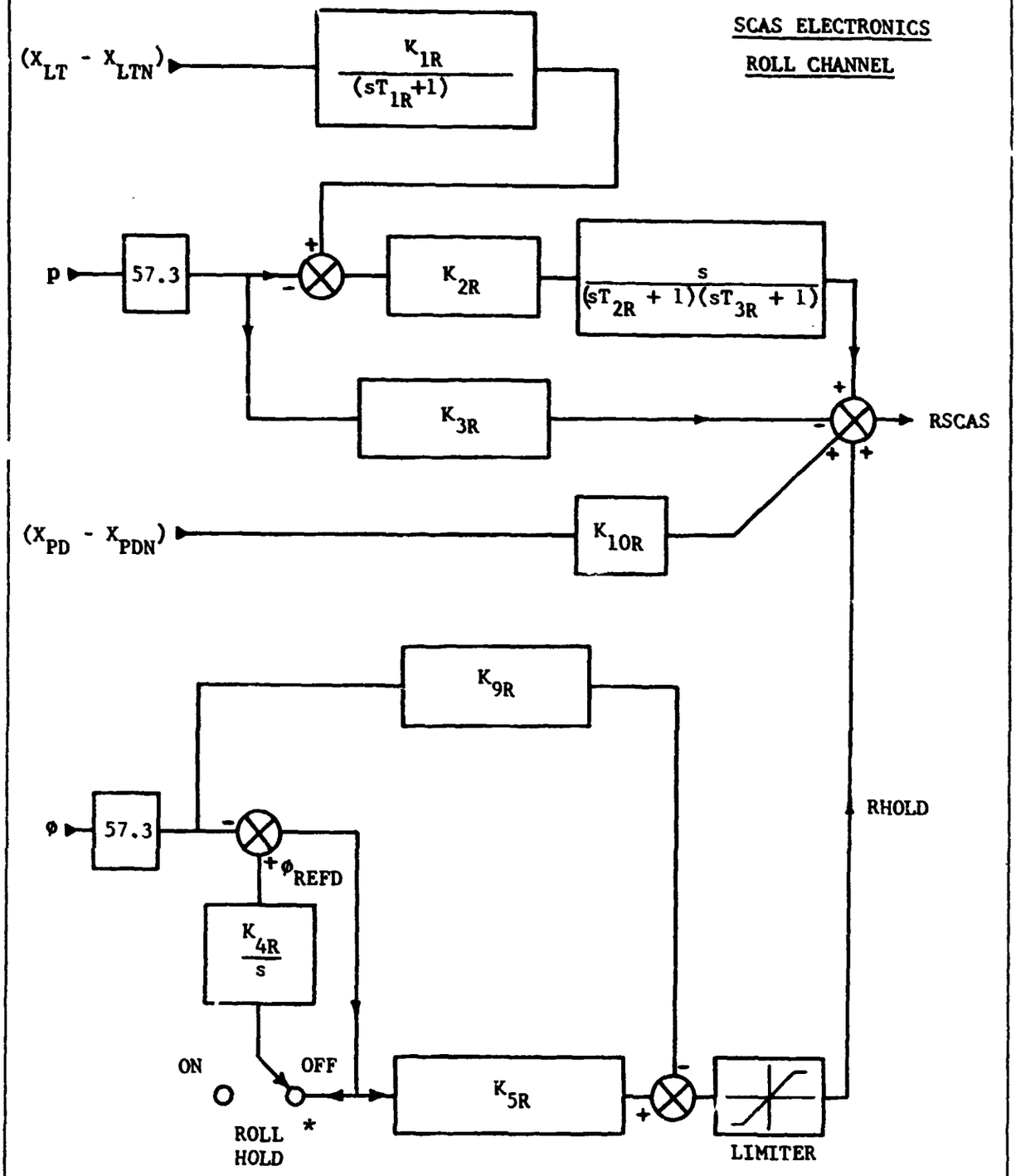

*See Note on Page A-120

Roll SCAS Parameters

$$K_{1R} = K_{1RU} * K_{1R\phi_M}$$

$$K_{2R} = K_{2RU} * K_{2R\phi_M}$$

$$K_{3R} = K_{3RU} * K_{3R\phi_M}$$

$$K_{9R} = K_{9RU} * K_{9R\phi_M}$$

If IFUH = 0, $K_{5R} = K_{5RUC} * K_{5R\phi_M 0}$

If IFUH = 1, $K_{5R} = K_{5RU1} * K_{5R\phi_M 1}$

$$K_{10R} = K_{10R}$$

$$ESAS = SIGN\ (\overline{PSCAS}) * MIN\ \ ESAS_{max},\ ABS\ (\overline{PSCAS})$$

$$RSAS = SIGN\ (\overline{RSCAS}) * MIN\ \ RSAS_{max},\ ABS\ (\overline{RSCAS})$$

$$ASAS = SIGN\ (\overline{ASCAS}) * MIN\ \ ASAS_{max},\ ABS\ (\overline{ASCAS})$$

*NOTE

ATTITUDE/AIRSPEED HOLD SWITCH LOGIC

1. Turn all holds to Off if Mag brake release depressed
2. Turn pitch and airspeed holds Off if long stick is out of force detent.
3. Turn roll and yaw holds Off if Lat stick or pedal is out of force detent.

OUTPUTS:

Subsystem Block No.	Symbol	Units
8a	ESAS	Inch
	RSAS	Inch
	ASAS	Inch

APPENDIX B

INPUT DATA FOR MODEL 301

TILT ROTOR RESEARCH AIRCRAFT

TABLE I - MODEL 301 CG AND INERTIA DATA

DESIGN GW = 13000 lbs

	Aft CG	Fwd CG
$SL_{CG}\|\beta_m = 0$	301.2	291.7
$BL_{CG}\|\beta_m = 0$	0	0
$WL_{CG}\|\beta_m = 0$	81.65	81.65
$I_{XX}\|\beta_m = 0$	42379	42379
$I_{YY}\|\beta_m = 0$	14230	14351
$I_{ZZ}\|\beta_m = 0$	49459	49580

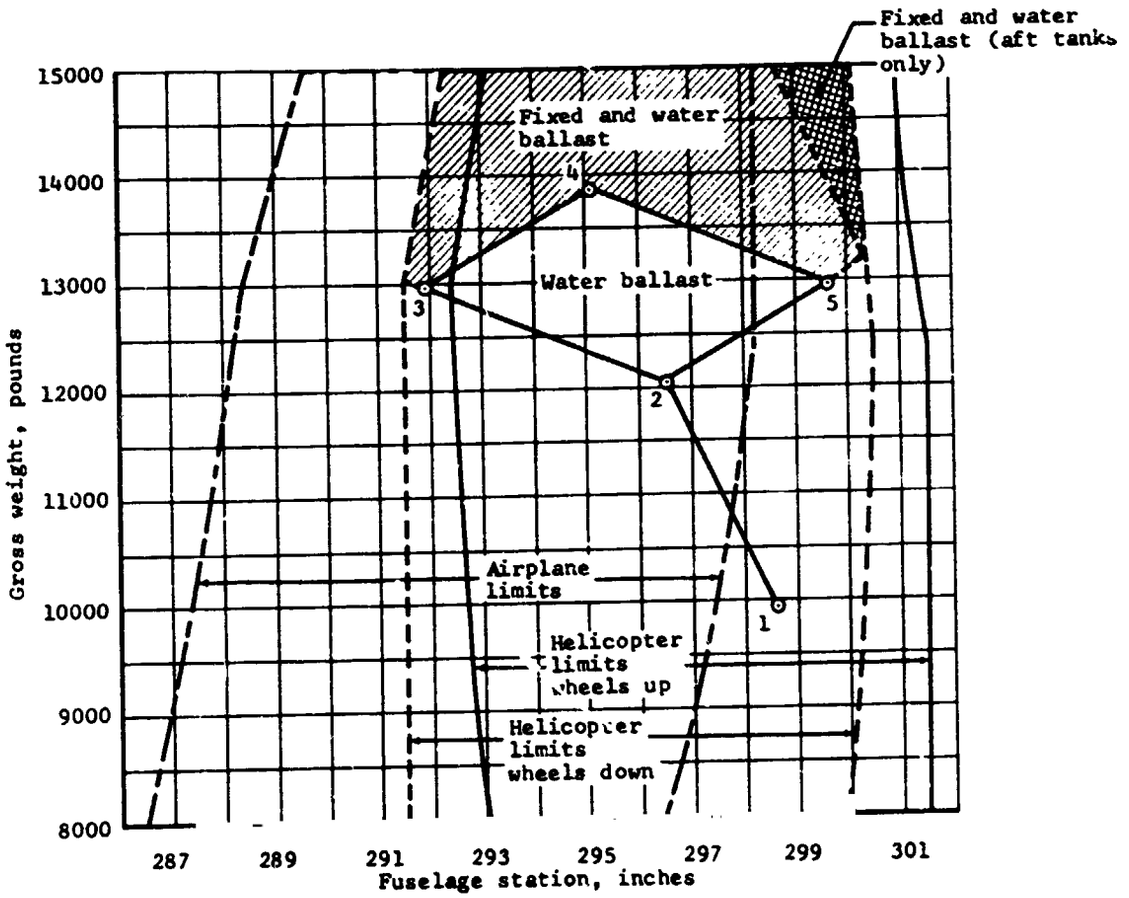

TABLE II-AIRCRAFT DESIGN DATA

ITEM	SYMBOL	M301 VALUE
Fuselage		
Center of pressure	SL_F	293.0 In.
	BL_F	0.0 In.
	WL_F	84.0 In.
Wing-Pylon		
Center of pressure	SL_{WP}	291.17 In.
	BL_{WP}	102.5 In.
	WL_{WP}	95.85 In.
Area	S_W	181.0 Ft^2
Span	b_W	32.17 Ft.
Chord	c_W	5.225 Ft.
Sweep	$\Lambda c/_4 W$	-6.5 Deg.
Aspect Ratio	AR_W	5.7
Trailing Edge	SL_{WTE}	
Horizontal Stabilizer		
Center of pressure	SL_H	560.0 In.
	BL_H	0.0 In.
	WL_H	103.0 In.
Area	S_H	50.25 $Ft.^2$
Span	b_H	12.83 Ft.
Chord	C_H	3.92 Ft.
Leading Edge	SL_{HLE}	548.25 In.
Vertical Stabilizer		
Center of pressure	SL_V	570.02 In.
	BL_V	77.0 In.
	WL_V	115.69 In.
Number of Panels		2.
Area (Per Panel)	S_V	25.25 $Ft.^2$

ITEM	SYMBOL	M301 VALUE
Vertical Stabilizer (Continued)		
Span	b_V	7.68 Ft.
Chord	c_V	3.725 Ft.
Leading Edge	SL_{VLE}	555.1 In.
Rotors		
Location of Shaft Pivot Point	SL_{SP}	300.0 In.
	BL_{SP}	193.0 In.
	WL_{SP}	100.0 In.
Number of Blades Per Rotor	n_b	3
Radius	R	12.5 Ft.
Chord	c_b	1.167 Ft.
Mast Length	ℓ_M	4.667 Ft.
Pitch-Flap Coupling	δ_3	-15.0 Deg.
Solidity	σ	0.089
Lock Number	γ	3.83
Direction of Rotation -inboard tip motion-helicopter/airplane		Aft/Up
Rotor RPM		
Helicopter		565 RPM
Conversion		565 RPM
Airplane		458 RPM
Blade Flapping Limits		±12 Deg.
Flapping Inertia per Blade	I_b	102.5 Slug-Ft.^{2}
Flapping Spring Rate/Rotor	$K_{FA}/,K_{LAT}$	225.0 Ft-L./Deg.
Blade Twist Distribution:	X_M, θ_M	
	X_{MO}, θ_{MO}	1.0, 0.0
	X_{M1}, θ_{M1}	0.6,10.2
	X_{M2}, θ_{M2}	0.5333, 12.3
	X_{M3}, θ_{M3}	0.4667, 14.5
	X_{M4}, θ_{M4}	0.4000, 17.75

ITEM	SYMBOL	M301 VALUE
Rotors (Continued)		
	X_{M5}, θ_{M5}	0.3333, 21.90
	X_{M6}, θ_{M6}	0.2667, 26.15
	X_{M7}, θ_{M7}	0.2000, 30.65
	X_{M8}, θ_{M8}	0.1333, 34.65
	X_{M9}, θ_{M9}	0.0667, 38.00
	X_{M10}, θ_{M10}	0.0 , 40.90
Angle of outboard tilt of mast axis		
Helicopter	ϕ_M	1.0* Deg.
Airplane		0 Deg.
Conversion range	β_M	-5 to + 90 Deg.
Pylon		
Center of Gravity	SL_P	291.7 In.
	BL_P	193.0 In.
	WL_P	118.0 In.
Weight (Two pylons)	W_P	3986 Lbs.
Inertia (Per pylon)	I_X	81.4 Slug-Ft.^{2}
	I_Y	431.0 Slug-Ft.^{2}
	I_Z	380.0 Slug-Ft.^{2}
Landing Gear		
Main Gear Coordinates	SL_{MG}	324.0 In.
	BL_{MG}	54.75 In.
	WL_{MG}	7.40 In.
Nose Gear Coordinates	SL_{NG}	139.0 In.
	BL_{NG}	0.0 In.
	WL_{NG}	4.95 In.

*The builtin dihedral of the pylon is 2.5 degrees; in hover elastic deformation reduces the dihedral to 1.0 degree. 0° was erroneously used during Phase I simulation.

7872 35426

Item	Symbol	M301 Value
Pilot Control Limits		
Collective Stick	X_{COL}	12.0 In.
Longitudinal Stick	X_{LN}	±4.8 In.
Lateral Stick	X_{LT}	±4.8 In.
Pedal	X_{PD}	±2.5 In.
Blade Pitch Governor Lever		7.5 In.
SCAS Actuator Limits		
Longitudinal	$ESAS_{max}$	1.54 In.
Lateral	$ASAS_{max}$	1.54 In.
Pedal	$RSAS_{max}$	0.8 In.
Pitch Attitude Hold	$PHOLD_{max}$	0.77 In.
Yaw Attitude Hold	$YHOLD_{max}$	0.4 In.
Roll Attitude Hold	$RHOLD_{max}$	0.77 In.
Engine Ratings		
2 Min. Contingency		1760 HP
10 Min. Takeoff		1550 HP
30 Min. Military		1400 HP
Normal Rated		1250 HP
Pilot Station Coordinates		
	SL_{PA}	215.25 In.
Pilot Station	BL_{PA}	17.00 In.
	WL_{PA}	50.5 In.

SUBSYSTEM NO. 1: MODEL 301 ROTOR AERODYNAMIC DATA

Equation	Constant	M301 Value
$a_{R,L}$	a_0	5.88
	a_1	9.20
	a_2	20.0
$C_{d_{fL,R}}$	δ_0	0.002
	δ_1	-.01
	δ_2	0.50
$Q_{3R,L}$	B	0.97

$\overline{T}_{R,L}$ $C_{\overline{T}} - f(\mu)$

μ	$C_{\overline{T}}$
0	.0146
.057	.0146
.114	.0144
.171	.0138
.228	.0132
.285	.0127
.342	.0125
.399	.0123
.456	.0122

$Q_{R,L}$ $x_{SS} - f(\mu)$

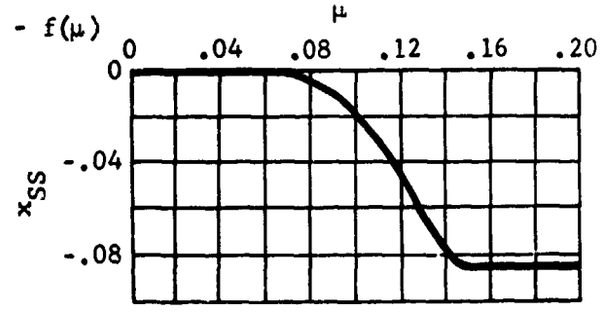

Equation	Constant	M301 Value
Blade Twist Constants K_{ijm}	X_{mi}, θ_{mi}	See Table II
TD3	TAN δ_3	0.268
Y'	I_b	102.7 Slug-Ft^2
C_{KFAR}	K_{FA}	225 Ft-Lb/Deg
C_{KLTR}	K_{LT}	225 Ft-Lb/Deg

SUBSYSTEM NO. 2: MODEL 301 AERODYNAMIC DATA

Equation	Constant	M301 Value
$W_i \mid R/W$	K_0	1.6
	K_1	0
	K_2	↓
	K_3	↓
	K_4	↓
$W_i \mid R/H$	h_0	- .5838
	h_1	.01158
	h_2	.5967
	h_3	.002547
	h_4	-2.2519

SUBSYSTEM NO. 3: MODEL 301 FUSELAGE AERODYNAMIC DATA

Equation	Constant	Model 301 Value
L_F	L_0	7.23
	L_1	0.905
D_F	D_0	1.56
	D_1	0.
	D_2	0.036 For Flaps Up Otnerwise = 0
	D_3	0.0023
	D_4	125.
M'_F	M_0	-146.6
	M_1	17 8 ($\alpha_F < 8°$)
	M_2	9.5
	M_α -f (α_F)	(Table F-1)
Y'_F	Y_0	0.
	Y_1	-1.44
	Y_2	0.
l'_F	l_0	0.
	l_1	-7.5
N'_F	N_0	0.
	N_1	-23.5

TABLE FI FUSELAGE PITCHING MOMENT COEFFICIENT (M_α)

α_F	M_α
-40	-282
-36	-282
-32	-282
-28	-282
-24	-282
-20	-282
-16	-282
-12	-320
-8	-287
-4	-217
0	-146
4	-75
8	-11.3
12	-56.5
16	-94.1
20	-112.9
24	-112.9
28	-103.5
32	-75.3
36	-75.3
40	-94.1

SUBSYSTEM NO. 4: MODEL 301 WING-PYLON AERODYNAMIC DATA

Equation	Constant	M301 Value
L_{iWPL}, L_{iWPL}, L_{WP}	$C_{L_{WP}} = f(\alpha'_F\|_W \,/\, \alpha_W, \beta_M, F_x, M_N)$	Tables WI, WII
L_{WP}	$C_{L_{\delta_a}} = f(F_x)$	Table A III
D_{iWPL}, D_{iWPR}, D_{WP}	$C_{D_{WP}} = f\alpha'_F\|_W \,/\, \alpha_W, \beta_M, F_x, M_N$	Tables W III, W IV
$M_{O_{WP}}$	$C_{M_{O_{WP}}} = f(F_x)$	+0.051 F_1(0/0) -0.057 - F_2(40/25) -0.?o - F_3(75/47) +0.085 - F_4(-28/-17.5)
$\Delta\alpha_{R/W}$	$x_{R/W} = f(\beta_M)$	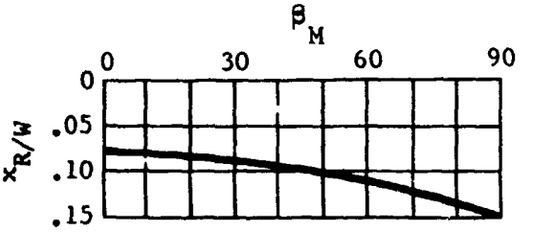
$\Delta\alpha_{W/ROT}$	$x_{W/ROT} = f(\mu)$	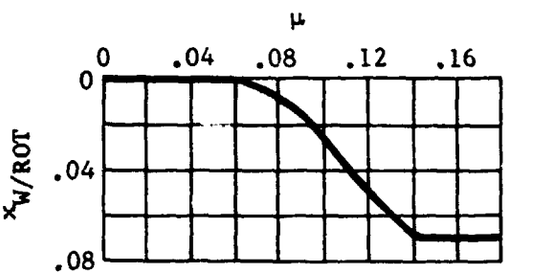

Equation	Constant	M301 Value
$\epsilon_{W/H}$	$\epsilon_{W/H} = f(\alpha'_F \Big\vert_W \Big/ \alpha_W \beta_M, F_X)$	Table W V
Y'_{WP}	$C_{Y_\beta} \Big\vert_{M_N = 0}$	0
	$\left.\dfrac{C_{Y_p}}{C_L}\right\vert_{M_N = 0}$	0
	$C_{Y_r} \Big\vert_{M_N = 0}$	0
l'_{WP}	$C_{l_\beta} \Big\vert_{\substack{C_L = 0 \\ M_N = 0}} = f(F_x, \beta_F, \beta_M)$	Table W VI
	$\left.\dfrac{C_{l_\beta}}{C_{L_{WP}}}\right\vert_{M_N = 0} = f(F_x, \beta_F, \beta_M)$	Table W VII
	$C_{l_p} \Big\vert_{\substack{C_L = 0 \\ M_N = 0}}$	- .774
	$\left.\dfrac{C_{l_r}}{C_{l_{WP}}}\right\vert_{M_N = 0}$	0.27
	$\left[\dfrac{\Delta C_{l_r}}{\left(\frac{\partial \alpha}{\partial \delta_F}\right) \delta_F}\right]$	-.0016
	$\partial\alpha/\partial\delta_F$	0.45

Equation	Constant	M301 Value
N'_{WP}	$C_{n_\beta}\Big\vert_{\substack{C_L = 0 \\ M_N = 0}}$	-.0315
	$\left(\frac{C_{n_\beta}}{C^2_{L_{WP}}}\right)\Big\vert_{M_N = 0}$	0.
	$\left(\frac{C_{n_r}}{C^2_{L_{WP}}}\right)$	-.016
	$\left(\frac{C_{n_r}}{C_{D_{O_{WP}}}}\right)$	-.32
l'_{WP}	$K_{l_{\delta_a}} = f(\alpha_W, \beta_M, F_x)$	Table A II
	$C_{l_{\delta_a}}\Big\vert_{\substack{F_l \\ \alpha_W < 8^o}}$	0.005
N'_{WP}	$\frac{C_{n_p}}{C_{L_{WP}}}\Big\vert_{M_N = 0}$	-.06
	K_{n_p}	1.0
	$K_{nO_{\delta_a}} = f(F_x, \beta_M)$	Table A IV
	$K_{n_{\delta_a}} = f(F_x, \beta_M)$	Table A IV

TABLE WI WING-PYLON LIFT COEFFICIENT (C_{LWP})

FLAP SETTING (F_X)		F_J (0/0)				
MAST ANGLE (β_M)		AIRPLANE (90^o)				HELICOPTER (0^o)
MACH NUMBER (M_N)		0-.2	.4	.5	.6	0-.4
	$\alpha'_{F\|W}/\alpha_W$					
	-40	-.93				-.68
	-36	-.84				-.58
	-32	-.84	Not			-.57
	-28	-.89	Defined	Not		-.62
	-24	-1.00		Defined	Not	-.72
	-20	-1.15	-.84		Defined	-.88
	-19.5	-1.15	-.86			-.88
	-16	-.95	-.94	-.675	-.49	-.73
	-15.5	-.91	-.945	-.680	-.49	-.70
	-13.0	-.75	-.85	-.805	-.50	-.57
	-12	-.67	-.772	-.800	-.50	-.50
	-11	-.60	-.68	-.795	-.50	-.45
	-8	-.383	-418	-.445	-.46	-.272
	-4	-.0625	-.075	-.094	-.105	-.045
	0	.257	.260	.272	.290	.183
	4	.577	.610	.630	.690	.412
	8	.88	.960	1.00	.925	.640
	11	1.10	1.23	1.10	.945	.800
	12	1.19	1.28	1.09	.940	.870
	13	1.26	1.29			.930
	16	1.48	1.23			1.095
	17	1.50			Not	1.100
	20	1.38		Not	Defined	.98
	24	1.22	Not	Defined		.80
	28	1.20	Defined			.78
	32	1.27				.86
	36	1.40				.98
	40	1.46				1.06

TABLE WII WING-PYLON LIFT COEFFICIENT (C_{LWP})

FLAP SETTING (F_x)	F_2 (40/25)		F_3 (75/47)		F_4 (-28/-17.5)	
MAST ANGLE (β_M)	90^0	0^0	90^0	0^0	90^0	0^0
MACH NUMBER (M_N)	M_N = 0 - .40					
$\alpha_{F\|W}/\alpha_W$						
-90	0	0	0	0		
-80	-.325	-.245	-.235	-.190		
-70	-.520	-.400	-.385	-.305		
-60	-.610	-.480	-.450	-.333		
-50	-.590	-.420	-.390	-.220		
-40	-.410	-.265	-.240	-.105	-1.17	-.96
-36	-.400	-.250	-.220	-.090	-1.08	-.83
-32	-.425	-.260	-.240	-.095	-1.06	-.805
-28	-.515	-.300	-.275	-.120	-1.11	-.85
-24	-.660	-.380	-.340	-.160	-1.21	-.945
-21.5	-.690	-.440	-.400	-.210	-1.31	-1.03
-21.0	-.680	-.440	-.400	-.210	-1.33	-1.06
-20	-.640	-.395	-.367	-.188	-1.37	-1.10
-19.2	-.580	-.360	-.310	-.140	-1.38	-1.12
-16	-.320	-.165	-.048	.040	-1.23	-.95
-12	0	.0628	.272	.268	-.95	-.73
-8	.320	.291	.591	.496	-.68	-.502
-4	.64	.581	.910	.724	-.3843	-.275
0	.96	.749	1.237	.952	-.0643	-.0460
4	1.24	.975	1.460	1.170	.2557	.182
8	1.49	1.205	1.680	1.390	.5757	.408
11.0	1.68	1.380	1.80	1.50	.770	.590
12	1.75	1.433	1.79	1.47	.840	.638
13.6	1.80	1.500	1.71	1.39	.950	.730
16	1.70	1.400	1.60	1.24	1.10	.864
18.4	1.56	1.260	1.49	1.16	1.20	.950
20	1.51	1.200	1.46	1.14	1.15	.890
24	1.48	1.15	1.46	1.16	.93	.680
28	1.48	1.20	1.54	1.29	.87	.630
32	1.69	1.32	1.69	1.38	.91	.680
36	1.76	1.41	1.78	1.44	1.05	.80
40	1.80	1.47	1.80	1.48	1.14	.89

TABLE WIII WING-PYLON DRAG COEFFICIENT (C_{DWP})

FLAP SETTING (F_X)	F_1 (0/0)				
MAST ANGLE (β_M)	90°				0°
MACH NUMBER (M_N)	0-.2	.4	.5	.6	0-.2
$\alpha_F \mid W / \alpha_W$					
-40	.575				.685
-36	.505	Not			.635
-32	.425	Defined	Not		.580
-28	.327		Defined	Not	.522
-24	.230	.312		Defined	.450
-20	.150	.175	.275		.370
-16	.089	.089	.135	.240	.295
-12	.042	.042	.050	.110	.246
-8	.025	.0250	.025	.052	.219
-4	.0170	.0170	.0170	.040	.212
0	.0170	.0170	.0170	.040	.212
4	.0353	.0353	.0353	.0555	.231
8	.0602	.0602	.0700	.1150	.262
12	.1000	.1100	.1500	.2500	.300
16	.1620	.1850	.2800		.354
20	.247	.3050			.436
24	.354	.500		Not	.512
28	.493		Not	Defined	.580
32	.600	Not	Defined		.642
36	.660	Defined			.698
40	.705				.748

TABLE WIV WING-PYLON COEFFICIENT (C_{DWP})

FLAP SETTING (F_X)		F_2 (40/25)		F_3 (75/47)		F_4 (-28/-17.5)	
MAST ANGLE (β_M)		90^o	0^o	90^o	0^o	90^o	0^o
MACH NUMBER (M_N)		M_N = 0 - .4					
	$\alpha'_{F\|W} / \alpha_W$						
	-90	1.18	.93	1.145	.90		
	-80	1.10	.91	1.050	.878		
	-70	.93	.855	.89	.822		
	-60	.705	.775	.67	.740		
	-50	.565	.665	.507	.640		
	-40	.430	.540	.450	.550	.622	.734
	-36	.335	.468	.400	.525	.566	.682
	-32	.245	.405	.350	.500	.500	.632
	-28	.180	.352	.309	.480	.430	.575
	-24	.130	.310	.278	.462	.345	.502
	-20	.090	.282	.260	.450	.255	.422
	-16	.065	.263	.243	.440	.186	.350
	-12	.058	.253	.246	.445	.130	.298
	-8	.063	.254	.261	.464	.086	.267
	-4	.081	.282	.288	.494	.055	.248
	0	.109	.313	.328	.536	.047	.239
	4	.148	.356	.378	.590	.0471	.243
	8	.200	.410	.444	.658	.0653	.258
	12	.275	.490	.530	.728	.0950	.284
	16	.380	.566	.642	.789	.138	.332
	20	.528	.630	.730	.839	.195	.402
	24	.630	.690	.790	.880	.287	.476
	28	.710	.748	.838	.920	.414	.540
	32	.764	.800	.883	.955	.510	.600
	36	.805	.845	.950	.985	.583	.648
	40	.865	.888	1.025	1.015	.640	.695

TABLE WV WING WAKE DEFLECTION ON HORIZONTAL STABILIZER ($\epsilon_{W/H}$)

MACH NUMBER (M_N)	M_N = 0 - .2			
FLAP SETTING (F_X)	F_1(0/0)	F_2(40/25)	F_3(75/47)	F_4(-28/ 7.5)
α_W				
AIRPLANE MODE (β_M = 90°)				
-90	0	0	0	0
-25.0	0	0	0	0
-17.94	0	0	2.40	0
-8.82	0	2.00	5.48	0
-2.353	1.92	4.38	7.70	0
0.0	2.52	5.25	8.50	.800
12	6.00	9.90	12.58	4.88
13.8	6.50	10.75	12.80	5.70
16	7.18	11.40	12.35	6.24
16.5	7.40	11.40	12.10	6.40
18.8	7.20	10.60	11.10	6.80
20	6.7	10.00	10.40	6.55
24	4.20	6.50	7.10	4.00
28	0	0	0	0
40	0	0	0	0
HELICOPTER MODE (β_M = 0°)				
-90	0	0	0	0
-28.65	0	0	0	0
-22.15	0	0	0	0
-17.8	0	0	0	0
-15.5	0	0	0	0
-12.41	0	1.2	2.0	0
-7.6	0	3.2	3.75	0
-2.94	2.0	5.0	5.4	0
0.0	3.1	6.15	6.3	1.00
8	6.3	9.25	9.2	3.72
12	7.8	11.00	10.7	5.08
13.0	8.30	11.40	11.0	5.40
14.8	9.00	11.95	11.5	6.00
16.0	9.6	11.90	11.4	6.44

TABLE WV WING WAKE DEFLECTION ON HORIZONTAL STABILIZER (CONT)

		F_1(0/0)	F_4(40/25)	F_3(75/47)	F_4(-28/-17.5)
	α_W				
HELICOPTER MODE (CONT)					
	18.0	10.00	11.20	11.2	7.00
	20	9.30	10.20	10.20	6.70
	24	6.00	6.80	6.80	4.20
	28-40	0	0	0	0

TABLE W VI - WING-PYLON DIHEDRAL STABILITY

AT $C_{L_{WP}} = 0$ $\{C_{l_{\beta_{WP}}} \Big|_{M_N}^{C_L} = 0\}$ PER RAD.

FLAP	F_1(0/0)&F_4(-28/-17.5)			F_2 (40/25)			F_3 (75/47)		
SIDESLIP/β_F/	0	5	10	0	5	10	0	5	10
β_M									
0	-.06	-.065	+.045	-.2	-.094	-.045	-.223	-.015	-.125
30	-.032	-.061	-.02	-.079	-.074	-.147	-.085	-.087	-.225
60	-.021	-.051	-.052	.067	-.052	-.148	-.008	-.088	-.222
90	-.025	-.025	+.035	-.11	-.025	-.025	+.033	-.04	-.08

TABLE W VII - WING-PYLON DIHEDRAL STABILITY

AS A FUNCTION OF WING LOADING $[C_{l_{\beta_{WP}}}/C_{L_{WP}}]$

FLAP	F_1(0/0)&F_4(-28/-17.5)			F_2 (40/25)			F_3 (75/47)		
SIDESLIP/β_F/	0	5	10	0	5	10	0	5	10
β_M									
0	0	0	0	+.105	+.013	+.035	+.104	-.045	+.110
30	+.049	+.079	-.016	+.069	+.062	+.062	+.049	+.047	+.107
60	+.039	+.071	-.018	+.032	+.061	+.058	-.013	+.055	+.082
90	-.065	-.065	0	0	-.085	-.065	-.043	-.045	0

TABLE AI AILERON EFFECTIVENESS ($C_{l_{\delta a}}$)

$C_{l_{\delta a}}$ = .005/deg $\quad \alpha_W < 8°$

Where $\delta_a = (\delta_l - \delta_r)/2$

for δ_F = 0/0; (F_1)

$\beta_M = 90°$; (Airplane)

TABLE AII AILERON EFFECTIVENESS CORRECTION FOR FLAP AND MAST ($K_{l_{\delta a}}$) FOR $\alpha_W < |8°|$

Flap Setting	Mast Angle	$K_{l\delta a}$ (1)
F_1	0°	.68
	90°	1.00
F_2	0°	.66
	90°	.73
F_3	0°	.45
	90°	.34
F_4	0°	.67
	90°	.90

($K_{l\delta a}$ =0 @ $\alpha_W = \pm 25°$)

(1) Straight Line Variation with Mast Angle

TABLE AIII AILERON EFFECT ON WING LIFT ($C_{L_{\delta a}}$)

Flap Setting	Mast Angle	$C_{L\delta a}$ (per Deg)
F_1	All	0
F_2	All	0
F_3	All	0
F_4	All	0

TABLE AIV AILERON YAW ($C_{n_{\delta a}}$)

$$C_{n_{\delta a}} = K_{no_{\delta a}} + K_{n_{\delta a}} C_L C_{l_{\delta a}}$$

Where:

Flap Setting	Mast Angle	$K_{nc_{\delta a}}$	$K_{n_{\delta a}}$
F_1	0°	.00046	-.0348
	30°	.00092	-.0354
	90°	.00143	-.0238
F_2	0°	.00046	-.0137
	30°	.00109	-.0052
	90°	.00103	-.0137
F_3	0°	-.00003	-.0232
	30°	.00035	-.0050
	90°	.00029	-.0157
F_4	0°	0	-.0205
	30°	0	-.0301
	90°	0	-.0215

SUBSYSTEM NO. 5: MODEL 301 HORIZONTAL TAIL AERODYNAMIC DATA

Equations	Constant	M301 Value
α_{HL}	τ_e	0.0 for $M_N < 1.0$
(For lift)		0.565 for $M_N > 1.0$
α_{HD}	τ_e	0.565
(For drag)		
q_H	η_H	1 [The effect is included in calculating $\epsilon_{W/H}$]
I_H	$C_{L_H} = f(\alpha_H, \delta_e, M_N)$	Tables HI, HII
	$C_{L_{H\beta}}$	-.0017
D_H	$C_{D_H} = f(\alpha_H, M_N)$	Table H IV
M'_H	$C_{M_H} = f(\alpha_H, M_N)$	0
α_H	$K_e = f(\delta_e, M_N)$	Table H III

TABLE HI HORIZONTAL STABILIZER LIFT COEFFICIENT (C_{LH})

ELEVATOR ANGLE	0°	10°	15°	20°	-10°	-15°	-20°
MACH NUMBER	M_N = 0 - .2						
α_H							
-90	0	0	0	0	0	0	0
-80	-.425	-.560	-.580	-.600	-.360	-.285	-.220
-70	-.720	-.865	-.890	-.920	-.600	-.490	-.380
-60	-.900	-1.060	-1.090	-1.120	-.770	-.640	-.510
-50	-1.002	-1.175	-1.205	-1.240	-.890	-.745	-.600
-40	-1.050	-1.240	-1.260	-1.300	-.960	-.800	-.640
-36	-1.030	-1.230	-1.255	-1.290	-.890	-.735	-.600
-28	-1.010	-1.210	-1.240	-1.280	-.840	-.680	-.560
-24	-.980	-1.185	-1.220	-1.260	-.780	-.615	-.500
-20	-.930	-1.160	-1.198	-1.235	-.690	-.500	-.420
-18.4	-.920	-1.200	-1.210	-1.240	-.660	-.540	-.480
-17.5	-.930	-1.260	-1.250	-1.250	-.710	-.565	-.450
-16.8	-.990	-1.310	-1.290	-1.310	-.740	-.550	-.420
-16.0	-1.12	-1.40	-1.330	-1.330	-.710	-.510	-.380
-15.6	-1.10	-1.44	-1.380	-1.350	-.700	-.480	-.350
-14.2	-1.01	-1.40	-1.55	-1.450	-.610	-.400	-.270
-12.5	-.880	-1.31	-1.49	-1.60	-.480	-.280	-.150
-12	-.852	-1.260	-1.464	-1.59	-.444	-.240	-.110
8	.568	.160	-.044	-.18	.976	1.180	1.330
12.0	.850	.442	.240	.100	1.250	1.420	1.500
12.2	.860	.450	.260	.120	1.270	1.430	1.480
13.0	.920	.520	.330	.170	1.30	1.370	1.450
15.0	1.0	.650	.450	.290	1.200	1.270	1.360
15.0	.98	.690	.475	.320	1.160	1.240	1.320
16.8	.94	.700	.490	.340	1.150	1.200	1.320
18.0	.89	.680	.500	.370	1.130	1.220	1.340
20	.88	.600	.465	.380	1.180	1.280	1.380
24	.935	.660	.455	.330	1.300	1.380	1.440
28	1.00	.730	.500	.380	1.370	1.440	1.500
32	1.05	.780	.540	.400	1.430	1.490	1.540
36	1.08	.820	.560	.410	1.470	1.535	1.570
40	1.10	.840	.570	.410	1.510	1.560	1.590

TABLE HII HORIZONTAL STABILIZER LIFT COEFFICIENT (C_{LH})

ELEVATOR ANGLE		$\delta_e = 0°$			
MACH NUMBER (M_N)		0 - .2	.4	.5	.6
	α_H				
	-20	-.930	Not	Not	Not
	-16	-1.12	Defined	Defined	Defined
	-12.2	-.870	-.92		
	-12.0	-.852	-.92		
	-8.8	-.630	-.680	-.72	
	-8.0	-.568	-.620	-.660	-.50
	-6.5	-.460	-.500	-.540	-.55
	-4.0	-.284	-.310	-.330	-.350
	0	0	0	0	0
	4.0	.284	.310	.330	.350
	4.2	.310	.330	.340	.390
	8.0	.568	.620	.600	.440
	16.5	.820	.800	.570	
	12.0	.850	.798	.560	Not
	15.5	1.00	Not	Not	Defined
	16.0	.980	Defined	Defined	
	20.0	.880			

TABLE HIII - ELEVATOR/RUDDER EFFECTIVENESS (τ_e/τ_r)
CORRECTED FOR MACH NO. AND DEFLECTION EFFECTS

ELEVATOR ANGLE - DEG	MACH NUMBER	K_e OR K_r
±15°	0-.2	1.0
	.4	.965
	.5	.950
	.6	.930
±15°	0-.2	1.0
±20°		.920

TABLE HIV HORIZONTAL STABILIZER DRAG COEFFICIENT (C_{DH})

ELEVATOR ANGLE		$\delta_e = 0^\circ$			
MACH NUMBER (M_N)		0-.2	.4	.5	.6
	α_H				
	-90	.92			
	-80	.91			
	-70	.87			
	-60	.81	NOT		
	-50	.72	DEFINED	NOT	
	-40	.60		DEFINED	NOT
	-36	.54			DEFINED
	-32	.47			
	-28	.39			
	-24	.30			
	-20	.20			
	-16	.115	.135		
	-12	.068	.068	.088	
	-8	.035	.035	.035	.045
	-4	.015	.015	.015	.015
	0	.00875	.00875	.00875	.00875
	4	.015	.015	.015	.015
	8	.035	.035	.045	.065
	12	.068	.075	.105	
	16	.115	.145		
	20	.20			NOT
	24	.34		NOT	DEFINED
	28	.48	NOT	DEFINED	
	32	.61	DEFINED		
	36	.72			
	40	.80			

SUBSYSTEM NO. 6: MODEL 301 VERTICAL FIN AERODYNAMIC DATA

Equations	Constant	M301 Value
β_{VL,R_o}	$\left(1 - \frac{\partial\sigma}{\partial\beta_F}\right) = f(\beta_F, \beta_M, F_X, \alpha_F)$	Tables V IV, V V, V VI
$\beta_{VYL,R}$ & $\beta_{VDL,R}$	$K_R = f(\delta_r, M_N)$	Table H III
	τ_r	.385
	$\frac{\partial\sigma}{\partial\hat{p}}$	-0.1
	$\frac{\partial\sigma}{\partial\hat{r}}$	0.0
$q_{VL,R}$	η_V	1
$Y_{VL,R}$	$C_{Y_V} = f(\beta_V, \delta_r, M_N)$	Tables VI, VII
$D_{VL,R}$	$C_{D_V} = f(\beta_V, \delta_r, M_N)$	Table V III

TABLE VI VERTICAL STABILIZER LIFT COEFFICIENT (C_{Y_V})

RUDDER ANGLE		0°	10°	20°	-10°	-20°
MACH NUMBER		M_N = 0 - .2				
	β_V					
	-90	0	0	0	0	0
	-40	-1.0	-.96	-.92	-1.07	-1.11
	-32	-.93	-.84	-.82	-1.02	-1.12
	-28	-.94	-.90	-.87	-1.02	-1.09
	-26	-.98	-.93	-.91	-1.07	-1.11
	-24	-1.03	-.98	-.92	-1.11	-1.15
	-22	-1.05	-.98	-.85	-1.14	-1.19
	-20	-1.05	-.88	-.74	-1.15	-1.22
	-18	-.96	-.77	-.64	-1.14	-1.24
	-16	-.86	-.66	-.52	-1.05	-1.18
	-12	-.635	-.45	-.30	-.84	-.99
	-8	-.425	-.225	-.09	-.63	-.76
	8	.425	.625	.76	.23	.10
	12	.635	.84	.99	.44	.31
	16	.86	1.05	1.78	.66	.52
	18	.96	1.14	1.24	.77	.64
	20	1.05	1.15	1.22	.88	.74
	22	1.05	1.14	1.19	.98	.85
	24	1.03	1.11	1.15	.98	.92
	26	.98	1.07	1.11	.93	.91
	28	.94	1.02	1.09	.90	.87
	32	.93	1.02	1.12	.84	.82
	40	1.0	1.07	1.11	.96	.92
	90	0	0	0	0	0

TABLE VII VERTICAL STABILIZER LIFT COEFFICIENT (C_{Y_V})

RUDDER ANGLE		$\delta_r = 0^\circ$			
MACH NUMBER (M_N)		0-.2	.4	.5	.6
	β_V				
	-24	-1.05	NOT DEFINED	NOT DEFINED	NOT DEFINED
	-22	-1.05			
	-20	-.96			
	-16	-.86	-.60	-.45	
	-12	-.635	-.60	-.45	-.32
	-10	-.52	-.575	-.445	-.34
	-8	-.425	-.52	-.44	-.34
	-6	-.33	-.43	-.405	-.33
	-4	-.22	-.30	-.32	-.30
	0	0	0	0	0
	4	.22	.30	.32	.30
	6	.33	.43	.405	.33
	8	.425	.52	.44	.34
	10	.52	.575	.445	.34
	12	.635	.60	.45	.32
	16	.86	.60	.45	
	20	.96	NOT DEFINED	NOT DEFINED	NOT DEFINED
	22	1.05			
	24	1.05			

TABLE VIII VERTICAL STABILIZER DRAG COEFFICIENT (C_{D_V})

RUDDER ANGLE		$\delta_r = 0^o$			
MACH NUMBER	(M_N)	0 - .2	.4	.5	.6
	β_V				
	-90	.800			
	-40	.600			
	-32	.550	Not Defined		
	-28	.435		Not Defined	Not Defined
	-24	.290			
	-20	.162			
	-16	.080	.165		
	-12	.040	.0750	.100	.160
	- 8	.0120	.0220	.0350	.060
	- 4	.0070	.0070	.0075	.010
	0	.00355	.00355	.00355	.00355
	4	.0070	.0070	.0075	.010
	8	.0120	.0220	.0350	.060
	12	.040	.0750	.100	.160
	16	.080	.165		
	20	.162			
	24	.290		Not Defined	Not Defined
	28	.435			
	32	.550	Not Defined		
	40	.600			
	90	.800			

TABLE VIV - SIDEWASH FACTOR $(1-\partial\sigma/\partial\beta_F)$ FOR FLAPS F_1 & F_4

FLAPS		F_1 (0/0) AND F_4 (-28/-17.5)						
		SIDESLIP ANGLE $\lvert\beta_F\rvert$ - DEG						
β_M DEG	α_F DEG	0	4	8	12	16	20 TO 50	>50
0	<-12	1.0	1.0	1.0	1.0	1.0	1.0	1.0
	-3	1.0	1.1	1.05	1.015	0.985	1.01	1.0
	0.4	1.0	1.038	1.044	0.965	0.933	1.0	1.0
	6.8	1.0	0.863	0.810	0.772	0.787	0.958	1.0
	13.2	1.0	0.524	0.517	0.474	0.491	0.673	1.0
	> 28	1.0	1.0	1.0	1.0	1.0	1.0	1.0
30	<-10.5	1.0	1.0	1.0	1.0	1.0	1.0	1.0
	-3.	1.0	1.13	1.072	0.97	1.025	1.0	1.0
	0.5	1.0	1.248	1.093	0.977	1.015	1.056	1.0
	6.9	1.0	0.995	0.961	0.865	0.845	0.953	1.0
	13.3	1.0	0.677	0.595	0.523	0.526	0.681	1.0
	> 28	1.0	1.0	1.0	1.0	1.0	1.0	1.0
60	< -9	1.0	1.0	1.0	1.0	1.0	1.0	1.0
	-3.	1.0	1.15	1 05	1.0	1.06	1.1	1.0
	0.5	1.0	1.21	1.08	0.975	1.02	1.025	1.0
	6.9	1.0	0.945	0.975	0.9	0.88	0.92	1.0
	13.3	1.0	0.69	0.645	0.585	0.59	0.7	1.0
	> 28	1.0	1.0	1.0	1.0	1.0	1.0	1.0
90	< -8	1.0	1.0	1.0	1.0	1.0	1.0	1.0
	-3.	1.0	1.09	1.10	1.18	1.15	1.04	1.0
	0.2	1.0	1.0	1.0	1.0	1.0	1.0	1.0
	7.0	1.0	0.834	0.865	0.866	0.842	0.924	1.0
	13.5	1.0	0.659	0.676	0.622	0.642	0.680	1.0
	> 28	1.0	1.0	1.0	1.0	1.0	1.0	1.0

TABLE VV SIDEWASH FACTOR $(1 - \frac{\partial\sigma}{\partial\beta_F})$ FOR FLAPS F_2

FLAPS		F_2 - (40/25)						
		SIDESLIP ANGLE $\lvert\beta_F\rvert$ - DEG						
β_M DEG	α_F DEG	0	4	8	12	16	20 to 50	>50
0	≤ -22.0	1.0	1.0	1.0	1.0	1.0	1.0	1.0
	-3.2	1.0	1.315	1.26	1.185	1.1	1.059	1.0
	1.0	1.0	1.228	1.208	1.12	1.045	1.0	1.0
	7.3	1.0	0.89	0.91	0.86	0.809	0.86	1.0
	13.5	1.0	0.535	0.59	0.396	0.443	0.678	1.0
	≥ 28.0	1.0	1.0	1.0	1.0	1.0	1.0	1.0
30	≤ -21.0	1.0	1.0	1.0	1.0	1.0	1.0	1.0
	-3.1	1.0	1.065	1.027	1.055	1.14	1.055	1.0
	1.1	1.0	1.1	1.115	1.058	1.12	1.065	1.0
	7.4	1.0	1.025	.935	.972	.882	.86	1.0
	13.6	1.0	.884	0.82	0.629	0.456	0.689	1.0
	≥ 28.0	1.0	1.0	1.0	1.0	1.0	1.0	1.0
60	≤ -19.5	1.0	1.0	1.0	1.0	1.0	1.0	1.0
	-3.0	1.0	1.02	1.03	1.08	1.117	1.04	1.0
	1.2	1.0	0.945	1.07	0.998	1.05	1.09	1.0
	7.4	1.0	1.03	0.985	1.015	0.95	0.908	1.0
	13.6	1.0	0.915	0.9	0.8	0.61	0.745	1.0
	≥ 26.0	1.0	1.0	1.0	1.0	1.0	1.0	1.0
90	≤ -18.0	1.0	1.0	1.0	1.0	1.0	1.0	1.0
	-3.1	1.0	1.07	1.121	1.16	1.072	1.04	1.0
	1.2	1.0	0.984	1.15	1.09	1.05	1.064	1.0
	5.4	1.0	0.982	1.035	1.03	0.993	1.015	1.0
	14.0	1.0	0.842	0.74	0.77	0.695	0.725	1.0
	≥ 28.0	1.0	1.0	1.0	1.0	1.0	1.0	1.0

7872 55426

TABLE VVI SIDEWASH FACTOR $(1 - \frac{\partial\sigma}{\partial\beta_F})$ FOR FLAPS F_3

FLAPS	F3 (75/47)							
β_M DEG	α_F DEG	SIDE SLIP ANGLE β_F - DEG						
		0	4	8	12	16	20 to 50	>50
0	≤ -30.0	1.0	1.0	1.0	1.0	1.0	1.0	1.0
	-3.1	1.0	1.8	1.22	1.155	1.105	1.048	1.0
	1.2	1.0	1.128	1.185	1.125	1.045	1.01	1.0
	5.3	1.0	0.846	0.99	0.948	0.92	0.862	1.0
	13.5	1.0	0.535	0.65	0.44	0.51	0.65	1.0
	≥ 28.0	1.0	1.0	1.0	1.0	1.0	1.0	1.0
30	≤ -29.0	1.0	1.0	1.0	1.0	1.0	1.0	1.0
	-3.0	1.0	1.05	1.072	1.14	1.135	1.08	1.0
	1.3	1.0	0.979	1.01	1.105	1.1	1.035	1.0
	5.5	1.0	0.82	0.862	0.998	0.986	0.932	1.0
	13.5	1.0	0.65	0.72	0.7	0.52	0.78	1.0
	≥ 28.0	1.0	1.0	1.0	1.0	1.0	1.0	1.0
60	≤ -28.0	1.0	1.0	1.0	1.0	1.0	1.0	1.0
	-3.0	1.0	1.025	1.082	1.15	1.115	1.075	1.0
	1.3	1.0	0.915	1.005	1.1	1.1	1.04	1.0
	5.5	1.0	0.855	0.90	1.015	0.955	0.995	1.0
	13.5	1.0	0.73	0.8	0.8	0.61	0.82	1.0
	≥ 28.0	1.0	1.0	1.0	1.0	1.0	1.0	1.0
90	≤ -26.0	1.0	1.0	1.0	1.0	1.0	1.0	1.0
	-2.9	1.0	1.058	1.15	1.145	1.075	1.04	1.0
	1.3	1.0	1.0	1.12	1.12	1.05	1.088	1.0
	5.6	1.0	0.905	1.005	1.03	0.99	1.028	1.0
	13.5	1.0	0.782	0.76	0.72	0.66	0.71	1.0
	≥ 28.0	1.0	1.0	1.0	1.0	1.0	1.0	1.0

SUBSYSTEM NO. 7: MODEL 301 LANDING GEAR DATA

Equation	Constant	M301 Value
D_{MG}	$D_{OMGD}f(t)$	
D_{NG}	$D_{ONGD}f(t)$	

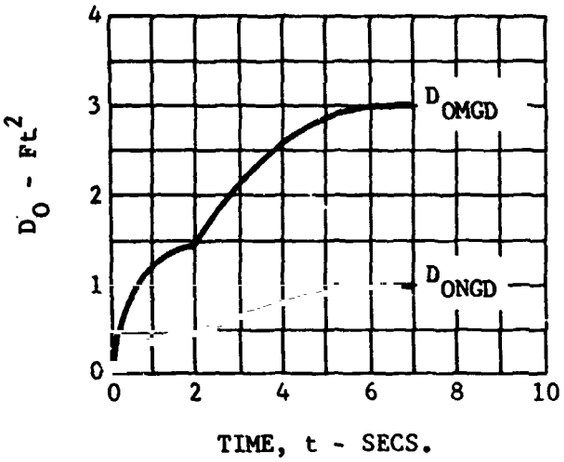

D_{MG}	$D_{OMGU}f(t)$	
D_{NG}	$D_{ONGU}f(t)$	

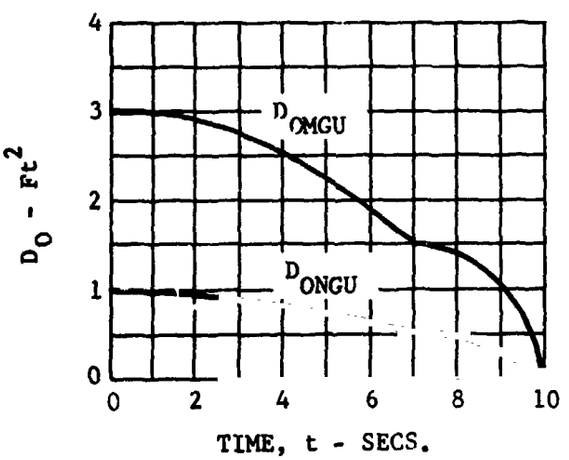

SUBSYSTEM NO. 8(a): MODEL 301 CONTROL SYSTEM DATA

Equation	Constant	M301 Value
θ_{OL}, θ_{OR}	$\frac{\partial \theta_0}{\partial X_{COL}}$	Table C IV
	$\theta_{0_{LL}} = f(\beta_M)$	Table C IV
	$\frac{\partial \theta_0}{\partial X_{LT}} = f(\beta_M)$	Table C III
B_{1R}, B_{1L}	$\frac{\partial B_1}{\partial X_{LN}} = f(\beta_M)$	Table C I
	$\frac{\partial B_1}{\partial X_{PD}} = f(\beta_M, V_T)$	Table C II
δ_e	$\frac{\partial \delta_e}{\partial X_{LN}}$	-4.16
δ_R	$\frac{\partial \delta_R}{\partial X_{PD}}$	8.0
δ_a	$\frac{\partial \delta_a}{\partial X_{LT}}$	+ 3.93
β_M	$\dot{\beta}_M = f(\beta_M)$	Table C V
i_H	$i_{H0}\|_{X_{LN}} = X_{LNN}$	$\begin{bmatrix} 0 \end{bmatrix}$
	i_{H1} $\quad$ $i_{H3}\|_{X_{COL}} = 0$	
	i_{H2} $\quad$ i_{H4}	

TABLE CI FORE AND AFT CYCLIC PITCH ($\partial B_1/\partial X_{LN}$)

MAST ANGLE (DEG)	$\frac{\partial B_1}{\partial X_{LN}}$ (°/in)
0	2.1
10	2.09
20	1.98
30	1.81
40	1.60
50	1.35
60	1.04
70	.71
80	.362
90	0

(X_{LN} = ±4.8 in) (B_1 = 10.0625° @ β_M = 0°)

TABLE CII DIFFERENTIAL CYCLIC PITCH ($\partial B_1/\partial X_{PD}$)

MAST ANGLE (DEG)	$\frac{\partial B_1}{\partial X_{PD}}$ (°/in)		
	0 - 60 KTS	80 KTS	100 KTS→
0	1.6	1.04	.40
10	1.58	1.025	.394
20	1.51	.975	.375
30	1.39	.90	.345
40	1.225	.795	.305
50	1.035	.67	.257
60	.803	.52	.200
70	.55	.325	.137
80	.28	.18	.069
90	0	0	0

X_{PD} = ±2.5 in

ΔB_1 = ±4.0° 0-60
±2.6° 80
±1.0° 100

TABLE CIII DIFFERENTIAL COLLECTIVE PITCH

MAST ANGLE (DEG)	$\partial\theta_o/\partial X_{LT}$ (°/in)
0	0.625
10	.606
20	.575
30	.541
40	.50
50	.438
60	.365
70	.293
80	.209
90	.121

($X_{LT} = \pm 4.8$ in)
($\Delta\theta_o = \pm 3^\circ$ @ $\beta_M = 0$)

TABLE CIV COLLECTIVE PITCH ($\partial\theta_o/\partial X_{Coll}$; $\theta_{o_{LL}}$)

MAST ANGLE (DEG)	$\partial\theta_c/\partial X_{Col}$ (°/in)	$\theta_{o_{LL}}$ (DEG)
0	1.17	35.5
10	1.12	36.0
20	1.08	37.1
30	1.00	39.5
40	0.85	42.7
50	0.69	46.6
60	0.50	50.4
70	0.31	53.5
80	0.13	55.9
90	0	57.5

TABLE CV CONVERSION RATE ($\dot{\beta}_M$)

MAST ANGLE (DEG)	$\dot{\beta}_M$ (°/Sec)
-5	3.0(1)
0	3.0(1)
2	3.0(1)
2.5	15.0(2)
10	14.25
20	13.3
30	12.45
40	11.7
50	11.4
60	11.4
70	11.63
80	12.5
87	14.0(2)
87.5	2.8(1)
90	2.8(1)

(1) When conversion starts at mast angle of -5, 0 or 90; $\dot{\beta}_M$ = 2.8 or 3.0. When conversion stops at mast angle of -5, 0, or 90; $\dot{\beta}_M$ = 0

(2) Δt from quarter rate to max rate; Δt = .05 sec

TABLE CVI X_{THR} VS X_{COL}

X_{COL} (INCH)	X_{THR} (DEG)
0	46.0
1.0	51.0
2.0	56.2
3.0	61.2
4.0	65.8
5.0	70.5
6.0	75.0
7.0	79.3
8.0	83.7
9.0	88.0
10.0	92.3
11.0	96.2
12.0	100.0

TABLE CVII β GOVERNOR GAIN

β_M (DEG)	K_{RPG}
0	0.1
15	0.1
30	0.1
45	0.1
60	0.1
75	0.1
90	0.1

TABLE CVIII β GOVERNOR LIMIT

β_M	θ_{0_C} Max
0	-6, +32
15	-6, +32
30	-6, +32
45	-6, +32
60	-6, +32
75	-6, +32
90	-6, +32

SUBSYSTEM 8(b): MODEL 301 FORCE GRADIENT DATA

Equation	Constant	M301 Values
F_{LN}	F_{LN0}	2
	F_{LN1}	0 for $V_T < V_1$
		.0264 for $V_T \geq V_1$
	F_{LN2}	0 for $V_T < V_2$
		.056 for $V_T \geq V_2$
	V_1	35
	V_2	175
F_{LT}	F_{LT0}	1
	F_{LT1}	0 for $V_T < V_1$
		.0107 for $V_T \geq V_1$
	F_{LT2}	0 for $V_T < V_2$
		.0336 for $V_T \geq V_2$
	V_1	35
	V_2	175
F_{PD}	F_{PD0}	6
	F_{PD1}	0 for $V_T < V_1$
		.148 for $V_T \geq V_1$
	F_{PD2}	0 for $V_T < V_2$
		1.21 for $V_T \geq V_2$
	V_1	0
	V_2	135

F_{COL}	F_4	0

NOTE: Breakout forces are adjusted by the pilot by varying the friction.

SUBSYSTEM NO. 9: M301 INERTIA COEFFICIENT DATA (AFT CG)

Equation	Constant	M301 Value
I_{XX}	K_{I1}	20.5 Slugs - Ft^2/deg
I_{YY}	K_{I2}	11.24 Slugs - Ft^2/deg
I_{ZZ}	K_{I3}	9.26 Slugs - Ft^2/deg
I_{XZ}	K_{I4}	1.76 Slugs - Ft^2/deg

SUBSYSTEM NO. 14: M301 GROUND EFFECT ROLLING MOMENT COEFFICIENT DATA

Equation	Constant	M301 Value
l_A	l_{GO}	$-8270 \frac{\text{Ft. lbs.}}{\text{Deg.}}$
	l_{G1}	$26186 \frac{\text{Ft. lbs.}}{\text{Deg.-Ft.}}$
	l_{G2}	$-23369 \frac{\text{Ft. lbs.}}{\text{Deg.-Ft}^2}$
	l_{G3}	$6336 \frac{\text{Ft. lbs.}}{\text{Deg.-Ft}^3}$

SUBSYSTEM NO. 17: M301 COLLECTIVE GOVERNOR DATA

Equation	Constant	M301 Value
$\bar{\theta}_{OG}$	$\frac{\delta\Omega_{OINT}}{\delta\Omega_{RO}}$	11.3
	$K_{1G}\ (\beta_M)$	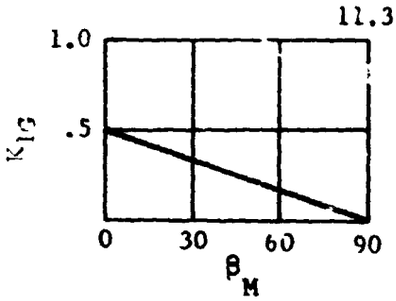
	$K_{RPG}\ (\beta_M)$	Table C VII
	$\theta_{OG_{max}}$ $\theta_{OG_{min}}$	Table C VIII

SUBSYSTEM NO. 18: MODEL 301 ENGINE DATA

Equations	Constant	M301 Value
HP	K_1	-0.94
	K_2	1.0
	K_3	0
RPM_{RO}	K_4	13100
	K_5	235
	K_6	475
T_a	K_7	288
HP_{ROC}	K_8	0.266
	K_9	-8.97
	K_{10}	0
	K_{11}	0.0032
	K_{12}	0.875
	K_{13}	0.00125
	K_{14}	0
ϵ_s	t_D	0.1
$\frac{dHP_{ROS}}{dt_{PTG}}$	pctmxs	6.0
$\frac{dHP_{ROS}}{dt_{TH}}$	pctmxp	6.0

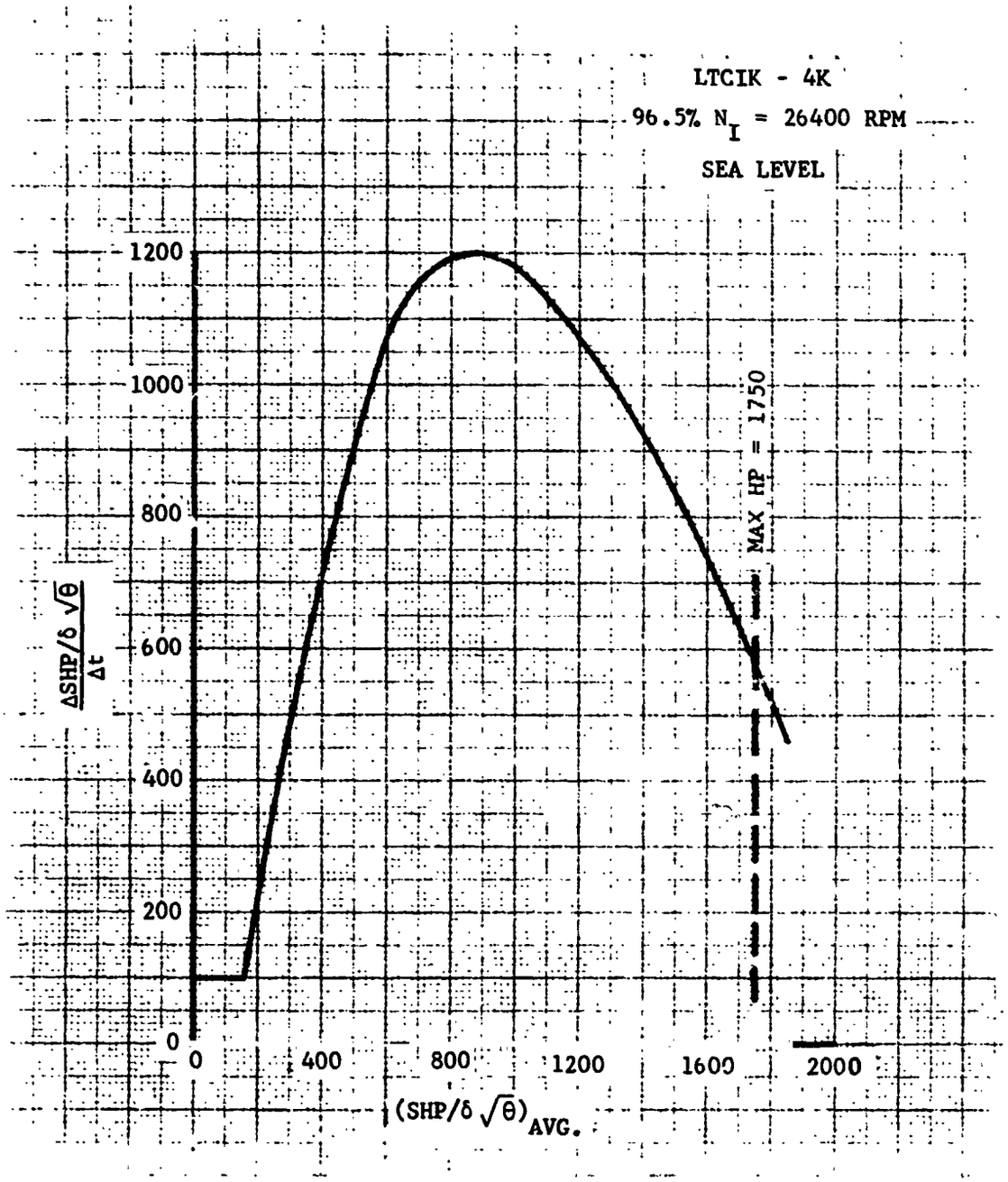

Figure B1. T53 Engine Acceleration Characteristics

SUBSYSTEM NO. 19: MODEL 301 DRIVE SYSTEM DATA

Equation	Constant	M301 Value
$\ddot{\xi}$	$I_{\perp}$	824.0 Slug-Ft^2
$F_1(t)$, Ω_{RPT}	θ_{RPT1}	35.2
Ω_{INT}	θ_{INT1}	11.3
Ω_R	Ω_{RO}	

SUBSYSTEM NO. 20: M301 SCAS DATA

Equation	Constant	M301 Value
PSCAS	K_{1PU} (U)	Table SAS I
	K_{9PU} (U)	
	$K_{1P\beta_M}$ (β_M)	Table SAS I
	$K_{10P\beta_M}$ (β_M)	
	T_{1P}	0.5 Sec
	T_{2P}	3.15 Sec
	T_{3P}	3.15 Sec
	T_{4P}	1.0 Sec
YSCAS	K_{1YU} (U)	Table SAS II
	K_{5YU} (U)	
	$K_{1Y\beta_M}$ (β_M)	Table SAS II
	$K_{5Y\beta_M}$ (β_M)	
	T_{1Y}	0.6 Sec
	T_{2Y}	2.7 Sec
	T_{3Y}	2.7 Sec
	T_{4Y}	1.0 Sec
RSCAS	K_{1RU} (U)	Table SAS I
	K_{9RU} (U)	

Equation	Constant	M301 Value
	$K_{1R\beta_{1'}}(\beta_M)$	Table SAS III
	$K_{10R\beta_M}(\beta_M)$	
	T_{1R}	1.0 Sec
	T_{2R}	3.0 Sec
	T_{3R}	3.0 Sec
ESAS	$ESAS_{max}$	1.54 Inch
RSAS	$RSAS_{max}$	0.80 Inch
ASAS	$ASAS_{max}$	1.54 Inch
PHOLD	$PHOLD_{max}$	0.77 Inch
YHOLD	YHOLD	0.4 Inch
RHOLD	$RHOLD_{max}$	.77 Inch

TABLE SAS 1 - Gains for Pitch SCAS Electronics

K_{4P} = 10.0 K_{6P} = 0 K_{7P} = 10.0

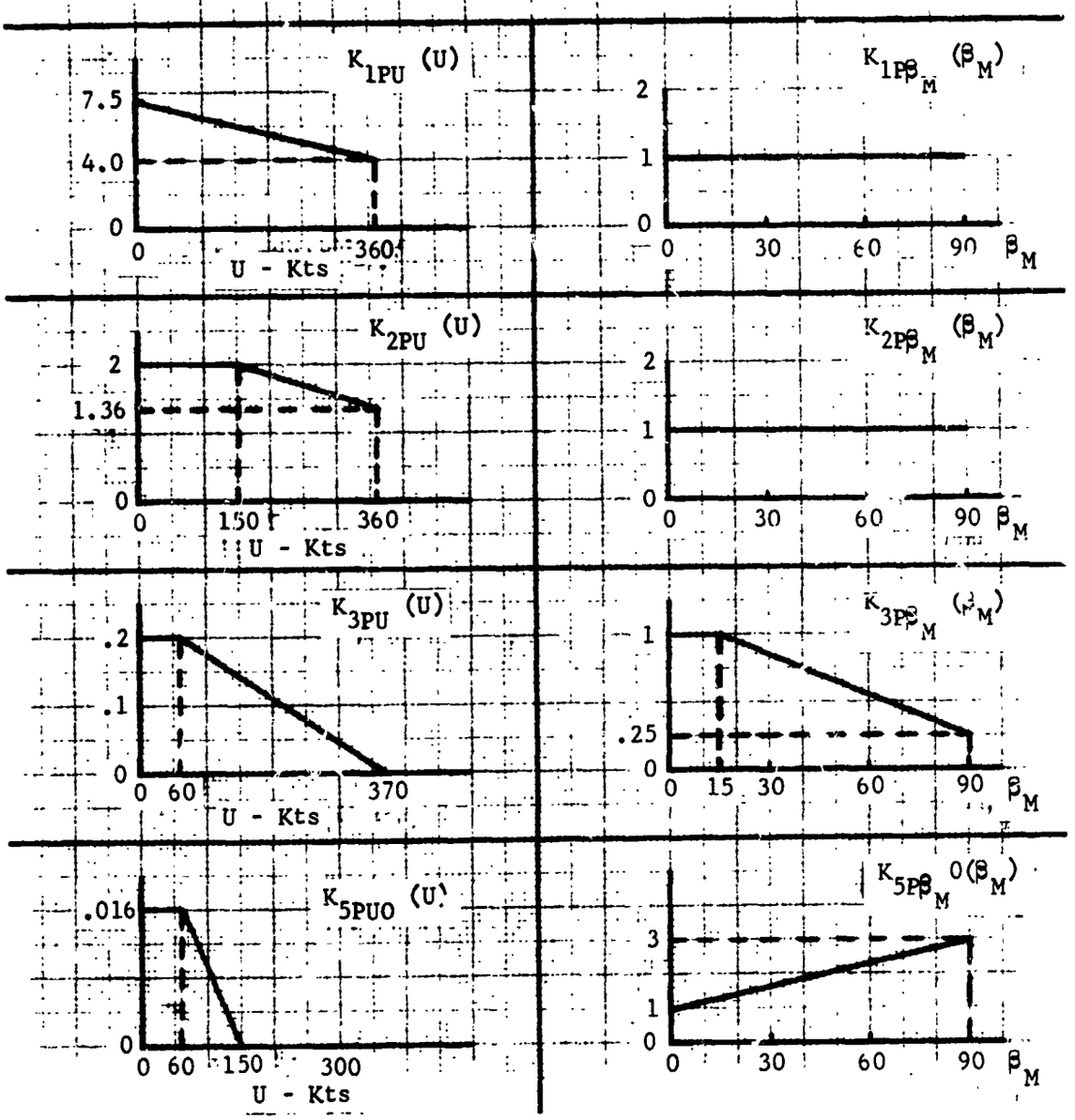

TABLE SAS I (Contd)

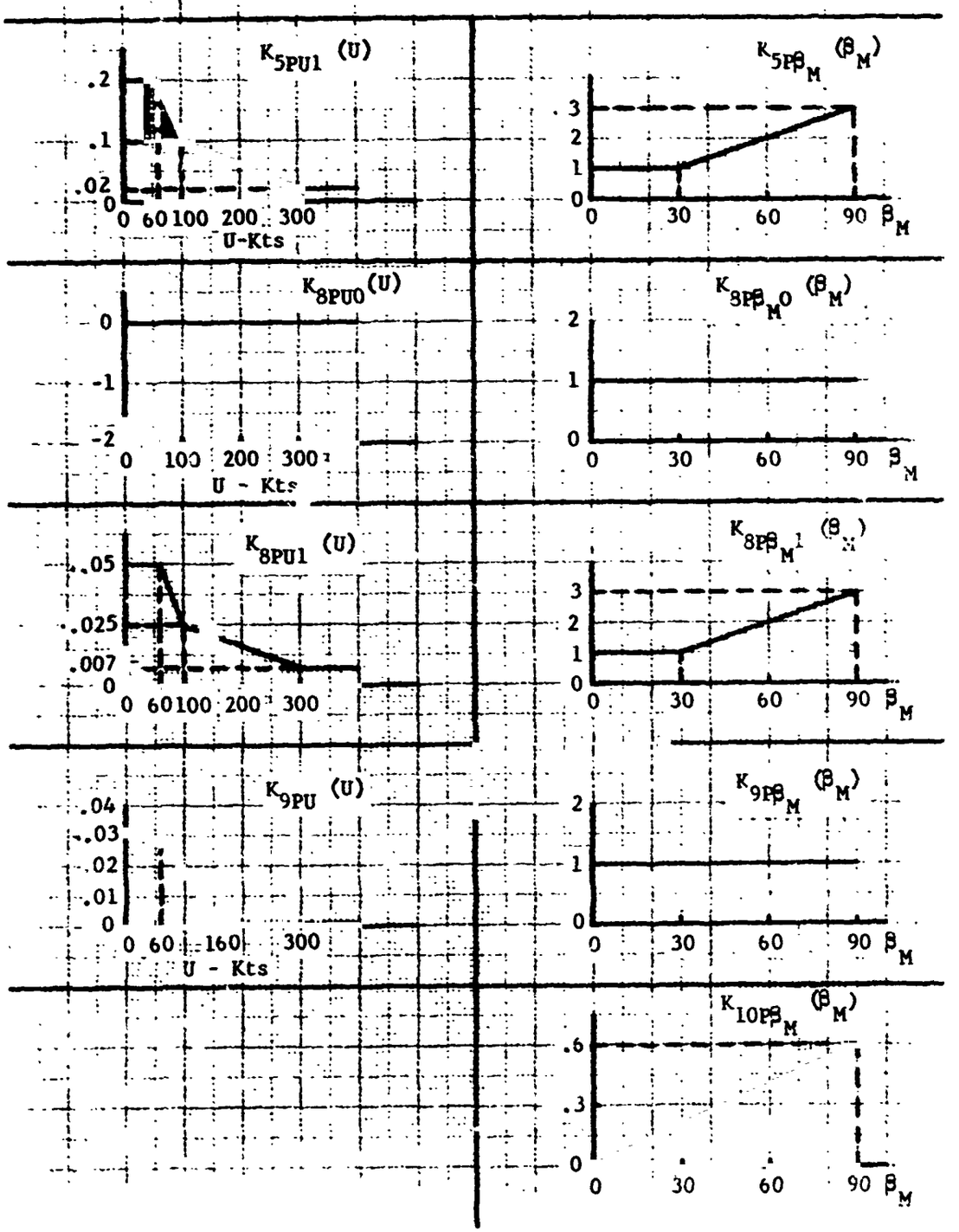

TABLE SAS II - Gains for Yaw SCAS Electronics

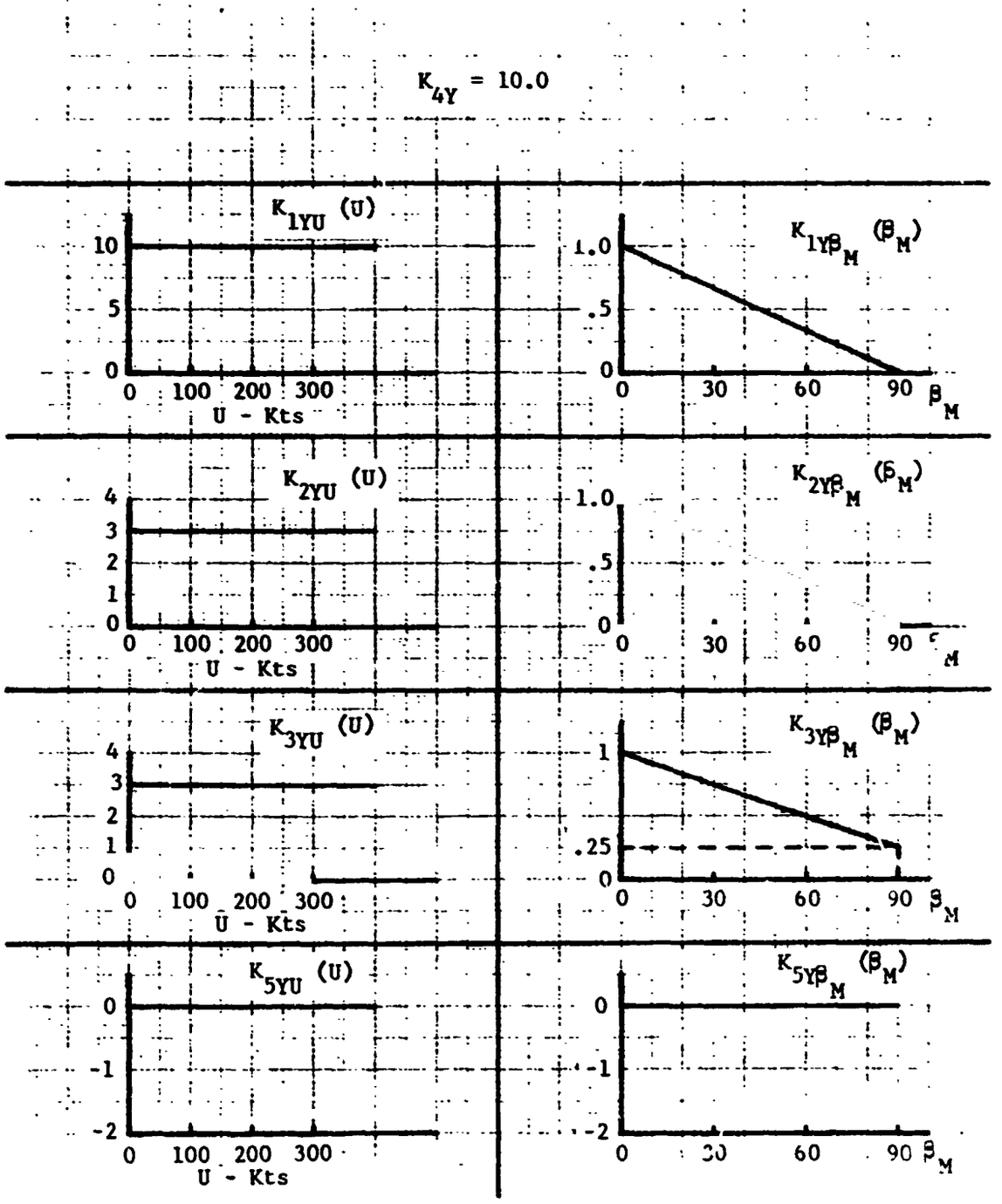

TABLE SAS II - Contd

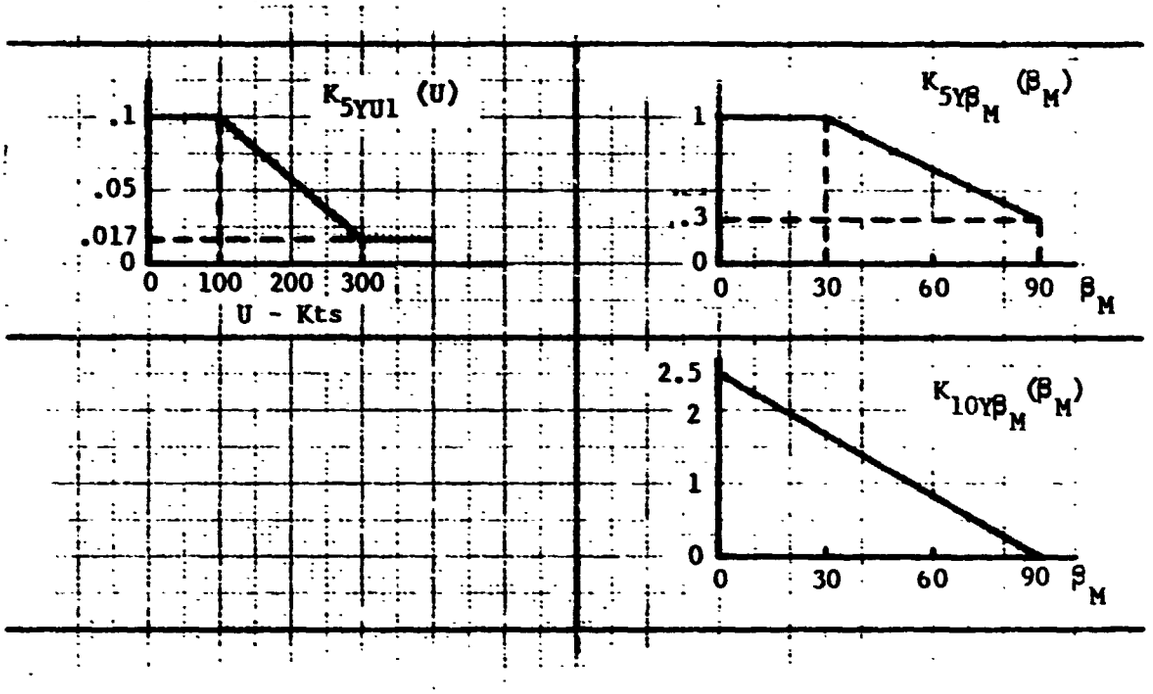

TABLE SAS III - Gains for Roll SCAS Electronics

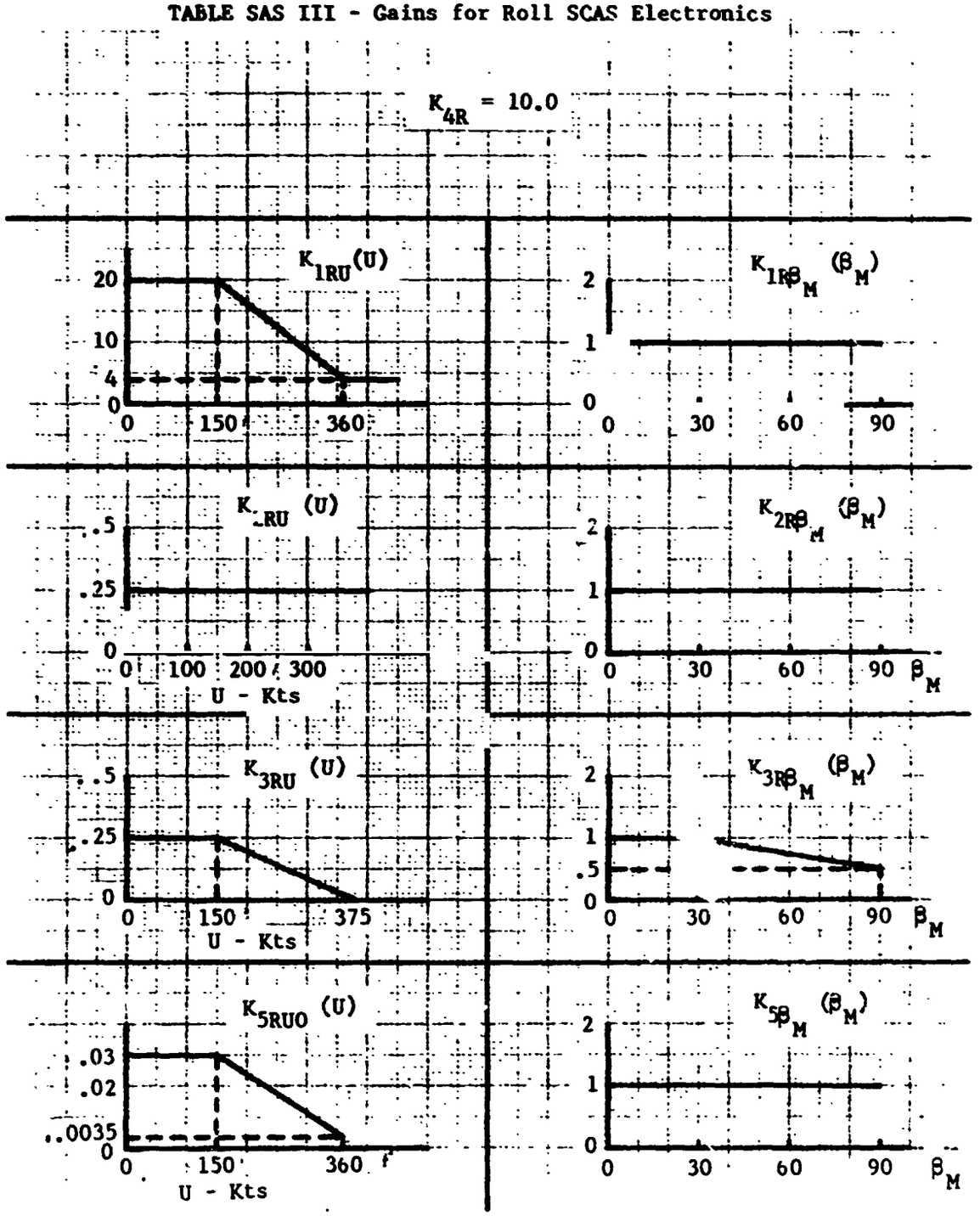

TABLE SAS III - Contd